Hydraulics and Dynamics of North Inlet, South Carolina, 1974-75

by

Robert J. Finley

GITI REPORT 10

September 1976

Prepared for
U.S. Army Coastal Engineering Research Center
under
Contract Nos. DACW72-72-C-0032 and DACW72-74-C-0018
by
University of South Carolina
Columbia, South Carolina 29208

GENERAL INVESTIGATION OF TIDAL INLETS

A Program of Research Conducted Jointly by
U.S. Army Coastal Engineering Research Center, Fort Belvoir, Virginia
U.S. Army Engineer Waterways Experiment Station, Vicksburg, Mississippi

Department of the Army
Corps of Engineers

Cover Photo: North Inlet, South Carolina, April 1962
Courtesy of National Ocean Survey

REPORT DOCUMENTATION PAGE		READ INSTRUCTIONS BEFORE COMPLETING FORM
1. REPORT NUMBER GITI Report 10	2. GOVT ACCESSION NO.	3. RECIPIENT'S CATALOG NUMBER
4. TITLE (and Subtitle) HYDRAULICS AND DYNAMICS OF NORTH INLET, SOUTH CAROLINA, 1974-75		5. TYPE OF REPORT & PERIOD COVERED Final Report
		6. PERFORMING ORG. REPORT NUMBER
7. AUTHOR(s) Robert J. Finley		8. CONTRACT OR GRANT NUMBER(s) DACW72-72-C-0032 DACW72-74-C-0018
9. PERFORMING ORGANIZATION NAME AND ADDRESS U.S. Army Engineer Waterways Experiment Station Hydraulics Laboratory P.O. Box 631, Vicksburg, Mississippi 39180		10. PROGRAM ELEMENT, PROJECT, TASK AREA & WORK UNIT NUMBERS F31019
11. CONTROLLING OFFICE NAME AND ADDRESS Department of the Army Coastal Engineering Research Center Kingman Building, Fort Belvoir, Virginia 22060		12. REPORT DATE September 1976
		13. NUMBER OF PAGES 188
14. MONITORING AGENCY NAME & ADDRESS(If different from Controlling Office)		15. SECURITY CLASS. (of this report) UNCLASSIFIED
		15a. DECLASSIFICATION/DOWNGRADING SCHEDULE

16. DISTRIBUTION STATEMENT (of this Report)

Approved for public release, distribution unlimited

17. DISTRIBUTION STATEMENT (of the abstract entered in Block 20, if different from Report)

18. SUPPLEMENTARY NOTES

19. KEY WORDS (Continue on reverse side if necessary and identify by block number)

Beach and inlet morphology   North Inlet, S.C.   Tidal hydraulics   Tidal inlets   Wave parameters

20. ABSTRACT (Continue on reverse side if necessary and identify by block number)

Detailed quarterly studies at North Inlet, South Carolina, have shown variation in wave parameters, beach and inlet morphology, and tidal hydraulics which are related to seasonal climatic patterns. Wind magnitude and direction, occurrence of northeast storms, and brackish water influx from adjacent Winyah Bay are significant process variables. Over 800 unique visual wave observations indicate that annual resultant wave energy flux is directed to the south.

(continued)

DD FORM 1 JAN 73 1473   EDITION OF 1 NOV 65 IS OBSOLETE

However, an energy flux reversal due to ebb tidal delta morphology results in longshore transport of sediment toward the inlet, adding to swash bars, the channel-margin linear bars, and a northward recurving spit. An estimate of the volume of inlet-directed longshore sediment transport (3.5×10^5 cubic meters per year), based on observed energy fluxes, gives a value which is 83 percent of the annual longshore transport rate (4.3×10^5 cubic meters per year), based on 39 years of spit and shoal growth.

Beach profiles at 11 locations show that erosion is primarily due to northeast storms and that the shoreline is transgressive. A maximum of 7 meters of foredune retreat was observed during the winter of 1972-73, contributing abundant sediment to the ebb tidal delta, which has a present volume of over 35,700,000 cubic meters. The only beach not severely eroding lies immediately south of the inlet where the ebb tidal delta affords protection from northeast storm wave approach, and onshore migration of swash bars provides sediment to the longshore transport reversal.

The southern channel-margin linear bar of the ebb tidal delta has increased in width and length during recovery from the February 1973 northeast storm. Reduction in the cross-sectional area of the inlet throat during the fall and winter months is related to sediment added to the northern channel-margin linear bar. The flood tidal delta is migrating westward under the influence of waves at high tide and is being dissected by ebb flow from a minor tidal creek.

Hydrographic observations over complete spring, mean, and neap tidal cycles have been used to determine the volume of the tidal prism, examine current velocity distributions, and determine coefficients of friction and repletion. Prism volume varies from 7.43×10^6 to 25.52×10^6 cubic meters, depending on tidal phase and meteorological influences, with a mean of 14.96×10^6 cubic meters. Maximum tidal current velocities reach 120 centimeters per second and time-velocity asymmetry is present. Average Manning's n friction coefficients have been found to range from 0.032 to 0.041. Keulegan repletion coefficients are applicable to tidal flow at North Inlet, despite the complex nature of flow into a marsh-filled area and the hydraulic connection to adjacent Winyah Bay. The two major channels must be considered separately, and extreme values of n which coincide with slack water must be excluded from any analyses.

FOREWORD

This report results from work performed under Contract Nos. DACW72-72-C-0032 and DACW72-74-C-0018 between the Coastal Engineering Research Center (CERC) and the University of South Carolina, Columbia, South Carolina. It is one in a series of reports from the Corps of Engineers' General Investigation of Tidal Inlets (GITI), which is under the technical surveillance of CERC and is conducted by CERC, the U.S. Army Engineer Waterways Experiment Station (WES), other government agencies, and by private organizations.

The report was prepared by Robert J. Finley, and is based on a dissertation which fulfilled the thesis requirement for a Ph.D. degree in geology. Dr. Miles O. Hayes served as principal investigator on the contracts and supervised preparation of the report. Assistance in data collection and analysis was provided by Sandra Finley, Stan Humphries, Jeff Knoth, J.J. Gonsiewski, and other members of the Coastal Research Division, University of South Carolina. The Belle W. Baruch Institute for Marine Biology and Coastal Studies provided additional logistical support. CERC contract technical monitor was C. Mason.
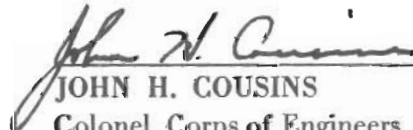
Technical Directors of CERC and WES were T. Saville, Jr., and F.R. Brown, respectively.

Comments on the publication are invited.

Approved for publication in accordance with Public Law 166, 79th Congress, approved 31 July 1945, as supplemented by Public Law 172, 88th Congress, approved 7 November 1963.

JOHN L. CANNON
Colonel, Corps of Engineers
Commander and Director
Waterways Experiment Station

JOHN H. COUSINS
Colonel, Corps of Engineers
Commander and Director
Coastal Engineering Research Center

3

PREFACE

1. The Corps of Engineers, through its Civil Works program, has sponsored, over the past 23 years, research into the behavior and characteristics of tidal inlets. The Corps' interest in tidal inlet research stems from its responsibilities for navigation, beach erosion prevention and control, and flood control. Tasked with the creation and maintenance of navigable U.S. waterways, the Corps routinely dredges millions of cubic yards of material each year from tidal inlets that connect the ocean with bays, estuaries, and lagoons. Design and construction of navigation improvements to existing tidal inlets are an important part of the work of many Corps' offices. In some cases, design and construction of new inlets are required. Development of information concerning the hydraulic characteristics of inlets is important not only for navigation and inlet stability, but also because inlets, by allowing for the ingress of storm surges and egress of flood waters, play an important role in the flushing of bays and lagoons.

2. A research program, General Investigation of Tidal Inlets (GITI), was developed to provide quantitative data for use in design of inlets and inlet improvements. It is designed to meet the following objectives:

To determine the effects of wave action, tidal flow, and related phenomena on inlet stability and on the hydraulic, geometric, and sedimentary characteristics of tidal inlets; to develop the knowledge necessary to design effective navigation improvements, new inlets, and sand transfer systems at existing tidal inlets; to evaluate the water transfer and flushing capability of tidal inlets; and to define the processes controlling inlet stability.

3. The GITI is divided into three major study areas: (a) inlet classification, (b) inlet hydraulics, and (c) inlet dynamics.

   a. Inlet Classification. The objectives of the inlet classification study are to classify inlets according to their geometry, hydraulics, and stability, and to determine the relationships that exist among the geometric and dynamic characteristics and the environmental factors that control these characteristics. The classification study keeps the general investigation closely related to real inlets and produces an important inlet data base useful in documenting the characteristics of inlets.

   b. Inlet Hydraulics. The objectives of the inlet hydraulics study are to define the tide-generated flow regime and water level fluctuations in the vicinity of coastal inlets and to develop techniques for predicting these phenomena. The inlet hydraulics study is divided into three areas: (1) idealized inlet model study, (2) evaluation of state-of-the-art physical and numerical models, and (3) prototype inlet hydraulics.

4

(1) The Idealized Inlet Model. The objectives of this model study are to determine the effect of inlet configurations and structures on discharge, head loss and velocity distribution for a number of realistic inlet shapes and tide conditions. An initial set of tests in a trapezoidal inlet was conducted between 1967 and 1970. However, in order that subsequent inlet models are more representative of real inlets, a number of "idealized" models representing various inlet morphological classes are being developed and tested. The effects of jetties and wave action on the hydraulics are included in the study.

(2) Evaluation of State-of-the-Art Modeling Techniques. The objectives of this part of the inlet hydraulics study are to determine the usefulness and reliability of existing physical and numerical modeling techniques in predicting the hydraulic characteristics of inlet-bay systems, and to determine whether simple tests, performed rapidly and economically, are useful in the evaluation of proposed inlet improvements. Masonboro Inlet, North Carolina, was selected as the prototype inlet which would be used along with hydraulic and numerical models in the evaluation of existing techniques. In September 1969 a complete set of hydraulic and bathymetric data was collected at Masonboro Inlet. Construction of the fixed-bed physical model was initiated in 1969, and extensive tests have been performed since then. In addition, three existing numerical models were applied to predict the inlet's hydraulics. Extensive field data were collected at Masonboro Inlet in August 1974 for use in evaluating the capabilities of the physical and numerical models.

(3) Prototype Inlet Hydraulics. Field studies at a number of inlets are providing information on prototype inlet-bay tidal hydraulic relationships and the effects of friction, waves, tides, and inlet morphology on these relationships.

c. *Inlet Dynamics.* The basic objective of the inlet dynamics study is to investigate the interactions of tidal flow, inlet configuration, and wave action at tidal inlets as a guide to improvement of inlet channels and nearby shore protection works. The study is subdivided into four specific areas: (1) model materials evaluation, (2) movable-bed modeling evaluation, (3) reanalysis of a previous inlet model study, and (4) prototype inlet studies.

(I) Model Materials Evaluation. This evaluation was initiated in 1969 to provide data on the response of movable-bed model materials to waves and flow to allow selection of the optimum bed materials for inlet models.

(2) Movable-Bed Model Evaluation. The objective of this study is to evaluate the state-of-the-art of modeling techniques, in this case movable-bed inlet modeling. Since, in many cases, movable-bed modeling is the only tool available for predicting the response of an inlet to improvements, the capabilities and limitations of these models must be established.

(3) Reanalysis of an Earlier Inlet Model Study. In 1975, a report entitled, "Preliminary Report: Laboratory Study of the Effect of an Uncontrolled Inlet on the Adjacent Beaches," was published by the Beach Erosion Board (now CERC). A reanalysis of the original data is being performed to aid in planning of additional GITI efforts.

(4) Prototype Dynamics. Field and office studies of a number of inlets are providing information on the effects of physical forces and artificial improvements on inlet morphology. Of particular importance are studies to define the mechanisms of natural sand bypassing at inlets, the response of inlet navigation channels to dredging and natural forces, and the effects of inlets on adjacent beaches.

4. This report presents results of the first phase of a field study to define the hydraulics and dynamics of North Inlet, South Carolina, a natural Atlantic coast tidal inlet. Exploratory field and office studies conducted during 1972-74 preceded an intensive field survey during 1974-75. Historical and recent bathymetric data are used to define the long- and short-term stability of the inlet and adjacent beaches. Wave and tidal data are used to correlate observed bathymetric changes with causative processes, and to provide basic information on the local variability in wave conditions and inlet hydraulic characteristics. A subsequent report on the last year of the field study (1975-76) will present additional data and analyses and a summary of significant results.

CONTENTS

CONTENTS--Continued

CONTENTS

TABLES--Continued

FIGURES

CONTENTS

FIGURES—Continued

CONVERSION FACTORS, U. S. CUSTOMARY TO METRIC (SI)
UNITS OF MEASUREMENT

U.S. customary units of measurement used in this report can be converted to metric (SI) units as follows:

Multiply	by	To obtain
inches	25.4	millimeters
	2.54	centimeters
square inches	6.452	square centimeters
cubic inches	16.39	cubic centimeters
feet	30.48	centimeters
	0.3048	meters
square feet	0.0929	square meters
cubic feet	0.0283	cubic meters
yards	0.9144	meters
square yards	0.836	square meters
cubic yards	0.7646	cubic meters
miles	1.6093	kilometers
square miles	259.0	hectares
acres	0.4047	hectares
foot-pounds	1.3558	newton meters
ounces	28.35	grams
pounds	453.6	grams
	0.4536	kilograms
ton, long	1.0160	metric tons
ton, short	0.9072	metric tons
degrees (angle)	0.1745	radians
Fahrenheit degrees	5/9	Celsius degrees or Kelvins[1]

[1] To obtain Celsius (C) temperature readings from Fahrenheit (F) readings, use formula: $C = (5/9) (F - 32)$. To obtain Kelvin (K) readings, use forumla: $K = (5/9) (F - 32) + 273.15$.

SYMBOLS AND DEFINITIONS

a_o = ocean tide amplitude

a_b = bay tide amplitude

A_B = surface area of basin

A_c = inlet cross-sectional area

C_g = group wave velocity

d_b = stillwater depth in which wave breaks

$\overline{E}$ = specific energy (total wave energy per unit surface area)

g = gravitational acceleration

H_1 = elevation of water in basin referred to mean sea level (MSL)

H_2 = elevation of water in ocean referred to MSL

H_b = height of breaker at surf zone

H_o = deepwater wave height

K = Keulegan repletion coefficient

L = wavelength

L = length of connecting channel (in friction and repletion coefficient calculations)

L_o = deepwater wavelength

m = a coefficient taken as 1 for assumed uniform velocity for an inlet cross section

n = Manning's friction coefficient

P = tidal prism volume

P_h = tidal prism determined hydraulically from flow measurements

P_{1s} = longshore energy flux factor

Q = annual longshore sediment transport rate

R = hydraulic radius

S = energy slope

T = tidal period (12.42 hours)

T_b = breaker wave period

a_b = breaker angle

λ = Keulegan's friction coefficient

ρ = mass density of water

ΔH_1 = fall necessary to accelerate ocean water to velocity, V

ΔH_2 = fall necessary to overcome inlet channel resistance

HYDRAULICS AND DYNAMICS OF NORTH INLET, SOUTH CAROLINA, 1974-75

by
Robert J. Finley

I. INTRODUCTION

1. The Problem.

The primary goals of this study were to gain a better understanding of those processes which determine the morphology and hydraulics of a natural tidal inlet and to determine seasonal and longer term changes in process variables through detailed field studies. Variations in littoral processes, especially longshore current velocity and wave energy flux, were investigated and correlations made with physiography of the beaches adjacent to the inlet and the ebb tidal delta. Significant seasonal patterns tied to seasonal climatic changes, and the importance of storms brought out by observations during all types of weather conditions, are reported in detail.

Inlet hydraulics has primarily been treated theoretically or through use of published tables and charts (O'Brien and Clark, 1973; King, 1974; Mehta and Hou, 1974). These data certainly bear analysis, but in many cases, as O'Brien (1971) pointed out, surveys concentrate on navigation channels and, in some cases, shoals are drawn without correction between successive published surveys. The problem, then, is to evaluate hydraulic parameters, such as the Keulegan repletion coefficient (Keulegan, 1967), and the influence of inlet morphology on tidal flow at a natural inlet. In the real situation, the simplifying assumptions which are often made in hydraulic analysis do not apply. Therefore, the study of complex natural inlet systems will help greatly to improve the understanding of the limitations of simple hydraulic mathematical models.

2. Methodology.

Preliminary fieldwork was carried out from June 1972 to June 1973, with most of the effort concentrated from June to August 1972. The fieldwork included a general reconnaissance of the inlet area, establishment of beach profile localities, some basic mapping and bathymetric profiling, and current velocity measurements at 11 stations, with the addition of temperature, conductivity, salinity, turbidity, and Secchi disc-extinction depth measurements at selected stations. Beach profiling was generally done monthly, with special emphasis on the effects of a northeast storm on 10 and 11 February 1973, the most severe storm affecting the area between June 1972 and May 1975.

From June 1973 to June 1974, beach profiles were monitored regularly, and extensive trenching of beach and overwash features was performed. Quarterly 2-week periods of intensive study were conducted in July and September 1974, and January and March 1975. Beach observations, mapping and profiling in subtidal through supratidal environments,

current velocity and direction measurements, aerial photography, and the continuous recording of tidal fluctuations were carried out. Each study period corresponded to the 2-week springtide to springtide period and, as the data later indicated, provided a good sampling of seasonal climatic variation.

II. PHYSICAL SETTING

1. Geology.

North Inlet is located in Georgetown County, South Carolina (Fig. 1). Approximately 17,000 acres of beach, marsh, and adjacent woodland between Winyah Bay and the Atlantic Ocean are being held in trust by the Belle W. Baruch Foundation and preserved as a completely natural area for scientific research. The inlet and adjacent beaches provide an unmodified area for geomorphic and hydrodynamic investigations.

North Inlet lies within the lower Coastal Plain of South Carolina. The underlying sediments consist of gently seaward-dipping and thickening sedimentary units whose relative elevations reflect fluctuations in ocean level over the past 120 million years, as well as regional warping of the continental margin. A relatively continuous sedimentary sequence is present from the Lower Cretaceous through the Pleistocene and Recent. The surface topography of Georgetown County and the county to the immediate north, Horry County, represents predominantly depositional landforms composed of late Miocene to Recent marine and fluvial deposits (Thom, 1967). These deposits have been partially modified by subsequent erosional processes. Five phases of coastal progradation have been recognized on the upper South Carolina coast, as evidenced by Pleistocene terrace deposits. Thom (1967) determined that these deposits in Horry County consisted of a barrier island behind which had accumulated lagoonal and fluvial sediments. Relative elevations above present sea level for the five surfaces are:

Horry. . . . 60 to 115 feet
Conway. . . 35 to 60 feet
Jaluco . . . 30 to 55 feet
Myrtle . . . 5 to 35 feet
Recent . . . 0 to 15 feet

Thom (1967) placed the Pleistocene-Recent contact at North Inlet at the western edge of the present salt marsh, which is shown as a dashline in Figure 2 (National Ocean Survey (NOS) chart 11532). Elevations along the marsh margin are 6 to 8 feet, indicating that this is probably a continuation of the Myrtle surface.

A well drilled in 1973 a few tens of feet west of the Pleistocene-Recent contact in the study area revealed unconsolidated sand and clay with a shell hash at its base down to the 18.5-meter depth. At that point a sharp contact with a dense microcrystalline limestone was encountered, indicating the top of the Upper Cretaceous, probably the Black Creek Formation (D. Comer, personal communication, 1973).
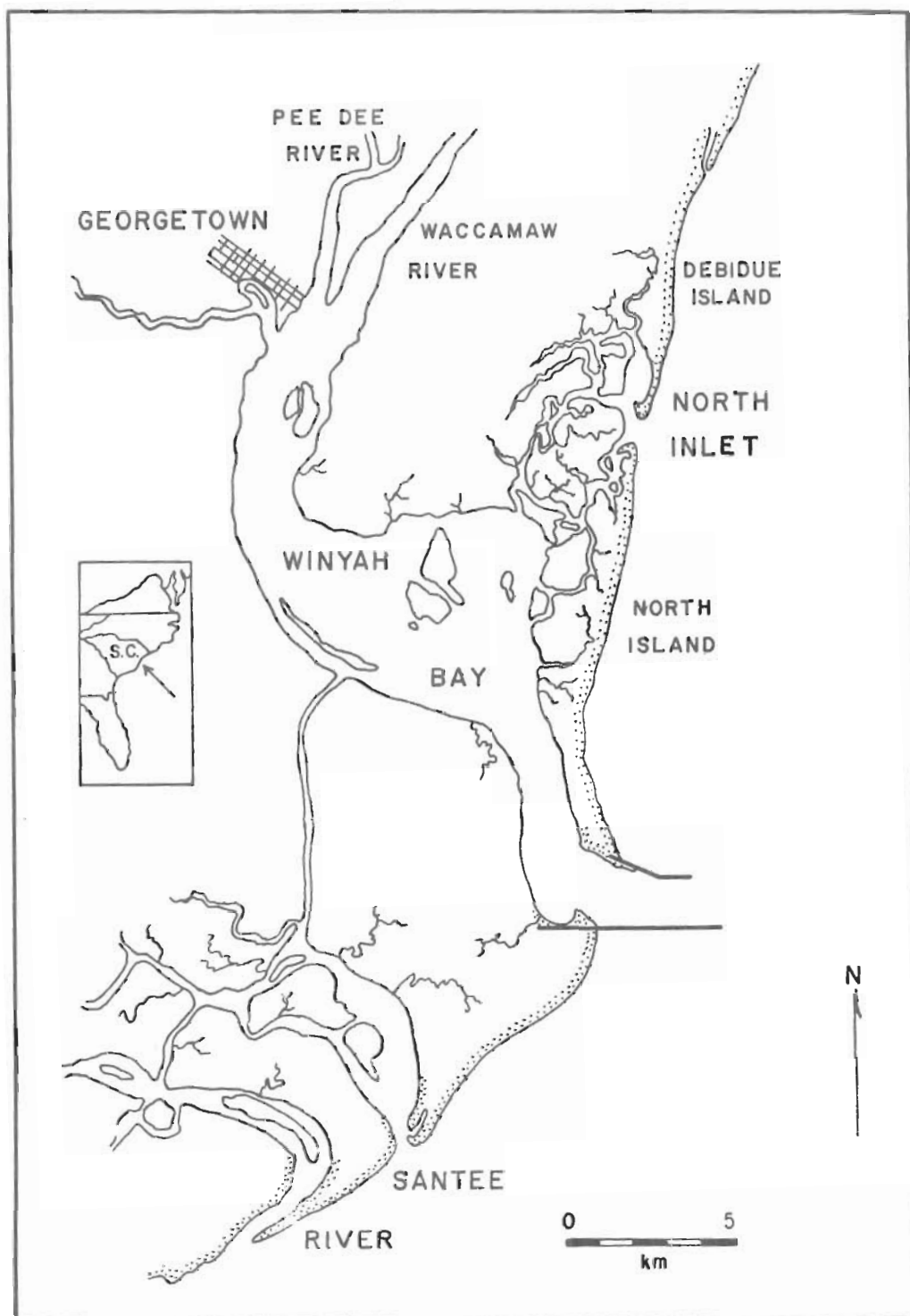
Figure 1. Location map of North Inlet and vicinity.
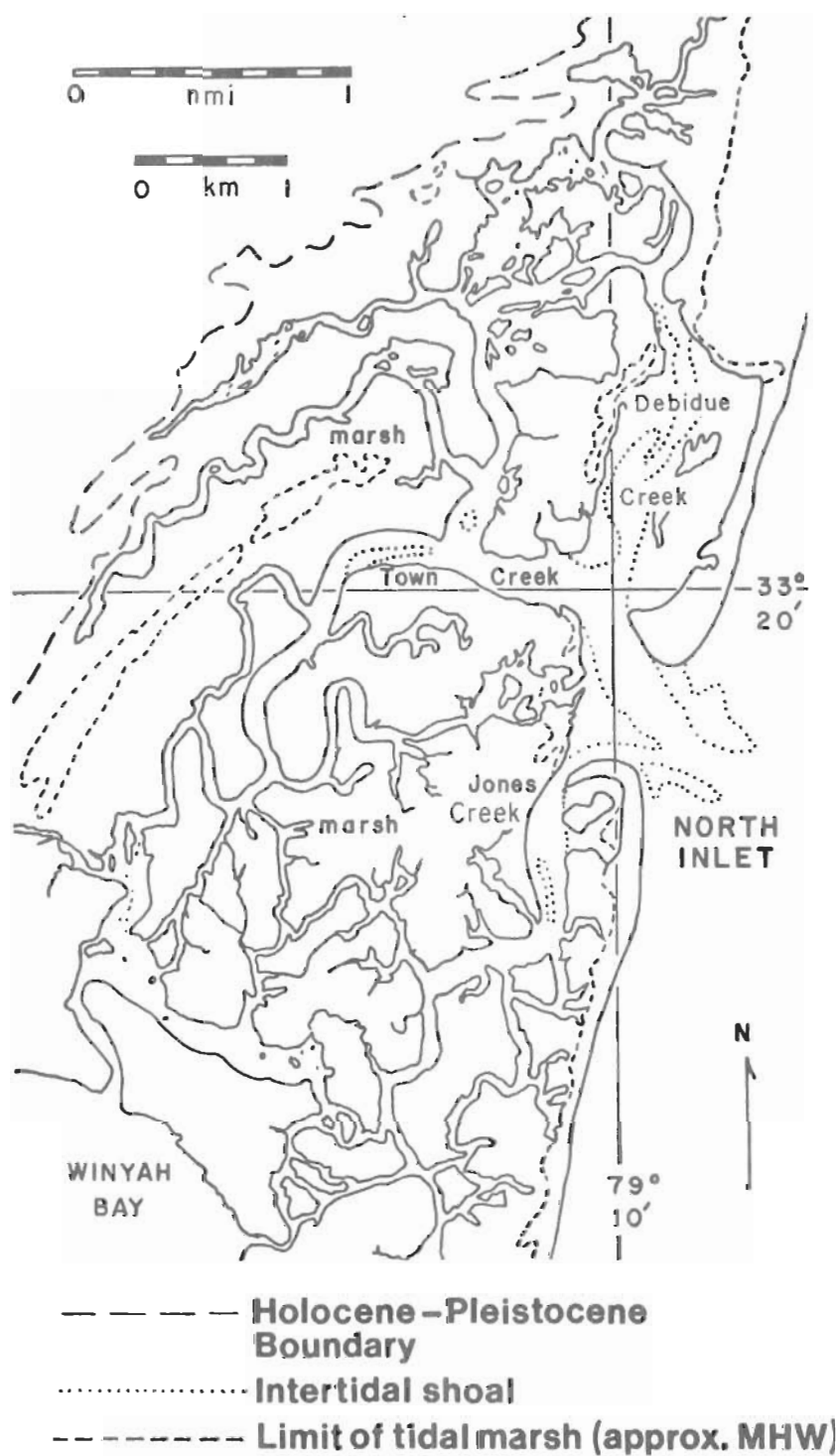
Figure 2. Detail of North Inlet bay area (based on NOS chart 11532).

2. Regional Climate.

Rainfall and temperature characteristics at North Inlet, interpolated from data contoured by Landers (1970), are as follows for the base period 1935 to 1964:

  (a) Annual average rainfall: 124 centimeters (48 inches),

  (b) January average maximum temperature: 14°Celsius (57°Fahrenheit),

  (c) January average minimum temperature: 3.5°Celsius (38°Fahrenheit),

  (d) July average maximum temperature: 31°Celsius (88°Fahrenheit), and

  (e) July average minimum temperature: 23°Celsius (73°Fahrenheit).

Wind patterns observed aboard ship for the 2° latitude observation square off the coast of South Carolina are summarized in Figures 3 and 4 (U.S. Naval Weather Service Command, 1970). The overall pattern (Fig. 3, a) shows the influence of extra-tropical cyclones, or northeast storms, by the presence of peaks in the northeast and eastern sectors. These winds are the dominant winds on the South Carolina coast and are the most important wave generators. Southeasterly and southerly winds generally result from circulation around the western sides of high-pressure systems. Anticyclonic circulation around these highs prevails during the summer months, bringing warm, moist air to the southeast. This pattern is modified locally by thunderstorms which build up in the afternoon hours. To complete the pattern, west and northwest winds usually result from approaching frontal systems, notably winter cold fronts, and are often of considerable velocity, but not approaching that of severe northeast storms passing over or south of the study area. Northeast storm centers passing north of the study area may also produce west or northwest winds.

Figure 3, b shows the percentage frequency of winds greater than 21 knots. This cutoff point was selected since the next lower velocity category in U.S. Naval Weather Service Command (1970) includes data in the relatively broad category of 11 to 21 knots. Westerly, northwesterly, and northerly winds are often strong and associated with frontal passage, but their offshore direction does not generate waves with any major effect on the North Inlet beaches. Most cyclonic storms travel along the eastern edge of cold, high-pressure airmasses with the result that offshore-directed northwest winds "blow down" the sea developed by northeasterly winds as the front moves into the coastal area. Such a movement pattern of a low-pressure system along a cold front was followed by the major northeast storm of February 1973.

Wind patterns (Fig. 4) are clearly seasonal. January is influenced by the westerly, northwesterly, and northerly winds of frontal passage; March shows a pattern intermediate between winter and summer, with southerly and southwesterly wind frequency beginning to increase; July shows the prevailing southwest summer wind; and September is influenced by the dominant northeast stormwind. These months were chosen because they correspond to the months of quarterly field studies during the 1974-75 study period. Note that a subordinate northeast peak is present for the January and March periods, as northeast storms do occur, but with lesser frequency through the winter and into the early spring.

a. All Readings

Shoreline Trend

b. Winds over 21 kn

10   **5**   0
pct
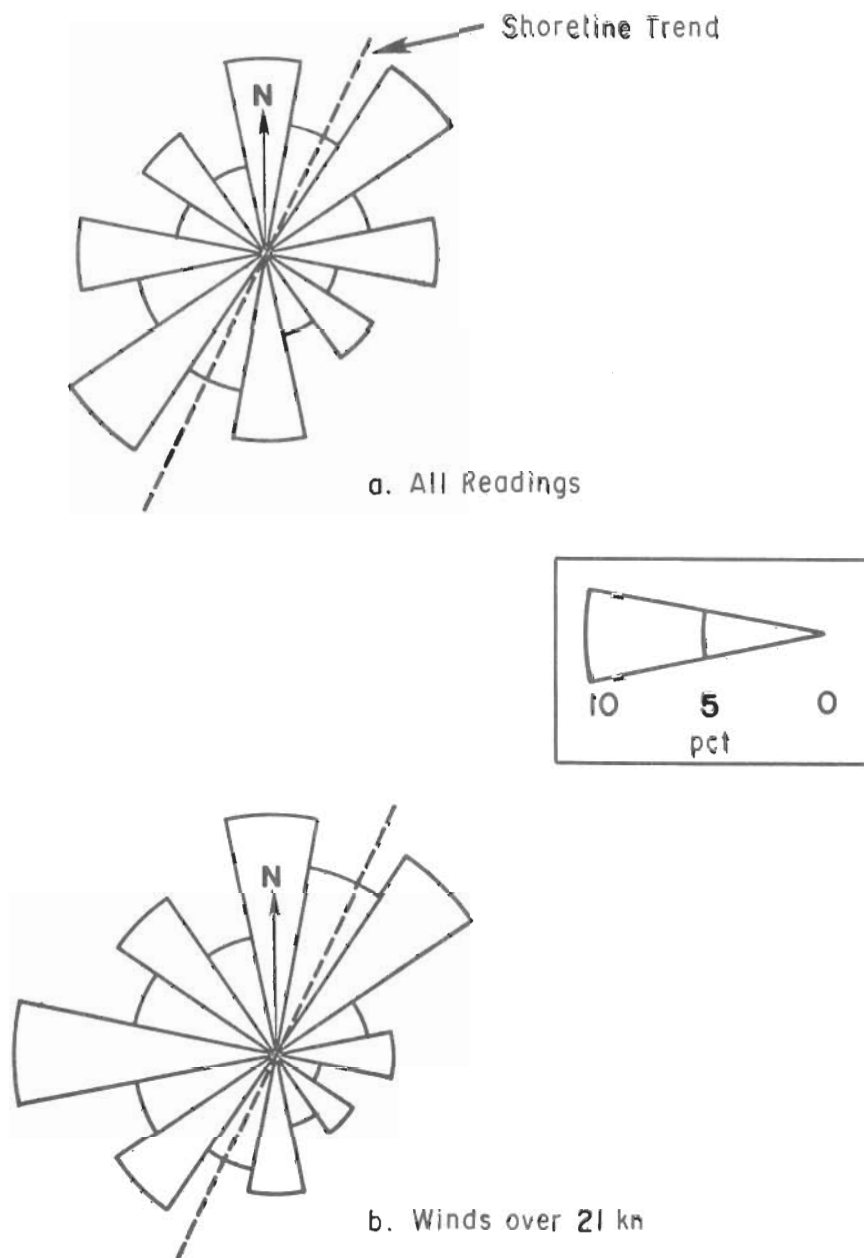
Figure 3. Annual wind directional frequency, offshore South Carolina (based on U.S. Naval Weather Service Command, 1970).

Shoreline Trend

a. Jan.

b. Mar.

20 15 10 5

pct

c. July

d. Sept.
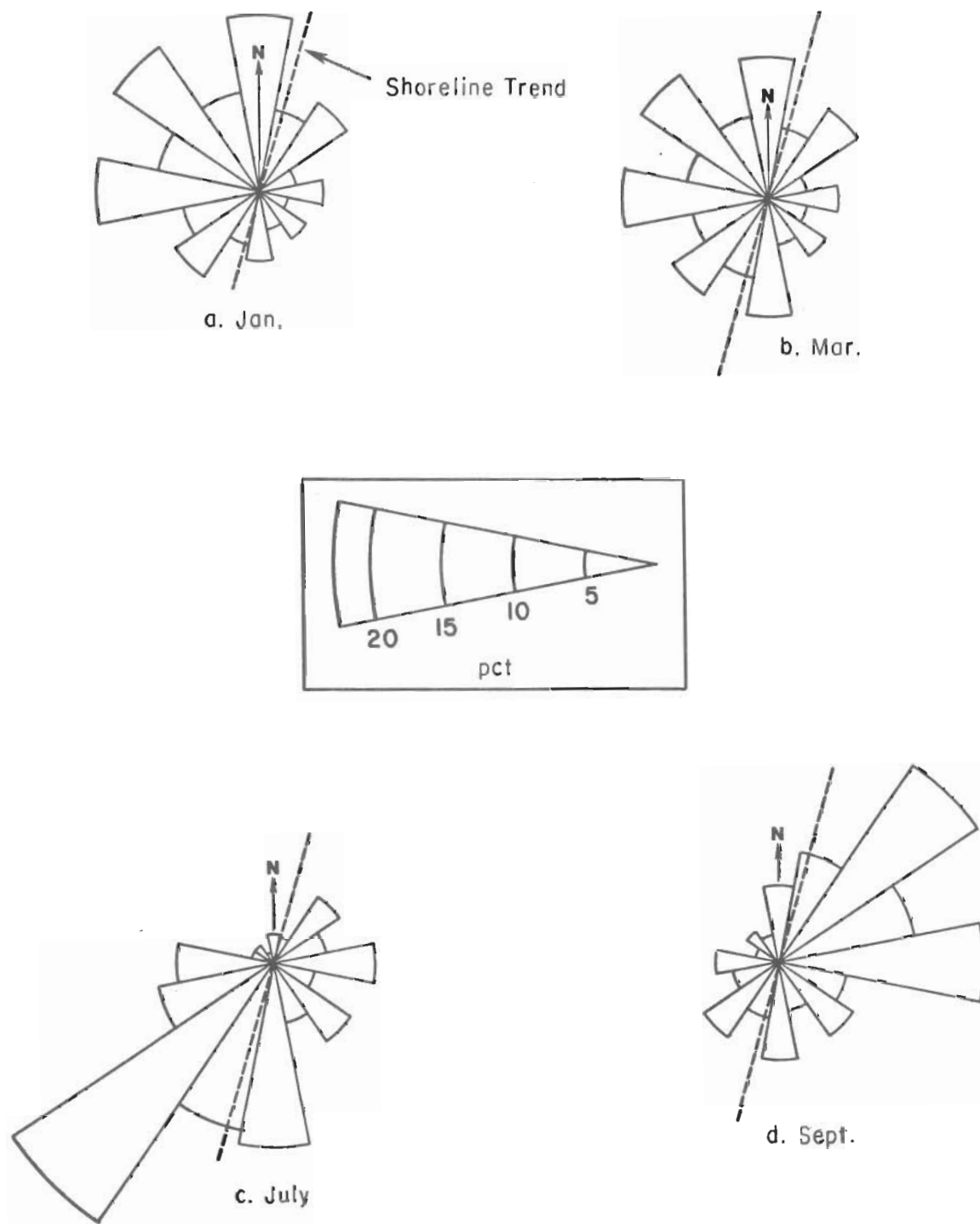
Figure 4. Quarterly wind directional frequency, offshore South Carolina
(based on U.S. Naval Weather Service Command, 1970).

Shipboard surface wind velocities are shown in Figure 5 for the area from 30° to 35°N. latitude and 75° to 80°W. longitude (U.S. Army Engineer District, Charleston, 1970). Also shown is surface wind data at Charleston, South Carolina, including average wind velocities for a 47-year period. These data again indicate a prevailing wind from the southwest, but the dominant or strongest wind from the northeast.

The Middle Atlantic States suffer hurricane damage due to storms moving onshore from the Atlantic Ocean, moving offshore after crossing overland from the Gulf of Mexico, or moving parallel to the coast. The latter movement results from prevailing westerly winds altering the storm tracks toward the northeast as they leave the tropics and move north of 30°N. latitude and is the most common according to Alaka (1968). The most recent hurricane damage occurred on 15 October 1954, when winds reaching 100 miles per hour were recorded 50 kilometers north of North Inlet at Myrtle Beach. Destruction due to tropical storms has occurred 10 to 15 times in the period 1901 to 1955 for South Carolina, according to data contoured by the U.S. Weather Bureau (Landers, 1970).

3. Local Climate at North Inlet.

During the quarterly 2-week field periods, wind velocity and direction were measured at North Inlet during daylight hours. Observations were made hourly in July, but became bihourly with additional readings during times of wind change for the other periods. During January field studies, northeast winds predominated (Fig. 6, a), and 44.2 percent of all readings fell between north-northeast and east-northeast; the strongest winds also came from those directions (Table 1). Weather during the period was generally poor with heavy overcast, much rain, and wind gusts up to 20 miles per hour recorded from the northeast. Compared to the longer term wind pattern (Fig. 4, a), fewer offshore-directed winds associated with frontal passage occurred than would have been expected.

March winds (Fig. 4, b) appear to be a transition between the winter pattern and the summer trend toward southerly and southwesterly airflow, as the frequency of the latter begins to increase. March field observations (Fig. 6; Table 1) show northeast and eastern peaks which were accompanied by stormy weather, heavy rains (up to 2.05 inches in 24 hours), and extensive flooding in South Carolina rivers. North Inlet salinities were lowered (described in Section VI).

The general summer pattern of southwest winds (Fig. 4, c) was not seen at North Inlet (Fig. 6, c); instead, southerly winds dominated. It is possible that this shift represents the effect of friction over the land surface, since the long-term data are derived from shipboard observations (D. Nummedal, personal communication, 1975). Thunderstorms occurred almost daily, most often from 1200 to 1400 hours and 1700 to 1900 hours. Associated winds were gusty and highly variable in direction, with one instance of 30-mile per hour winds lasting just over 1 hour, accompanied by gusts up to 45 miles per hour. Thunderstorms generally moved from the southwest to the northeast, but several storms reversed direction when reaching the ocean and headed back toward land with a strong onshore wind component. An increase in wave height was almost immediate in such cases, with high waves lasting several hours after the thunderstorm had dissipated.

SURFACE WINDS (OFFSHORE STATION)

LEGEND

Pct Calm

(4 to 10) kn
(11 to 16) kn
(17 to 27) kn
(> 28) kn

SURFACE WINDS (ONSHORE STATION)

LEGEND

Pct Calm

Average wind velocity
for 47-year period

9.5 mi/h
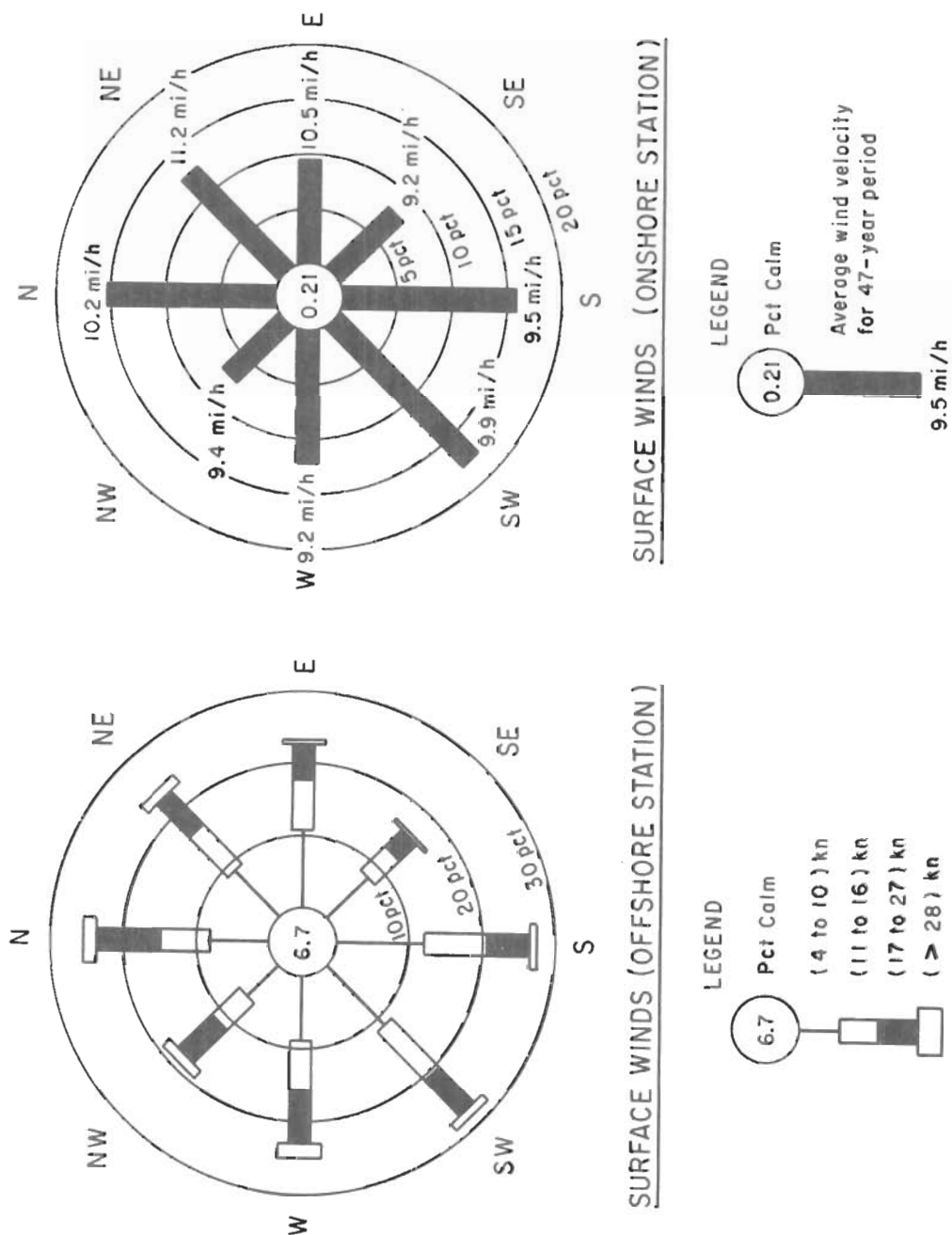
Figure 5. Offshore and onshore wind directional distribution
(U.S. Army Engineer District, Charleston, 1970).

N = 57

Shoreline Trend

a. Jan.

N = 58

b. Mar.

25 20 15 10 5

pct

N = 135

c. July

N = 58

d. Sept.

N = No. of Observations
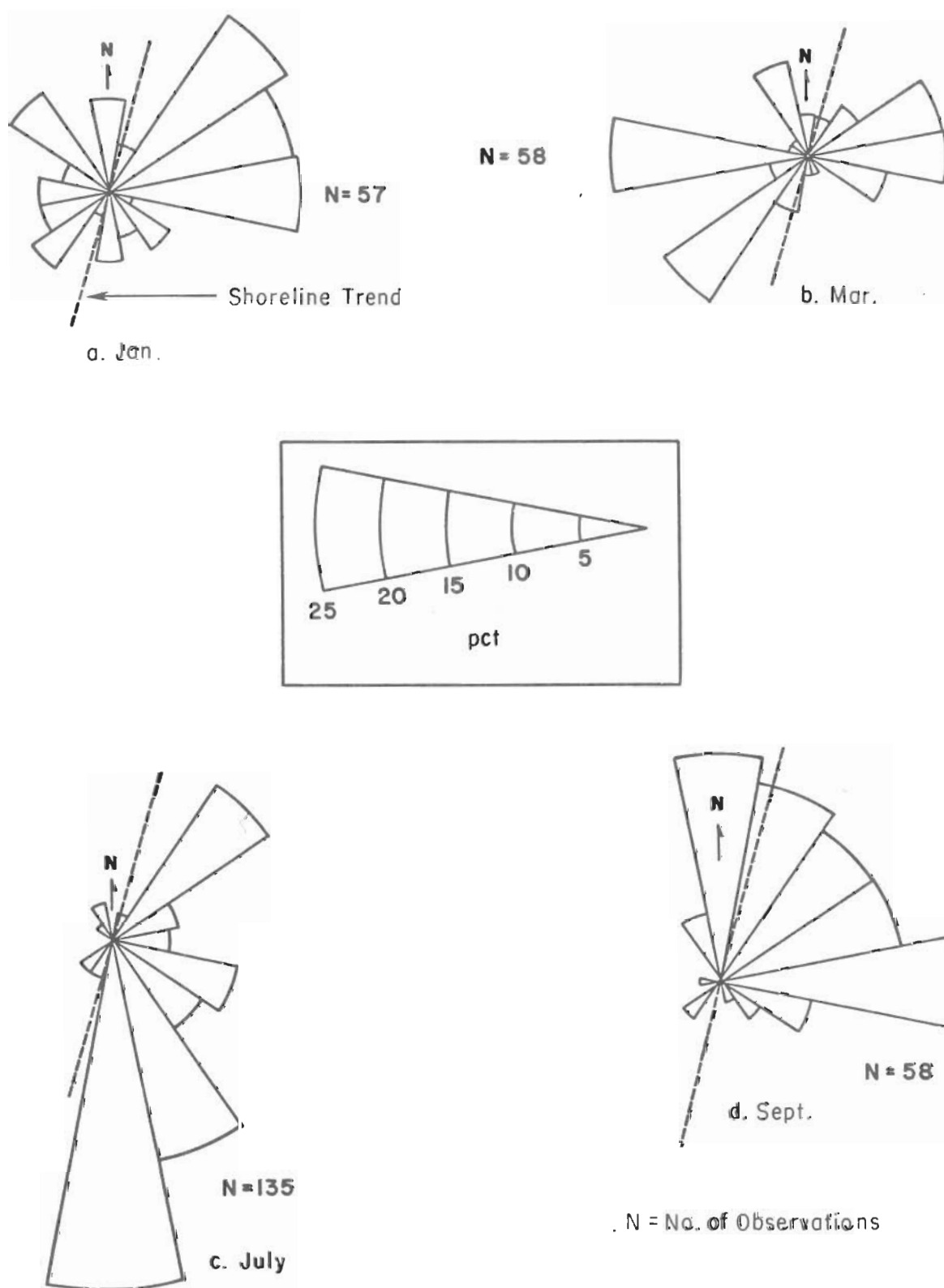
Figure 6. Observed wind directional distribution, North Inlet.

Table 1. Mean wind velocities (miles per hour) observed at North Inlet.

Dir.	Observation periods			
	1974		1975	
	26 July to 2 Aug.	15 to 28 Sept.	2 to 15 Jan.	14 to 26 Mar.
NNE.	5.3 (3)[1]	12.9 (9)	3.0 (2)	10.5 (2)
NE.	6.7 (20)	11.1 (8)	8.2 (9)	13.0 (3)
ENE.	10.5 (6)	7.8 (8)	10.1 (8)	15.0 (7)
E.	7.4 (7)	5.3 (10)	6.0 (7)	8.9 (7)
ESE.	6.1 (11)	8.3 (4)	5.0 (1)	11.0 (4)
SE.	7.4 (13)	5.0 (2)	8.7 (3)	------------[2]
SSE.	7.9 (23)	8.0 (1)	--------------	5.0 (1)
S.	10.7 (36)	--------------	6.7 (3)	5.0 (1)
SSW.	6.0 (4)	--------------	4.0 (1)	12.0 (3)
SW.	3.8 (4)	4.5 (2)	6.8 (4)	14.0 (6)
WSW.	--------------	--------------	7.3 (3)	9.5 (2)
W.	--------------	4.0 (1)	8.7 (3)	11.5 (10)
WNW.	--------------	--------------	--------------	9.0 (1)
NW.	2.0 (2)	--------------	8.3 (4)	14.0 (1)
NNW.	3.4 (5)	5.7 (3)	--------------	9.6 (5)
N.	--------------	--------------	--------------	--------------

[1] Figures in parenthesis indicate number of readings contributing to each mean.
[2] No reading occurred within compass point.

The September wind pattern (Figs. 4, d and 6, d; Table 1) showed highest velocities and greatest frequencies from the northeast quadrant. A substantial northeast storm occurred during the study period, resulting in several days of northeast winds and the greatest frequency of southward-directed wave energy flux of any field period.

Since June 1972, the most severe storm was the extra-tropical cyclone of 10 and 11 February 1973, which began in the Gulf of Mexico, moved across northern Florida, and was located off South Carolina and North Carolina by 1300 hours e.s.t. on 10 February, with a central pressure of 988 millibars. A recording anemometer at North Inlet failed after readings of 60 miles per hour. A Sverdrup-Munk-Bretschneider wave hindcast (U.S. Army, Corps of Engineers, Coastal Engineering Research Center, 1975) gave an estimated significant wave height of 10.5 feet, and an estimated significant wave period of 13 seconds at North Inlet. The results of this storm are discussed in Section V, 2.

4. Tidal Regime and Short-Term Sea Level Changes.

The tidal regime at North Inlet is semidiurnal with a pronounced diurnal inequality. The published Tide Tables (National Oceanic and Atmospheric Administration, 1974) give the following data, which should be considered only as approximations:

Mean tide level above mean low water (MLW) datum: 67 centimeters (2.2 feet),

mean range: 137 centimeters (4.5 feet),

average spring range: 162 centimeters (5.3 feet), and

extreme neap range: 64 centimeters (2.1 feet).

The average diurnal inequality calculated for June, July, and August 1972 was 37 centimeters (1.21 feet), with extreme values of 0 during a neap phase to 67 centimeters (2.2 feet) during a spring phase. This inequality contributes to the significant variation in volume between successive flood and ebb tidal prisms considered in Section VI.

Tidal elevations were continuously recorded at three North Inlet locations: An ocean gage off North Island, and tidal creek gages in Town Creek and Jones Creek (Fig. 7). Mean tidal range was greater than the published predictions, and a statistically significant difference in range has been found among these three locations. Using the November 1974 data as an example, the mean range (calculated for 62 tidal cycles) was 150.6 centimeters for the ocean, 144.9 centimeters for Town Creek, and 140.2 centimeters for Jones Creek.

Hicks and Crosby (1974) presented plots of yearly mean sea levels (MSL) (average of hourly sea level heights obtained from an analog tide gage over a period of 1 calendar year) from various NOS tide gages. Figure 8 was taken from these plots and includes the curve for Charleston, South Carolina, some 60 miles to the south of North Inlet, as well as for other east coast locations. The Charleston rate of rise of 3.61 millimeters per year is based on the slope of a least-square line of regression fit to the data series, which for Charleston extends from 1922 to 1972. Computing sea level rise from 1927 (the date of the North American MSL map datum) through 1974, the 3.61-millimeter rate yields a 16.96-centimeter relative sea level rise at North Inlet. This extrapolation appears reasonable since the adjacent curves are similar in shape to the Charleston curve.

To determine water level differentials, all gages were leveled to a common datum using a Wilde T-2 theodolite. The survey was carried to a triangulation station termed *inlet*, located on a sandy ridge in the marsh northwest of the intersection of Town Creek and Debidue Creek. The recorded elevation of this station, 1.4 meters above MSL, could be ±1 meter in error (Dracup, 1973). Therefore, the 1927 MSL datum could not be entered into the tide records. A local mean water level (MWL) was established at the ocean and Town Creek gages by averaging sets of hourly water levels over a 2-week period of tide records from January 1975. Some 480 data points were used at each location.

5. Sediment Characteristics.

Sands at North Inlet generally have a mean size in the medium (0.50 to 0.25 millimeter, 1 to 2 phi) to fine (0.25 to 0.125 millimeter, 2 to 3 phi) size range. The finest material occurs on ebb tidal delta shoals, while the coarsest occurs in the subtidal channels, where it is intermixed with shell fragments, primarily the oyster *Crassostrea virginica* which grows
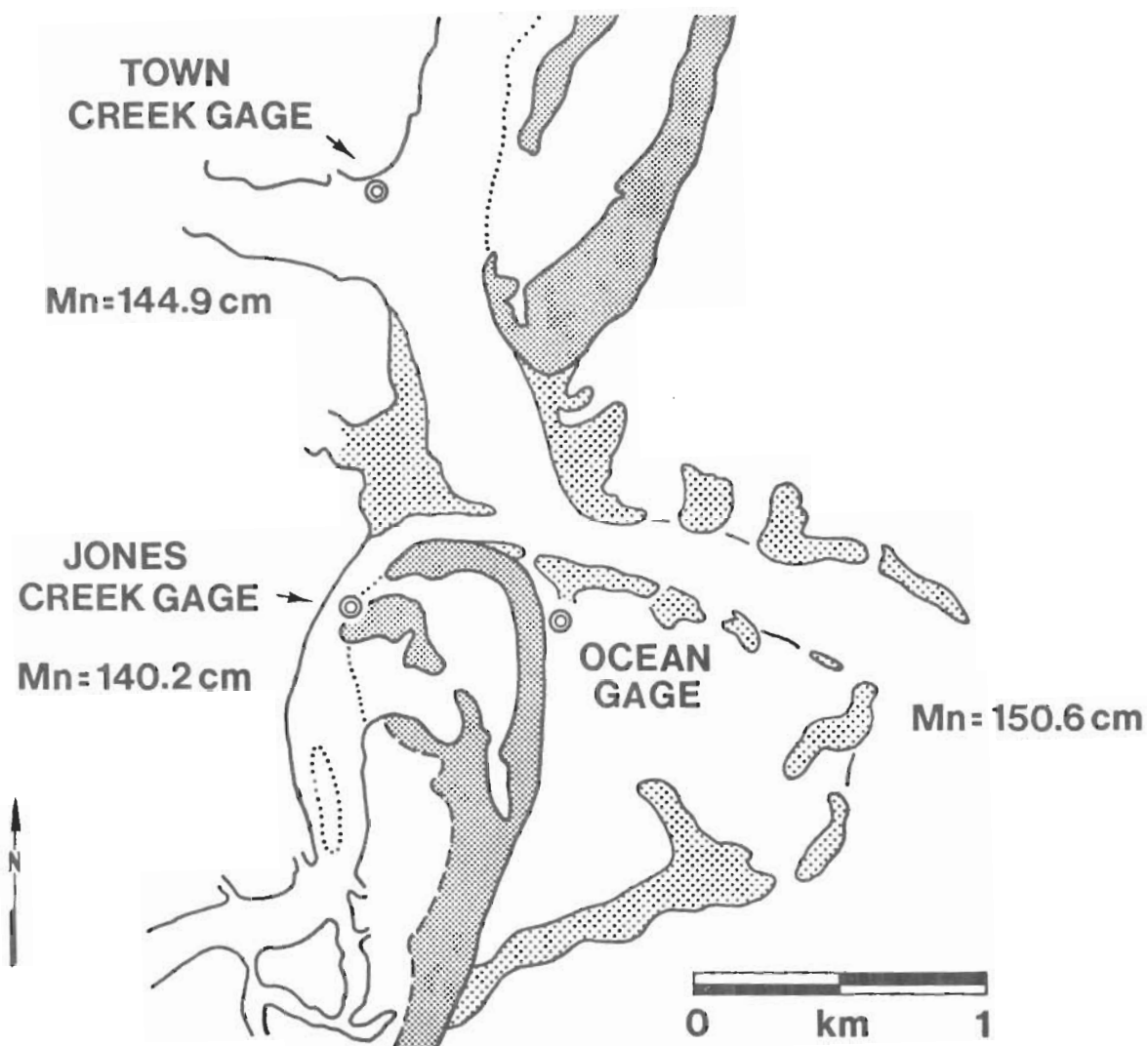
Figure 7. Tide gage locations and mean ranges (Mn) for November 1974 (based on 62 observations).
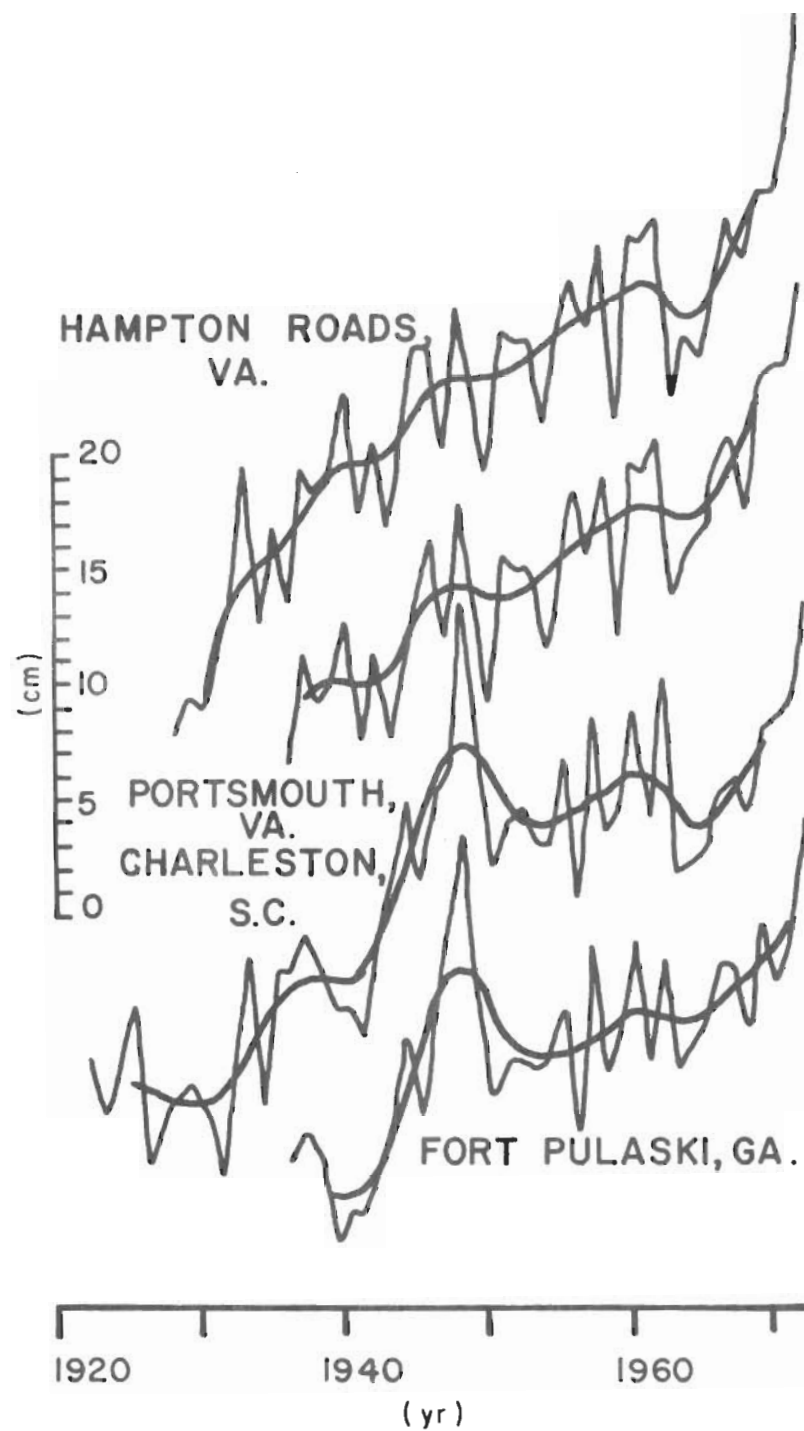
Figure 8. Sea level rise curves (based on Hicks and Crosby, 1974).

abundantly along the creek banks and in free-standing reefs in the tidal creeks. Mineralogically, the sand-size sediment consists of quartz with 5- to 10-percent shell debris and a heavy mineral fraction of ilmenite, epidote, hornblende, staurolite, and ziron (Thom, et al., 1972). Rivers supply hornblende and epidote, which are primarily derived from the Piedmont, because the Coastal Plain sediments are relatively deficient in these less stable mineral species (Neiheisel, 1965).

All sediment samples in the beach and intertidal shoal environments were collected by removing the top layer, which generally contains a lag of sand-size shell fragments, and by sampling a layer several grains thick immediately below. Channel bottom samples were taken with a Van Veen grab sampler. Laboratory analysis utilized the settling velocity principle of the Hydraulic Equivalent Sediment Analyzer built by Anan (1972); parameters were calculated using the graphic statistics of Folk (1968).

The average mean grain size of 17 midtide level beach samples collected on Debidue Island (at 0.10-mile intervals) in August 1972, was 2.05 phi. A similar set collected in December 1972, had an average mean of 1.93 phi which is a very small difference compared to the earlier data (Table 2). Average standard deviations of 0.35 and 0.37 phi, respectively, indicate very well sorted sediments; therefore, no difference is apparent between summer and winter intertidal beach sediments on Debidue Island.

A selection of sediment characteristics from the dune, berm, and intertidal environments is given in Table 3. Within each environment and at each location the samples collected were spaced 6 meters apart along the profile line. A mean size of 2.02 phi for the dune samples and 2.17 phi for all other beach samples indicates the dominance of fine sand throughout the North Inlet environment, which is corroborated by additional sediment data presented in Table 4. The entire South Carolina coast is dominated by fine (2 to 3 phi), river-supplied sediment because the rivers rework Coastal Plain sediments and also drain deeply weathered Piedmont rocks, although the absolute amount of sand reaching the coast is small. The nearest major river, the Santee (Fig. 1), has lower reaches dominated by bottom sediments finer than 2 phi (0.25 millimeter) in median diameter (Stephens, et al., 1975). The generally well sorted (S = 0.35 to 0.50 phi) to moderately well sorted (S = 0.50 to 0.71 phi) nature of all the samples indicates the textural uniformity of the sediments; therefore, it seems that there is little finer sand available to be preferentially incorporated into windblown dunes.

Samples (Table 4) were collected at the locations shown in Figure 9, which, in most cases, were each occupied at least twice during the four quarterly field study periods. Consistently, fine sands (average mean size = 2.34 phi for eight samples) were found on the channel-margin linear bars (stations 9 and 11), where constant wave action results in very well to well-sorted fine sediments. Channel bottom sands of the ebb tidal delta (stations 13 to 16) are medium sands, swept free of fines by tidal currents, and containing much shell lag material. This is especially true of station 16 at the inlet throat where currents remove most sand and the sampler recovers primarily shell (5 to 15 centimeters) and small

Table 2. Debidue Island intertidal sediment characteristics.

| Loc. | Aug. 1972 | | Dec. 1972 | |
	M[1] (phi)	S[2] (phi)	M (phi)	S (phi)
−1	2.16	0.30	2.04	0.31
0 (DBI-10)	2.13	0.37	2.26	0.21
1	2.12	0.44	1.71	0.38
2	1.86	0.40	1.43	0.36
3	2.08	0.31	1.94	0.37
4 (DBI-20)	2.01	0.31	1.75	0.53
5	1.91	0.42	1.88	0.45
6	1.78	0.38	1.99	0.29
7 (DBI-25)	1.99	0.40	1.99	0.32
8	2.05	0.35	2.05	0.35
9	2.04	0.32	1.91	0.31
10	2.13	0.32	1.76	0.41
11 (DBI-30)	2.11	0.32	2.56	0.52
12	2.01	0.33	1.77	0.35
13	2.19	0.34	2.02	0.29
14	2.14	0.38	1.87	0.41
15	2.10	0.29	1.86	0.36

[1]Graphic mean size.

[2]Graphic standard deviation (sorting).

NOTE: Location indicates distance south (negative) or north (positive) of profile DBI-10 (zero) in 1/10-mile increments, as shown on sketch below.

Table 3. Debidue Island sediment characteristics.

Loc.	Environment	M[1] (phi)	S[2] (phi)
DBI-10	dune	1.94	0.48
DBI-10	dune	2.05	0.49
DBI-20	dune	1.87	0.51
DBI-20	dune	2.07	0.35
DBI-20	dune	2.01	0.45
DBI-20	dune	1.75	0.75
DBI-20	dune	2.41	0.45
DBI-20	dune	2.09	0.45
DBI-20	berm	1.86	0.51
DBI-20	berm	2.14	0.37
DBI-20	intertidal	1.96	0.40
DBI-30	berm	2.05	0.49
DBI-30	berm	2.23	0.43
DBI-30	intertidal	2.14	0.39
DBI-30	intertidal	2.25	0.37
DBI-30	intertidal	2.23	0.41
DBI-30	intertidal	2.44	0.36
DBI-30	intertidal	2.36	0.39

[1] Graphic mean size.

[2] Graphic standard deviation (sorting).

Table 4. Quarterly sediment data.

Sta.	Loc.	July 1974		Sept. 1974		Jan. 1975		Mar. 1975	
		M[1] (phi)	S[2] (phi)	M (phi)	S (phi)	M (phi)	S (phi)	M (phi)	S (phi)
1	DBI-ftd	-------	-------	-------	-------	-------	-------	2.28	0.38
2	DBI-ts	-------	-------	-------	-------	2.05	0.36	1.74	0.32
3	DBI-6	-------	-------	-------	-------	1.91	0.52	2.18	0.45
4	DBI-8	-------	-------	-------	-------	-------	-------	2.24	0.42
5	NI-ftd	-------	-------	-------	-------	2.24	0.55	1.99	0.23
6	NI-ts	-------	-------	2.30	0.42	2.46	0.44	2.71	0.51
7	NI-6	2.43	0.43	-------	-------	-------	-------	-------	-------
8	NI-8	2.17	0.47	-------	-------	-------	-------	-------	-------
9	shoal	2.34	0.51	2.42	0.38	2.48	0.44	2.40	0.45
10	shoal	1.75	0.61	-------	-------	2.14	0.38	1.49	0.58
11	shoal	2.42	0.32	2.36	0.35	2.13	0.35	2.20	0.24
12	shoal	1.55	0.81	-------	-------	-------	-------	-------	-------
13	channel	-------	-------	-------	-------	-------	-------	1.39	0.47
14	channel	1.56	0.46	-------	-------	-------	-------	1.23	0.29
15	channel	1.42	0.65	-------	-------	-------	-------	1.80	0.59
16	channel	-------	-------	0.62	0.32	-------	-------	0.97	0.70
17	channel	2.25	0.41	1.76	0.46	1.84	0.39	2.34	0.34
18	channel	0.69	0.31	0.43	0.65	0.69	0.41	0.34	0.54
19	channel	-------	-------	-------	-------	-------	-------	0.79	0.52
20	channel	-------	-------	-------	-------	0.47	0.46	1.38	0.60
21	channel	0.86	0.80	1.36	0.60	-------	-------	0.59	0.71
22	channel	1.07	0.69	0.58	0.39	-------	-------	0.90	0.57
23	channel	1.96	0.51	-------	-------	-------	-------	-------	-------

[1] Graphic mean size.

[2] Graphic standard deviation (sorting).

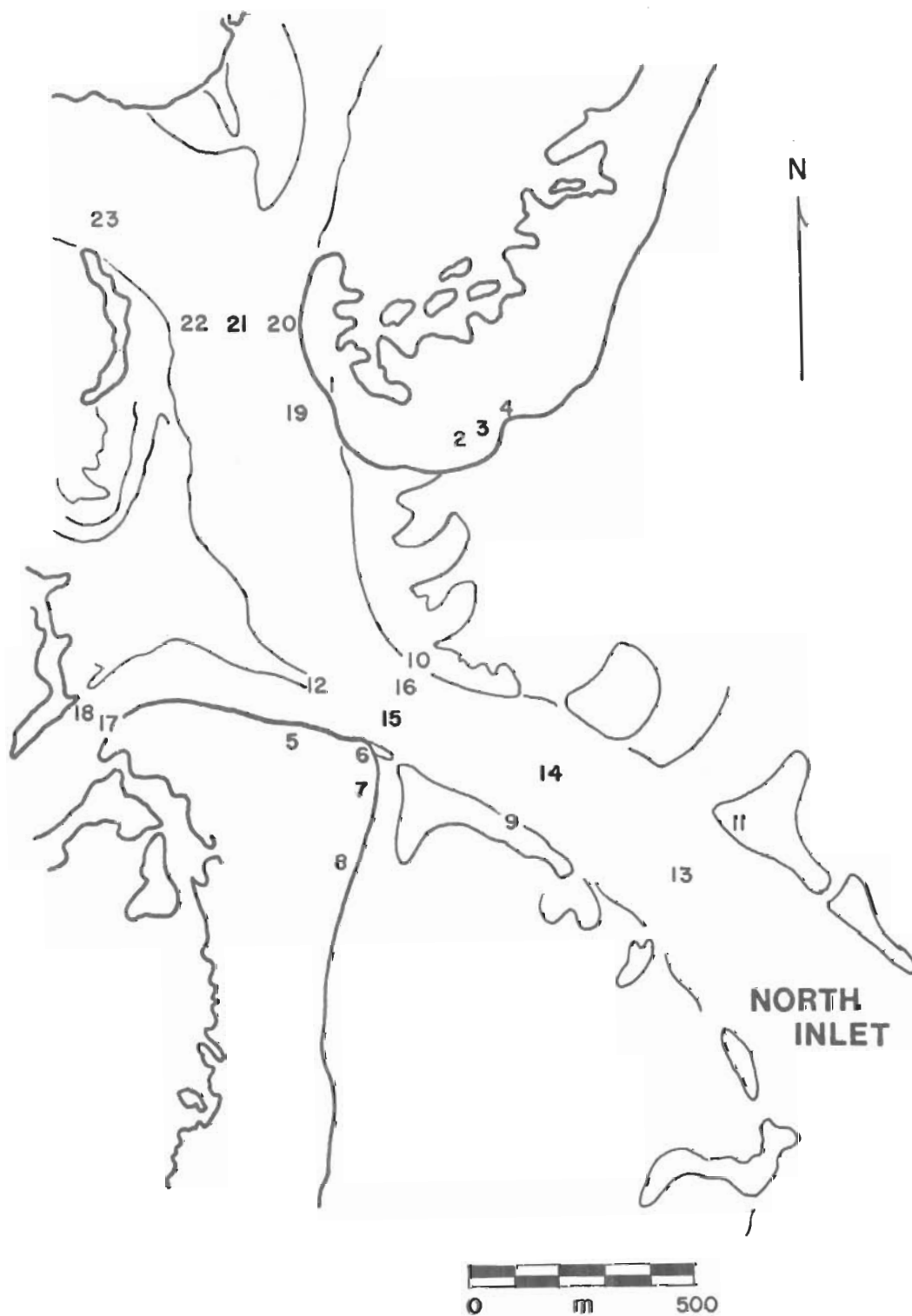NOTE: Position of stations 1 to 8 shown later in Figure 10.

Figure 9. Sediment sample station locations, midtide level beach (1 to 8), intertidal shoal (9 to 12), and subtidal (13 to 23).

33

fragments of beach rock. It is likely that the bottom here is entirely covered by a coarse shell lag similar to that found on the ebb spit of the flood tidal delta. It is difficult to obtain a truly representative sample with the grab sampler in areas of high shell content since the jaws are often jammed open and the enclosed material is partially washed on the way up. Table 4 results are based on sand taken from the sampler after the exposed surface of the sample has been discarded. Other channel localities where shell material is generally found, although in lesser abundance, are stations 18 to 20 and in smaller (2 to 5 centimeters) fragments at stations 21 and 22.

Seasonal variation among the samples at each repetitively sampled station is minimal and, as described previously, this may be attributed to the uniformity of material supplied to the shore zone, as well as little "new" sediment influx to the area. It is unlikely that any significant amount of sand-sized material from the Pee Dee River or Waccamaw River escapes Winyah Bay (Barrell, personal communication, 1975). The Santee River supplied virtually no sandy material to the coastal zone since the building of the Santee-Cooper Dam in 1942 and the diversion of the Santee's flow into Charleston harbor. The diversion reduced the Santee River discharge from 525 to 14 cubic meters per second and the river's lower distributaries are now acting as a sand sink rather than as a sand source (Stephens, et al., 1975). Considering these factors in addition to the obvious sand deficit indicated by the erosional state of the shorelines, it can be concluded that a limited amount of nearshore and eroded beach sand is being continually redistributed within the beach-inlet system, and little seasonal variation may be expected. Maximum variability of about 0.80 phi unit is found in the channels, where sampling techniques may contribute to observed change, while intertidal shoal sands on the ebb tidal delta change only 0.29 phi unit among the seasonal samples.

Winyah Bay and the Santee River supply abundant suspended sediment to the nearshore zone, making the waters at North Inlet extremely turbid throughout the year. This factor precludes effective diving operations in the area. The Santee River currently discharges about 1.3×10^4 tons per year of suspended sediment (Stephens, et al., 1975). The suspended material at North Inlet, both organic and inorganic, results in Secchi disc-extinction depths which usually range from 0.6 to 1.2 meters, depending on tidal stage, wind conditions, and locality. With a flooding springtide at locations near the inlet, extinction depths of 1.8 to 1.9 meters have been recorded, indicating the presence of clearer ocean water. In the interior waterways, disc readings have been as low as 0.38 meter due to high content of mud and organic detritus, much of which is derived from decaying cordgrass, *Spartina alterniflora*. Wind-driven waves increase turbidity by resuspending sediment from the tidal creek banks.

A turbidimeter, the Beckman Envirotrans model, was used to measure total turbidity through the water column. The probe has a built-in light source and measures light attenuation over a 10-centimeter path. Transmittance ranges from 40 to 50 percent for ebb

flow from small, completely marsh-enclosed creeks, to values of 80 to 90 percent for flooding ocean water. The light beam is attenuated due to both absorption and scattering by water molecules, and by naturally occurring suspended matter. Vertical profiles of turbidity taken 14 August 1972, along the thalweg of Town Creek and at one-third ebb flow, vary from 96, 92, and 89 percent at 1 meter to 65, 63, and 57 percent at the 5-meter depth. At the mouth of small marsh creek tributaries (< 10 meters wide), transmittance ranges from 51 to 47 percent through a 1.5-meter water column.

Actual total suspended matter concentrations were measured by filtration of water samples on 0.45-micrometer pore-size glass fiber filters. Samples were collected from the 2-meter depth with a Kemmerer sampler. This depth was selected because it was the shallowest and considered not to be affected by velocity fluctuations near the air-water interface; the velocity at 2 meters seemed representative of the entire flow. Total suspended matter concentrations ranged from 1.02 milligrams per l as a winter low to 51.26 milligrams per l for a summer high. Much of this variation was due to changes in suspended organic matter content, but for any particular tidal cycle, concentrations generally varied from 5 to 25 milligrams per l. Variation with absolute current velocity was not conclusive.

III. LITTORAL PROCESSES

1. Goals and Methods.

A network of beach profiles was established in June 1972 and expanded in June 1974, to examine beach changes on Debidue and North Islands adjacent to North Inlet (Fig. 10).

Beach changes result from the action of wind, waves, and wave-induced longshore currents. These active processes were monitored during quarterly 2-week periods of study at profiles DBI-10, DBI-25, NI-14, and NI-20 to quantify the process variables affecting the inlet, determine their seasonal variation, and establish relationships between energy flux and volumetric changes in tidal deltas and the shallow nearshore zone. The stations were selected so that DBI-10 and NI-14 were well within the zone of wave refraction around the ebb tidal delta. NI-20 was less influenced by wave refraction; DBI-25, some 1.3 kilometers (0.8 mile) north of the ebb tidal delta margin, was least affected by refraction around the intertidal shoals.

Profile localities were marked with pairs of metal fenceposts with additional stakes in the dunes to provide a backup in case of severe storm erosion. Surveys utilized the horizon method of Emery (1961), with a data point every 3 to 6 meters. Localities were selected on the basis of small changes in strike of the shoreline, changes in character of the eroding foredune ridge, or variation in the nearshore morphology. Presentation of profiles and related results are discussed in Section V.

Littoral process observations were made bihourly during daylight hours at each of the four profile station points (Fig. 10), with an additional late evening and early morning observation at DBI-10 and DBI-25, respectively. Station DBI-10 was manned 24 hours a day to safeguard the weather instruments at that location, take the additional late and early process data, and to report on unusual weather conditions.
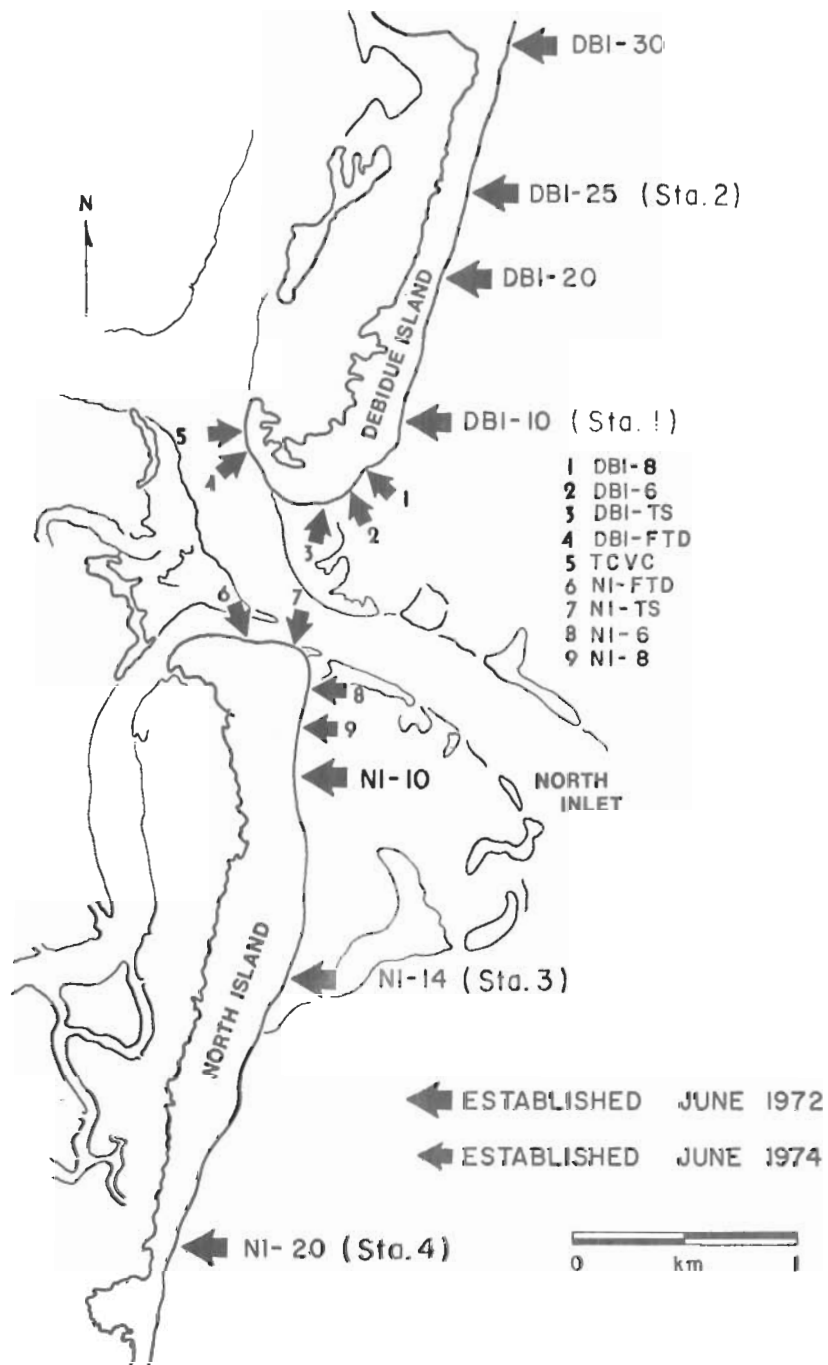
35

Figure 10. Beach profile localities. Stations 1 to 4 are localities of littoral process measurements between July 1974 and March 1975.

Extensive instrumentation was not available for the surf zone data collection. Therefore, wave heights were estimated visually and breaker angle was measured by wading into the surf zone and measuring the strike of the breaker with a hand-held Brunton compass. Angle is probably the most difficult parameter to measure accurately (Galvin and Nelson, 1967), especially at low angles. Breaker height, breaker depth, and the stillwater depth in which the wave breaks, were measured by wading into the surf with a graduated profile rod. Weather instruments to measure wind velocity and direction, and rainfall were set up on a dune crest at station DBI-10. Longshore current velocity was measured by releasing fluorescein dye or tracking slightly buoyant rubber balls in the surf zone.

2. Comparison with Previous Studies.

Observations of selected variables in the nearshore environment on a time series basis have been obtained by Harrison and Krumbein (1964), Dolan, Ferm, and McArthur (1969), Davis and Fox (1971), Fox and Davis (1971, 1972), Abele (1972), and Owens (1975). However, these studies differ from the present study; here, emphasis is placed on the way in which littoral processes affect a tidal inlet. Usually, as in the latter three studies, data were obtained continuously at 2- or 3-hour intervals for periods up to about 30 days. In the studies by Abele (1972) and Owens (1975), data were obtained under both summer and winter conditions and the technique of Fourier analysis was used to describe the cyclic nature of the coastal processes. As both these studies were primarily aimed at beach process analysis, manpower was available for continuous monitoring on a 24-hour basis and greater instrumentation was used. At North Inlet the process data were collected only on a 12-hour basis to allocate manpower and resources for the remaining parts of this study of littoral processes, inlet morphology, and tidal hydraulics.

This study represents an integration of the major process-response activity in the area, with a great deal of depth added by the four-season approach to the fieldwork. Results, such as the observed weather patterns previously described, seem to validate this approach to seasonal studies. In addition, monthly beach profile runs between quarterly studies have filled the interim periods with more response data. It is considered, then, that the variation in the beach parameters represents a reasonable synopsis of shore processes which occurred on a continuous basis. Only phenomena with periods entirely outside the 12 to 15 hours of data taken daily on Debidue Island would be completely missed during the quarterly studies.

3. Variable Analysis.

Water waves are an important factor in beach processes; therefore, a description of the littoral environment must include wave period, breaker height, breaker type, approach angle, and a measure of the longshore current motion. Breaker depth is an additional variable which is perhaps not as significant as the others, but was measured since it may be used in one form of the wave energy flux equations. The punchcard data were processed using the Statistical Package for the Social Sciences (SPSS) programs on the University of

37

South Carolina IBM 370 computer. The subprograms provided summary statistics and frequency tables of specified variables, linear correlation coefficients and significance levels, and scatter plots with selected statistics. The following discussion is concerned with basic parameter description and summaries to characterize wave regime and seasonal variation, including longshore current velocity and the derivation of predictive relationships.

Complete listings of original field data are not included here but may be obtained from the author or from the U.S. Army Coastal Engineering Research Center (CERC) as part of Quarterly Progress Report 2, 3, and 4, Contract DACW72-74-C-0018. Tables 5 to 10 contain selected statistics for the variables observed. Other statistics and frequency tables are also available from CERC. The stations are listed in geographical position from north at the top to south at the bottom with the inlet located between stations 1 and 3. The average values included the data for all stations monitored during the quarterly study of that particular month.

4. Descriptive Statistics and Pearson Correlations.

a. Breaker Type. Wave breaking generally occurs at a water depth of about 1.3 times the wave height. The form which the wave takes when it breaks is referred to as breaker type. Galvin (1972) describes *spilling, plunging, collapsing,* and *surging* breakers. At North Inlet spilling waves, with gradual breaking and foamy turbulent water at the crest, and plunging waves, with a curling of the crest and a concave wave front just before breaking, are the only types which have been observed. Wiegel (1964) stated that, in general, spilling breakers are associated with steep deepwater waves and beaches of low slope, and plunging breakers are related to waves of intermediate steepness and steeper beaches. Galvin (1972) considers the four types he describes as an ordered sequence, changing continuously from spilling to plunging, collapsing and surging with decreasing wave height, increasing wave period, and increasing slope. The percentages of spilling and plunging breakers are summarized in Tables 5 and 6, both by station and overall for each seasonal study. Note that observations were started at station 2 (profile DBI-25) in September 1974. The attachment of a large, intertidal swash bar just north of profile NI-14 (Fig. 10) created the flattest and generally widest intertidal zone of any station. As expected from Galvin's considerations, the mean percentage of spilling waves is greatest at this location consistently through all seasons (Table 5, station 3). At profile DBI-10, station 1, the next highest occurrence of spilling waves was observed as the slope here is relatively gradual due to the presence of the channel-margin linear bar immediately to the south. Conversely, the greatest percentage of plunging wave occurs (Table 6) at stations 2 (profile DBI-25) and 4 (profile NI-20) where the beach has the steepest slope and is generally the narrowest.

b. Breaker Height. Aside from its influence on breaker type, beach slope also affects breaker height by influencing the time and distance spent by the wave in the shallow-water zone (Galvin, 1972). More time and greater distance allow friction to have a greater effect in reducing breaker height, somewhat counteracting the effect of shoaling. Also affecting

Table 5. Percent spilling waves.

Sta.	Mean	Std. dev.	Median	Min.	Max.
July 1974					
2	-------[1]	-------	----------	--	------
1	69.2	33.8	75.0	0	100
3	71.6	33.2	invalid	0	100
4	48.8	33.9	47.0	0	100
Avg.	67.5	34.2	68.3	0	100
September 1974					
2	56.4	28.4	52.8	0	100
1	58.8	31.1	60.0	0	100
3	67.6	27.6	70.0	0	100
4	50.2	29.5	49.5	0	100
Avg.	57.8	29.7	54.6	0	100
January 1975					
2	44.5	32.7	45.0	0	100
1	53.8	31.6	57.3	0	100
3	60.6	28.6	61.8	0	100
4	35.8	31.2	33.8	0	100
Avg.	49.0	32.2	50.8	0	100
March 1975					
2	36.0	27.8	29.4	0	95
1	49.2	31.6	51.0	0	100
3	60.2	31.4	70.3	0	100
4	44.2	28.9	43.8	0	95
Avg.	46.7	31.0	46.6	0	100

[1] No reading.

Table 6. Percent plunging waves.

Sta.	Mean	Std. dev.	Median	Min.	Max.
July 1974					
2	------- [1]	-------	-----------	--	------
1	30.8	33.8	25.0	0	100
3	28.4	33.2	invalid	0	100
4	51.3	33.9	5.30	0	100
Avg.	32.5	34.2	31.7	0	100
September 1974					
2	43.6	28.4	47.2	0	100
1	41.2	31.1	40.0	0	100
3	32.4	27.6	30.0	0	100
4	49.8	29.5	50.5	0	100
Avg.	42.2	29.7	45.4	0	100
January 1975					
2	55.5	32.7	55.0	0	100
1	46.2	31.6	42.8	0	100
3	39.4	28.6	38.2	0	100
4	64.0	31.4	66.3	0	100
Avg.	51.0	32.2	49.0	0	100
March 1975					
2	64.0	27.8	70.6	5	100
1	50.8	31.6	49.0	0	100
3	39.8	31.4	29.8	0	100
4	55.9	28.9	56.3	5	100
Avg.	53.3	31.0	53.4	0	100

[1] No reading.

Table 7. Breaker height in centimeters.

Sta.	Mean	Std. dev.	Median	Min.	Max.
July 1974					
2	------[1]	-------	-------	----	------
1	53.5	16.2	51.7	25	150
3	50.3	20.4	43.8	10	95
4	65.0	18.1	62.5	30	110
Avg.	54.0	17.8	52.0	10	150
September 1974					
2	68.9	21.2	64.0	30	120
1	61.9	21.9	58.9	25	120
3	41.6	24.0	41.7	2	90
4	69.8	35.4	55.5	15	190
Avg.	61.7	27.4	58.6	2	190
January 1975					
2	59.1	20.3	58.3	20	100
1	49.4	18.0	48.0	20	100
3	48.9	16.4	49.8	20	100
4	57.3	24.7	52.7	20	120
Avg.	53.6	20.3	50.0	20	120
March 1975					
2	51.7	28.5	46.3	20	200
1	43.4	27.9	36.8	10	200
3	45.9	17.6	40.8	20	90
4	51.7	24.0	48.0	15	100
Avg.	47.9	25.7	41.1	10	200

[1] No reading.

Table 8. Breaker depth in centimeters.

Sta.	Mean	Std. dev.	Median	Min.	Max.
July 1974					
2	-------[1]	-------	-------	----	------
1	48.5	11.7	48.2	20	80
3	44.9	19.4	42.0	5	90
4	59.6	16.1	59.5	25	90
Avg.	48.9	14.9	48.3	5	90
September 1974					
2	52.1	14.4	50.0	30	85
1	47.7	12.6	47.7	25	85
3	35.4	16.7	35.0	0	70
4	54.7	20.3	53.5	15	95
Avg.	48.1	17.0	45.7	0	95
January 1975					
2	38.8	14.7	39.8	10	70
1	35.5	15.1	35.5	10	99
3	39.6	20.0	38.3	20	120
4	34.9	13.6	32.7	10	65
Avg.	37.2	15.9	37.7	10	120
March 1975					
2	57.2	27.9	50.6	10	150
1	47.5	20.7	49.6	10	100
3	54.4	26.2	51.3	17	100
4	49.5	23.5	46.3	15	100
Avg.	52.2	24.8	50.1	10	150

[1] No reading.

Table 9. Percentage frequency of wave period
for Charleston offshore area.[1]

Period (s)	July	Sept.	Jan.	Mar.
<6	65.0	46.3	45.5	47.4
6 to 7	26.7	30.7	29.9	31.9
8 to 9	5.8	14.4	13.3	12.9
10 to 11	1.8	5.7	4.9	5.3
12 to 13	0.4	1.9	5.7	1.6
>13	0.2	0.9	0.7	0.9

[1] U.S. Naval Weather Service Command, 1975.

Table 10. Degrees of observed breaker angle.[1]

Sta.	Dir.[2]	Mean	Std. dev.	Min.	Max.
July 1974					
2	N[3]	-------	-------	--	----
	S[3]	-------	-------	--	----
1	N	8.2	3.6	0	20
	S	5.8	4.8	1	15
3	N	9.3	4.5	4	16
	S	12.6	4.7	4	25
4	N[4]	-------	-------	--	----
	S	9.2	4.8	5	20
September 1974					
2	N	10.0	5.8	2	20
	S	9.3	1.2	8	11
1	N	12.0	5.0	2	26
	S[4]	-------	-------	--	----
3	N	4.4	3.2	2	12
	S	8.1	4.9	2	15
4	N	5.9	2.3	1	15
	S	7.3	3.8	3	15
January 1975					
2	N	9.4	6.3	2	25
	S	11.5	5.6	5	25
1	N	10.4	6.9	2	30
	S	5.0	0.0	5	5
3	N	9.3	3.3	5	15
	S	19.9	17.8	2	55
4	N	8.7	3.4	3	15
	S	13.8	10.2	2	40
March 1975					
2	N	14.4	9.6	5	32
	S	10.9	6.6	2	25
1	N	17.2	12.5	2	45
	S	14.0	12.1	3	25
3	N	16.6	9.8	5	40
	S	19.9	10.2	4	40
4	N	10.8	5.6	1	20
	S	15.1	9.6	4	35

[1] The angle measured is the acute angle between shoreline and breaker crest.

[2] N = Wave approach direction between east and north.
S = Wave approach direction between east and south.

[3] No readings.

[4] No waves from this direction.

breaker height is wave refraction, which is important at profile DBI-10 near the channel-margin linear bar and at profile NI-14 near the swash bar at the ebb tidal delta's southern margin (Fig. 10). The lowest mean breaker heights are observed at these locations (Table 7, stations 1 and 3); the highest mean breaker heights occur away from the inlet shoals at stations 2 and 4. As the wave orthogonals spread and energy per unit length of wave crest decreases, breaker height will tend to decrease in high refraction zones. This effect, working in the same direction as bottom friction, is indicated by the field data.

Munk (1949) derived relationships from solitary wave theory relating breaker height, H_b to breaker depth, d_b, as:

$$\frac{d_b}{H_b} = 1.28 \,. \tag{1}$$

This relationship, although also dependent on beach slope and wave steepness, should result in reasonably linear correlation between these two variables and, where such correlation breaks down, may give an indication of "noise level" of the data due to operator error and the data collection method. Pearson correlation coefficients between d_b and H_b over all stations are 0.4068, 0.5065, 0.8155, and 0.6891 for January, March, July, and September, respectively. Since breaker depth and height observations are dependent on the observer wading in the surf zone, the least reliable data could be expected in the winter when d_b often exceeded hip-boot depth and the least favorable weather conditions were encountered.

c. *Breaker Depth*. Summaries of breaker depth are presented in Table 8. The overall means and medians are similar for March, July, and September but are unusually low for January as a result of observation conditions. In part, the low breaker depth values may result from measuring a water level closer to the trough depth than the stillwater depth in the region of breaking.

d. *Wave Period*. Procedural difficulties prevented accurate visual estimates of wave periods at the sites. However, meteorological summaries for the Charleston offshore region (Table 9) indicate a seasonal pattern of low mean values in July and September with higher periods in January and March. This same pattern was seen in the seasonal North Inlet data.

e. *Breaker Angle*. The angle which waves make when approaching the shoreline determines the magnitude of the longshore component of motion of the breaking water mass. This motion is responsible for the longshore current flow as well as beach drift, the movement of sediment on the beach face resulting from swash oblique to the shoreline trend, and backwash perpendicular to it.

Galvin (1967) observed that single readings of wave angle are rarely accurate to within $2°$; it is probable that the North Inlet data (Table 10) are accurate to within $5°$ in most

45

cases. There is a definite operator preference for the values 5°, 7°, 8°, 10°, 15°, and further multiples of 5° to be recorded. The data have a positive skewness due to inclusion of higher values having a notably lower frequency; therefore, the median would be preferred by some (Campbell, 1967) as a measure of central tendency, rather than the mean. Overall median values range from 7.5° to 8.8°, with the low March value of 5.2° due to the inclusion of 86 values of 0° obtained when waves approached parallel to the beach.

5. Longshore Current Flow.

Waves affect sediment movement by initiating sediment motion and generating a current which flows parallel to the shoreline. The highest longshore current velocity is reached between the point of wave breaking and the stillwater level on the shore (Galvin, 1967). Much of the sediment moved in longshore current systems eventually becomes part of intertidal inlet shoals, is transported into tidal channels or estuary mouths behind the shoreline, or is trapped by manmade structures along the shore. All three processes are taking place in the vicinity of North Inlet; however, the first is of greatest relative importance at the inlet and will be considered with respect to morphological change with time.

The longshore current velocity statistics (Table 11) are based on each individual velocity measurement rather than the average of the three measurements made in conjunction with the observation set. This approach results in the inclusion of all data variability in the approximately 2,400 velocity readings. Inman and Quinn (1951) found that the variability in longshore velocity was such that the standard deviation often equaled or exceeded the measurement mean. Standard deviations for the North Inlet data never equal the mean but do approach it in all cases. The most active conditions occurred during the northeast storm in September 1974, when the Debidue Island stations experienced mean velocities to the south of 46.4 centimeters per second (station 2) and 54.6 centimeters per second (station 1). Maximums of 150 to 160 centimeters per second were encountered during the storm with the only observed similar value, 144 centimeters per second, resulting from an unusually strong July 1974 thunderstorm that developed an onshore wind component.

Resultant longshore current velocity vectors (Fig. 11) show currents dominantly to the south along Debidue Island, but mostly northerly currents south of the inlet. This northerly current reversal is opposed to the dominant current regime which from geomorphic evidence, energy flux calculations and the means of longshore current velocities (Table 12) were southerly. Refraction of waves around the ebb tidal delta is responsible for the reversal and this effect is also present at station 4 (profile NI-20), 0.75 kilometer south of the junction of the shoreline and the large swash bar of the ebb tidal delta. During the September 1974 studies, all resultant velocities were directed to the south as an effect of the northeast storm, and the very low southerly value at station 3 may be attributed to the mitigating effects of refracted waves. Correlations of longshore current velocity with tidal stage were not statistically significant, indicating that tidal flow was not a major factor in the current reversal. High northerly currents at stations 3 and 4 during July 1974, are

46

Table 11. Longshore current velocity in centimeters per second.

Sta.	Dir.[1]	No.[2]	Mean	Std. dev.	Median	Min.	Max.
July 1974							
2	N[3]	0	-------	-------	-------	-----	---------
	S[3]	0	-------	-------	-------	-----	---------
1	N	74	12.5	8.6	10.2	1.9	37.0
	S	298	22.2	15.5	20.0	0.6	144.0
3	N	118	39.8	20.4	38.4	2.4	87.4
	S	18	18.9	13.7	15.2	2.6	44.4
4	N	62	39.8	21.1	37.9	3.2	82.4
	S[4]	------	-------	-------	-------	-----	---------
September 1974							
2	N	21	13.8	10.0	10.0	2.0	36.4
	S	152	46.4	33.0	38.2	1.8	150.0
1	N	7	6.9	3.8	7.5	1.0	11.8
	S	185	54.6	34.3	50.0	2.0	160.0
3	N	38	16.1	13.9	13.6	1.2	47.4
	S	72	23.4	16.8	20.5	2.0	77.0
4	N	30	12.7	7.8	11.6	2.0	35.2
	S	91	31.4	27.4	25.6	2.0	138.0
January 1975							
2	N	61	22.7	14.0	20.1	2.0	54.8
	S	107	33.8	21.4	30.4	1.7	91.1
1	N	13	7.5	6.0	5.9	1.8	23.0
	S	162	33.5	20.2	30.2	0.0	114.5
3	N	65	24.4	19.5	18.5	1.2	73.6
	S	66	19.2	13.5	14.9	1.8	51.8
4	N	64	38.1	20.4	22.7	1.0	74.5
	S	58	24.1	19.8	18.5	1.8	74.8
March 1975							
2	N	72	24.4	18.3	18.7	1.4	77.4
	S	64	27.1	17.4	24.2	1.8	79.4
1	N	23	16.5	10.4	14.7	1.8	35.6
	S	151	28.8	20.0	25.7	1.2	110.0
3	N	86	29.4	18.6	26.7	1.4	95.4
	S	28	14.2	12.4	9.9	1.4	52.2
4	N	67	28.9	26.7	36.4	2.8	117.0
	S	43	22.1	13.1	20.2	2.8	54.0

[1] N = Wave approach direction between east and north.

S = Wave approach direction between east and south.

[2] Number of observations for that direction at that particular station.

[3] No reading.

[4] No southerly drift observations.
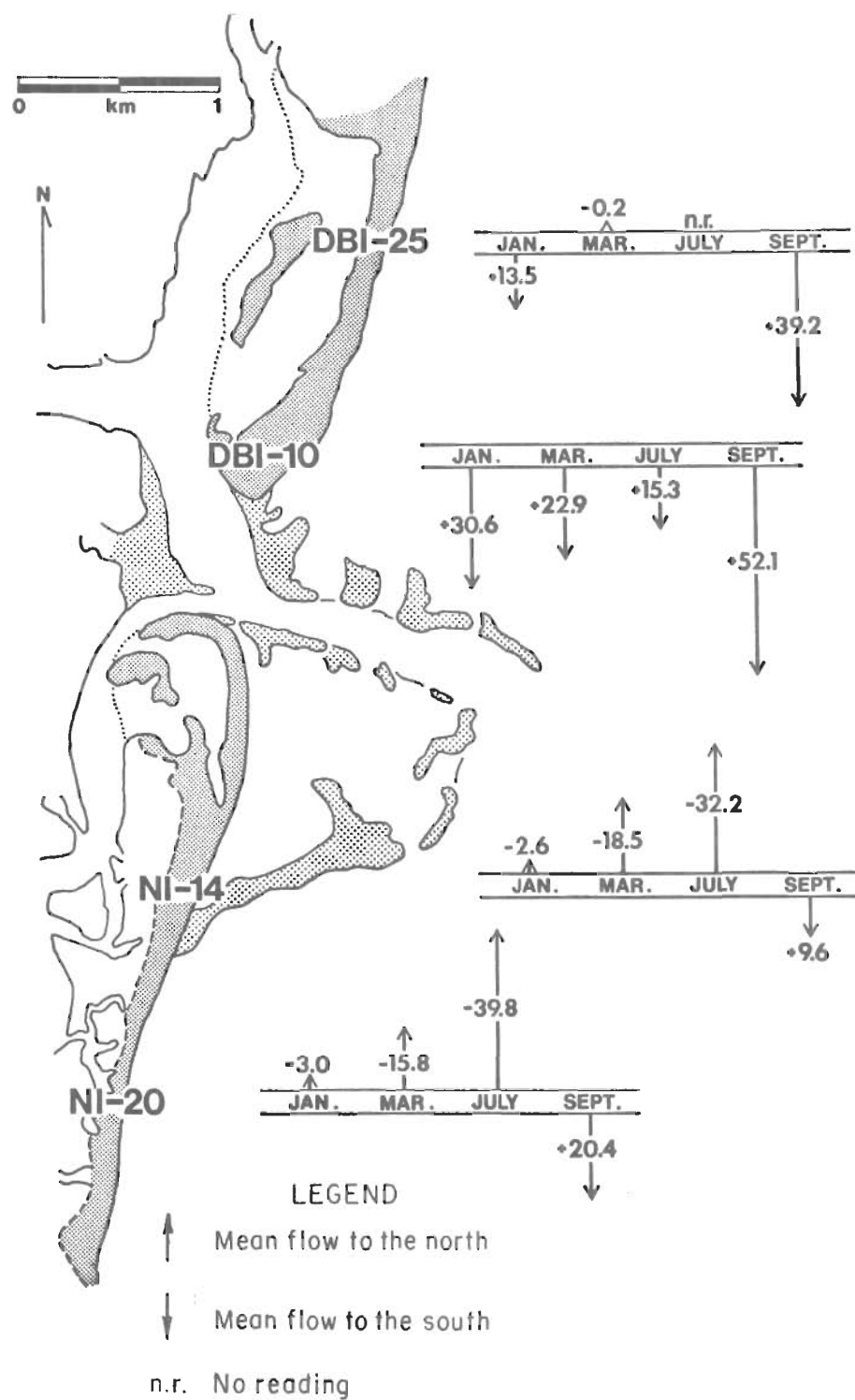
Figure 11. Resultant longshore current vectors (centimeters per second).

Table 12. Longshore energy flux factor by season and direction at each station.

Sta.[1]	Dir.[2]	July 1974			Sept. 1974			Jan. 1975			Mar. 1975		
		No.[3]	Mean	Median	No.	Mean	Median	No.	Mean	Median	No.	Mean	Median
Debidue Island													
2	N	----[4]	----	----	4	73	77	22	101	55	16	55	30
	S	------	----	----	46	88	64	27	65	42	18	127	51
1	N	9	36	12	0	----	----	2	68	----	2	27	----
	S	124	49	30	61	94	54	51	54	25	35	87	28
North Island													
3	N	39	57	32	10	39	21	17	102	66	15	80	50
	S	8	32	25	9	14	12	20	34	31	11	68	38
4	N	22	84	59	7	43	39	16	94	63	13	126	91
	S	0	----	----	19	61	24	17	64	49	14	83	39

[1] Stations 1 and 3 are closest to the inlet; stations 2 and 4, farthest on each side.
[2] Direction along shoreline.
[3] Number of observations.
[4] No reading.

attributable to the high frequency of southerly winds which coincides with the lowest southerly drift at station 1 where shielding is provided by the channel-margin linear bar. A resultant southerly current at station 1 was expected for all seasons in view of wave refraction into the corner between the Debidue shoreline and the ebb tidal delta.

6. General Characteristics of Beach Response.

Beach responses to littoral processes are most easily measured by repetitive beach profiles (Apps. A and B; Fig. 10). Most sandy beaches undergo a high-frequency cycle of erosion and deposition in response to storms (Hayes, 1972) and lower frequency changes due to barrier island growth and inlet migration. The severity of storm erosion depends on wave conditions, storm surge, tidal stage, and storm duration. Beaches adjacent to North Inlet show the typical pattern of a smooth, concave upward profile immediately after a storm, followed by landward-migrating ridge and runnel systems which may, depending on wave conditions, weld onto the backshore to form a small berm (Hayes and Boothroyd, 1969).

Storm-eroded beach sands are deposited as a sheet or bar in the surf zone which then forms the sediment source for ridge and runnel systems during poststorm recovery. Sands swept by longshore currents into intertidal shoals or tidal channel bottoms are not readily available for beach recovery, and in a sand-starved situation, as at North Inlet, this is a critical loss. Debidue Island and North Island beaches are characterized by small and ephemeral berms and, except just south of the inlet, a seaward-facing erosional scarp on the foredune ridge. The overall morphology of these beaches is closely related to migration of the inlet itself over the last 100 years which will be considered later in this report.

49

IV. WAVE ENERGY FLUX AS A PROCESS VARIABLE

1. Longshore Energy Flux.

Two methods of obtaining Q, the longshore sediment transport rate, which are often used (U.S. Army, Corps of Engineers, Coastal Engineering Research Center, 1975) are: (a) Evaluation of historical changes in the bathymetry of the littoral zone near a barrier to longshore transport, and (b) computation of wave energy flux from measured conditions, which is then related to the longshore transport rate with an empirical relationship. In this report, longshore energy flux was computed for the four beach observation stations to: (a) Examine its magnitude and direction in relation to the present ebb tidal delta, and (b) relate annual values of the longshore energy flux factor to historical changes of spit and shoal growth.

Total wave energy per unit surface area is termed specific energy, $\bar{E}$. Wave energy flux is the rate at which specific energy is transmitted in the direction of wave propagation along the orthogonal. Following the development in U.S. Army, Corps of Engineers, Coastal Engineering Research Center (1975), longshore energy flux per unit length of beach for waves approaching obliquely and evaluated at the surf zone is given by:

$$P_{ls} = \frac{\rho g}{16} H_b^2 Cg \sin 2a_b \quad . \tag{2}$$

Making several assumptions (Table 4-9 in U.S. Army, Corps of Engineers, Coastal Engineering Research Center, 1975) and using breaker height observed at the surf zone, P_{ls} may be calculated according to:

$$P_{ls} = 32.1 \, H_b^{5/2} \sin 2a_b \quad . \tag{3}$$

The result is P_{ls} as a longshore energy flux *factor* which is proportional to energy flux but not equal to it, and is the P_{ls} referred to subsequently in foot-pounds per second per foot of beach front.

Seasonal and annual summaries of the energy flux factor at each station for both directions are given in Tables 12 and 13. Although the median value is included here because, as previously described, it gives a better indication of the nature of the data in the case of a skewed distribution, the mean value is geologically more significant. Positive skewness is introduced into the longshore energy flux factor distribution by the occurrence of an infrequent event, the northeast storm, which generates high wave energy. Offshore data (Fig. 12) substantiate that the highest sea and swell which could affect the shoreline at North Inlet come from the northeast. Therefore, mean P_{ls} reflects these high storm values from periods during which major beach changes take place and intuitively the rate of sediment transport is greatest.

50

Table 13. Annual longshore energy flux factors.

Sta.	Dir.[1]	No.[2]	Mean	Std. dev.	Median	Min.	Max.
Debidue Island							
DBI-25	N	42	80.6	80.7	54.8	1.9	312.7
(2)	S	91	88.8	112.5	51.8	1.9	634.1
DBI-10	N	13	39.3	48.5	18.1	4.9	179.0
(1)	S	271	65.4	92.7	34.2	1.9	589.4
North Island							
NI-14	N	81	68.2	91.8	33.3	0.2	615.9
(3)	S	48	37.6	46.1	25.0	0.3	252.5
NI-20	N	58	91.3	96.4	55.8	2.2	434.4
(4)	S	50	68.1	82.2	36.3	0.9	402.0

[1] N = Wave approach direction between east and north.
S = Wave approach direction between east and south.

[2] Number of observations for that direction at that particular station.

During the September 1974 study, a northeast storm and the associated winds (Fig. 6) produced high mean southerly-directed P_{ls} on Debidue Island, but a northerly component, due to wave refraction around the ebb tidal delta, was present at the North Island stations. The same pattern prevailed in January and March 1975 (Table 12). Southerly and southeasterly winds in July 1974 generated flux components toward the north at profile NI-20 (station 4) and profile NI-14 (station 3); again, refraction resulted in virtually all energy being directed toward the south and the inlet shoals at profile DBI-10 (station 1). Lack of summer data at profile DBI-25 makes it only a guess, but presumably energy flux would be primarily directed to the north here under summer southerly wave approach conditions. Note that on an annual basis (Table 13) there is a significant component of energy flux toward North Inlet at all observation locations with an associated rate of sediment volume transport toward the inlet from both north and south. This is similar to the reversal of longshore transport direction described by Hayes, Goldsmith, and Hobbs (1970), but in the case of North Inlet extensive swash features on an ebb tidal delta platform have developed rather than a pronounced shoreline offset (Fig. 13).

Resultant vectors of the longshore energy flux factor (Fig. 14) show net flux toward the inlet when extrapolated to an annual basis, assuming that the 2 weeks of data are representative of each season. At DBI-10 (station 1), wave refraction virtually eliminates the northerly-directed component, while the profile DBI-25 net value, most representative of open coast conditions, is also inlet-directed but at a 42-percent lower rate. Note that the

SWELL DIAGRAM

SEA DIAGRAM

LEGEND

14.4 / 0.4 Pct No Swell
Pct Confused
Low (1 to 6 ft)
Moderate (6 to 12 ft)
High (>12 ft)

LEGEND

3.3 / 0.1 Pct Calm
Pct Confused
Slight (<3 ft)
Moderate (3 to 5 ft)
Rough (5 to 8 ft)
Very Rough (8 to 12 ft)
High (>12 ft)
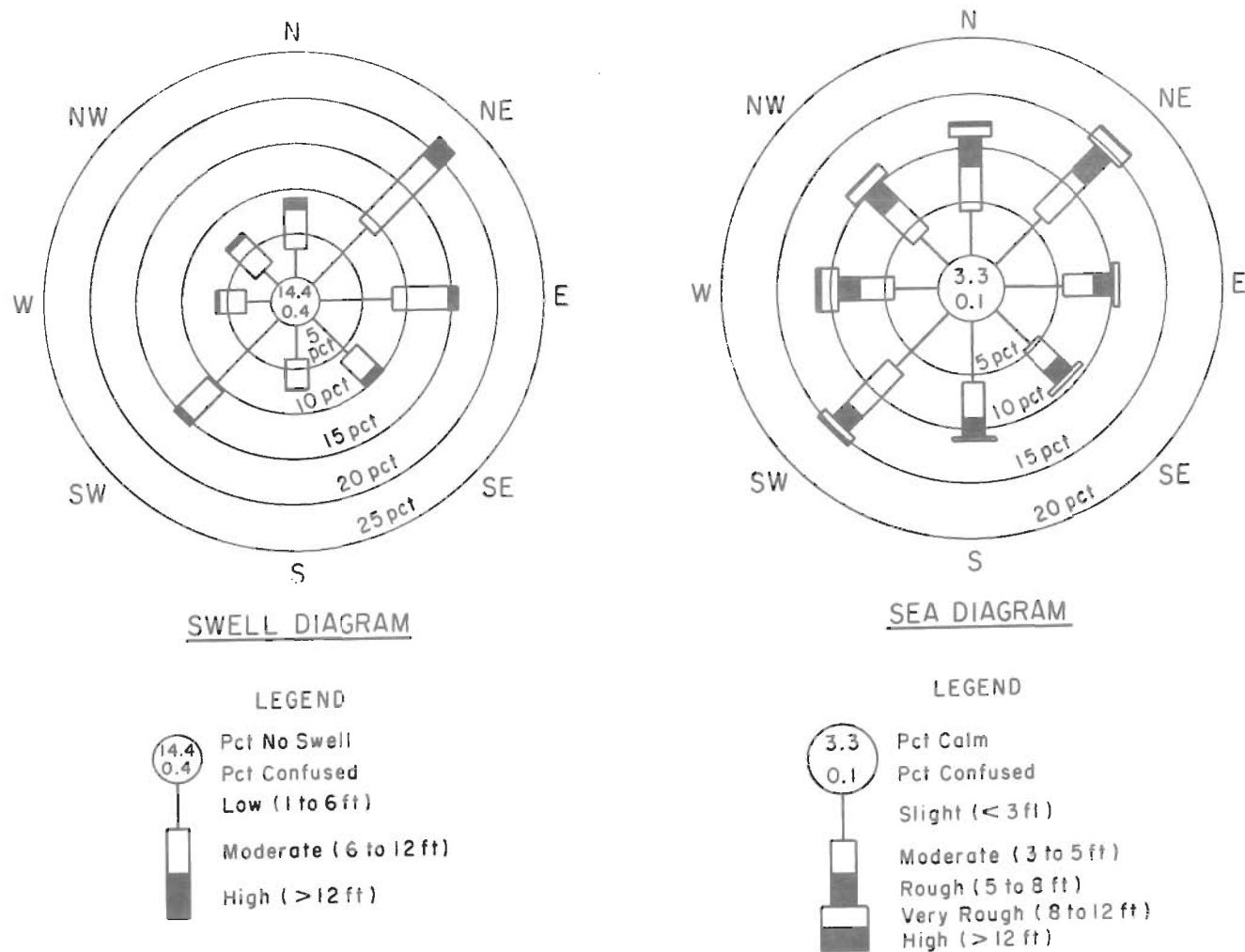
Figure 12. Frequency of occurrence of sea and swell and approach direction (for SSMO observation square off South Carolina) (from U.S. Army Corps of Engineers, 1970).
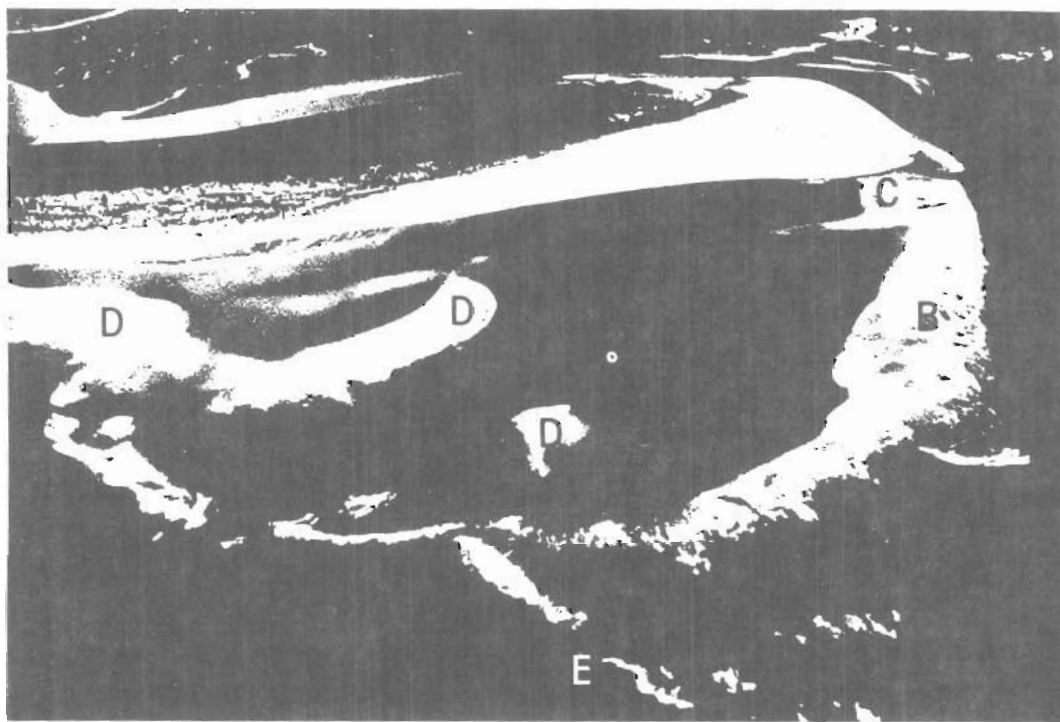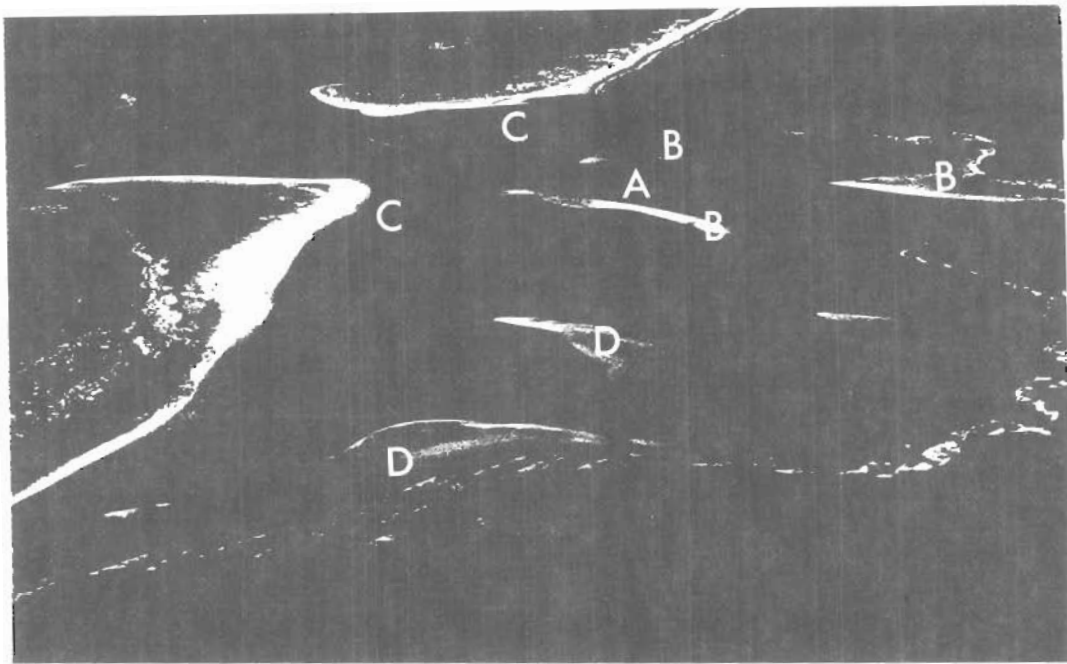
Figure 13. The North Inlet ebb tidal delta. Letters refer to: A, main ebb channel;
B, channel-margin linear bars; C, marginal flood channels; D, swash bar;
and E, terminal lobe.
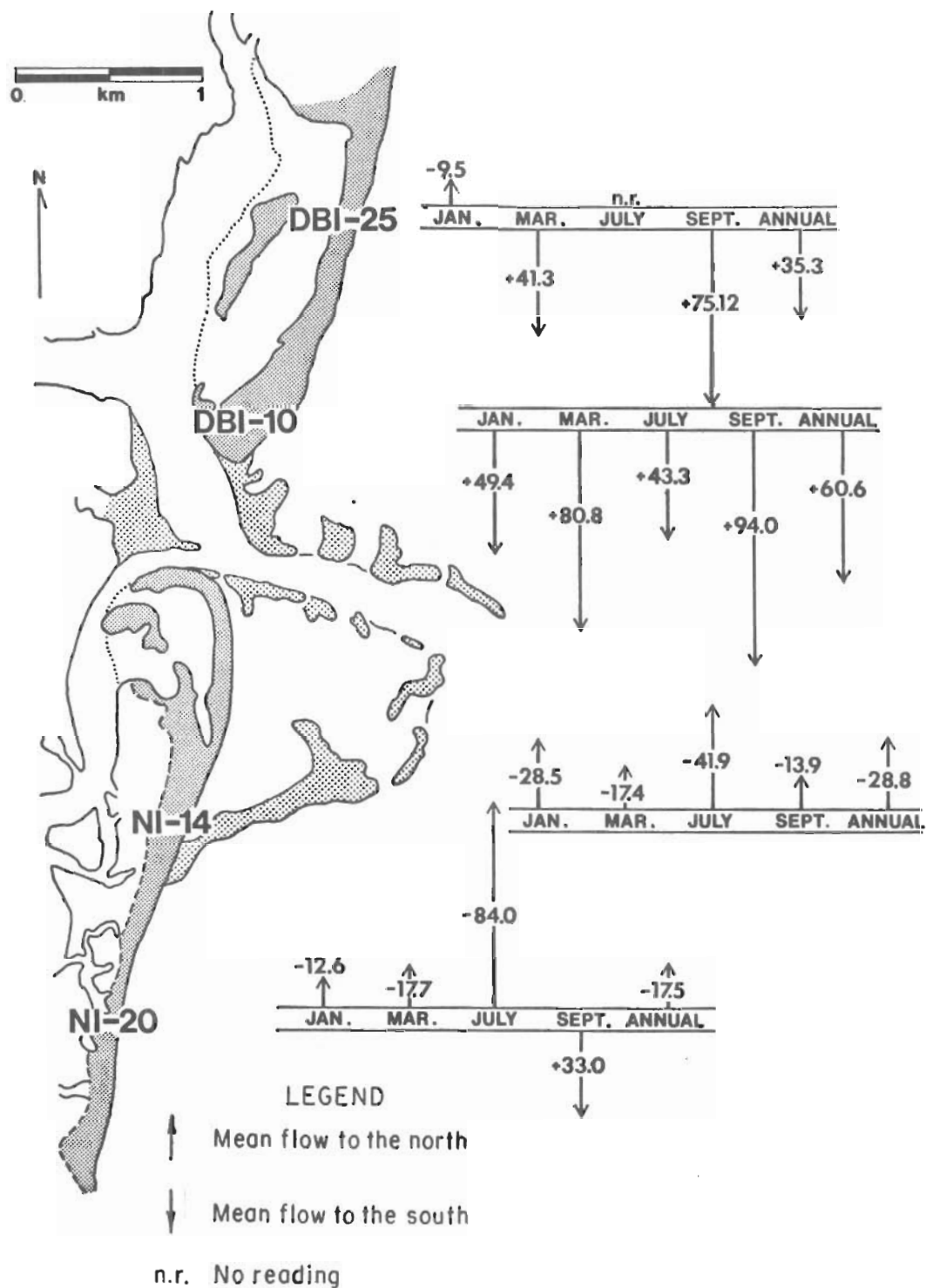
Figure 14. Resultant longshore energy flux vectors (foot-pounds per second per foot of beach).

mean annual value of the southerly-directed component (Table 13) is higher at profile DBI-25 than at profile DBI-10, which is related to higher mean breaker heights (Table 7) at profile DBI-25. Within this context, it was of considerable interest how the energy flux factor relates to the known historical changes as North Inlet migrated and the Debidue Island spit grew in the last 100 years.

2. Inlet Migration.

Since 1878, North Inlet has migrated southward to its present position (Fig. 15), as mapped in 1964. During this timespan, Debidue spit had extended to the south and the existing large ebb tidal delta developed, as described in Section V. Because the bathymetry of the 1878 survey is inadequate for detailed study, a comparison of the volumetric changes between the 1925 and 1964 surveys was made using the original U.S. Coast and Geodetic Survey (USC&GS) boat sheets. Using the method of Dean and Walton (1975), hypothetical no-inlet contours were superimposed over the original bathymetry and a 0.5-kilometer grid added to cover the nearshore area (Fig. 16). The difference between actual and no-inlet contours was determined at each grid point intersection and the four-corner values then averaged to give a mean increase in sediment thickness over the grid square. Summing these values over the entire grid system results in computed ebb tidal delta volumes of 19,674,000 cubic meters in 1925 and 35,674,000 cubic meters in 1964 (Fig. 17). These figures indicate a net addition of 16,900,000 cubic meters when 900,000 cubic meters is added for the growth of Debidue spit during the 39-year timespan. The annual rate of increase is 433,000 cubic meters or 566,000 cubic yards per year.

3. Energy Flux and Sediment Transport Rates.

Utilizing this value of 5.66×10^5 cubic yards per year with the relationship $Q = 7.5 \times 10^3 \, P_{ls}$ (U.S. Army, Corps of Engineers, Coastal Engineering Research Center, 1975) gives an indicated energy flux factor of 74 foot-pounds per second per foot which compares well with the mean annual inlet-directed components (Table 13) of 88.8 and 68.2 foot-pounds per second per foot (average = 78.5) at DBI-25 and NI-14, respectively. Resultant annual energy flux vectors (Fig. 14) of 35.3 (DBI-25) and 28.8 (NI-14) give a total inlet-directed sediment transport rate of 4.6×10^5 cubic yards per year, a value which is 81.5 percent of the historical change volume of 5.66×10^5 cubic yards per year. Since energy flux can be related to longshore transport rate of sediment, changes in spit and shoal growth over several decades may give a reasonable indication of the energy flux factor derived from littoral process measurements. Sediment transport predominantly in one direction, as indicated by geomorphic evidence, would probably be a necessary condition for this analysis.

Note that the DBI-25 (station 2) data do not include any summer values and that the annual mean to the south would probably come even closer to the derived energy flux factor by lowering the value of 88.8 if such data had been included. However, two factors remain unevaluated: (a) The magnitude of onshore-offshore component of sediment transport which may contribute to shoal growth, and (b) the amount of sediment bypassed

79°10′

33°20′

1878

1964

0   km   1

1878 Shoreline   1964 Shoreline

1878 Channel   1964 Channel

1964 Intertidal
shoals
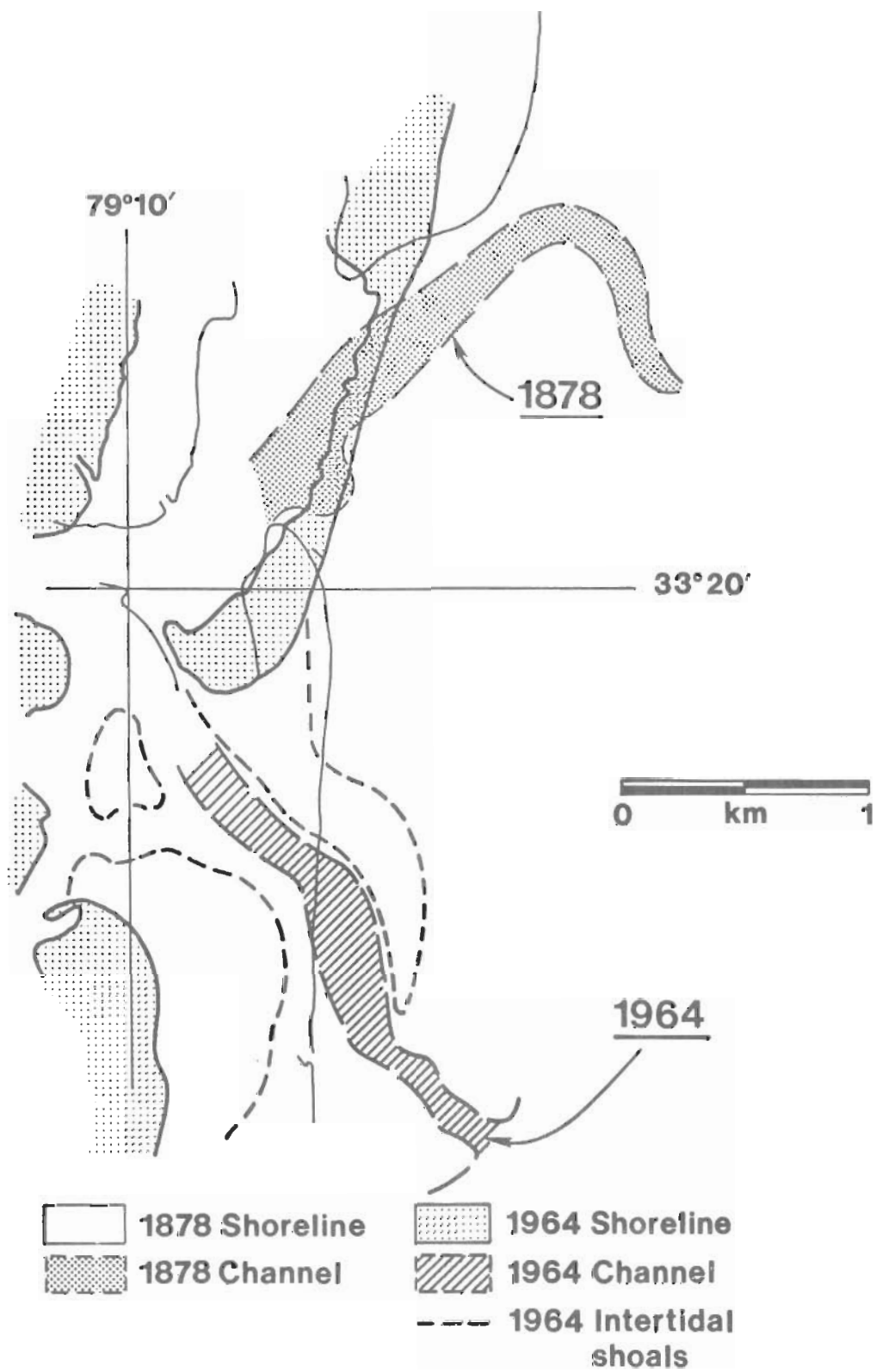
Figure 15. Summary of shoreline changes, 1878 to 1964
(based on USC&GS surveys H-1419 and H-8838).
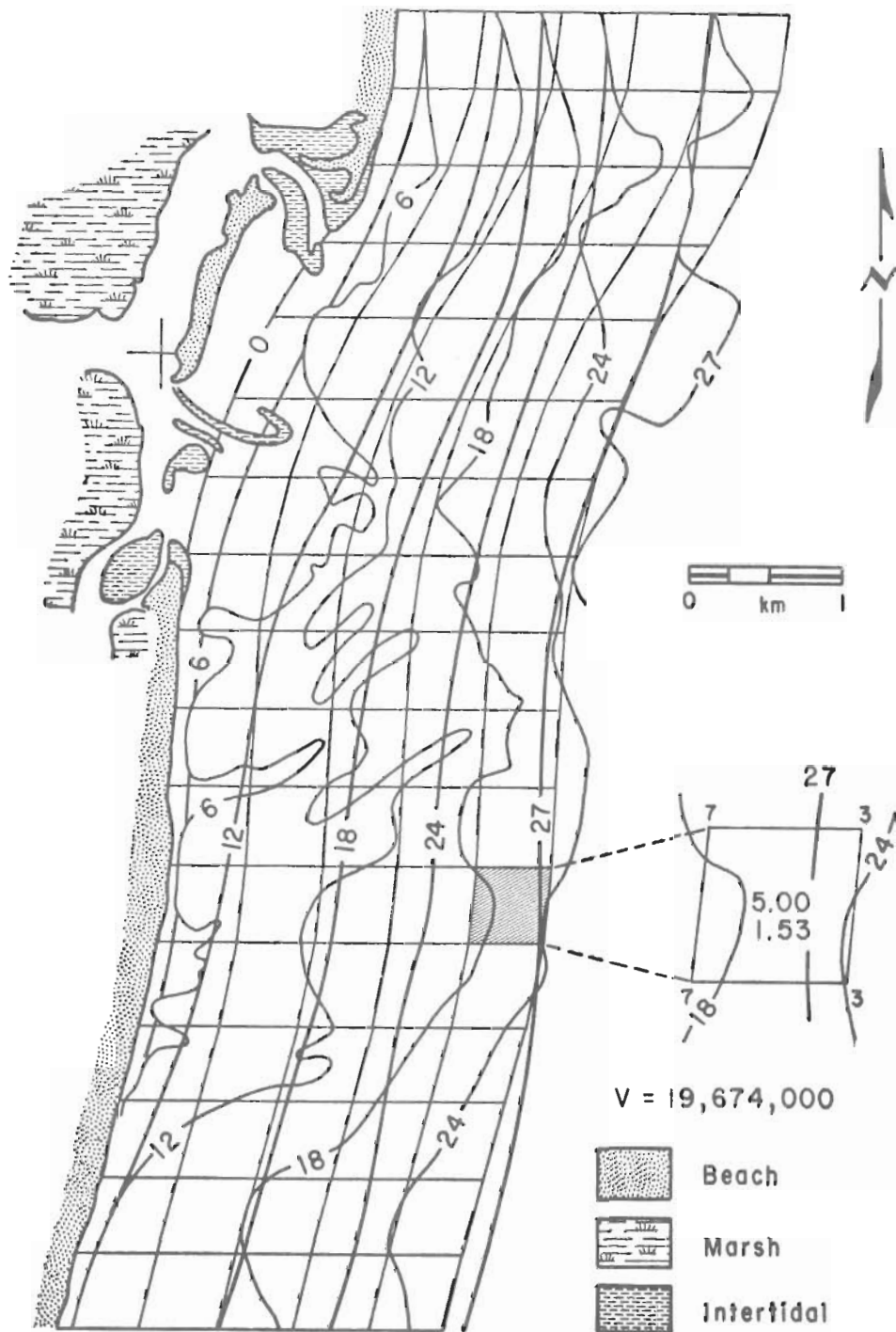
Figure 16. Ebb tidal delta volume in 1925 (based on USC&GS 1925 survey). An example of this method is shown on the right. The differences (feet) at the grid point intersections are 7, 3, 7 and 3; their mean is 5 feet (1.53 meters), which would then be the value for the grid square.

V = 35,673,700 m^3

Rate of Increase over 39 years
= 410,200 m^3/yr
= 550,000 yd^3/yr

Beach

Marsh

Intertidal
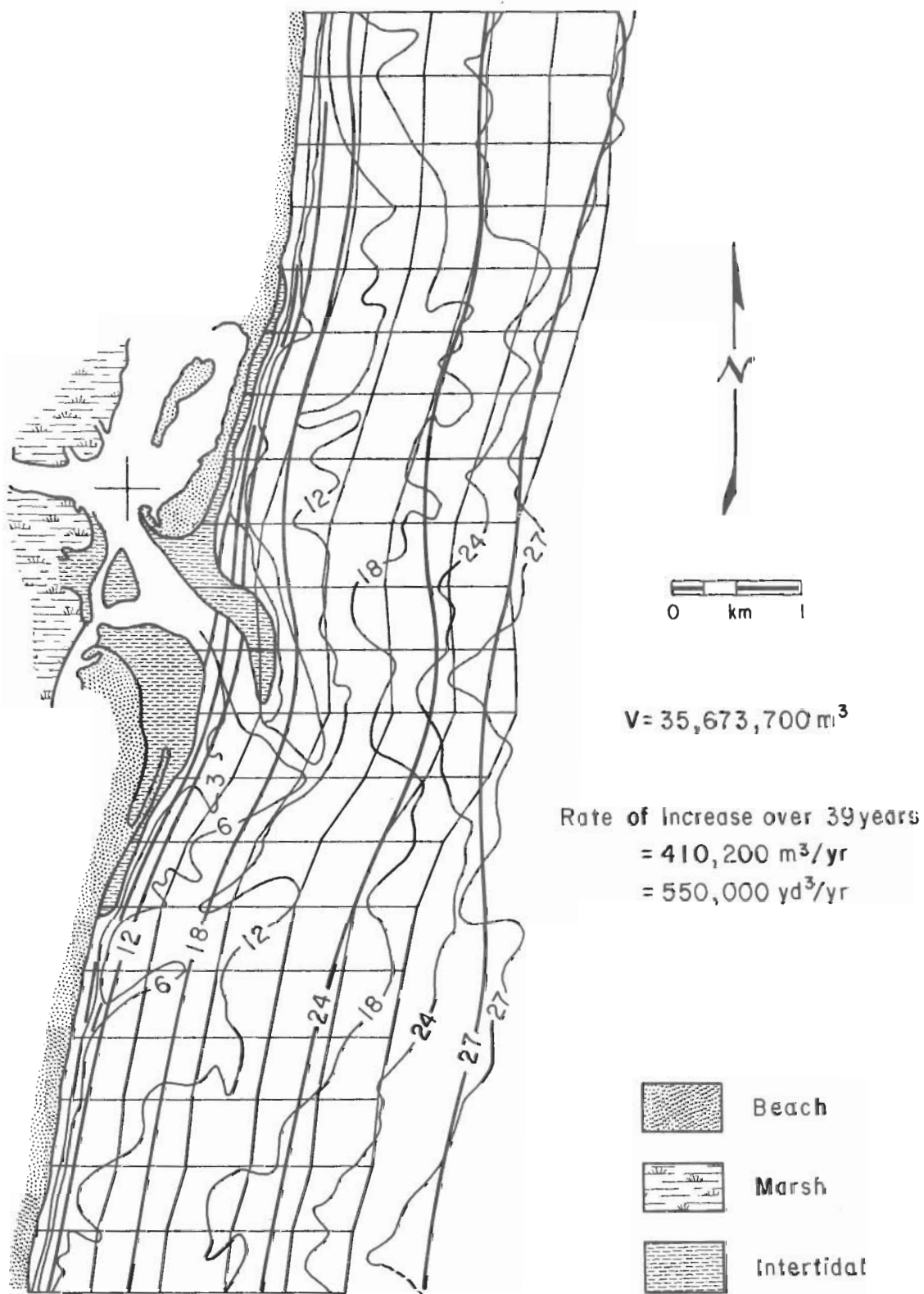
Figure 17. Ebb tidal delta volume in 1964 (based on USC&GS 1964 survey).

around the margin of the ebb tidal delta. Concerning the first, U.S. Army, Corps of Engineers, Coastal Engineering Research Center (1975) suggests that sand from the shelf is not a significant source in the sediment budget of the littoral zone, but further work on this point is clearly needed. With regard to bypassing, it would seem that this factor would tend to decrease as the inlet migration rate slowed and the ebb tidal delta grew in size and stabilized in approximately its present position. Air photos indicate this took place in the late 1930's which was probably the start of the drift reversal and the movement of North Island sands toward the inlet. The close agreement between the observed wave energy flux and the value derived from shoal growth indicates that the inlet shoals are highly efficient trapping mechanisms for littoral drift. Nevertheless, bypassing and onshore-offshore transport may be occurring to some extent.

V. MORPHOLOGIC HISTORY OF THE INLET, ADJACENT BEACHES, AND TIDAL DELTAS

1. Introduction and General Scope of Information.

Morphological changes between 1878 and 1964 are summarized in Figure 15. The triggering mechanism for this change, and the growth of Debidue Island spit a distance of 1.5 kilometers to the south between 1925 and 1939, are difficult to detect. Perhaps an overwash break in the North Island barrier opposite Town Creek created a more direct channel leading to abandonment of the channel to the north. Spit growth under the dominant northeast wind and wave approach then continued, ending about 1940. At that time the inlet stabilized in approximately its present position, and the tidal deltas began their growth. Lack of sediment supply, perhaps due to various coastal stabilization structures between North Inlet and the South Carolina-North Carolina border, and rising sea level (Fig. 8) are primary causes of the present transgressive nature of the shoreline.

The scope of information available to document morphologic change includes vertical and oblique aerial photos, original hydrographic boat sheets, early editions of coastal charts, and maps prepared during field studies. Vertical aerial photo coverage was obtained seven different times by various government agencies between 1939 and 1973. In addition, special purpose color infrared coverage was obtained by the U.S. Geological Survey (USGS) on 7 April 1974 and by National Oceanic and Atmospheric Administration (NOAA) on 27 March 1975. Oblique aerial photos were obtained quarterly corresponding with the 2-week field study periods. Original hydrographic survey sheets are available dating from 1878, 1925, and 1964; however, the earliest survey (USC&GS chart H-1419) showed little of the exact configuration of the inlet mouth (Fig. 18). Although eight editions of USC&GS chart 787 (now NOAA, renumbered 11532) exist, the North Inlet configuration and bathymetry have not been revised each time (Fig. 19). This chart is primarily used for the Winyah Bay entrance, which handles commercial traffic and provides access to the Intracoastal Waterway. Combining published information with field map and profile data, morphologic changes in the inlet, adjacent beaches, and shoals can be detailed.
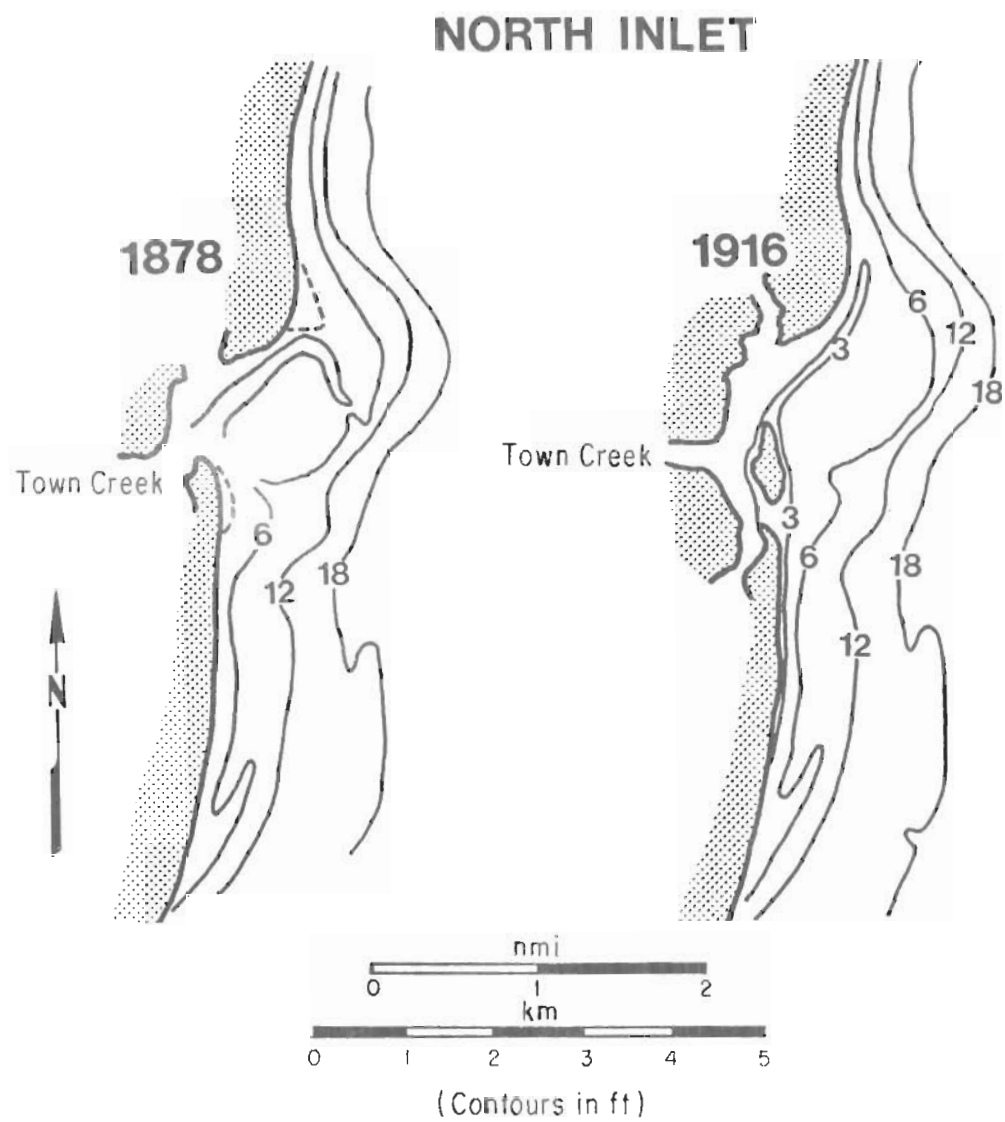
Figure 18. Early shoreline changes (after USC&GS).
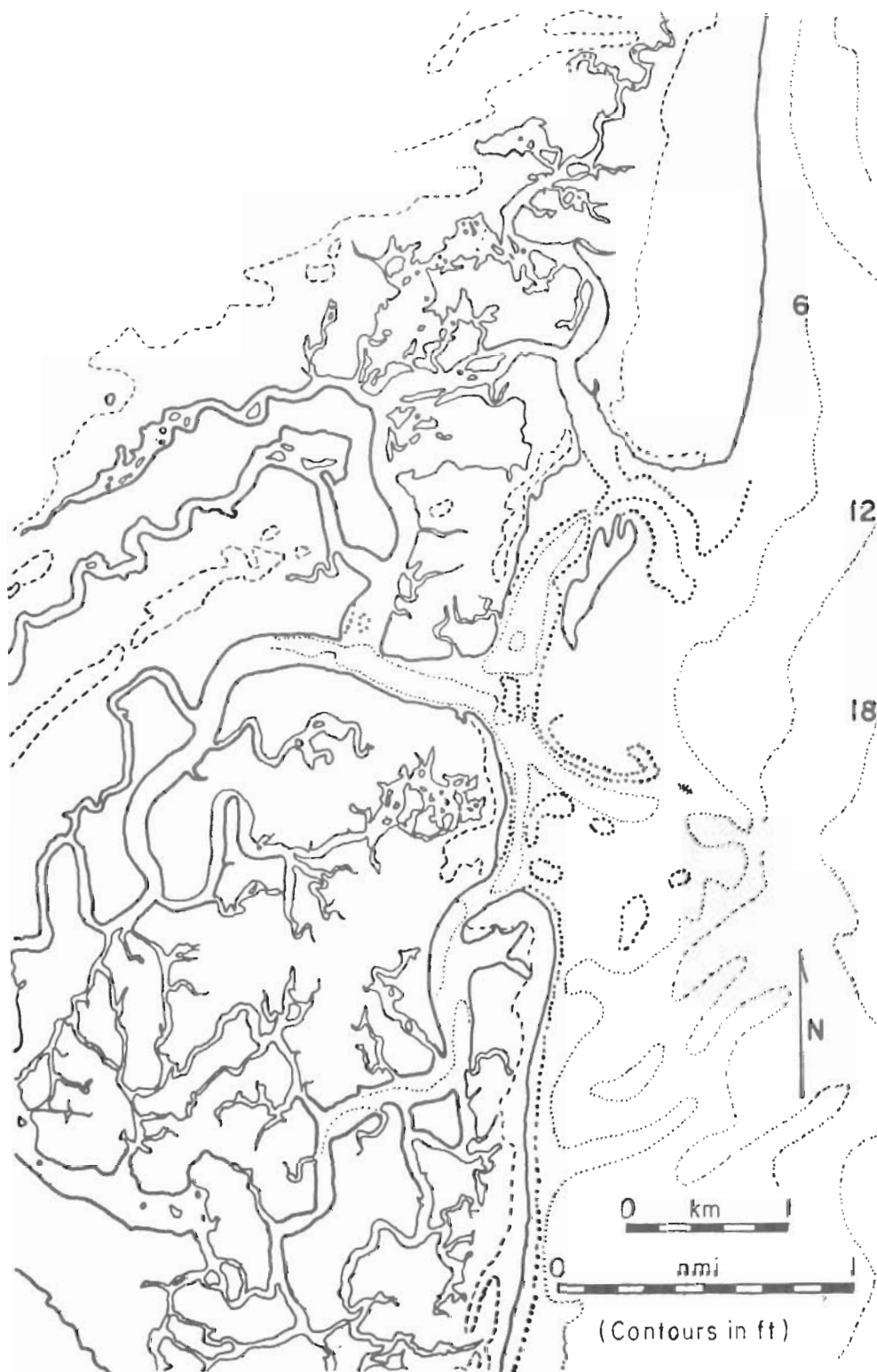
Figure 19. North Inlet, 1925 (based on USC&GS chart 787, 1st ed., 1938).

2. Inlet Migration and Morphology.

North Island was continuous south of the mouth of Town Creek in 1878; in 1916 (Fig. 18), a break was present near the present inlet throat southeast of the Town Creek mouth. This break may have originated as an overwash breach which was subsequently enlarged by Jones Creek flow finding a shorter route to the ocean. The supratidal part of the small island left by this break was eroded away to form the wide shoal off the mouth of Town Creek present in the 1925 survey (Fig. 19). The island present in this survey lies along the 1878 channel-margin linear bar, and probably represents upward growth of this feature, possibly by swash bar accretion, after the tidal flow shifted primarily to the southern channel. Between the time of the configuration published in 1916 and the 1925 field survey, the northern tip of North Island eroded, probably due to tidal flow through Jones Creek. As a result, a wide, shallow inlet existed in 1925, recurved spits were growing southward from Debidue Island; the northern channel was abandoned as the southern channel became more efficient in handling tidal flow from both Town and Jones Creeks.

Vertical aerial photos of 1939, the earliest available (Fig. 20), show that a thin recurved spit had extended southward as far as the southern margin of Town Creek. The main ebb channel was being pushed south by the advancing recurve and began to take on a southeast alinement. The ebb tidal delta began to develop in its present position, and the head area of Sixty Bass Creek began eroding due to wave exposure since the retreat of North Island. By 1954 (Fig. 20), erosion had opened up the creek to tidal flow from the east. The low tide photo (April 1962) is the earliest to show the extensive tidal delta development in detail. Drift reversal due to the ebb tidal delta had become an important process, feeding sediment to a large number of swash bars moving shoreward just south of the inlet. Small recurved spits developed on the tip of North Island. On Debidue Island a large ridge nearly welded to the backshore, and a wide ridge- and runnel-covered low tide terrace existed. The large ridge was continuous for the entire length of Debidue spit, ending in the form of a recurve near the inlet. The appearance of the entire system at that time was that of poststorm recovery following the effects of the northeast storm of March 1962, which did much damage to the entire east coast of the United States.

By February 1963, the swash bar off North Island had become a large ridge separated from the backshore by a berm runnel and had grown in length toward the inlet (Fig. 20). In 1964, a USC&GS ground survey resulted in the 3d edition of chart 787 (Fig. 21), documenting the changes since 1925. Buffington and Randall (1964) noted the growth of Debidue spit, the ebb tidal delta growth about 1,600 meters to the southeast and up to 300 meters of shoreline erosion 1.5 miles south of the inlet. This is about the location of NI-20 (station 4) where littoral materials are moving south due to the regional transport pattern as well as north in response to drift reversal about the growing ebb tidal delta. Erosion was also responsible for changes in tidal creek orientation.
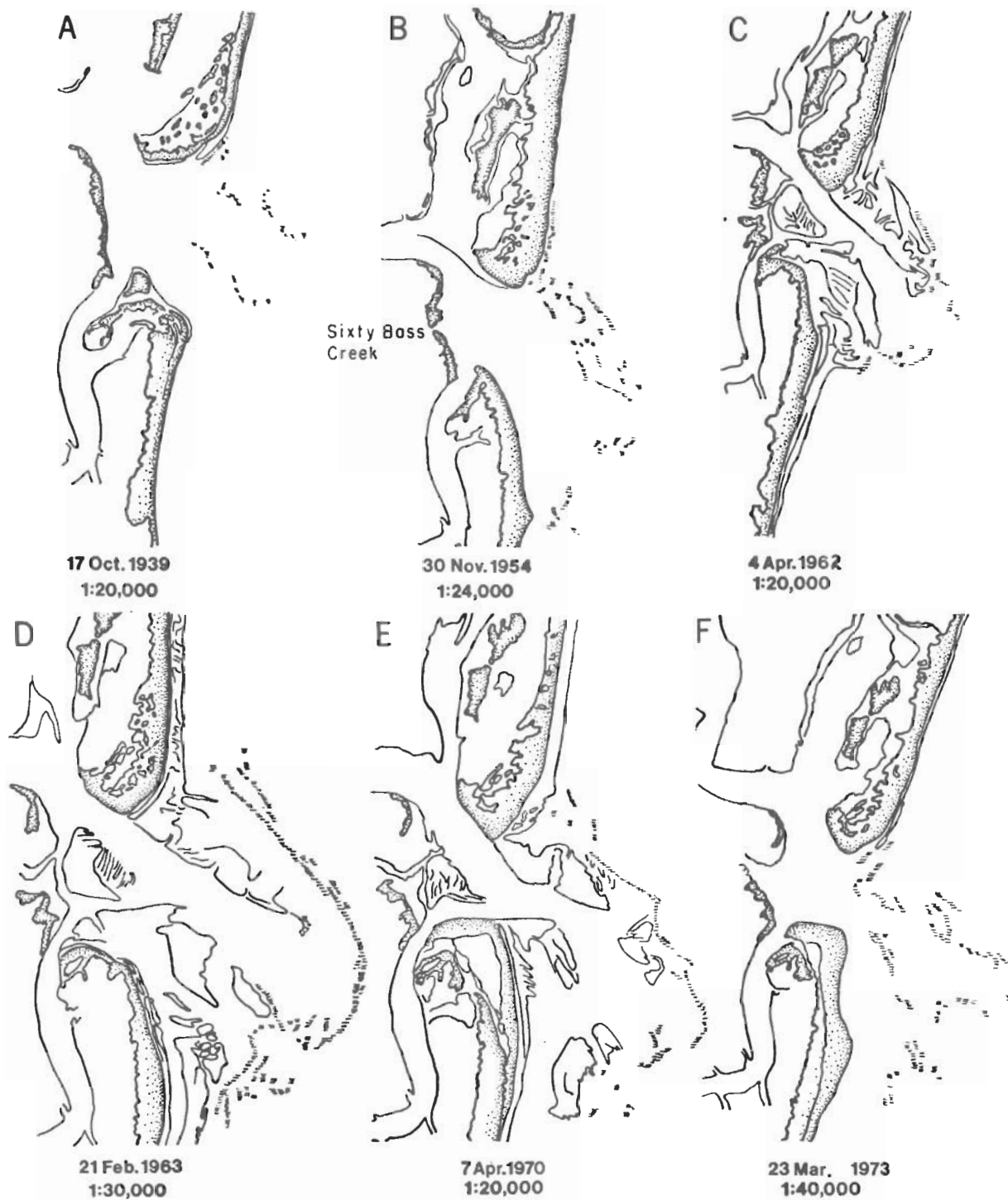
Figure 20. Historical changes at North Inlet. Sketches are based on vertical aerial photos. Beach areas interpreted to be above MHW are enclosed by heavier lines and are stippled. Pattern of short, parallel line segments indicates areas of breaking waves. On high tide photos (A, B, F), pattern gives the approximate location of shoals. Original photo scale indicated.

Within the figure:

A — 17 Oct. 1939 — 1:20,000
B — 30 Nov. 1954 — 1:24,000 — Sixty Bass Creek
C — 4 Apr. 1962 — 1:20,000
D — 21 Feb. 1963 — 1:30,000
E — 7 Apr. 1970 — 1:20,000
F — 23 Mar. 1973 — 1:40,000

63
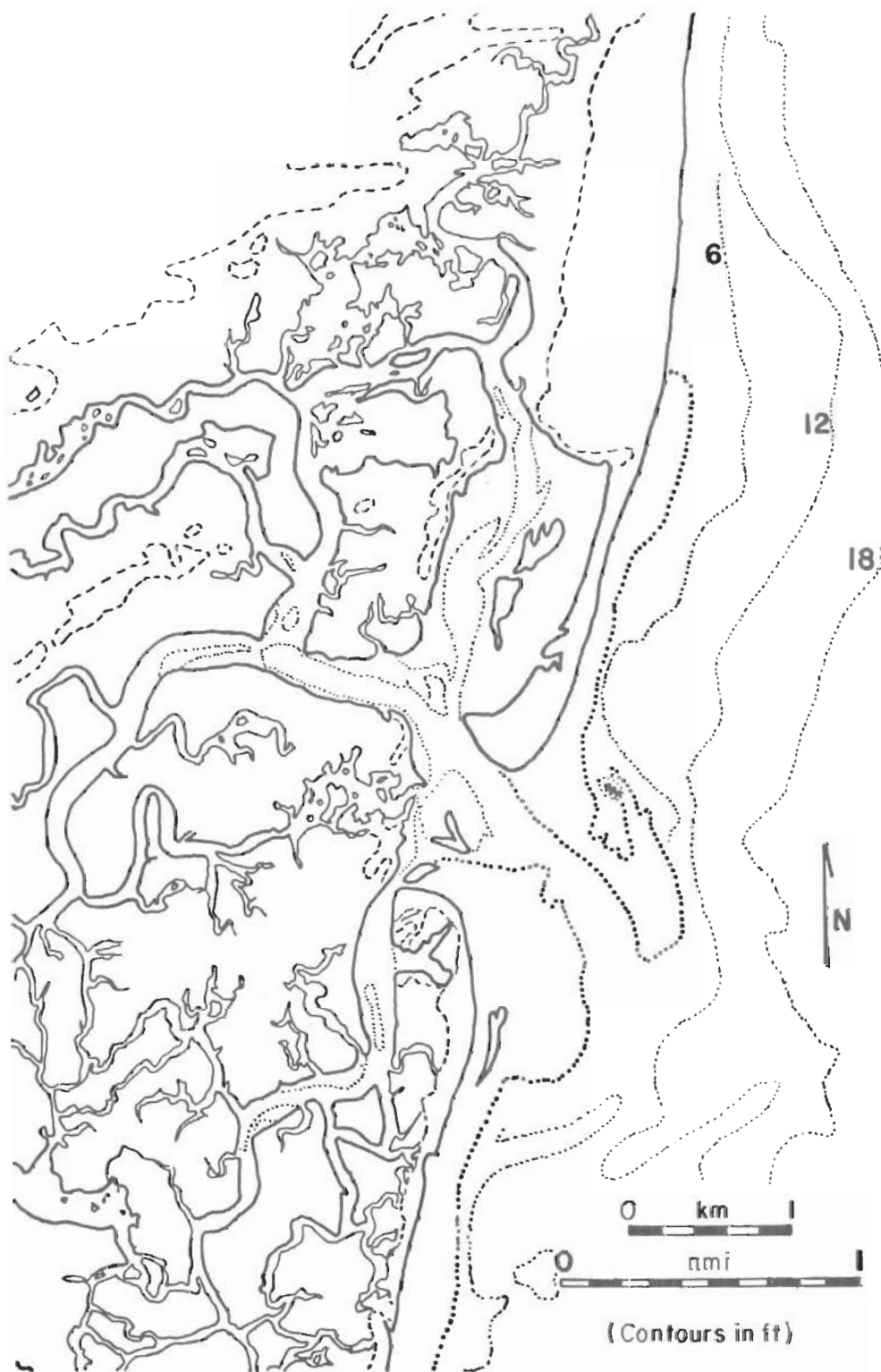
Figure 21. North Inlet, 1964 (based on USC&GS chart 787, **3d ed., 1964**).

The large northward-growing ridge on North Island coalesced with small swash bars and part of the southern channel-margin linear bar to form a large, L-shaped recurve spit by April 1970 (Fig. 20). The area behind the recurve began to fill in with windblown sand, mud, and organics carried in by tidal flow through a small creek created between the recurve and the old 1962-63 North Island shoreline. Figure 22 shows the stubby channel margin linear bars and relatively wide main ebb channel in April 1970. The large swash bar south of the inlet in 1970 (Fig. 20) (or a similar one) was responsible for the beach protuberance seen when this study began in June 1972, and also was present in March 1973. The approximate present configuration of the inlet is shown in Figure 2.
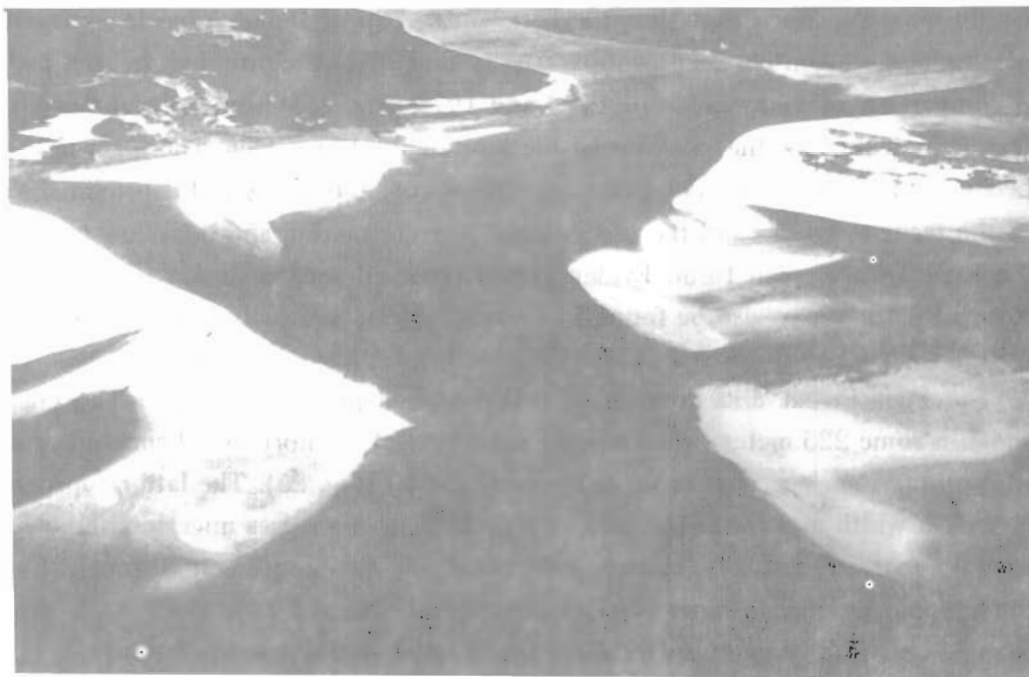
Figure 22. Channel-margin linear bars, April 1970.

3. Inlet Changes: 1972-75.

A detailed comparison of April 1970 and March 1973 photos (Fig. 20) shows no detectable southward retreat of the shore of North Island facing the inlet channel (Fig. 23). The development of the seaward-concave shoreline south of the inlet took place in the interim with some of the sand being incorporated into the flat behind the recurve by wind transport and some being incorporated into the channel-margin linear bar. Additional sand eroded from the northward-facing channel-parallel section of the North Island recurve appears to be filling in the area near the mouth of the small creek flowing behind the recurve. Replacement of this sediment is probably material brought in from the south by

the longshore drift reversal, with beach-welded swash features supplying much of the sediment (Fig. 23). The lack of evident southward inlet migration of North Inlet may also be related to the fact that the inlet has scoured into a cohesive, blue-gray, possibly Pleistocene back-barrier clay in the northern part of the throat channel. At high water depths of 8 meters, clay is occasionally brought up on the anchor, indicating that it probably directly underlies the surficial coarse sand-shell lag. Channel scouring of this material would be relatively difficult.

The Debidue shore of the inlet consists of a recurved spit along the margin of which smaller recurves generated by ridge and runnel systems migrate shoreward and into the inlet. In June 1972, a wide berm was created as windblown sand filled the area (Fig. 24) enclosed by the recurve. Since that time the berm on the tip of Debidue has become substantially narrower as erosion between profiles DBI-10 and DBI-TS continued, as seen in July 1974. A comparison of maps made in 1972 and 1974 (Fig. 25) shows substantial retreat of the beach, indicated by the position of the base of the beach face. The main part of the spit becomes unstable and erodes as the open beach, corresponding to the proximal, eastern end of the recurve, erodes and the processes of wave refraction and tidal flow tend to maintain the same recurve plan form. Evidence that recurved spits maintain a similar overall planform with time may also be found in Farrell (1969). As beach erosion proceeds, then, the inlet is widened by decreased width of the recurved spit on Debidue Island.

The inlet throat area consists of two morphological components: The main channel, which is some 225 meters wide, and the inner part of the northern channel-margin linear bar whose upper surface is near mean sea level (MSL) (Fig. 26). The latter approximates 550 meters in width and forms the base on which recurving ridges migrate around the Debidue Island recurved spit. A steady movement to the southwest through time of the topographically higher inner shoal margin (Figs. 20 and 26), along with the described changes on North Island, have localized the channel in its present position.

The major change observed in the inlet throat cross section came as a result of the severe northeast storm of February 1973. Fathometer profiles (Fig. 27), whose total length has been adjusted to nearly the same horizontal scale, show infilling by the channel-margin linear bar into the channel on the poststorm profile of 6 March 1973. This is evident when it is noted that the central highs, part of the seaward-projecting ebb spit, should be in approximately the same position. The sharp pinnacle in the 6 March 1973 profile is interpreted as a remnant, resulting from erosion in the area indicated, as tidal scour tended to restore the original cross-sectional area. By 5 May 1973, the pinnacle had been entirely scoured away, and, presumably, a near-equilibrium condition had been reestablished.

The inlet throat was surveyed eight times between 30 June 1974 and 26 April 1975 (Fig. 28). Length adjustments were made on the profiles such that all horizontal scales are between 34.63 meters (113.62 feet) and 38.63 meters (126.71 feet) per inch; only those profiles requiring substantial adjustment were changed and then to a scale of 37 meters per

66

Figure 23. North Island shoreline just south of the inlet (upper photo) and along the main inlet channel (left center, lower photo), August 1973 and July 1974, respectively.
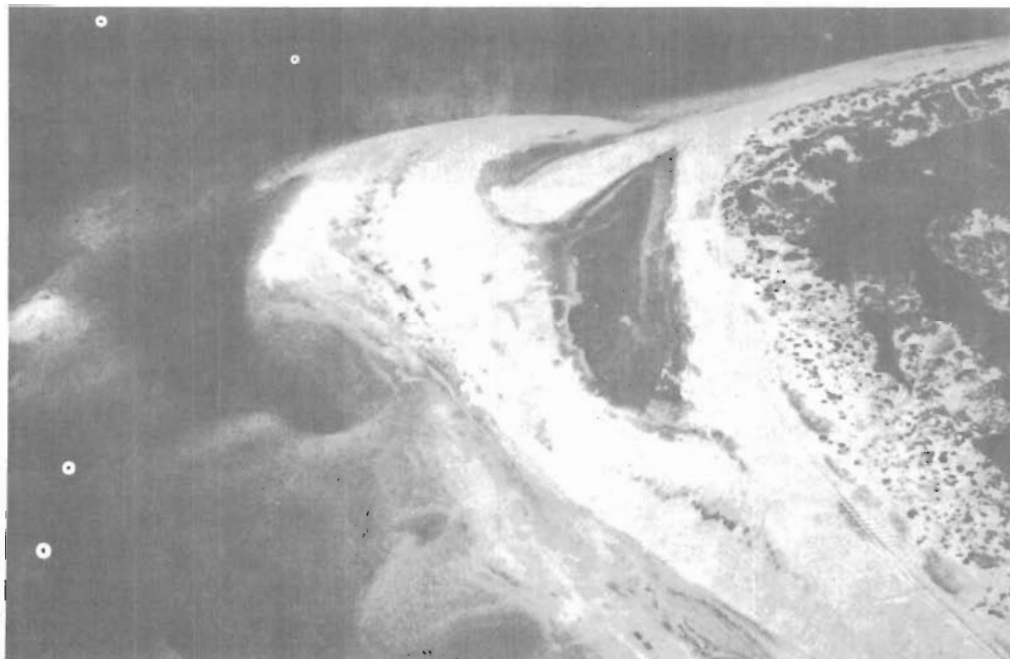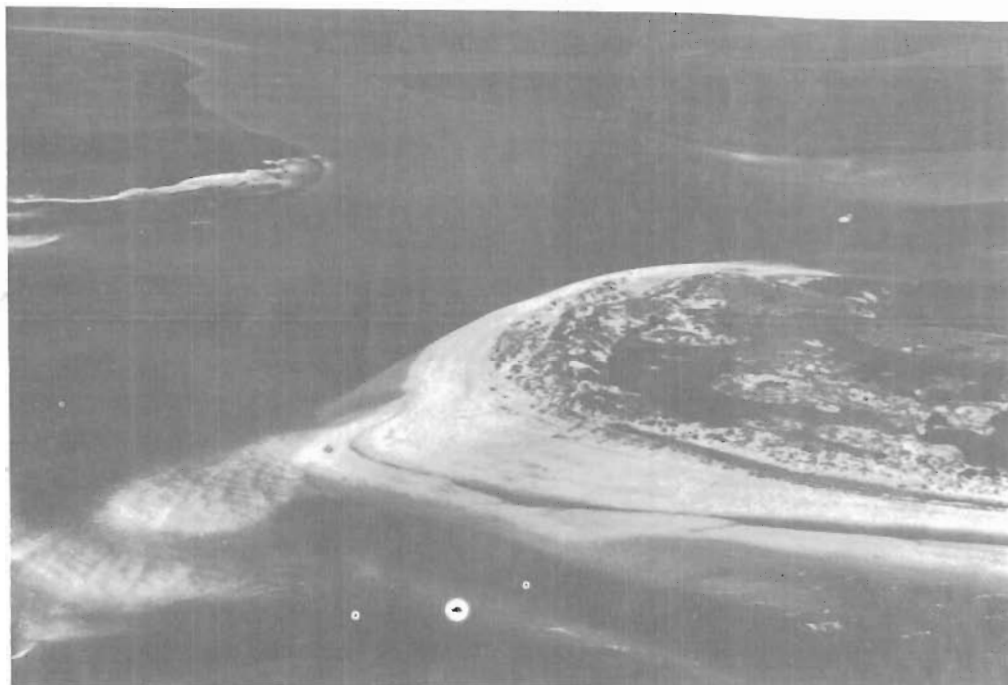
Figure 24. Southern tip of Debidue Island, June 1972 (lower photo)
and July 1974 (upper photo).

PLANFORM: 7 to 9 JULY 1972
CONTOURS: 28 SEPT. 1974

200
150
100
50
0

N

BASE OF BEACH FACE

C.I. = 50 cm

0   40   80
       m
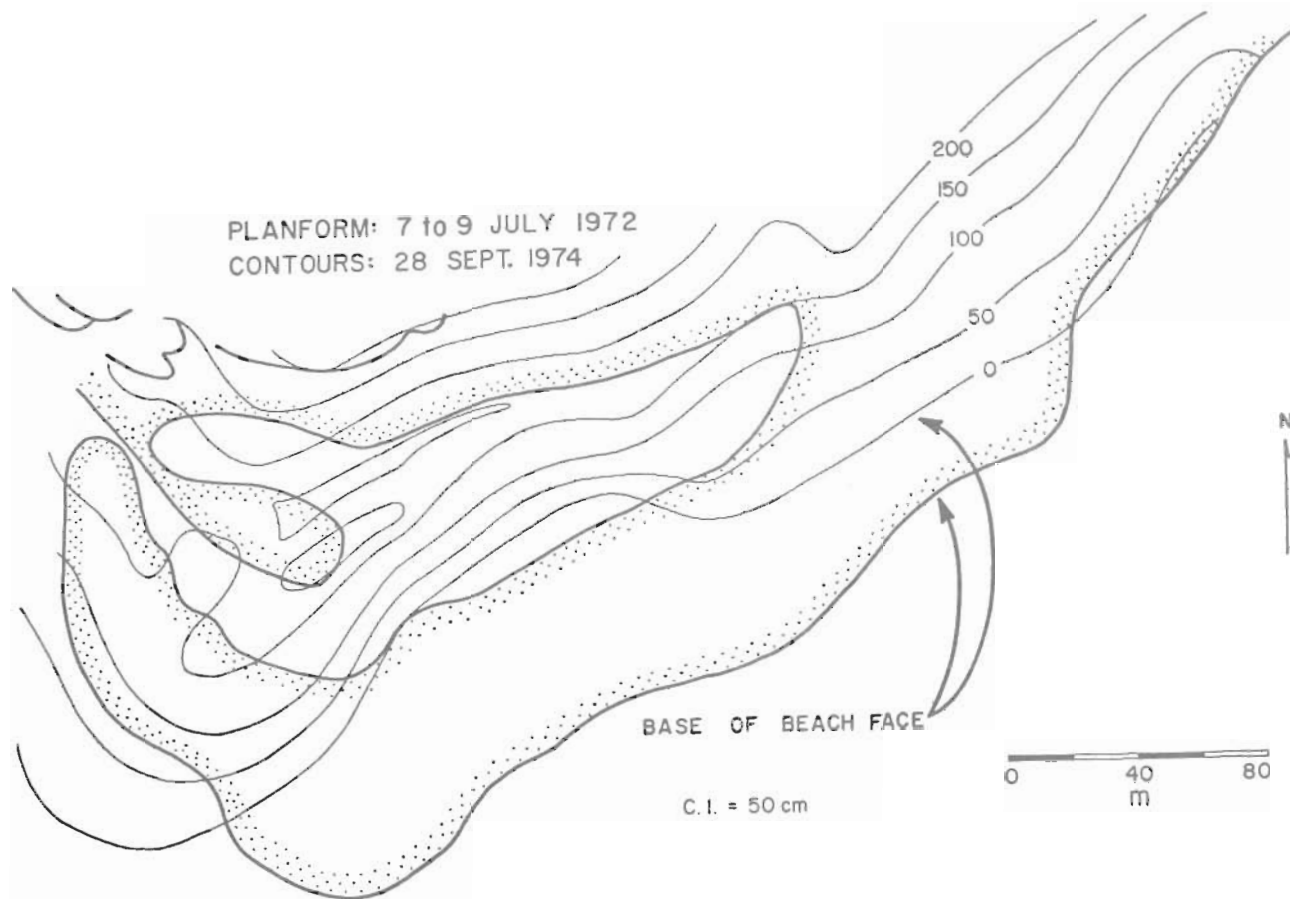
Figure 25. Debidue Island recurved spit maps. The planform map (stippled boundary) covers the area of the upper photo in Figure 24. The contour map shows elevations above the base of the beach face (0 contour), indicating retreat of 20 to 60 meters of this feature over a 2-year period.
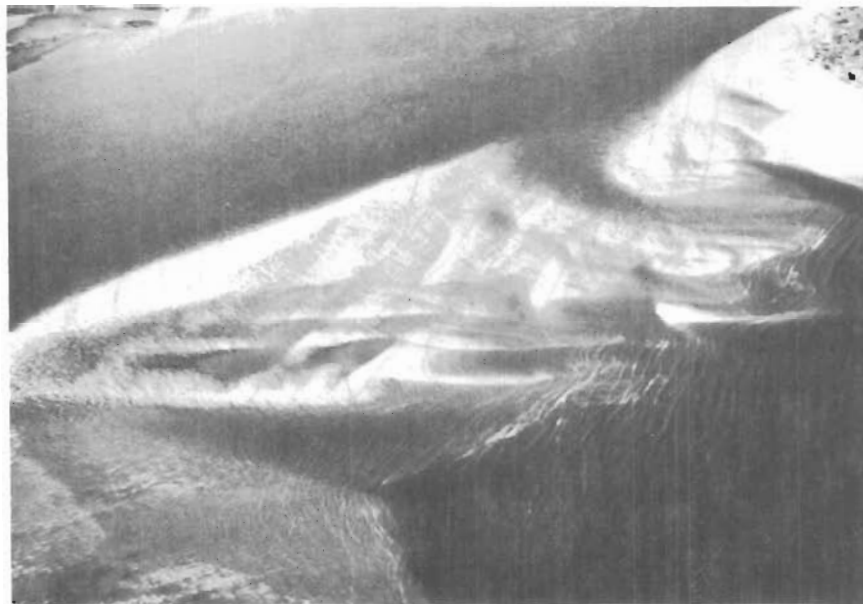
Figure 26. Inlet throat (upper photo) and channel-margin linear bar (lower photo), January 1975.
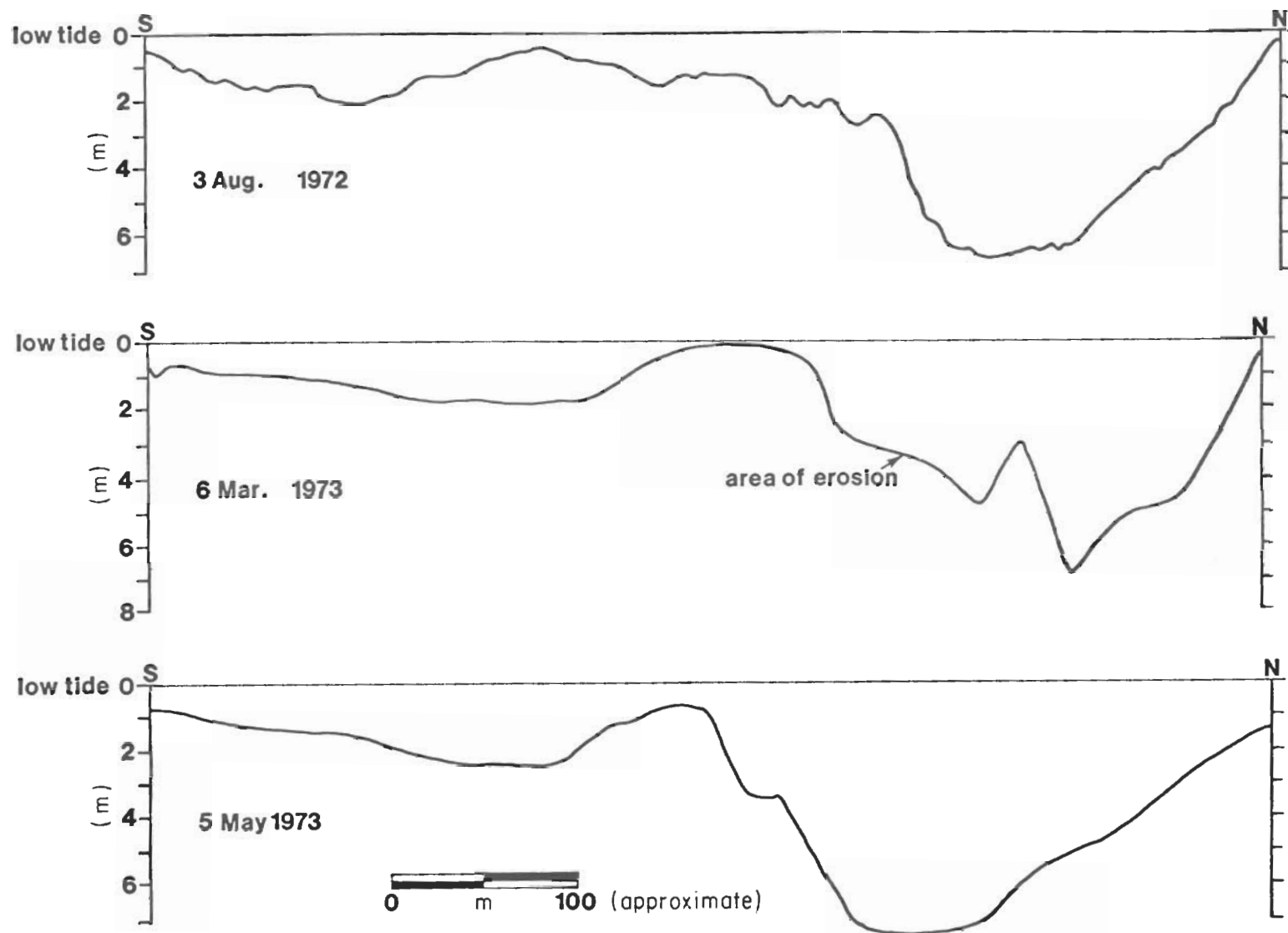
Figure 27. North Inlet throat bathymetry, 1972-73. Profiles run off location 7 (Fig. 10).
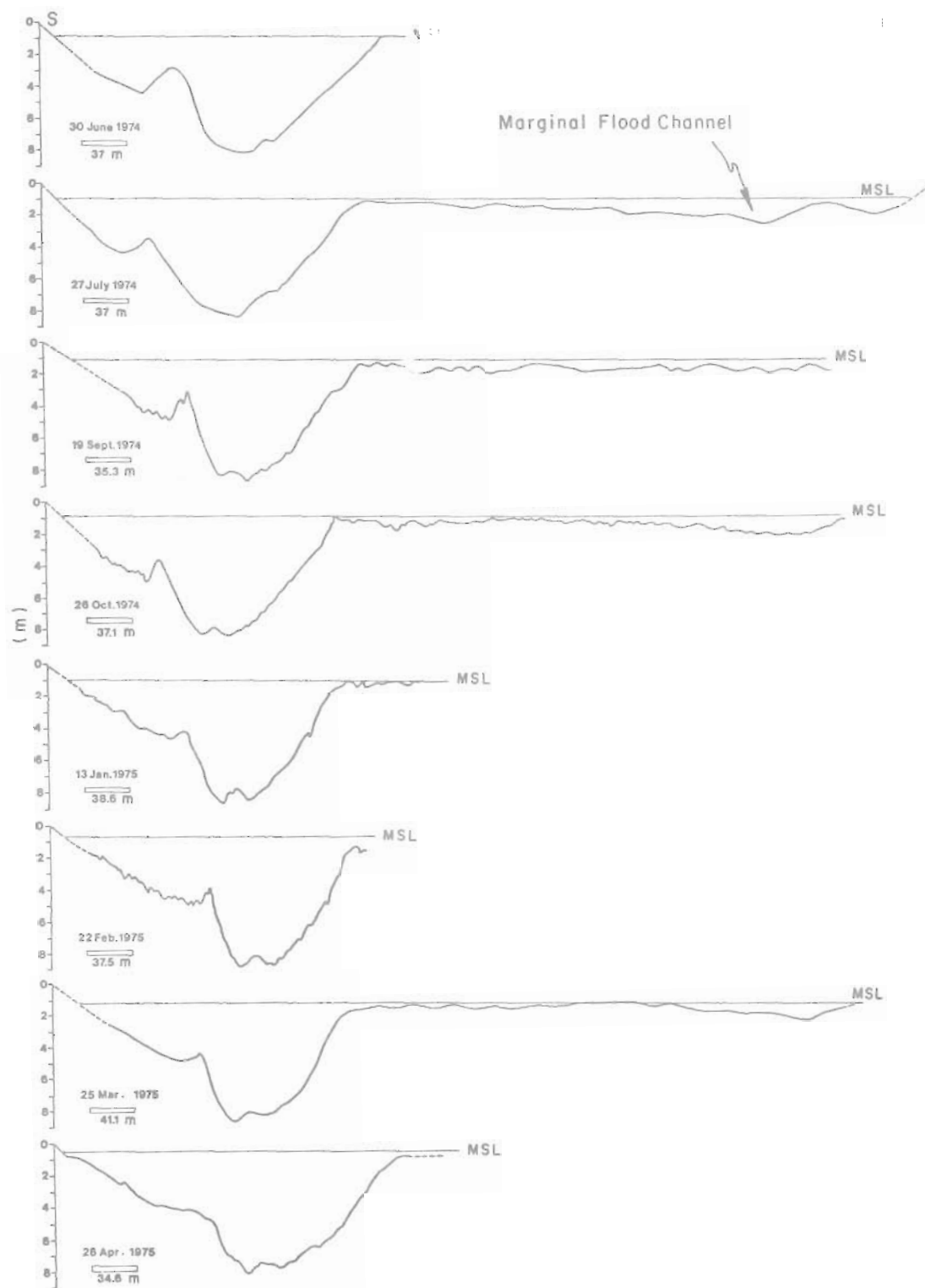
Figure 28. North Inlet throat bathymetry, 1974-75.
Profiles run between locations 7 and 3 (Fig. 10).

inch. A somewhat qualitative, rather than a precise quantitative, interpretation should be made of the horizontal scale, especially at the southern end of the profile where the boat was first being brought on course. MSL indicated on the profiles is derived from averaging hourly ocean water levels over a 2-week period of good quality tide records.

Two subchannels make up the main channel of the inlet. The seaward-projecting ebb spit of the flood tidal delta tends to divide the flow between that issuing from Jones Creek to the south and Town Creek to the north. Tidal current velocities and salinities vary across the ebb spit boundary, as described below in the hydraulics section. The elevation of the ebb spit is decreasing with time and is less evident on the last two profiles than on those of the summer and fall of 1974. Westward migration of the entire flood tidal delta under the influence of wave swash and tidal currents is responsible for this; however, this is a slow process, and the ebb spit is also armored with an oystershell lag deposit.

Inlet throat cross-sectional areas were computed along the throat profile to the margin of the intertidal shoal for each quarterly study. Areas measured were: 27 July 1974, 995 square meters (10,706 square feet); 19 September 1974, 886 square meters (9,533 square feet); 13 January 1975, 925 square meters (9,946 square feet); 25 March 1975, 894 square meters (9,619 square feet); and 26 April 1975, 968 square meters (10,412 square feet). Percentage changes based on the summer area are -11 percent for September, -7 percent for January, -10 percent for March, and -3 percent for April. A hypothetical error of ± 5 meters in channel width due to surveying error and rod-positioning error would result in a ± 2-percent error in the change values based on the March data. This may be taken as some indication of the accuracy of the data; random errors due to boat operation also exist but have not been evaluated. Comparison of the 27 July 1974 and 25 March 1975 profiles (Fig. 28) shows upward growth of the intertidal shoal and a shallowing of the marginal flood channel. Aerial photos (Figs. 26 and 29) suggest that this has resulted from the increasing size and number of swash bars migrating onto the shoal and growth of a small ebb-oriented spillover lobe near the Debidue shore. Although over the last 3 years the inlet has become wider due to decreasing width of the Debidue Island recurved spit, profiles spaced a few months apart do not show a substantial trend in this direction (Fig. 30). The response of the profiles seems to be more affected by short-term accretion and erosion.

4. Debidue Island and North Island Beaches.

The general morphological changes of the beaches adjacent to North Inlet have been summarized in connection with inlet migration between 1878 and the present. Sea level rise and the low rate of sand-sized sediment influx have caused significant erosion of both beaches. Extensive efforts at beach preservation have been made on Debidue, using dune fencing and artificial planting of sea oats (*Uniola paniculata*); however, westward retreat is continuing, and only a relatively narrow dune area is present in front of the tidal marsh and mudflat (Fig. 31). On North Island, short segments of subparallel beach ridges are present south of the recurved spit (Fig. 31), but this area has been receding over the last 3 years
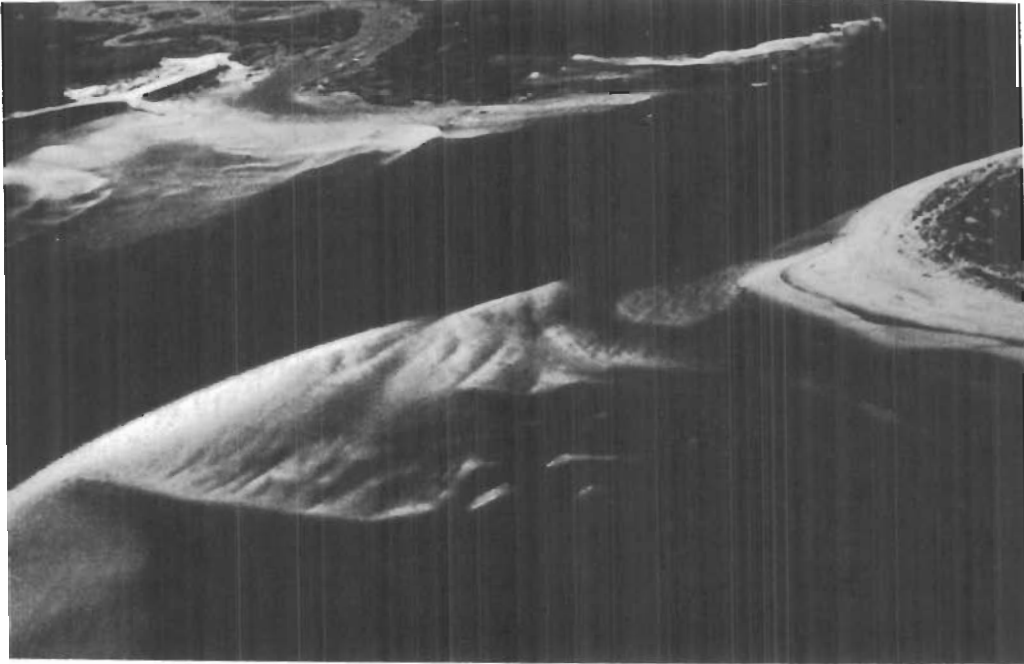
Figure 29. Inner channel-margin linear bar, July 1974.

DBI-TS (throat section)

23 Mar. 75

29 Oct. 74

8 Jan. 75

8 Jan. 75   23 Mar. 75

23 Mar. 75

2
1
0   10   20
        m

NI-TS (throat section)

25 Mar. 75

5 Jan. 75

27 Oct. 74
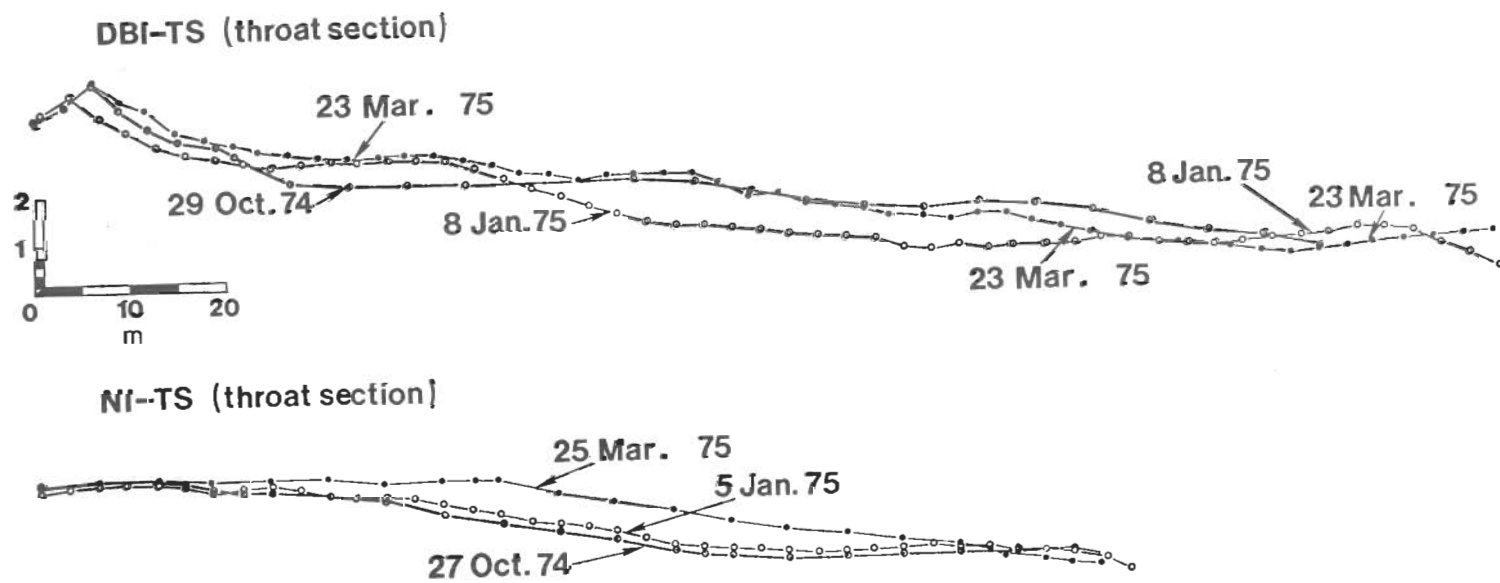
Figure 30. North Inlet throat section changes. Location of profiles shown in Figure 10.

Figure 31. Debidue Island (upper photo) and North Island (lower photo)
January 1975.

(compare with Fig. 23). South of the ebb tidal delta, near NI-20 (station 4, Fig. 10), the beach is exceedingly narrow, and several overwash fans (Fig. 32) are building back into *Spartina alterniflora* marsh. These fans are active during higher springtides. On the beach face, a very thin, active sand layer overlies a coarse shell hash with some coarser sand. The shell debris is almost exclusively oystershell which comes through the beach from the marsh as transgression continues.

a. Beach Profiles. Individual beach profiles are in Appendix B. A description of those surveyed between June 1972 and June 1973 is included in Finley (1973); profile response to the February 1973 northeast storm is discussed later. Profiles were obtained between June 1973 and May 1974 on an irregular basis at the seven original sites until the establishment of the additional sites in June 1974 (Fig. 10). Sequential plots are included in Appendix B. To examine the active sand envelope, quarterly profiles were plotted in correct relative position for the four beach observation stations.

These plots (Fig. 33) show that the beaches were in an accretionary phase in September 1974, before the northeast storm of 23 and 24 September. A berm with a landward slope and sharply defined berm crest had developed since the July 1974 profile at DBI-10, DBI-25, and NI-20. Erosion due to storm waves through the fall and winter resulted in approximate sediment losses of 23.6, 15.0, and 10.0 cubic meters per meter between July 1974 and March 1975 for these three localities. It would be expected that some of this loss would be recovered as storm wave frequency decreases toward the summer of 1975, but observations since 1972 indicate that the overall trend is net erosion. Profile NI-14 has shown a steady rise in level of the upper beach and a consistently landward-sloping berm. Accretion below the berm crest represents an addition of 124 cubic meters per meter of beach between July 1974 and March 1975. Northward migration of the point of swash bar attachment to the beach was responsible for the upward growth, since by March 1975, profile NI-14 was located on the wide south flank of the swash feature.

The loss of 10,000 to 15,000 cubic meters per kilometer of sand on Debidue Island over an 8-month period is comparable to the 11,000 cubic meters per kilometer of erosion measured by DeWall, Pritchett, and Galvin (1971) for the northeast storm of 16 to 18 December 1970, along the coast from Cape May, New Jersey, to Race Point, Massachusetts. This single event is roughly comparable in effect to a longer timespan which includes multiple minor erosive events. DeWall, Pritchett, and Galvin (1971) also noted that the storm erosion value is small compared to net longshore sand transport rates of 400,000 cubic meters per year estimated for the shoreline between Cape May and Race Point. This is also the case at North Inlet, where net addition to the ebb tidal delta (Fig. 17) indicates a longshore transport rate of 433,000 cubic meters per year toward the inlet.

b. Beach Response to Northeast Storms. The northeast storm of 10 to 11 February 1973 has already been described as the major storm event at North Inlet during the past 3 years. At profile DBI-10, 7.3 meters of foredune ridge was lost as the eroding face moved westward between 2 December 1972 and 15 February 1973 (App. A). At profile DBI-20, a
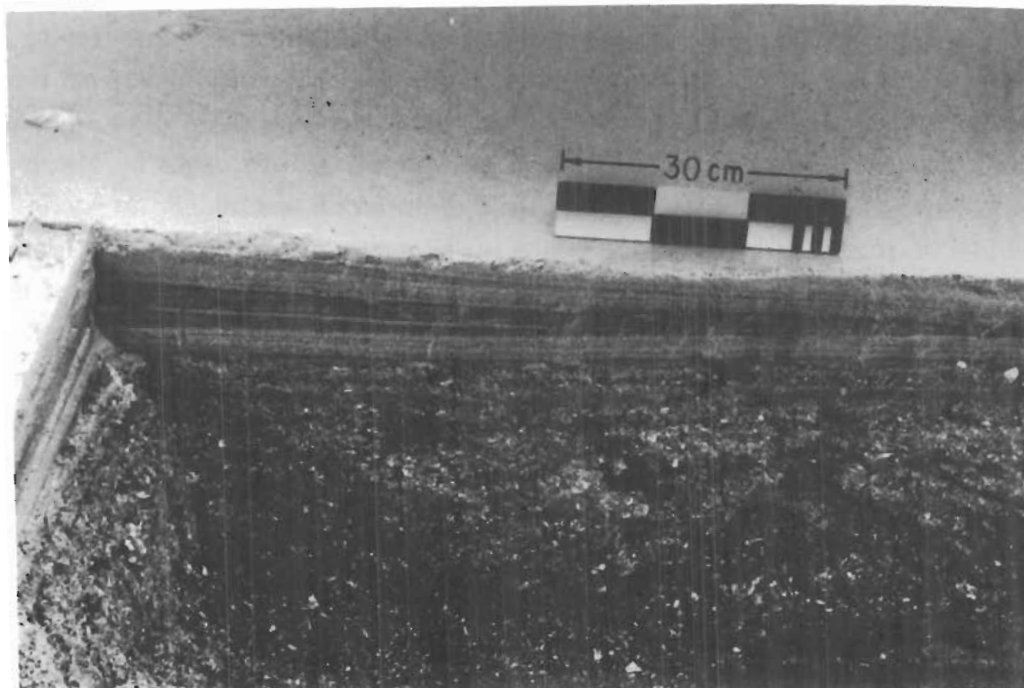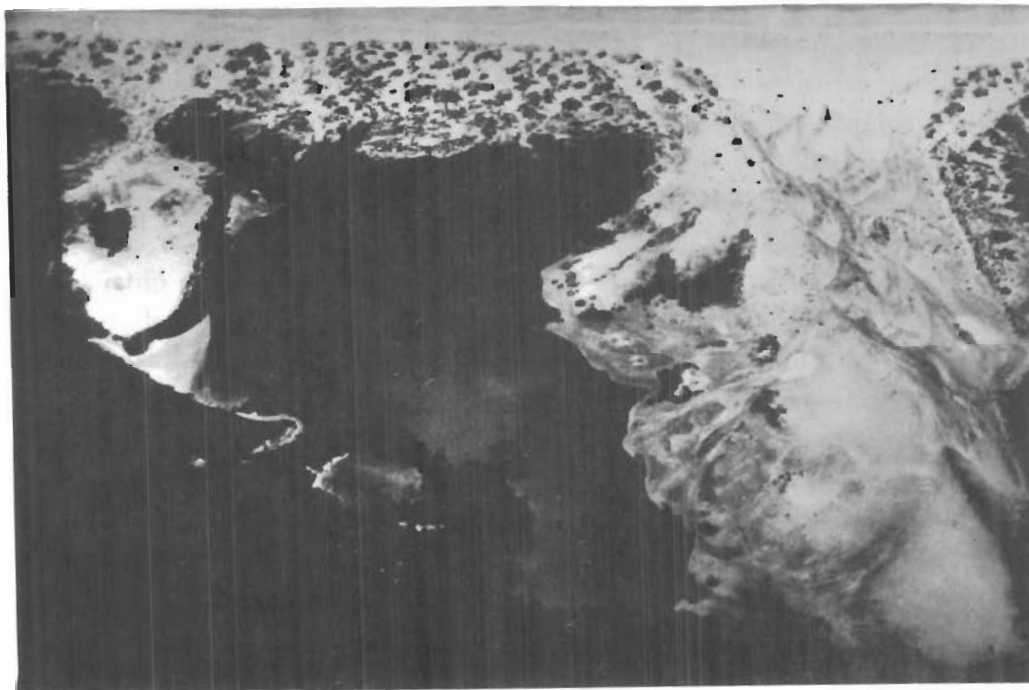
Figure 32. North Island overwash fans, July 1974 (upper photo) and trench in upper foreshore, July 1972 (lower photo).

DBI-10 (sta. 1)
8 Jan. 75
18 Sept. 74
22 July 74
20 Mar. 75

DBI-25 (sta. 2)
18 Sept. 74
22 July 74
8 Jan. 75
20 Mar. 75

NI-14 (sta. 3)
25 Mar. 75
9 Jan. 75
27 Oct. 74
22 July 74

NI-20 (sta. 4)
25 Mar. 75
18 Sept. 74
22 July 74
9 Jan. 75
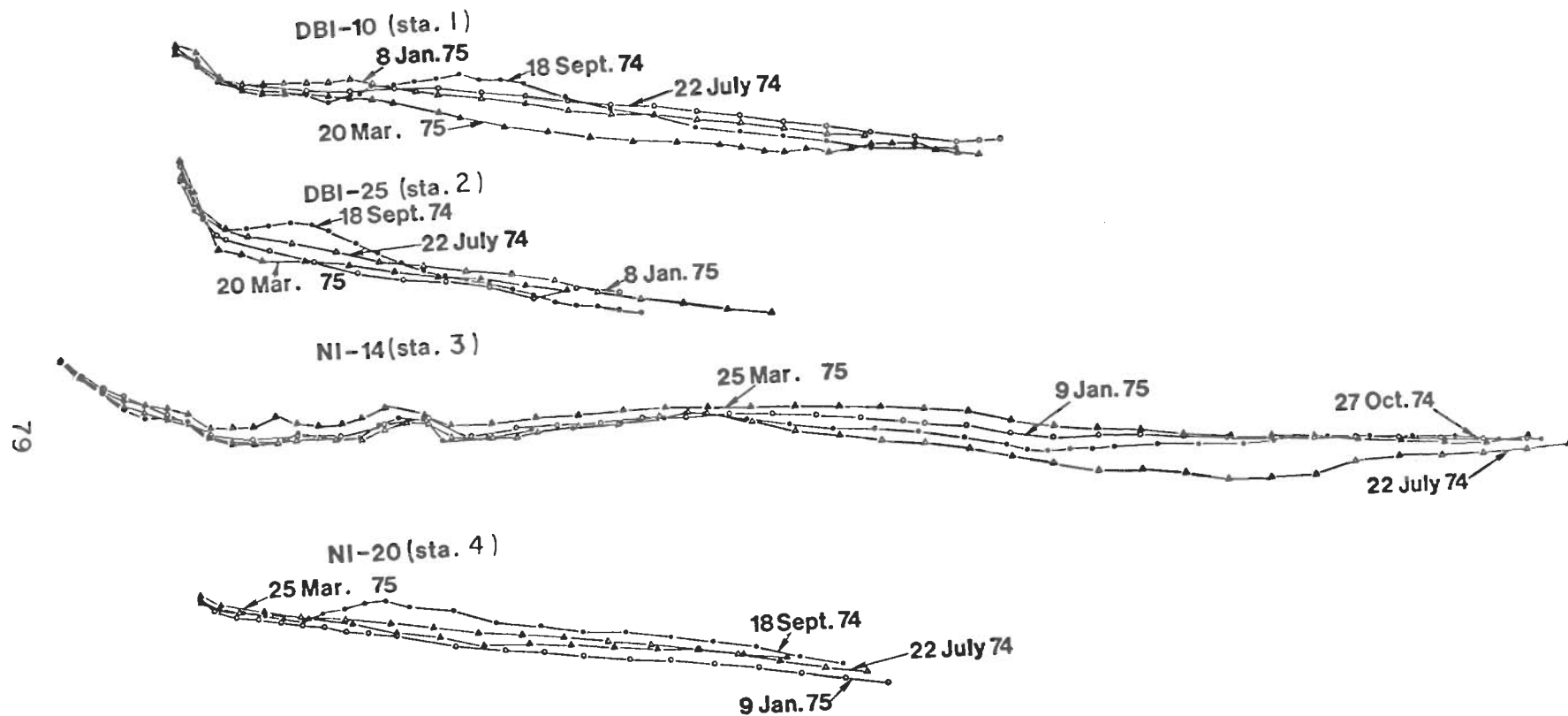
Figure 33. Quarterly beach profiles, July 1974 to March 1975.

2.6-meter-high vertical scarp was present after the storm, and a similar but lower scarp was found at profile DBI-25 (Fig. 34). Comparison of the eroded scarp at profile DBI-20 with the preceding profile measurement shows a loss above mean low water (MLW) of 31.6 cubic meters per meter of beach (43.8 cubic yards per foot of beach) which indicates that this storm caused erosion similar in magnitude to the 1970 storm studied by DeWall, Pritchett, and Galvin (1971). Tabulated single profile erosion extremes (U.S. Army, Corps of Engineers, Coastal Engineering Research Center, 1975) for the December 1970 storm (on New Jersey beaches) are 59.72, 24.26, and 34.28 cubic meters per meter.
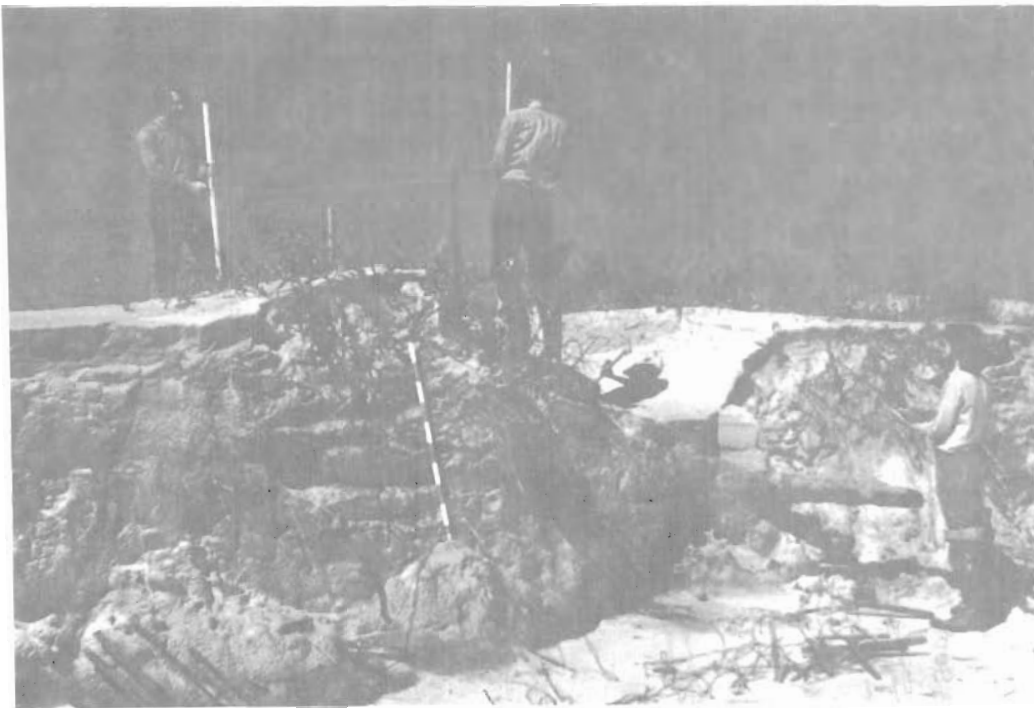
Figure 34. Foredune ridge scarp at profile DBI-25. Length of scale is 1 meter

Of the three original profile localities on North Island, the northern two profiles, NI-10 and NI-14, are sheltered from direct approach of northeast waves by the ebb tidal delta. As a result of this protection, no major erosion, as indicated by the position of the berm crest, occurred from 6 January to 17 February 1973, which included the northeast storm. The southernmost profile on North Island, NI-20, is beyond the zone of protection by offshore features and underwent erosion (Fig. 35). The *Spartina alterniflora* peat exposed on the lower foreshore probably underlies the entire beach sand prism which is only some 400 meters wide (from MLW to marsh margin) in this vicinity. Large quantities of oystershell lag are added to the beach sediments as the marsh peat is broken up and carried away (Fig. 35).

Figure 35. Foredune ridge scarp (upper photo) and peat exposure (lower photo) at profile NI-20. Length of scale is 1 meter.

A radiocarbon date of 920 ± 120 years Before Present (B.P.) was obtained for peat samples at the margin of the scarp, giving a very approximate long-term beach recession rate of 0.50 to 0.38 meter per year over the last 1,000 years. These data are consistent with the relative rise in sea level measured by Hicks and Crosby (1974) and may be indicative of eustatic sea level change and compactional subsidence on the south flank of the Cape Fear arch.

A low-intensity northeast storm on 23 and 24 September 1974 resulted in significant beach erosion and was the only storm of this type to occur during any of the quarterly 2-week study periods. Kana (in preparation, 1976) analyzed the development of an erosional scarp on Debidue Island, with profiles at the beginning and end of the 2-week period indicating losses of 6.7 cubic meters per meter of beach at DBI-10 and 13.1 cubic meters per meter at DBI-25 (Fig. 36). Note that the beach recovery was well underway by 27 September 1974, with the development of a landward-migrating ridge. Figure 37 shows that the scarp developed primarily in a 6-hour period on 23 September which coincided with a high tide, maximum breaker height (120 centimeters), maximum longshore current (140 centimeters per second), and greatest wind velocities (20 miles per hour with higher gusts). By 0850 hours on 24 September 1974, 13.4 cubic meters per meter of beach had been lost in a 24-hour period. Southward-directed energy flux factors (P_{1s}) for the midmorning and midafternoon of 23 September 1974 were 402 and 312 foot-pounds per second per foot and for 24 September 1974, 136 and 312 foot-pounds per second per foot. These data represent a significant contribution to the annual mean southward P_{1s} values, without which the close correspondence between longshore transport rate and derived P_{1s} would not exist. Here, then, is another instance of the significance of "extreme" events in contributing to the overall mean conditions on a section of coast.

5. The Flood Tidal Delta.

The flood tidal delta occupies a position facing the inlet between Town Creek to the north and Jones Creek to the south. It is strongly affected by wave action at high tide (Figs. 38 and 39). Although its morphologic components are quite similar to flood tidal deltas of New England estuaries, it is substantially smaller than other such features to the north along the east coast of the United States. This is a direct result of the limited area for flood tidal delta growth afforded when the inlet stabilized at its present position (Fig. 20), and the transgressive nature of the shoreline. While the main delta has shown continuous change and westward migration, the flood tidal delta at the junction of Town Creek and Debidue Creek changed very little between June 1972 and March 1975.

The landward ebb shield margin opposite the mouth of Sixty Bass Creek migrated some 42 meters westward from July 1972 through March 1973. Planform outlines of the delta at MLW (Fig. 40) show the westward retreat.

Successive bathymetric profiles, designated FTD (Fig. 41), show that as the tidal delta has retreated, the area to the east has deepened, possibly as much as 1 meter in some areas. Note that as with the throat bathymetric profiles, a semiquantitative rather than an exact

DB −10
Sta. 1

DBI−25
Sta. 2

Area=6.7 m²

27 Sept. 74

18 Sept. 74

Area=13.1 m²

27 Sept. 74

18 Sept. 74
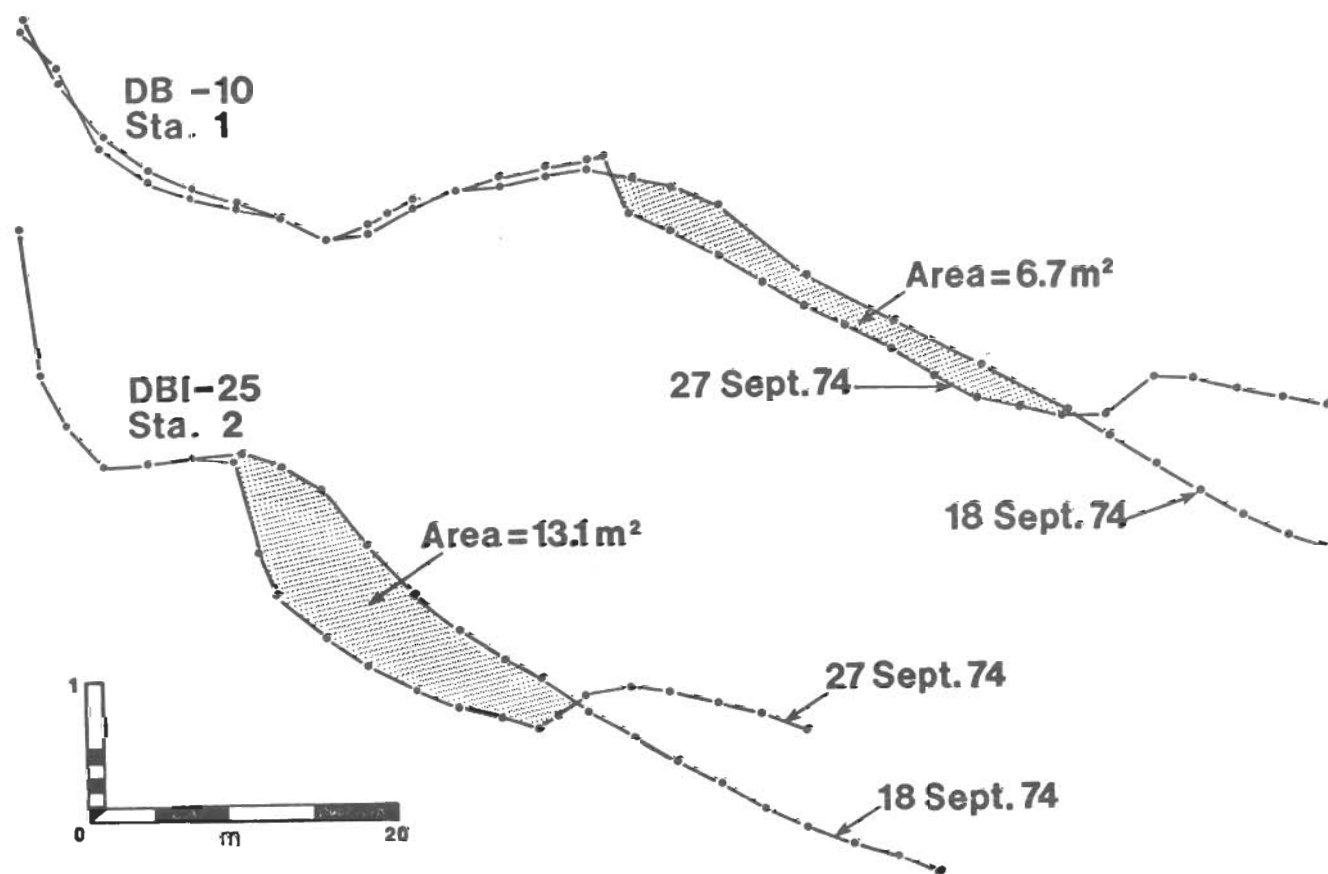
Figure 36. Debidue Island beach erosion, September 1974.
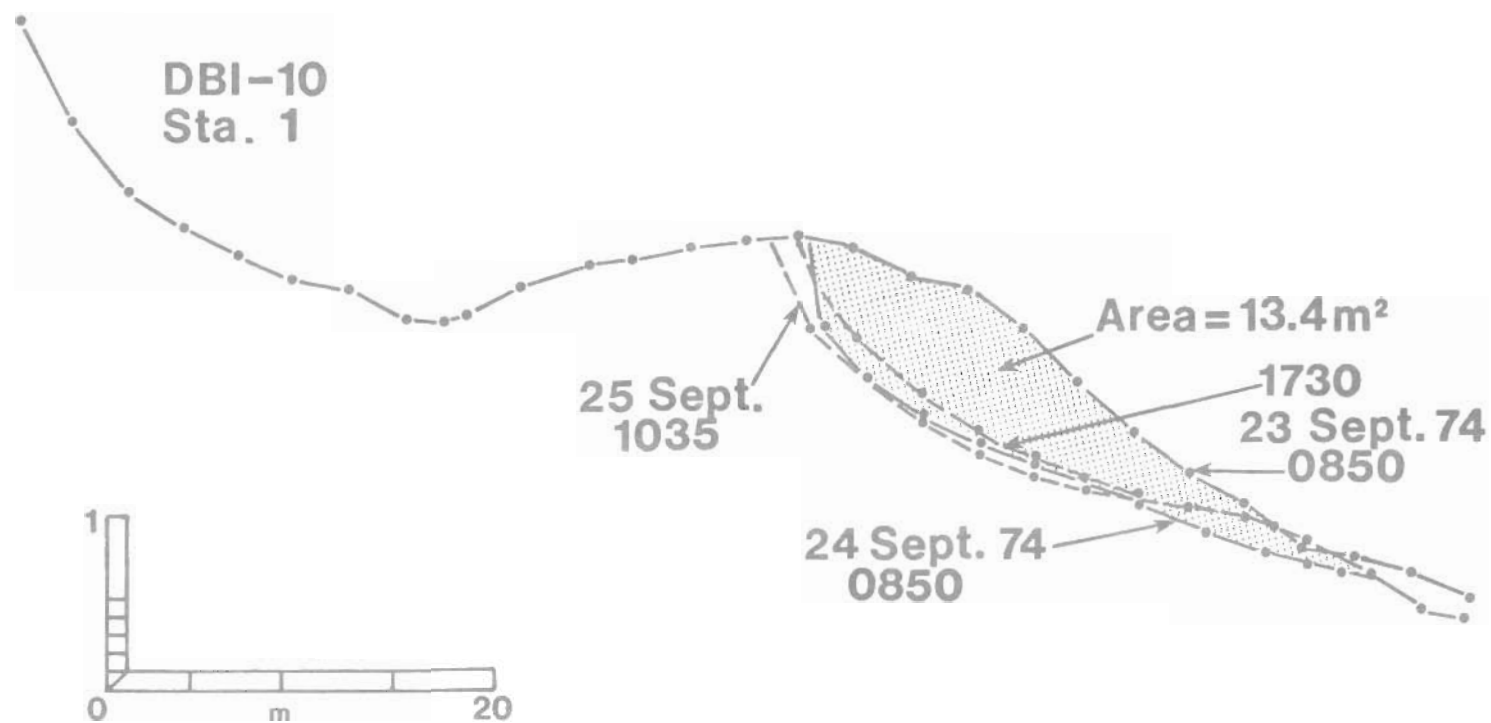
Figure 37. Debidue Island beach scarp development, September 1974.

Figure 38. Vertical view of North Inlet, April 1974 (USGS).
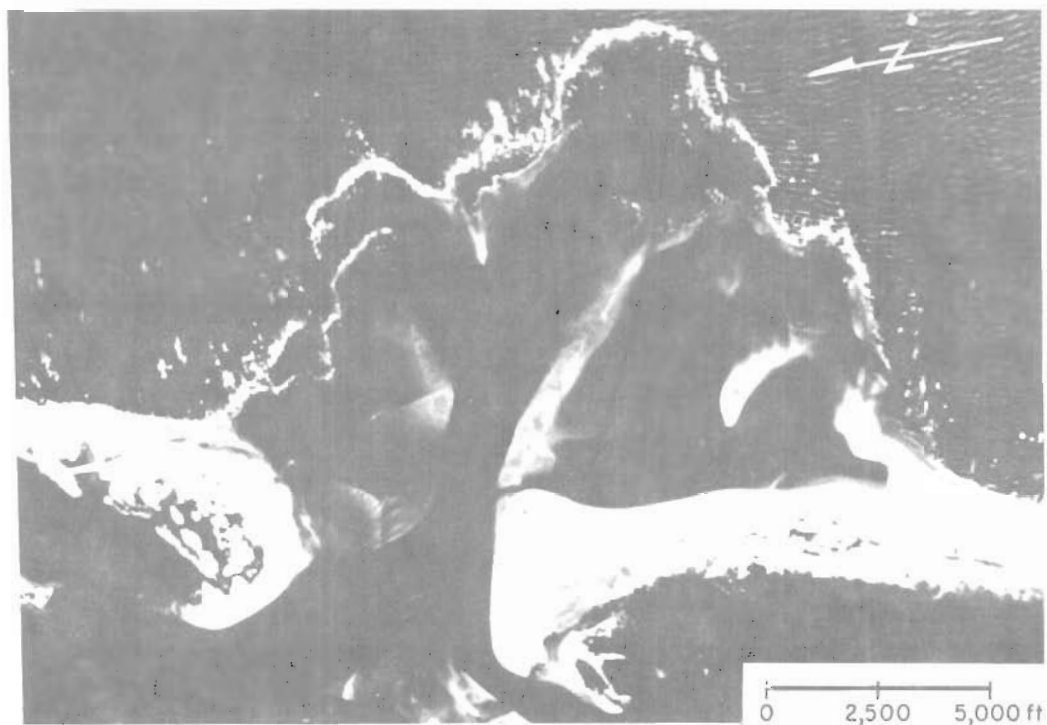
Figure 39. Vertical view of North Inlet, March 1975 (NOAA).
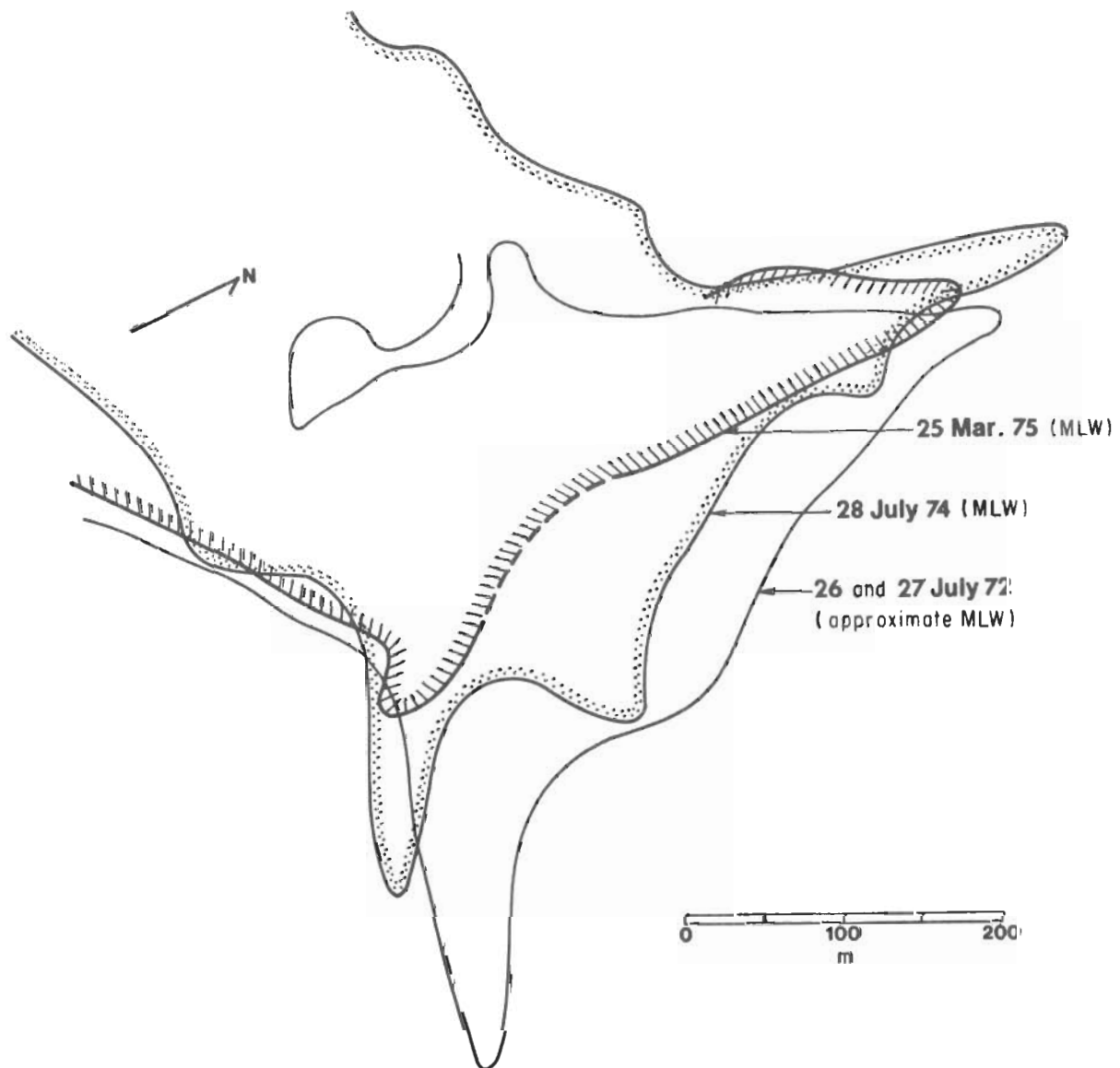
Figure 40. North Inlet flood tidal delta planforms.

25 Mar. 75 (MLW)

28 July 74 (MLW)

26 and 27 July 72 (approximate MLW)

N

0   100   200
         m
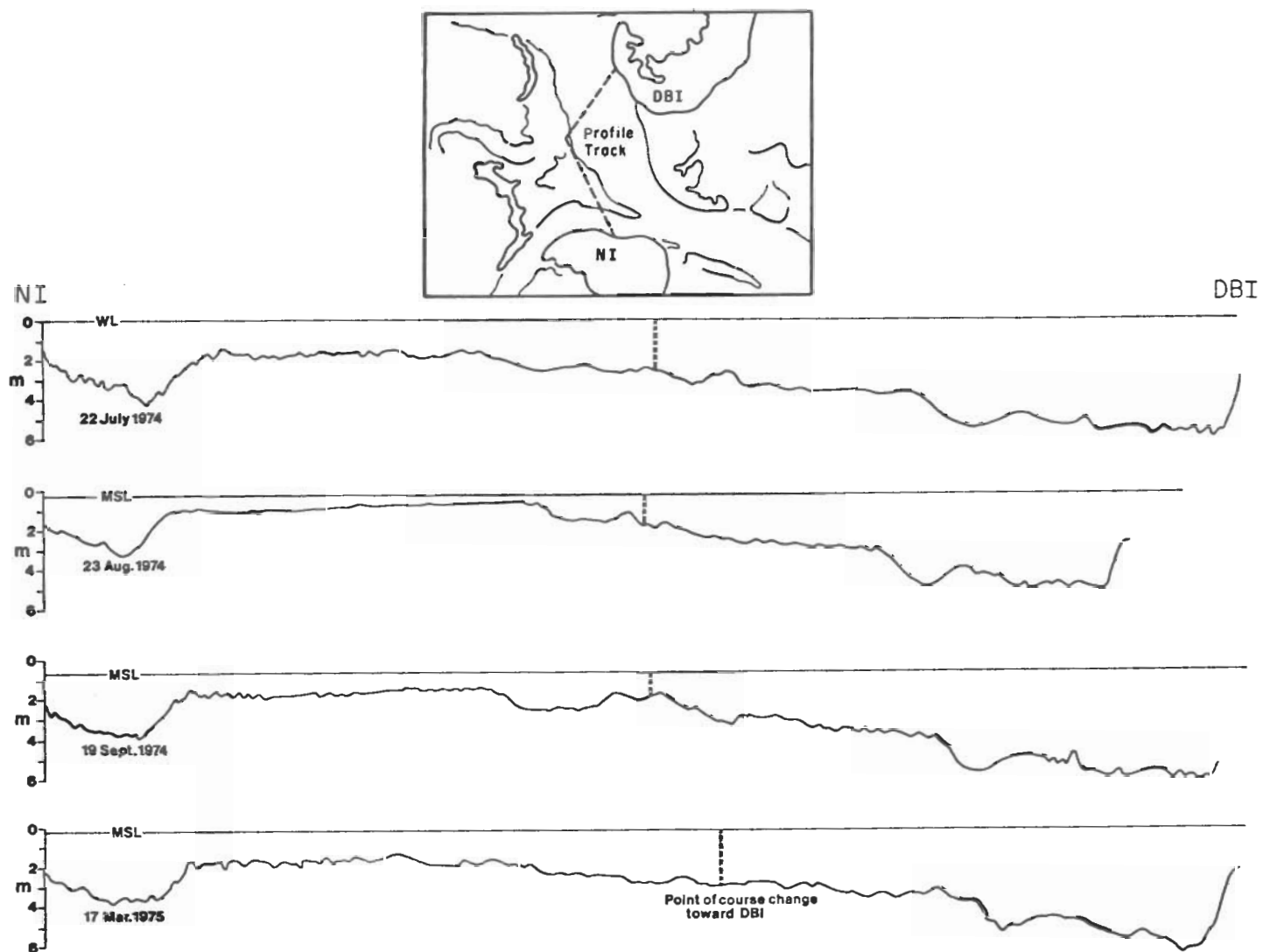
Figure 41. Flood tidal delta profiles.

interpretation should be made of the horizontal scale. Matching of the overall topography and similar depth are interpreted as indicating little change in the region of the Jones Creek and Town Creek channels.

The flood tidal delta is flanked by arcuate sand ridges, or washover berms, which are migrating westward and steadily inundating *Spartina alterniflora* marsh. The northern washover is the lower of the two and has an active slip face on its western margin (Fig. 42). Springtides in combination with an onshore wind are sufficient to cause washover at high tide; a major storm is not required. *Spartina* peat is gradually being uncovered on the seaward side of each ridge, and some recolonization by the grass is taking place.

6. The Ebb Tidal Delta.

The present ebb tidal delta began its growth in the late 1930's when the inlet stabilized near its present position. The high to midtide photo of 1939 (Fig. 20) shows two parallel zones of breaking surf, indicating the presence of channel-margin linear bars flanking the main ebb channel. These components are two of the five major components of the ebb tidal delta model described by Hayes, et al. (1973): (a) Main ebb channel, (b) channel-margin linear bars, (c) terminal lobe, (d) marginal flood channels, and (e) swash bars (Fig. 13). The overall morphology results from a balance of forces due to wave action, flood currents, and ebb currents, with the latter being dominant as described by Hayes, et al. (1973), Boothroyd (1973), and Hubbard (1973). In addition, the entire ebb tidal delta rests on a broad, elevated area termed the ebb tidal platform which is bounded by the terminal lobe.

The former ebb tidal delta, associated with the inlet position of 1878, is still evident as a seaward arc in the offshore bathymetry, especially the 12-foot contour surveyed in 1964 (Figs. 17 and 21). A short segment of a shore-parallel topographic high also remains about 1 kilometer offshore near profile DBI-30 (Fig. 43), and is interpreted as a southerly-directed segment of the old channel-margin linear bar. Another short segment, now evident as a shore-attached shoal, may have been part of the inner channel-margin linear bar. These features seem to appear on the DBI-30 offshore bathymetric profiles, especially that of 16 September 1974, which may have been slightly north of the true track and, therefore, picked up more of the offshore relict topography.

The intertidal features of the North Inlet ebb tidal delta are the channel-margin linear bars and a series of swash bars south of the inlet on the ebb tidal delta platform (Fig. 44). These have been studied primarily by aerial photos and quarterly bathymetric profiles from July 1974 through March 1975. General changes between the vertical aerial views of April 1974 and March 1975 (Figs. 38 and 39) are: (a) Increasing length and a slight increase in width of the southern channel-margin linear bar, (b) increase in width of the spillover channel breaking up the northern channel-margin linear bar, and (c) northward and shoreward migration of swash bars on the ebb tidal delta platform off North Island.

The northern channel-margin linear bar has become increasingly segmented by the widening of the spillover channel with time. This channel has also increased in length relative to its 1970 configuration (compare Figs. 20, 38, and 39). Bathymetric profile NI-6
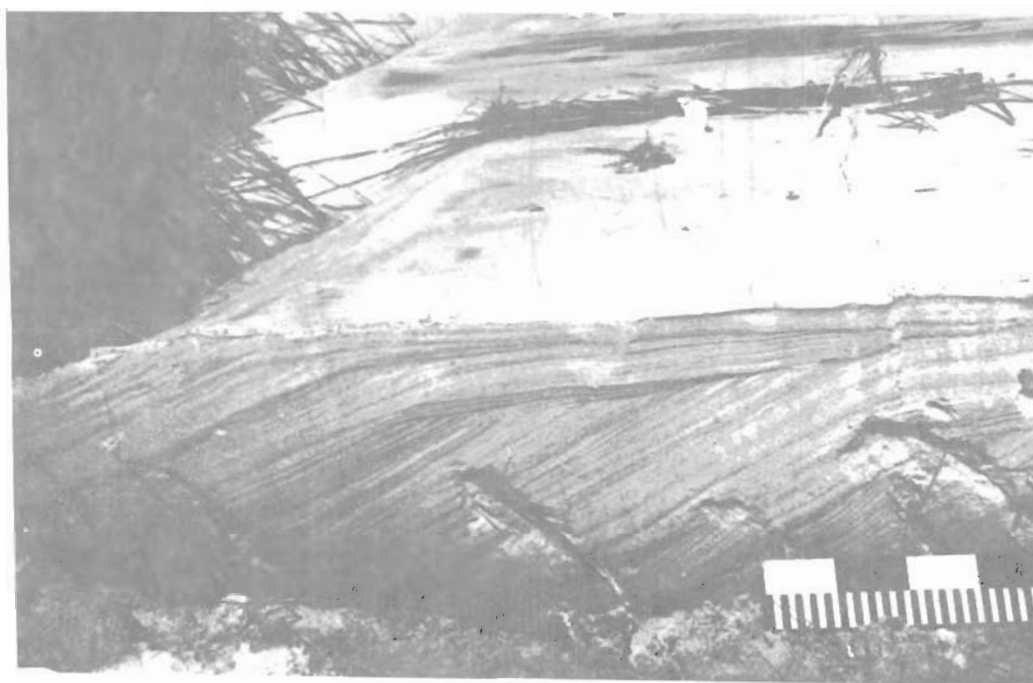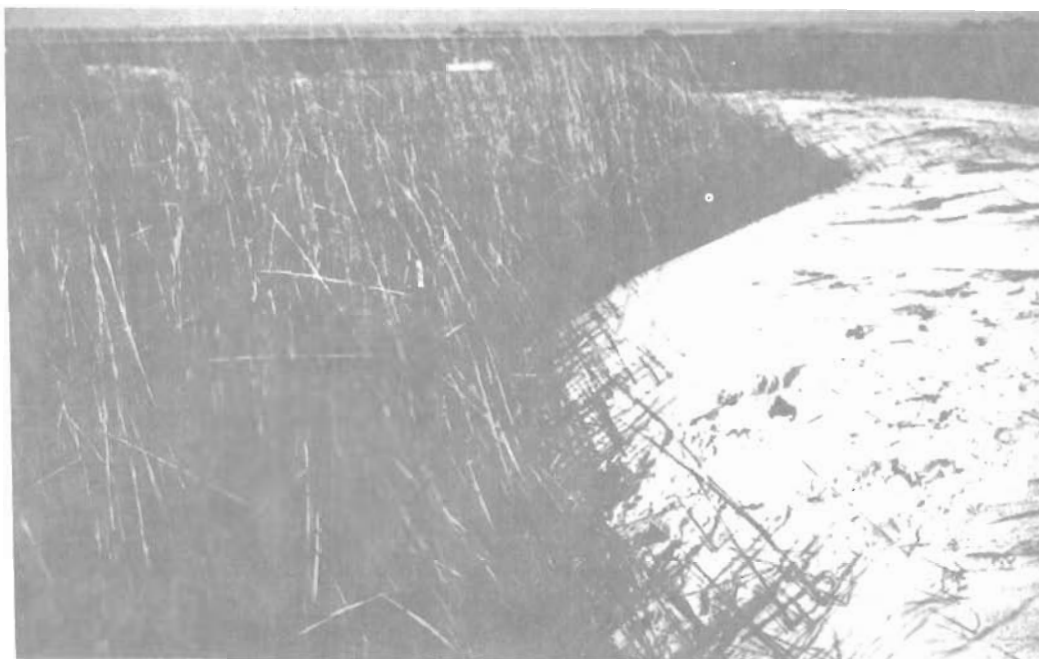
Figure 42. Washover berm (upper photo) and slip face cross section (lower photo)
(Larger divisions on scale are 10 centimeters.)
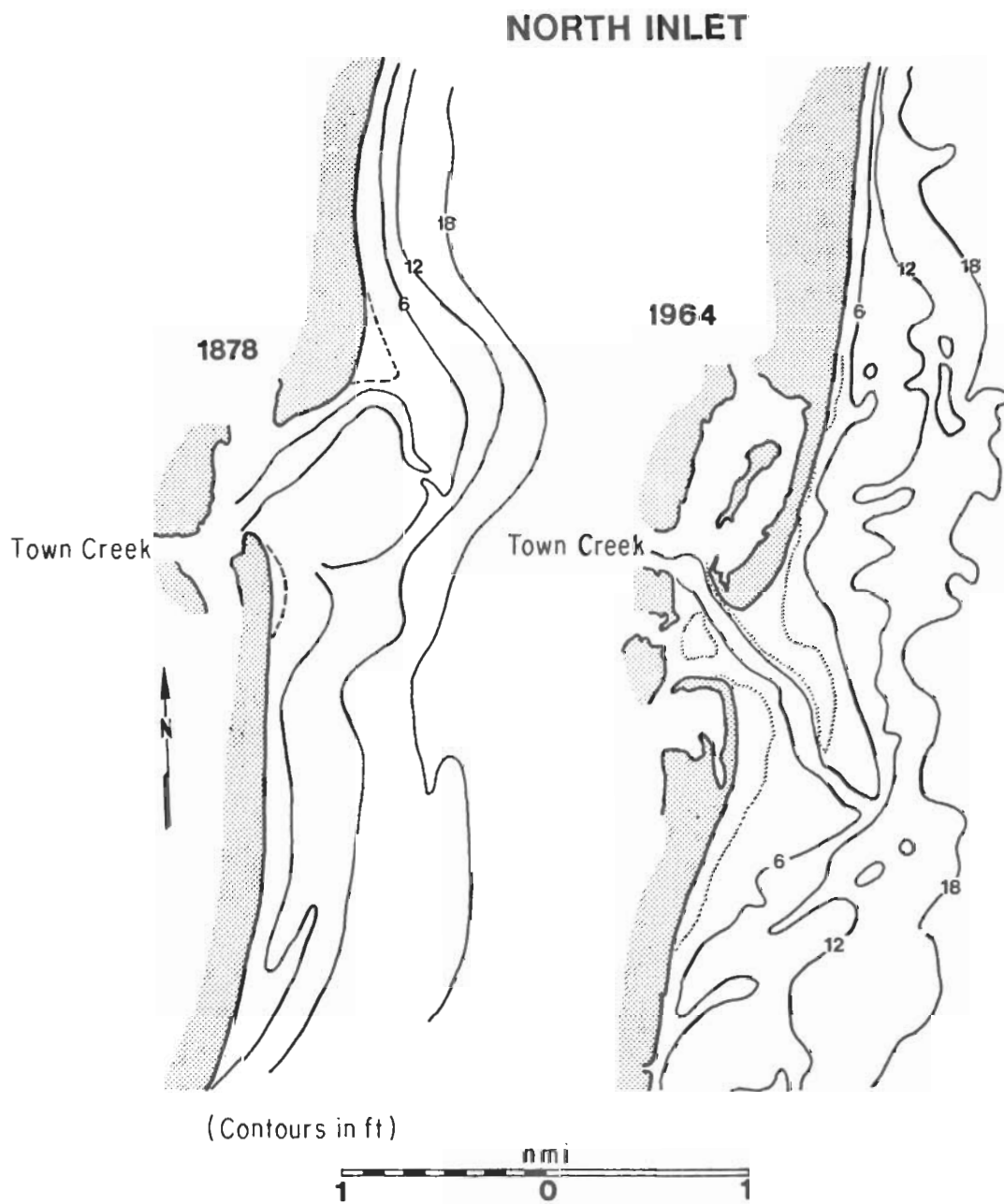
NORTH INLET

Figure 43. North Inlet offshore bathymetry, 1878 and 1964.
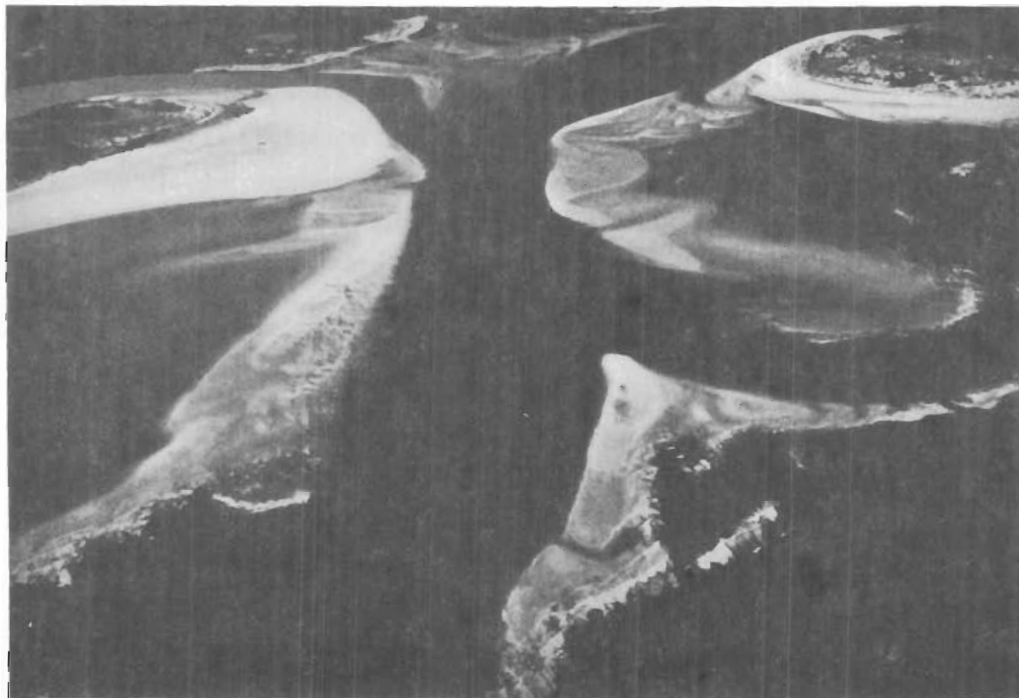
Figure 44. North Inlet channel-margin linear bars, January 1975.

runs offshore through the spillover and shows the gradual slope building up to the high topographic margin of the spillover followed by the rapid drop of the terminal lobe. The margin was some 60 to 70 centimeters higher in September 1974 than in the previous July. This probably represents a buildup by ebb tidal currents in a period which, as evidenced by berm development on beach profiles (Fig. 33), was accretionary. By March 1975, the margin was again lower by about 70 centimeters, representing destructive wave action, probably beginning with the 23 September 1974 northeast storm.

Since 1972 the inner part of the northern bar has grown in a southwestward direction with the addition of sand eroded from the Debidue Island shoreline. A pronounced ebb shield margin was present in January 1975, and profile DBI-6 indicates upward growth of the entire shoal relative to MSL. Shoaling of the channel-margin linear bar off profile DBI-8 was also recorded, and depths below MLW in the first 300 meters offshore have changed from some 60 centimeters to about 30 centimeters between July 1974 and March 1975.

The predominant bed forms seen on the channel-margin linear bar at low tide are megaripples formed in response to high-velocity ebb flow. This process is active even during high wave conditions, with surface modification by waves taking place as the bed forms emerge at low water (Boothroyd, 1973). The linear megaripples are formed at velocities of 40 to 65 centimeters per second, depending on water depth; the cuspate megaripples develop at velocities of 60 to 80 centimeters per second, depending on depth (Boothroyd and Hubbard, 1974). The megaripples on the channel-margin linear bar reverse orientation during flood and migrate across the bar toward the ebb channel. Trenches perpendicular to megaripple crests show bidirectional planar-tangential cross-lamination, or "herringbone" crossbedding, as a result of the two directions of transport. Transverse and horizontal trenches show trough cross-lamination resulting from megaripple migration.

The main ebb channel at North Inlet trends to the southeast at an azimuth of 135° and measured about 1,150 meters in length from inlet throat to terminal lobe in March 1975. Two morphological components of the channel bottom are evident: (a) A gradual upward slope from depths of 6 meters at the throat (this and subsequent depths referenced to MLW) to about 1 meter ending in an ebb-oriented slip face about 1 meter in height, followed by (b) a relatively level area with some large (100-meter wavelength) barlike features showing a slight rise toward the terminal lobe. Depths at this margin vary from 1.1 to 1.5 meters, beyond which is a rapid drop to 5 or 6 meters of water. The end of the gradual upward slope is located about 700 meters from the throat at the inner end of the spillover lobe through the northern channel-margin linear bar (Figs. 38 and 39). The section of the main ebb channel beyond this point is shallower because it is hydraulically adjusted to a lower volume of ebb flow, some of which was diverted into the spillover channel. During higher energy conditions with waves of 100 to 150 centimeters in height, e.g., 27 March 1975 (Figs. 38 and 39), waves break around the entire margin of the ebb tidal delta including the entrance to the main ebb channel.

The southern channel-margin linear bar has shown variation both in overall shape and in elevation with time. The February 1973 northeast storm pushed the bar to the southwest, obliterating much of it (Fig. 45) and leaving only a short channel-parallel segment. A swash bar covered with smaller swash features trailed off to the southeast in May 1973 and remained through August 1973. By March 1974, the channel-parallel segment of the bar had lengthened significantly in the seaward direction, probably incorporating the sand of the smaller swash features which were no longer evident. In July 1974, only a faint trace of the southeast trailing feature which had formed the stem of the "arrowhead" seen in May 1973 remained (Fig. 46). By this time, the bar was well developed along the channel margin and was growing upward by wave swash accretion along both margins, resulting in the low, central area of the bar between the accretion zones, which appears darker on the photo. Note also in this poststorm sequence that the bar is tending to reattach itself to the beach near the inlet throat as it was in June 1972. Figure 46 also shows the upward growth and increase in width of the bar which had taken place by January 1975, and the infilling of the marginal flood channel area.

Bed forms on the southern channel-margin linear bar, which is entirely beyond the inlet throat section, are primarily linear and cuspate megaripples. The cuspate features tend to be planed off during the late lower water depth stages of the ebb flow. Large linear to slightly cuspate megaripples (spacing 2 to 4 meters) are found in the marginal flood channel between the bar and North Island. When observed at low water, these bed forms are seen as ebb-modified, dominantly flood-oriented features.

The bathymetric profiles (DBI-6, NI-6, and NI-8) crossing the southern channel-margin linear bar have documented the gradual shoaling since July 1974. This process is probably related to buildup by southerly wave swash combined with low-intensity northeast storms activating the littoral transport reversal toward the inlet. The entire process has been one of recovery in the 2 years since the severe February 1973 storm. Comparison of DBI-6 profiles shows that the highest point on the bar margin was 60 centimeters above MLW in September 1974, while in March 1975, a broad area rose some 120 centimeters above MLW.

The ebb tidal delta platform south of the inlet is characterized by multiple shoreward-oriented swash features with slip faces 60 to 100 centimeters in height in some locations (Fig. 13). Attachment of individual swash bars to the beach has in the past resulted in development of a supratidal ridge and ultimately led to the growth of the North Island recurved spit (Fig. 20). In 1975 no major swash feature became shore-attached, and as a result there was a lack of sediment available for transport by the northerly-directed energy flux component. Therefore, beach erosion occurred (Figs. 33 and 47).

Northward migration of the point of attachment of the swash feature (bar A, Fig. 47) forming the southern margin of the ebb tidal delta occurred between July 1974 and March 1975. As this occurred, the large landward-pointed swash bar (bar B, Fig. 47) separated from the swash feature along the margin and migrated landward. Comparison of the vertical aerial
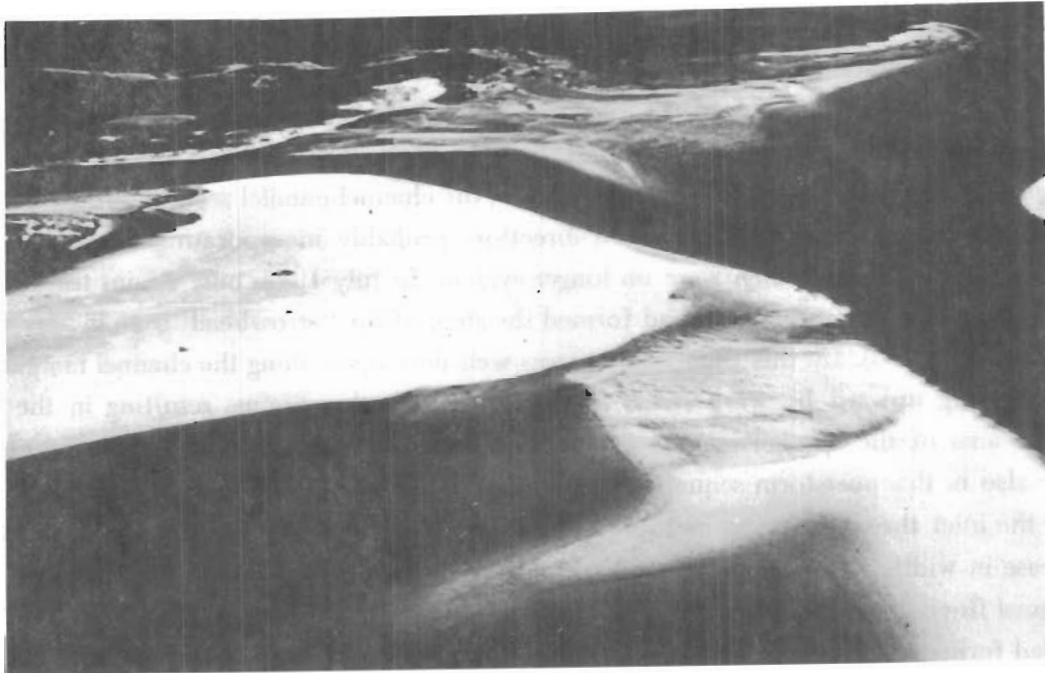
Figure 45. Southern channel-margin linear bar in June 1972 (upper photo) and May 1973 (lower photo).
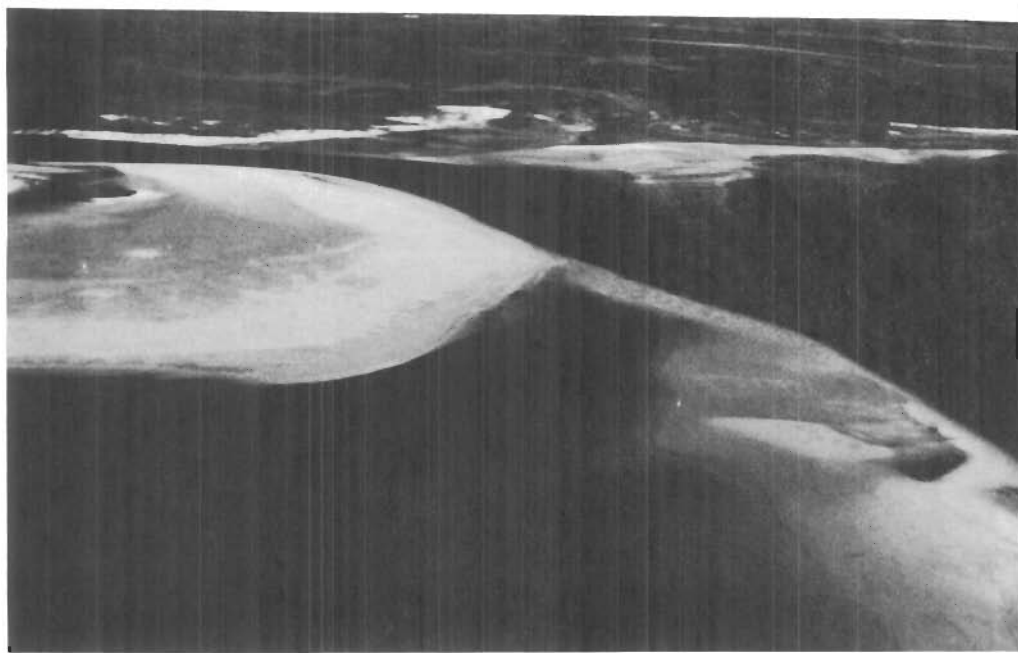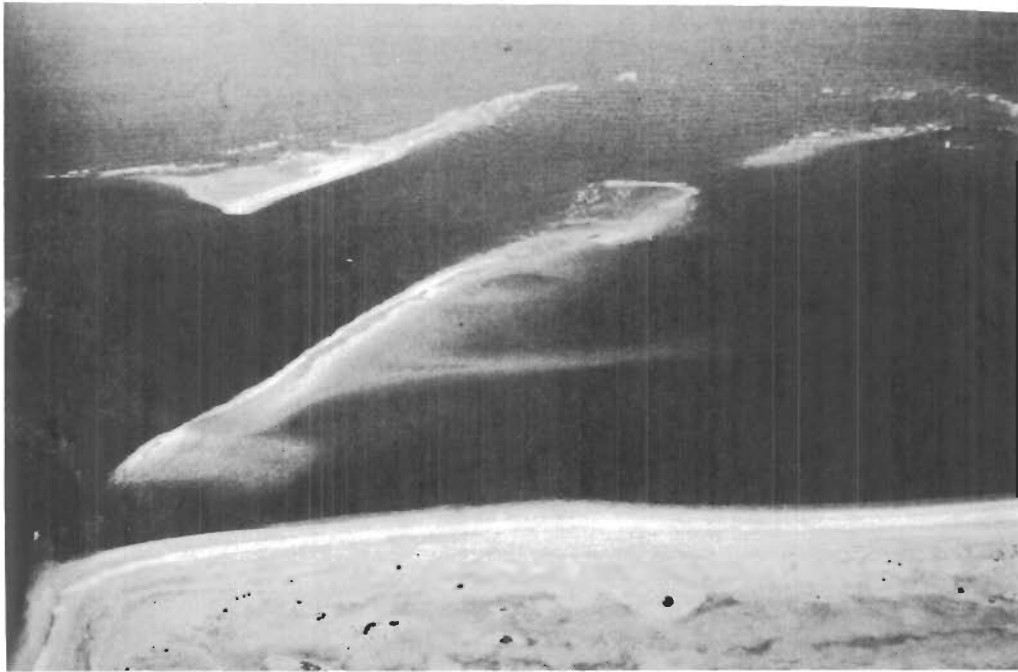
Figure 46. Southern channel-margin linear bar in July 1974 (upper photo) and January 1975 (lower photo).

Figure 47. Swash bars (A and B) south of the inlet, July 1974 (upper photo) and March 1975 (lower photo).

photos of April 1974 and March 1975 (Figs. 38 and 39) shows that this movement was on the order of 91 meters or an average of 7.9 meters per month. Movement of the former, delta platform margin feature at its point of attachment to the beach was on the order of 417 meters, or an average of about 36.3 meters per month. The major slip face on the marginal feature migrated some 98 meters to the northwest (shoreward) or about 8.5 meters per month. The driving force behind these changes was largely the residual shoreward motion associated with shoaling and breaking waves.

VI. TIDAL HYDRAULICS

1. General Introduction and Scope of Information.

The objective of this phase of the study is to examine the tidal hydraulics of this complex, natural tidal inlet under a variety of conditions to investigate several inlet hydraulic characteristics. Current velocity and direction measurements were obtained at 1-meter intervals of depth over complete tidal cycles, both at reconnaissance stations (Fig. 48), and repetitively at established cross sections (Fig. 49), beginning in July 1974. Salinity and temperature measurements were usually made. Bathymetric surveys to determine flow cross-sectional area were made in conjunction with velocity measurements at the Town Creek and Jones Creek velocity sections.

To examine the variation in tidal height and establish surface slopes across the inlet, three tide gages were installed (Fig. 7) at North Inlet. The ocean gage is a Bristol bubbler-type with an orifice installed just seaward of North Island. The creek gages are Leopold and Stevens float types with a stilling well (Fig. 7) which consisted of a 12-inch aluminum culvert held by lengths of iron pipe jetted at least 10 feet into the creek bottom.

Tidal height differentials were obtained by surveying the gages to a common reference level, that of the USC&GS triangulation station, INLET, located near the mouth of Town Creek. Using the reference level and periodic time checks entered into the record, dimensionless values of water surface slope may be calculated between each creek gage and the ocean level. Combined with current velocity data the Manning relationship may then be used to obtain a friction factor n. Analysis using Keulegan's (1967) equations requires a friction factor which is derived from Manning's n. Details of these procedures with specific results are presented below. In addition, current velocity data combined with gage water level elevations and bathymetric profiles have been used to compute the tidal prism and evaluate the relationship between tidal prism and throat cross-sectional area.

Data Collection Procedure for Currents and Salinity. During the first year (June 1972 to June 1973) tidal current measurements were completed over 14 full tidal cycles at 11 stations within the inlet area (Fig. 48). Time velocity asymmetry and current velocity asymmetry (Boothroyd and Hubbard, 1974; Hayes, et al., 1973) were observed. Typical velocity time histories at the 2-meter depth for these stations are in Appendix C; a discussion of these may be found in Finley (1973, 1975). Vertical variation in tidal current velocities is low (Fig. 49) with the exception of near-bottom and near-surface boundary effects, since the waters at North Inlet generally show no salinity stratification.

(Contours in ft)

0   km   1
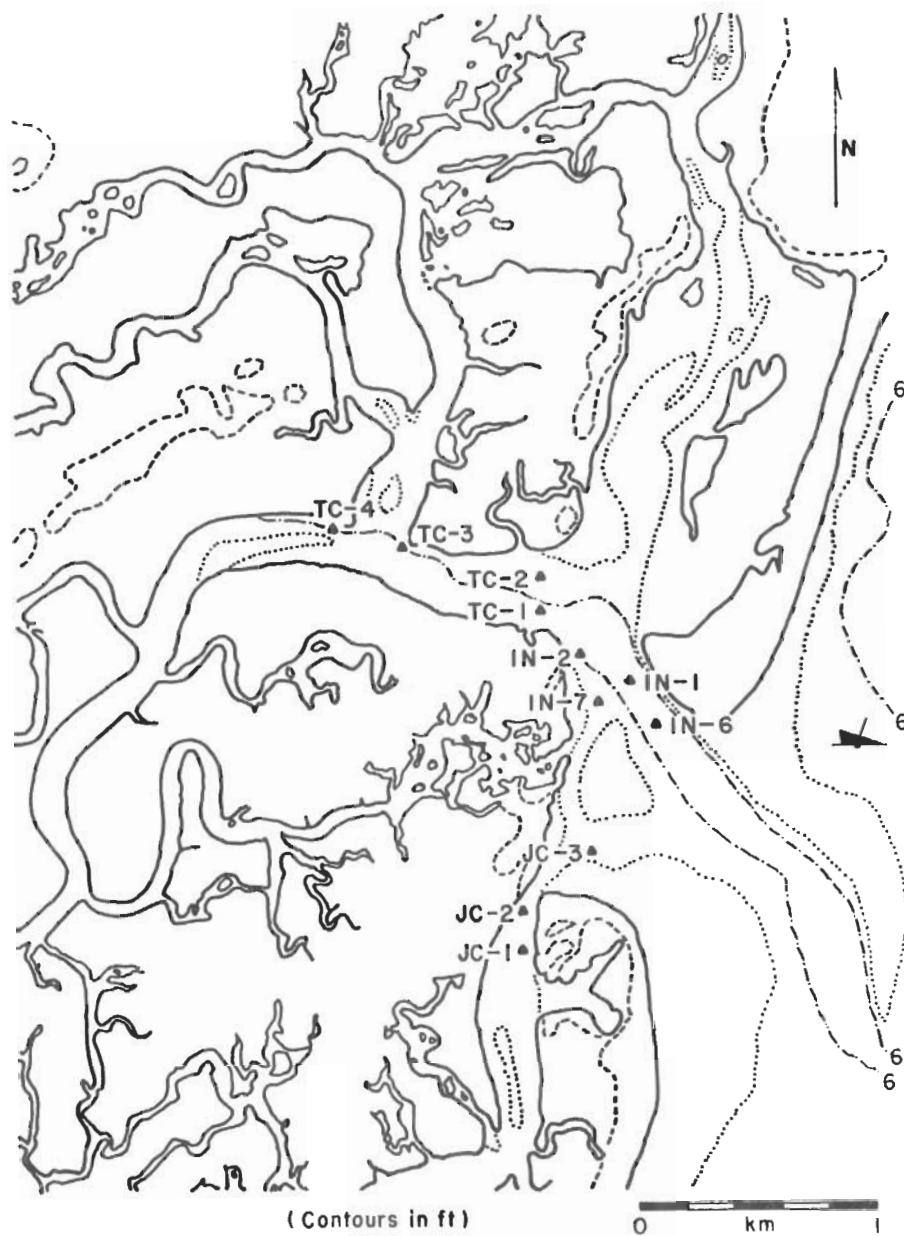
Figure 48. Location of 1972-73 hydrography stations.
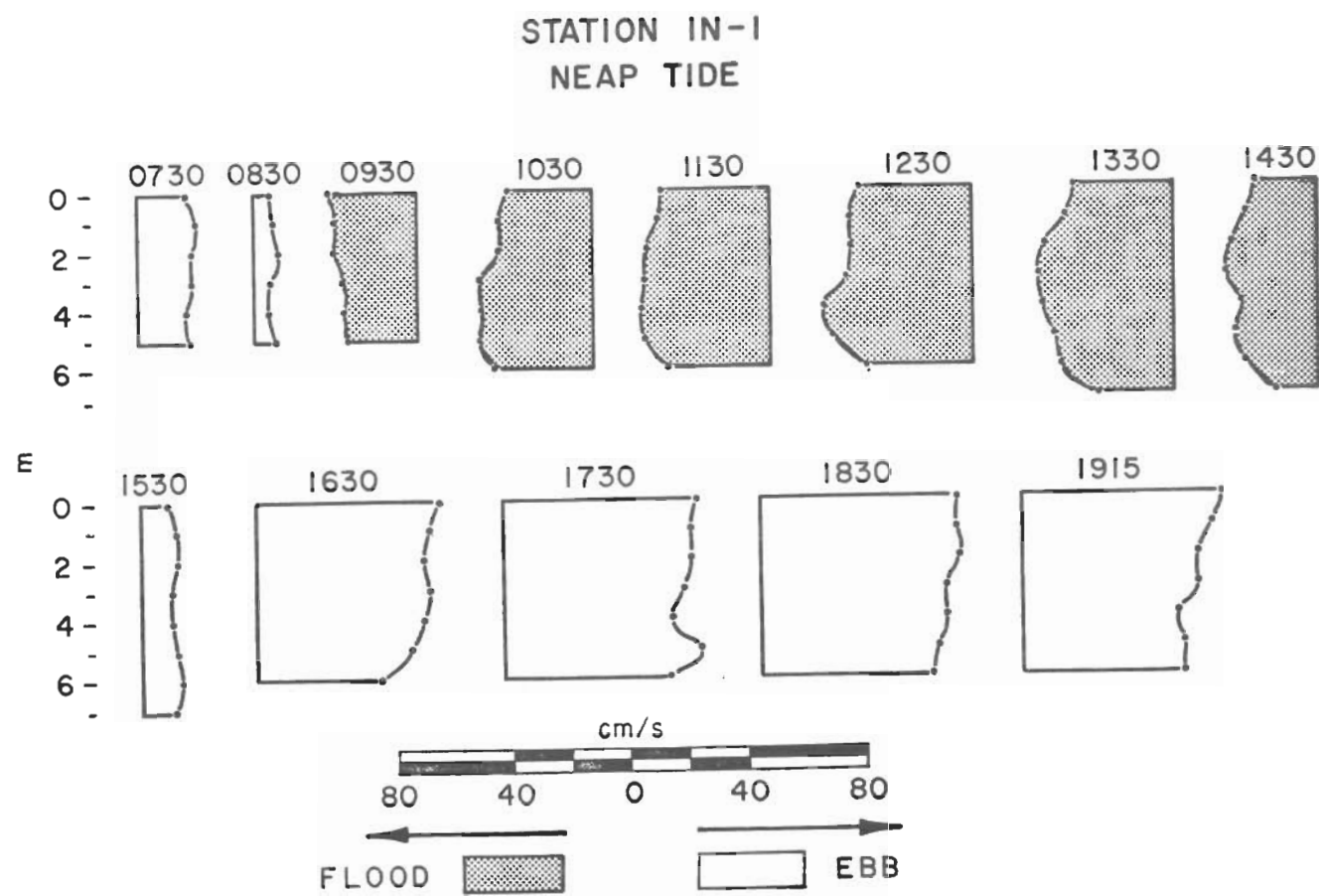
Figure 49. Vertical velocity profiles, 18 July 1972.

During the quarterly 2-week field studies beginning in July 1974, current velocity and direction, salinity, and temperature data were collected at three stations in the channel leading to Town and Debidue Creeks and at two stations in Jones Creek (Fig. 50). Measurements were made over full tidal cycles for spring, mean, and neap tides. In addition, several sets of data were obtained at two stations in the inlet throat. During March 1975, auxiliary velocity measurements were taken in Sixty Bass and Jones Creeks (Fig. 50) concurrently with data collection at the main velocity sections. An Endeco Type 110 current meter with velocity, direction, temperature, and depth readouts was utilized at the main stations along with a Beckman induction salinometer for salinity measurements.

2. Hydraulic Classification of the North Inlet System.

North Inlet best resembles O'Brien's (1971) category 1, a short, low-friction inlet channel connected to a lagoon. The lagoon is largely filled with marsh, leaving only a system of tidal creeks. North Inlet is not a true estuary according to Pritchard's (1967) definition, which requires measurable dilution with freshwater derived from land drainage. With the exception of unusually high runoff into Winyah Bay, or strong south to southwest winds bringing bay waters through the tidal creeks, North Inlet waters are undiluted by freshwater, and are vertically and horizontally homogeneous with respect to salinity. The hydraulic connection to a second bay, such as Winyah Bay, is a complication not present in most of the inlet field studies done to date.

3. Tidal Prism versus Cross-Sectional Area Relationships.

The relationships discussed by O'Brien (1931, 1969) suggest that the equilibrium configuration of an inlet depends on the balance between the tidal flow tending to enlarge the inlet throat cross section and the supply of sediment brought to the inlet by waves and currents tending to reduce the cross section. This tendency toward equilibrium suggested that a specific relationship may exist between entrance area and tidal prism, which for O'Brien's (1931) original Pacific coast data, was:

$$A_c = 4.69 \times 10^{-4} P^{0.85} . \tag{4}$$

Here, A_c = minimum flow cross section of the inlet (throat section) measured below MSL, in square feet, and P = tidal prism corresponding to the diurnal or spring range of tide, cubic feet. O'Brien (1969) introduced another relationship which seemed to be more representative of natural inlets with no jetties:

$$A_c = 2.0 \times 10^{-5} P . \tag{5}$$

Johnson (1973), utilizing mean instead of spring tidal prisms, found as an average for six unjettied inlets on the Pacific coast:

$$A_c = 1.82 \times 10^{-5} P . \tag{6}$$
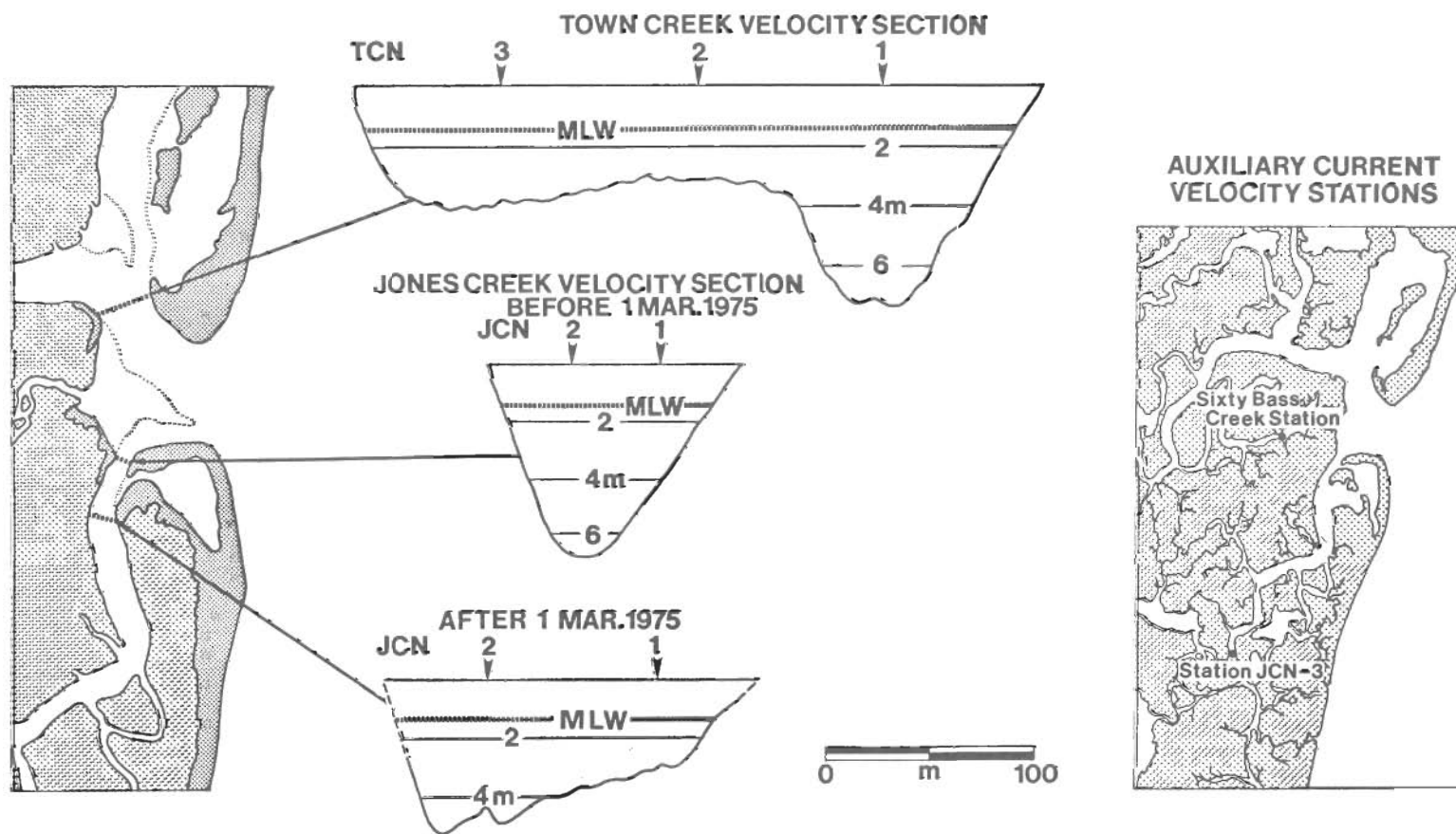
Figure 50. Location of 1974-75 hydrography stations.

Jarrett (1976) has investigated inlets on all three coasts of the United States and noted possible differences in prism-area relationships due to varying tidal range and wave climate on Atlantic, Pacific, and gulf shorelines. His analysis included 108 inlets, 59 of which are located on the Atlantic coast. Results indicated that natural or single-jettied inlets on the Atlantic coast have larger cross sections for a given tidal prism than on the Pacific coast.

At North Inlet, 17 total discharge versus time curves were constructed (App. D), and the resulting ebb and flood tidal prisms computed (Table 14). The mean tidal prism, or volume exchanged on an average ebb or flood half-tidal cycle, based on all discharge calculations, is 14.963×10^6 cubic meters, or 5.283×10^8 cubic feet, which is near the lower end of the range of data developed by Jarrett (1976). Spring and mean tidal prisms versus cross-sectional areas for the quarterly data and for the throat section hydrography of April 1975, have been plotted on a section of Jarrett's diagram (Fig. 51). Although within the 95-percent confidence limits of Jarrett's data, the North Inlet springtide data tend to plot above the regression line.

a. Seasonal Variation in A_c. The section on recent inlet morphology detailed the percentage changes in the inlet cross-sectional area (Fig. 28). Since the April 1975 value is only some 3 ± 2 percent less than the July 1974 value, it appears that the inlet area is tending to return to an equilibrium summer configuration after winter deposition. This may be an indication of a seasonal cycle with about a 10-percent decrease during fall and winter periods when storms result in increased littoral drift supply to the inlet, and then an opposite trend in the late spring and summer. Superimposed on this trend are the longer term changes which have been noted, such as erosion of the flood tidal delta's ebb spit at the throat section and overall widening of the inlet.

b. Differences in Ebb versus Flood Tidal Prisms. Variation in ebb and flood tidal prisms (Table 14) measured during any complete 12.42-hour tidal cycle results from: (a) The diurnal inequality between successive high and low waters, (b) meteorological effects of onshore or offshore winds, and (c) hydraulic effects due to the connection of North Inlet waters to Winyah Bay. Of the total 16 complete cycles monitored, 7 had larger ebb prisms, 7 had larger flood prisms, and 2 had ebb versus flood prisms varying by 1.1×10^6 cubic meters (6 percent) or less. An attempt at assessing these factors is made in Table 15. In several cases, the diurnal inequality, expressed as a percentage of the maximum range for the tidal cycle, is of the same magnitude as the percentage difference between ebb and flood tidal prisms. In 5 (20 July 1974, 24 August 1974, 21 September 1974, 27 October 1974, and 4 January 1975) of the 17 cases, the direction of the diurnal inequality would indicate a prism excess opposite to that actually measured, but in 3 of these cases either Winyah Bay runoff reaching North Inlet or a steady onshore wind would be acting in the same direction as the measured prism difference. However, the fourth case in this group (27 October 1974) is one in which the tidal prisms are essentially in balance; therefore, it seems that at least qualitatively the diurnal inequality, wind and bay runoff account for the observed ebb and

Table 14. North Inlet ebb and flood tidal discharge.

Date	Tide	Flood	Ebb	Mean	Mean
		Prism			
		(millions of m^3)			(10^8 ft^3)
1974					
20 July	spring	20.976	15.876	18.426	6.506
26 July	mean	18.036	13.050	15.543	5.488
1 Aug.	neap	18.864	13.680	16.272	5.746
24 Aug.	mean	15.624	16.452	16.038	5.663
15 Sept.	spring	25.524	20.052	22.788	8.046
21 Sept.	mean	15.480	18.162	16.821	5.939
27 Sept.	neap	16.614	13.860	15.232	5.378
27 Oct.	mean	17.010	18.117[1]	16.557	5.846
1975					
4 Jan.	mean	14.796	11.196	12.996	4.589
7 Jan	neap	10.044	11.304	10.674	3.769
12 Jan.	spring	13.716	20.232	16.974	5.994
22 Feb.	mean	13.068	16.452	14.760	5.211
19 Mar.	neap	7.819	12.737	10.278	3.629
21 Mar.[2]	mean	7.433	11.954	9.694	3.423
22 Mar.	mean	10.604	12.765	11.685	4.126
24 Mar.	spring	10.855	19.369	15.112	5.336
26 Apr.[2]	spring	16.668	12.387	14.528	5.130

[1] Estimate based on two-thirds of ebb cycle measured.
[2] Based on two throat section stations.
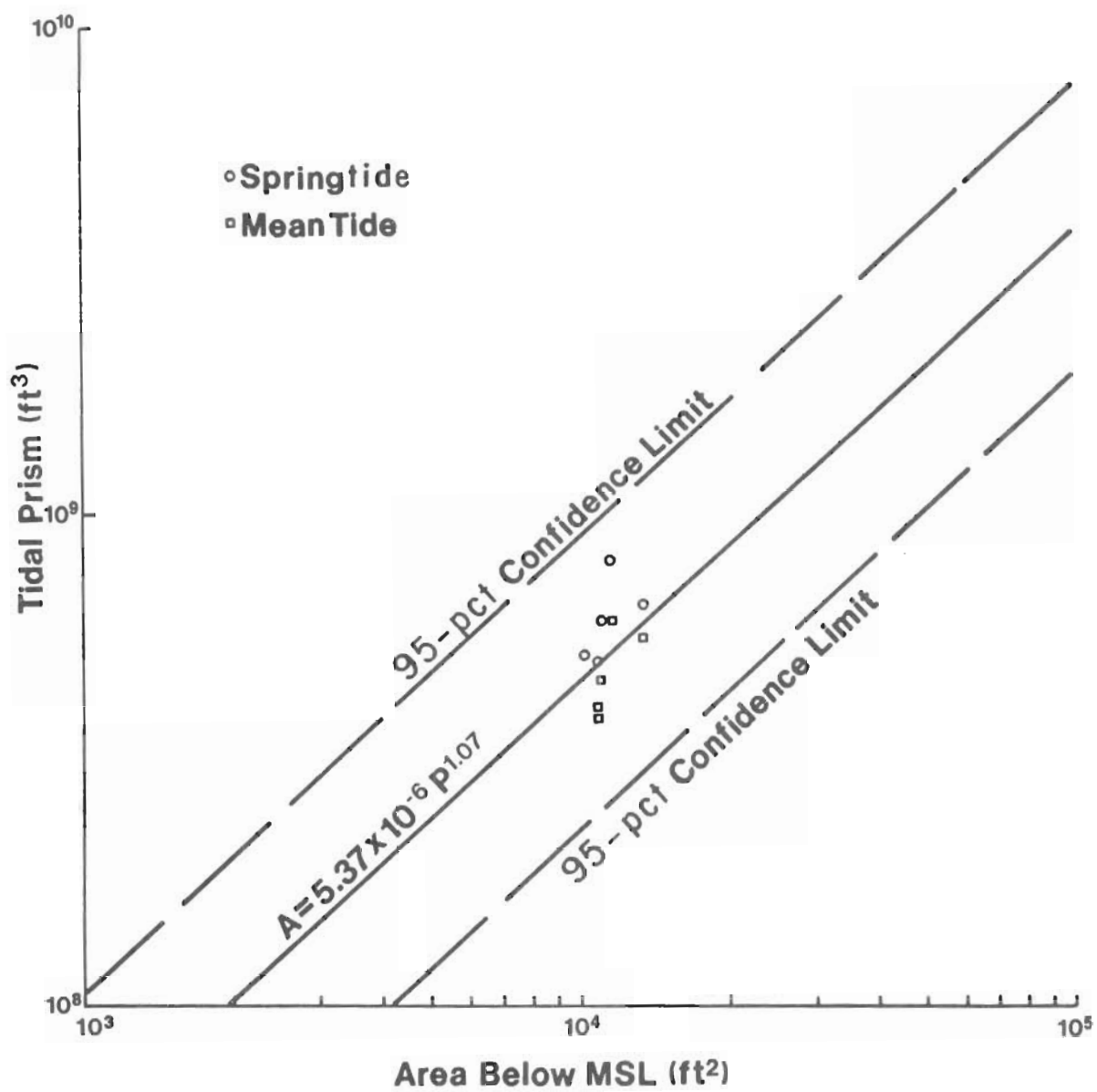
Figure 51. Tidal prism versus cross-sectional area, North Inlet (after Jarrett, 1976).

Table 15. Factors influencing tidal prism inequality.

Date	Predicted tide	Daily mean range[1] (cm)	Prism			Diurnal inequality[2]	Wind[3]	Winyah Bay runoff[4]
			Flood	Ebb	Pct. excess	+ = higher	+ = onshore	
			(millions of m^3)		+ = flood − = ebb	− = lower	− = offshore	
1974								
20 July	spring	184	20.976	15.876	+24.3	(L) −3.5	0[5]	no
26 July	mean	136	18.036	13.050	+27.6	(L) +8.1	+8	----
1 Aug.	neap	146	18.864	13.680	+27.5	(H) +20.3	0	----
24 Aug.	mean	122	15.624	16.452	−5.0	(L) +14.0	----	yes
15 Sept.	spring	188	25.524	20.052	+21.4	(H) +3.7	+7	no
21 Sept.	mean	125	15.480	18.162	−17.3	(L) +19.6	0	yes (minor)
27 Sept.	neap	117	16.614	13.860	+16.6	(H) +14.0	+8	-----
27 Oct.	mean	133 (J)	17.010	18.117	−6.1	(H) +2.6	----	no
1975								
4 Jan.	mean	151 (J)	14.796	11.196	+24.3	(L) −12.4	0	no
7 Jan.	neap	130	10.044	11.304	−11.1	(L) −15.0	0	no
12 Jan.	spring	155	13.716	20.232	−32.2	(L) −2.2	0	no
22 Feb.	mean	141	13.068	16.452	−20.6	(L) −21.6	-----	-----
19 Mar.	neap	132	7.819	12.737	−37.3	(L) −51.2	−12	yes
21 Mar.[6]	mean	114	7.433	11.954	−37.8	(L) −1.9	0	yes
22 Mar.	mean	139	10.604	12.765	−16.8	(L) −24.5	−14	yes
24 Mar.	spring	171	10.855	19.369	−44.2	(H) −7.9	−15	yes
26 Apr.[6]	spring	185 (J)	16.668	12.387	+25.7	(H) +18.7	-----	yes

[1] Measured at Town Creek gage, except when gage out, then at Jones Creek (J).

[2] Difference in elevation between high (H) or low (L) tide 12½ hours after starting point, expressed as a percentage of higher range.

[3] Wind at a steady velocity of 7 knots or more for 3 hours or more; ----- indicates no readings.

[4] Presence of Winyah Bay brackish water as indicated by lowered salinities at North Inlet; ----- indicates no readings.

[5] Not effective.

[6] Based on two throat section stations.

flood tidal prism differences. This inference is further substantiated by the fact that the largest imbalances occur in the ebb direction in March 1975, when all three factors were tending to reinforce each other in the ebb direction. The lowered salinities indicating Winyah Bay runoff were due to substantial rains along the coast that occurred early during the 2-week quarterly study, and the winds were from the south and southwest.

The dominant ebb discharge of Jones Creek at Noble Slough (JCN-3 in Fig. 49) on 19 March 1975 (App. D, Fig. D-13), is further evidence of the importance of the connection to Winyah Bay. During 11.5 hours of measurement, floodflow from North Inlet occurred for a period of only about 3 hours, and the relative volumes were about 576,000 cubic meters flood discharge and 1,908,000 cubic meters ebb discharge.

c. Division of Discharge Between Jones and Town Creeks. The total tidal prism at North Inlet has been computed from the sum of the flow through the Jones Creek and Town Creek measurement sections except for the 21 March and 26 April 1975 data, which were computed from inlet throat measurements. The only flow which is not measured at these two sections is that which flows into Sixty Bass Creek behind the flood tidal delta, a route which may be taken during approximately one-half the tidal cycle from midflood through high water to midebb and probably accounts for less than 5 percent of the tidal prism. Incomplete measurements in Sixty Bass Creek (App. D, Fig. D-18) show that easterly ebb flow occurs for 2.5 to 3 hours during a mean tidal cycle before direction reversal occurs and the ebb waters flow west into Town Creek.

The volumes of water flowing only through the Town Creek channel (Table 16) indicate that on the average 73.4 percent of the flood prism and 74.0 percent of the ebb prism discharge through the Town Creek measurement section. When Winyah Bay brackish waters are detected, salinities tend to be lower in Jones Creek than in Town Creek. Excluding the incomplete data of 27 October 1974, 9 of the 14 tidal prisms (Table 16) show 2 to 9 percent greater ebb flow than floodflow through Jones Creek. Therefore, Winyah Bay waters may be regularly contributing to the ebb tidal prism measured at North Inlet.

Ebb currents from Town and Jones Creeks formed the trailing ebb spit of the flood tidal delta which acted as a barrier between the two zones of flow. This was often indicated by a foam line at the water mass boundary which trailed seaward from the spit during ebbtide. To determine the current patterns on either side of the foam line, a dye streak was rapidly spread across the inlet throat about one-half hour before a typical low water. Figure 52 shows Jones Creek was still ebbing, causing the dye to bow seaward, while Town Creek was essentially slack.

4. Influence of Morphology on Flow Pattern.

Typical tidal current velocity curves (Fig. 53) for stations TCN-1 and TCN-2 (Fig. 49) at the Town Creek velocity section show that over the shallow subtidal flat at TCN-2 flood currents are dominant. This velocity asymmetry occurs because the station area is shielded

Table 16. Town creek tidal prisms.

Date	Tide	Prism (10^6 m^3)		Total Prism (pci)	
		Flood	Ebb	Flood	Ebb
1974 20 July	spring	16.983	11.412	80.9	71.9
26 July	mean	12.996	10.188	72.1	78.1
1 Aug.	neap	12.924	8.550	68.5	62.5
24 Aug.	mean	12.366	12.708	79.2	77.3
15 Sept.	spring	18.864	13.266	73.9	66.2
21 Sept.	mean	10.692	13.608	69.1	74.9
27 Sept.	neap	12.330	9.552	74.2	68.7
27 Oct.	mean	11.538	16.983[1]	67.8	93.7[1]
1975 4 Jan.	mean	10.962	8.784	74.1	78.5
7 Jan.	mean	6.228	6.804	62.0	60.2
12 Jan.	spring	9.000	15.048	65.6	74.4
22 Feb.	mean	10.512	12.888	80.4	78.3
19 Mar.	neap	5.771	8.413	79.0	72.1
22 Mar.	mean	7.666	8.943	78.0	75.7
24 Mar.	spring	9.017	16.270	76.6	77.7

[1] Estimate based on two-thirds of ebb cycle measured.

from Town Creek ebb flow which does not turn southeast and seaward until it is blocked by Debidue Island just north of station TCN-1. At TCN-1 ebb dominance is typically present for this reason, and the tendency is for ebb currents to be stronger in the deeper channel due to the confining effect of the channel walls as the water level drops. Station TCN-3 also shows flood dominance and is usually the first to show floodflow as the tide turns, while a slight ebb current may still be present at TCN-1.

In Jones Creek at the flow section occupied before March 1975, station JCN-1 (Fig. 50) is shielded from floodflow by the northeast tip of the North Island recurve. This locality also shows slightly lower ebb velocities, as the ebb current follows the outer bank of the curved channel near station JCN-2. Ebb currents are generally 10 to 20 centimeters per second greater at this station. A near-vertical upper channel wall developed west of JCN-2 as currents cut into *Spartina alterniflora* peat.
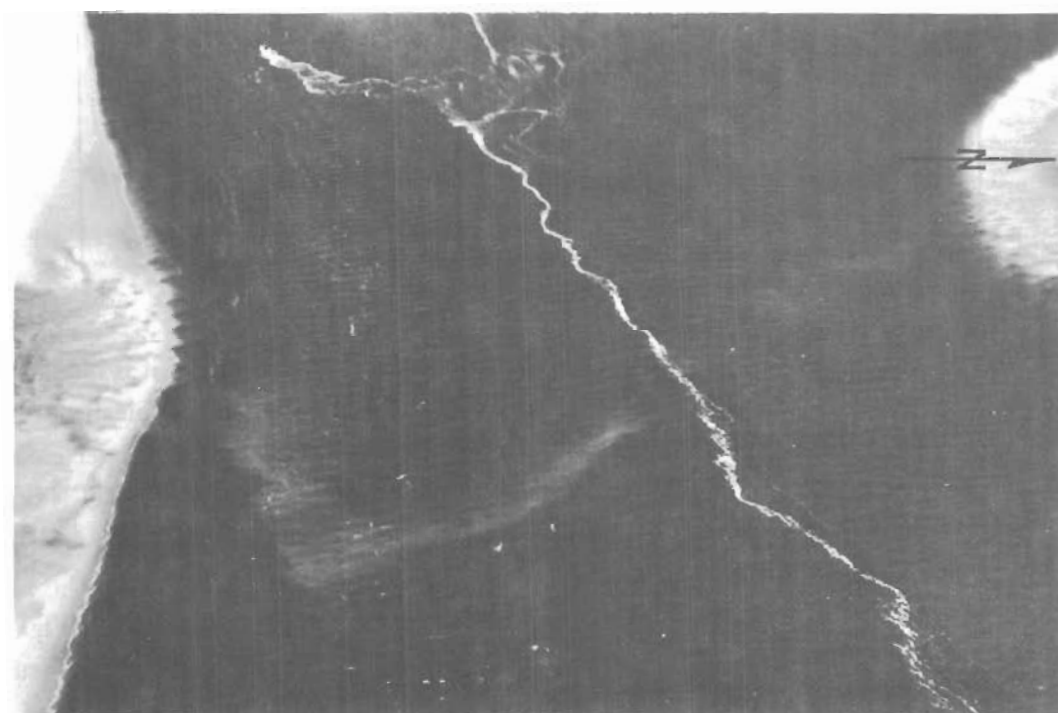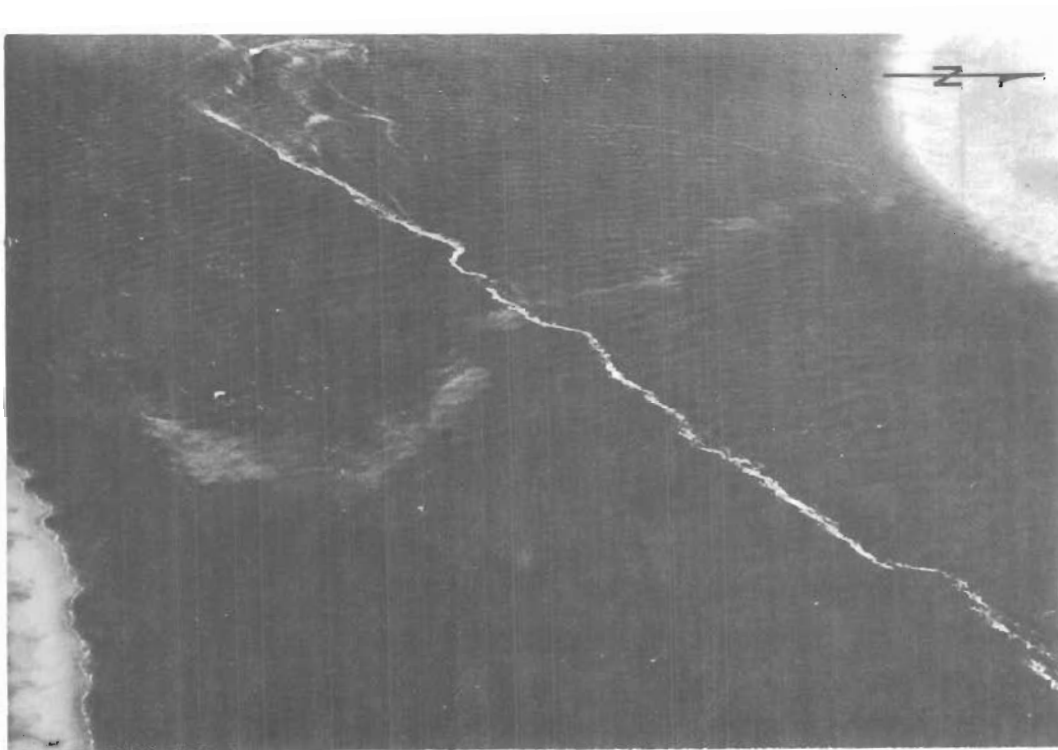
Figure 52. Variation in ebb flow between Jones Creek (upper photo) and Town Creek (lower photo). Upper photo was taken 4 minutes before lower photo.
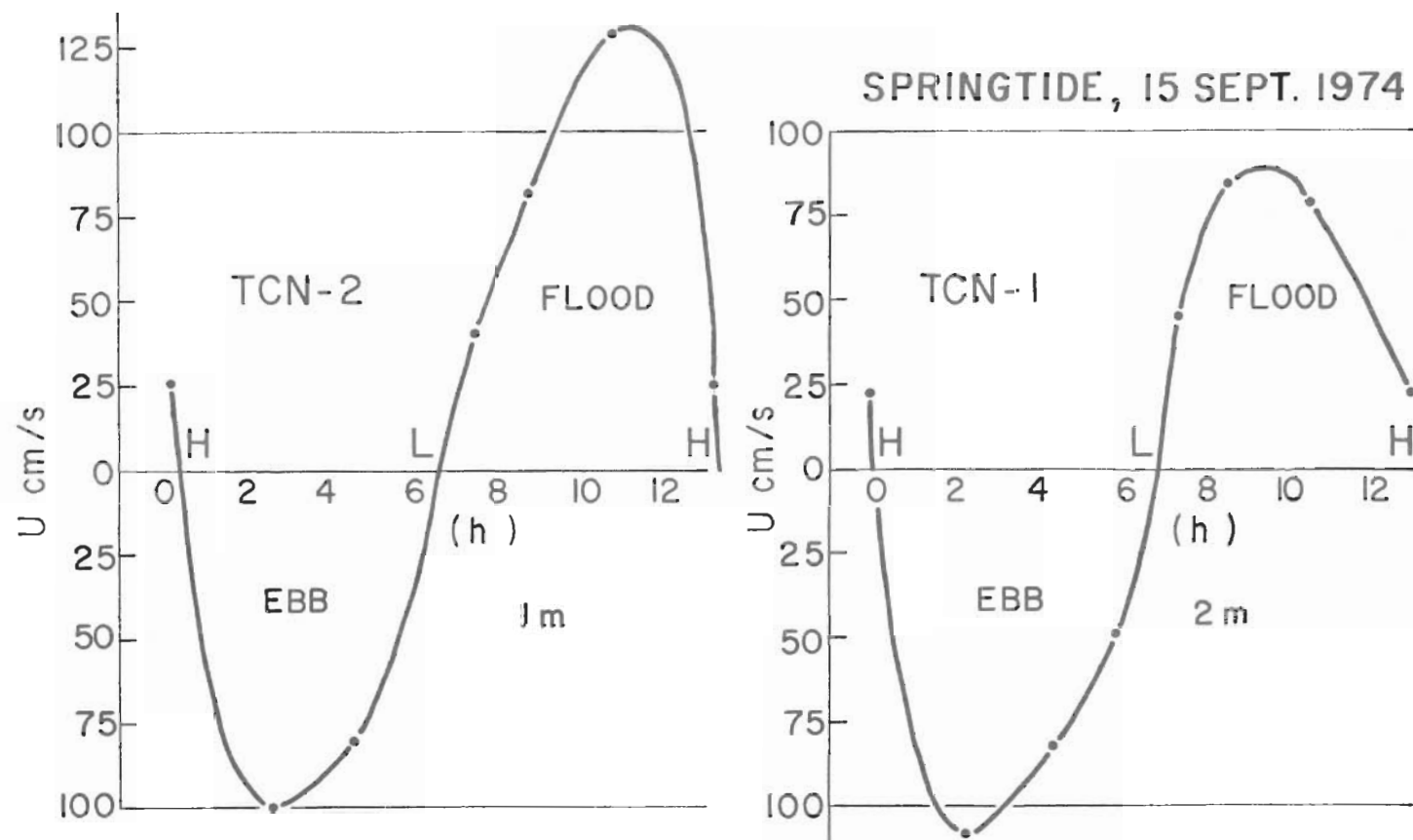
Figure 53. Tidal current velocities at stations TCN-1 and TCN-2.

5. Water Level Differences and Tidal Flow Velocities.

a. Range of Tidal Elevation. Jones Creek and Town Creek tide gage records from 31 October to 31 December 1974 were analyzed to investigate additional parameters. This period was selected because it runs from October high springtides to December high springtides, and the records were uninterrupted. A paired t-test (Dixon and Massey, 1969) was run using 119 values of tidal range from each location with results indicating that, at the 95-percent confidence level, the tidal range at Town Creek averages 4.2 centimeters greater. Both Town Creek and Jones Creek tidal ranges have already been shown to be smaller than the ocean range based on November 1974 data.

The lower ranges at the two interior gages may most likely be attributed to energy loss due to frictional resistance of the channel. Keulegan (1967) expressed this type of loss as a head loss "necessary to overcome the resistance of the connecting channel" with the formula:

$$\Delta H_2 = \lambda \frac{L}{r} \frac{V^2}{2g}, \tag{7}$$

where ΔH_2 is head loss due to friction, λ is a friction coefficient, L is the length of the connecting channel, r is hydraulic radius, and V is mean current velocity. This expression represents a static balance between water level differential across the inlet and inlet channel friction. Entrance and exit losses are not considered nor are inertial effects. Factors leading to the higher tidal range at the Town Creek gage than at Jones Creek may be: (a) More direct alinement with the main inlet channel, and (b) relatively less friction loss in the wider channel between the gage and the inlet throat.

b. Water Surface Slopes and Tidal Velocities. Keulegan's (1967) analysis shows that the elevation difference between ocean and basin can be related to the mean velocity by:

$$V^2 = \frac{2gr}{\lambda L + mr} (H_2 - H_1), \tag{8}$$

where H_2 is the ocean surface elevation above a reference plane and H_1 is the bay surface elevation above a reference plane. The difference,

$$H_2 - H_1 = \Delta H_1 + \Delta H_2, \tag{9}$$

has two components, ΔH_1 and ΔH_2, the latter having been introduced as the fall necessary to overcome channel resistance. The first, ΔH_1, is the fall necessary to accelerate the water from the sea to the velocity, V, at the entrance channel.

Malfunction of the tide gages allowed calculation of water level differences only for those dates shown in Figures 54 to 57. Analysis was concentrated on the Town Creek versus ocean gage, since 70 percent or more of the flow (Table 16) moves through the Town Creek velocity section. However, two analyses of Jones Creek flow were made for comparison purposes. The velocities shown (Figs. 54 to 57) are mean velocities obtained by averaging all individual readings in the flow section and plotting at an average time of measurement. Also shown are values of Manning's n, a coefficient of friction considered in the following section.

The velocity curves, in some cases (12 January 1975, 22 March 1975 at Town Creek, 24 March 1975), show deflections which correspond to small variations in the water level differential. This would seem logical in view of the relationships just described. However, an instance (12 January 1975 at Jones Creek) of unexpected variation in water level differences was observed and may have been due to abnormal water level fluctuation around the ocean gage orifice. The orifice is semienclosed by the channel-margin linear bar and the swash bars of the ebb tidal delta platform; therefore, wind stress and wave approach may alter the rate of rise and fall of the ocean tide. Such an effect may also occur in the reach of the tidal creeks where the gages are located, leading to irregularities in the water level differentials.

6. Manning's n Friction Coefficient.

A formula introduced by Manning (Chow, 1959) is the most widely used of all uniform flow formulas for steady open channel flow computations. The formula, in metric units, takes the form:

$$V = \frac{1}{n} R^{2/3} S^{1/2} , \tag{10}$$

where V is the mean velocity (meters per second), R is the hydraulic radius (meters), S is the slope of the energy line, and n is Manning's friction coefficient. Using the data graphed in Figures 54 to 57, and assuming that the water surface slope approximates the energy slope, Manning's n values have been calculated for the time of each mean velocity reading and are plotted on the same figure. The channel lengths used in determining water slope were 1,507 meters from the throat section to the Town Creek gage and 793 meters from the throat section to the Jones Creek gage.

Behrens, Watson, and Mason (in preparation, 1976) found that n generally increased during the ebb or flood half of a tidal cycle at New Corpus Christi Pass, Texas. After each slack water, n was a minimum, increasing with time during the following flow conditions. This was also the case at North Inlet for the ebb cycles measured (Figs. 54 to 57), with the exception of 24 March 1975. This is a notable similarity since tides at Corpus Christi are diurnal or mixed with a diurnal range of 0.52 meter and those at North Inlet are semidiurnal
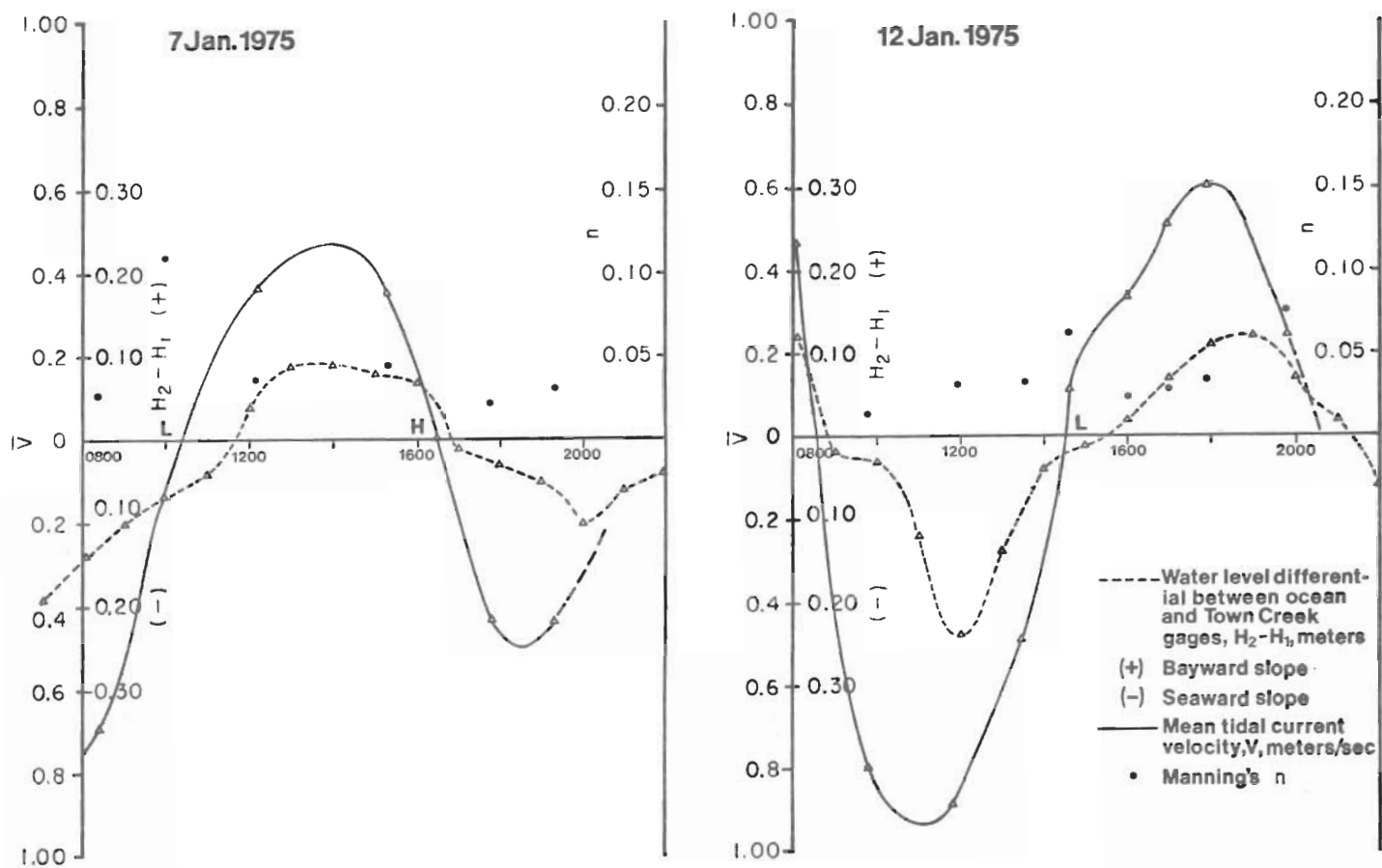
Figure 54. Time histories of tidal differential, currents, and Manning's n at Town Creek, 7 and 12 January 1975.
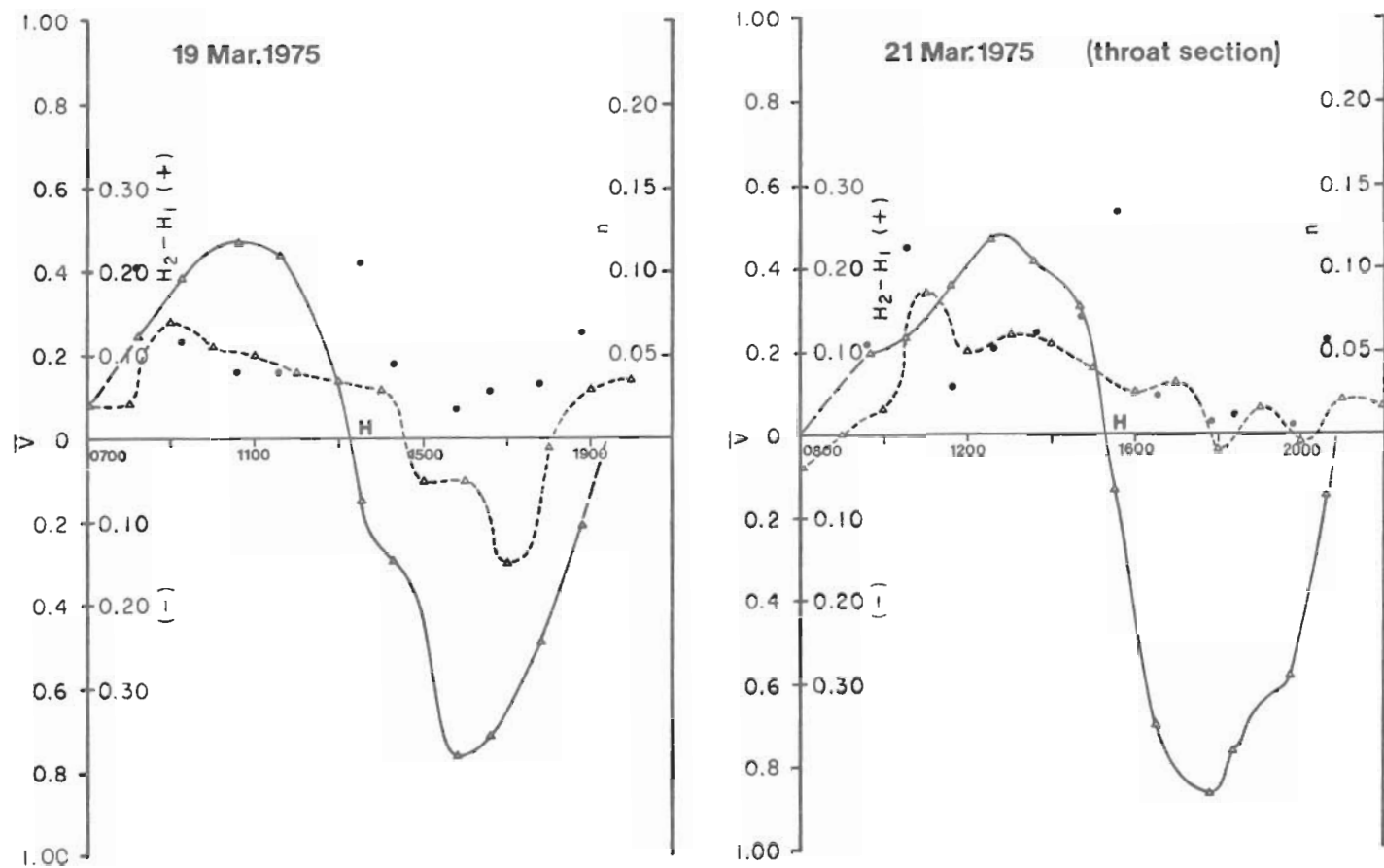
Figure 55. Time histories of tidal differential, currents, and Manning's n at Town Creek, 19 March 1975, and throat section, 21 March 1975.
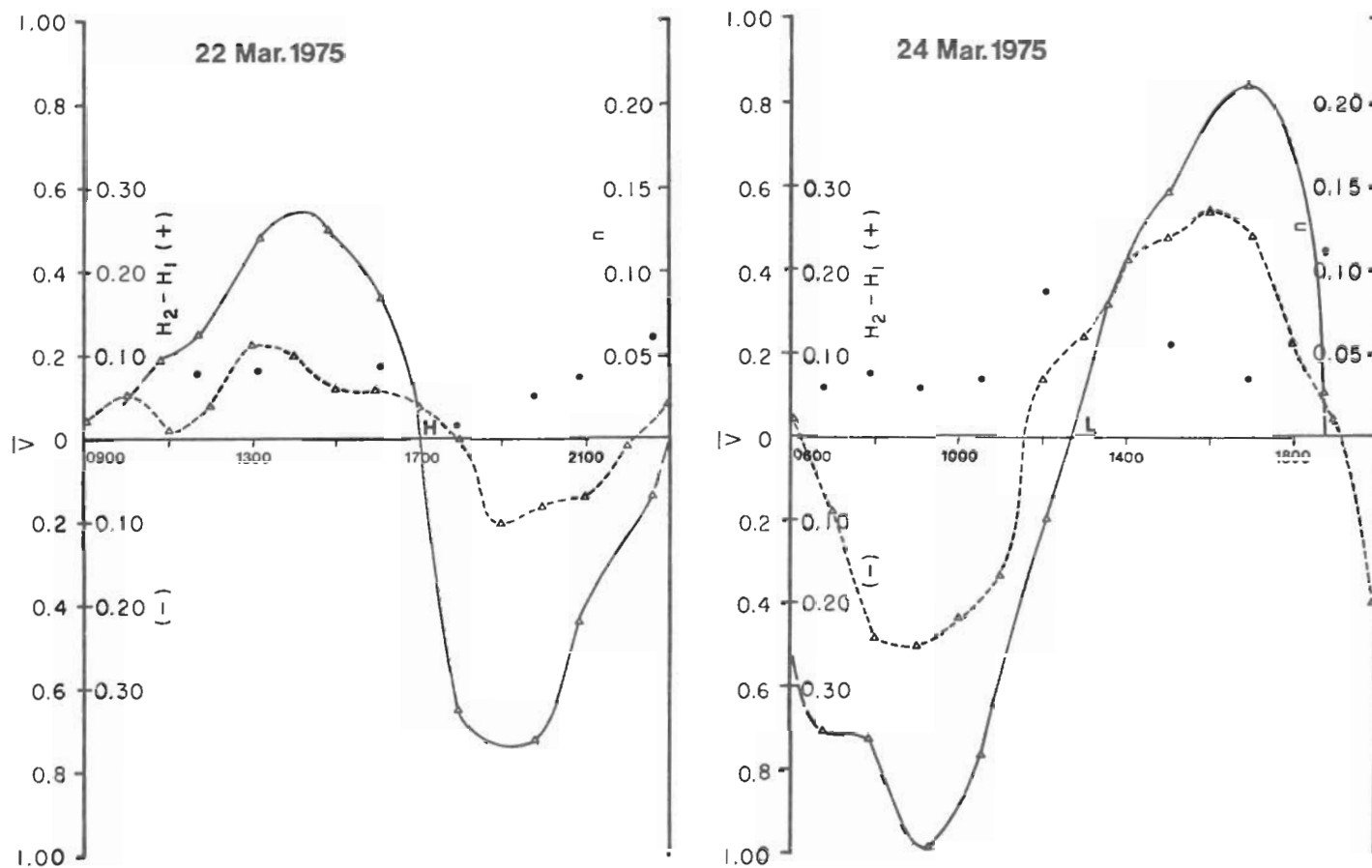
Figure 56. Time histories of tidal differential, currents, and Manning's n at Town Creek, 22 and 24 March 1975.
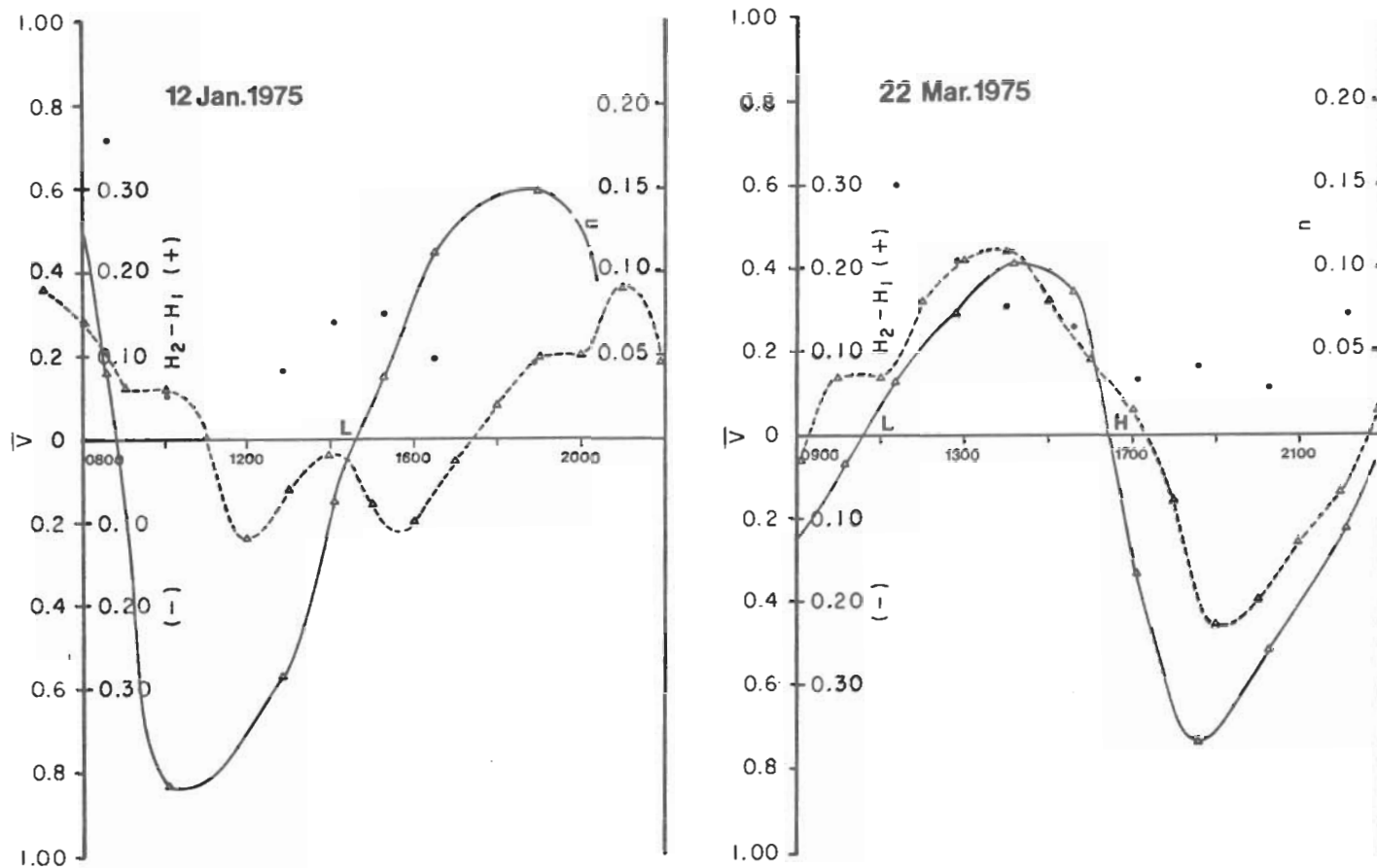
Figure 57. Time histories of tidal differential, currents and Manning's n at Jones Creek, 12 January and 22 March 1975.

with a spring range of about 1.80 meters. During the flood cycle at North Inlet, however, n remains fairly constant or decreases as high slack water is approached, with the exception of the 12 January 1975 Town Creek data. This may result from variations in channel depth and width during the flood phase. Compared to New Corpus Christi Pass, relatively greater changes in depth occur at North Inlet due to the greater Atlantic coast tidal range. Since partially full channels possess greater n values than full conduits (Chow, 1959), n values decrease as high slack water is neared and proportionately less fluid is influenced by channel boundary friction. Width is involved also, since narrow channels have higher n values than wide channels. A natural inlet channel gains greatly in effective width compared to a regular, nearly prismatic dredged channel, since at low water the former is divided by many intertidal to barely subtidal shoals which are covered by 1 to 3 meters or more of water at high tide. Behrens, Watson, and Mason (in preparation, 1976) noted that velocities below 0.20 meter per second do not give reliable values for n (values with less than 15-percent error). They also indicated that the percent error will be larger at low water level differentials and that both very low and very high values of n occur at low differentials, as was also found at North Inlet. Behrens, Watson, and Mason attributed the early low values of n to flow over bed forms oriented in the opposite direction (i.e., early floodflow over ebb-oriented bed forms). The later high values of n were considered to result from bed forms oriented with flow (i.e., floodflow over flood-oriented bed forms), which produced higher frictional resistance due to the greater turbulence associated with steeper downstream slip faces.

In any case, high or low values of Manning's n appear to be related to the reversing and continuously varying nature of tidal flow, which differs markedly from the open channel uniform flow for which equation (10) applies. Nevertheless, n has been used by Brown (1928), Keulegan (1967), and O'Brien and Clark (1973) as a friction coefficient. In view of the above analysis and the reluctance of O'Brien and Clark (1973) to use the computation of n except in channels of fairly regular configuration, Manning's n must be interpreted with caution. Table 17 gives mean Manning's n values for each tidal cycle. Individual values near times of slack water (generally less than 0.01 or greater than 0.07) were not included. These data compare well with values of 0.022, 0.051, 0.039, 0.071, and 0.038 for seven inlets which O'Brien and Clark (1973) consider to be of a configuration suitable for calculation of Manning's n. Also included in Table 17 are Keulegan's coefficient of friction and the value of K, the repletion coefficient.

7. Keulegan Repletion Coefficient.

The repletion coefficient, K, developed by Keulegan (1967) indicates the efficiency of tidal exchange through a channel. It includes the effects of the channel length, form and frictional losses, channel and bay geometry, and the period and range of ocean tidal fluctuations. A number of simplifying conditions are applied in Keulegan's (1967) analysis,

Table 17. Calculated friction and repletion coefficients.

Date 1975	Flow section measured	Friction factor n	Friction factor λ	Keulegan K
7 Jan.	Town Creek	0.032	0.0135	3.72
12 Jan.	Town Creek	0.034	0.0152	2.07
12 Jan.	Jones Creek	0.040	0.020	2.19
19 Mar.	Town Creek	0.041	0.022	2.41
22 Mar.	Town Creek	0.041	0.022	1.97
22 Mar.	Jones Creek	0.042	0.025	1.45
24 Mar.	Town Creek	0.036	0.017	1.83

including the assumption that flow in the channel is governed by Manning's formula, hence the need to determine Manning's n as an indication of channel friction. The relationship which may be used in the calculation of K is:

$$K\sqrt{H} = \frac{T\sqrt{2g}}{2\pi}\sqrt{\frac{R}{\lambda L + R}\frac{a}{A}}, \tag{11}$$

where H is the semirange of tide in the ocean, T is the period of the tide (12.42 hours), R is the hydraulic radius of the inlet cross section, λ is a friction coefficient, L is the channel length, a is the inlet cross-sectional area, and A is surface area of the basin. The friction coefficient, λ, corresponding to each value of n (Table 17), is derived from the relationship:

$$\lambda = \left(\frac{n\sqrt{2g}}{1.486\ R^{1/6}}\right)^2. \tag{12}$$

The larger the value of K the more efficient is the tidal exchange. K is directly proportional to tidal period and inlet cross-sectional area, but inversely proportional to tidal range, bay area, friction, and channel length.

The morphology of North Inlet, with two main channels divided by the trailing ebb spit of the flood tidal delta, has led to consideration of each channel separately in repletion coefficient analysis. This approach also seems reasonable because of the differences in: (a) Tidal ranges at the Town Creek and Jones Creek gages; (b) overall channel configuration between the inlet throat and the cross sections of velocity measurement; and (c) tidal flow,

as shown in Figure 52 and Table 16. In addition, the computation of bay area presents a special problem when the bay is really a marsh-filled lagoon with a series of complex tidal creeks fed by two main channels. An approximate area for the tidal creek network was computed as 7.333×10^6 square meters using a 1:24,000 USGS topographic map as a base, along with aerial photos and field knowledge of the area as aids. Although an area adjacent to Winyah Bay known to be dominated by brackish bay water was excluded, it would be nearly impossible to assign distinctive areas to Jones Creek and Town Creek flows. Therefore, the approach of O'Brien and Dean (1972) was adopted, and an equivalent bay area was computed as:

$$A_B = \frac{P_h}{2a_b}. \tag{13}$$

where P_h is the hydraulic tidal prism computed from the flow measurements through a velocity section and a_b is the bay tide amplitude.

Examination of the results (Table 17) indicates that the highest values of K resulted from neap tide flow through Town Creek on 7 January 1975 (K = 3.72), and flow through the inlet throat section on 21 March 1975 (K = 3.37) at a somewhat lower than mean tide. In Town Creek the small value of tidal range is the primary reason for the greater value of K, since the value of K = 2.07 on 12 January 1975, was determined at the same hydraulic radius, but during springtides. Channel length, L, was considered to be 1,005 meters (3,300 feet) for the Town Creek flow.

A comparison of Jones Creek and Town Creek repletion coefficients for the 12 January 1975 springtides shows similar values of K, despite the greater friction of the Jones Creek channel, part of which is due to the channel's curving configuration. However, the greater friction is compensated for in shorter channel length, 792 meters (2,600 feet) at Jones Creek as opposed to 1,005 meters (3,300 feet) for Town Creek. The low values of K measured on 22 March 1975 are probably due to augmentation of the ebb flow by Winyah Bay waters due to southwesterly winds and high runoff conditions (Table 15). Ebb velocity asymmetry was very pronounced at both Town Creek and Jones Creek (Figs. 54 to 57). A larger ebb prism would increase the mean value of the tidal prism used to compute A_B, the hydraulic equivalent area, a factor which would reduce the value of K.

VII. SUMMARY

Tidal inlets are of immense importance for navigation, food production, and maintenance of the coastal ecosystem. By combining study of littoral processes, morphology of the inlet and adjacent beaches, and tidal hydraulics on a detailed seasonal basis, the results obtained at North Inlet may be used as a model for the behavior of many natural tidal inlets. The quarterly collection of a large amount of field data, combined with

analysis of morphological change over the last 100 years, has led to an understanding of inlet processes which would not otherwise have been possible.

Historical study shows that tidal flow through an overwash breach around 1916 may have been responsible for the formation of the present channel. Erosion of North Island north of this break and abandonment of the 1878 inlet channel allowed spit growth to occur as a result of southward sediment transport. Thus, North Inlet stabilized at its present position in the late 1930's following the growth of the Debidue Island recurved spit.

Net longshore sediment transport from north to south results from an annual net wave energy flux to the south, which is caused by high-energy conditions during northeast storms. The fall and winter months are dominated by these northeast winds, with the addition of west and northwest winds associated with winter cold fronts. During the spring a transition is seen between this pattern and the south to southwest summer winds associated with high-pressure systems.

The present ebb tidal delta began to grow when sediment moving toward the inlet was deposited in the area of interaction between waves and inlet tidal currents. As waves refracted around the growing ebb tidal delta a longshore sediment transport reversal developed just south of the inlet, building a northward recurving spit, adding to swash bars and increasing the size of the ebb tidal delta. The seasonal wave energy flux and resulting sediment transport pattern have been documented by about 800 littoral process observation sets at four stations, two on either side of the inlet.

These data include weather observations which show a seasonal pattern of winds, which in turn influences the wave climate, depending on the magnitude of the onshore or offshore component.

Comparison of bathymetric surveys from 1925 and 1964 indicates an annual increase in spit and shoal volume of 4.33×10^5 cubic meters per year. An estimate of the inlet-directed longshore sediment transport based on wave energy flux gives a value which is 81.5 percent of the annual rate of increase during the 39 years between surveys. Therefore, shoal volume changes may be used to give an indication of long-term energy flux before actual field measurements.

Beach profiles at 11 locations have shown that the severely eroding shoreline adjacent to North Inlet is degraded by northeast storms. Lack of sediment influx to the area and a relative rise in sea level contribute to the transgressive character of the shoreline. The uniformity in mean sediment size and sediment sorting also results from lack of new sediment influx and the continuous reworking of a limited amount of sedimentary material.

Beach erosion, which reached a maximum of 7 meters of foredune ridge retreat during the winter of 1972-73, contributes abundant sediment to the ebb tidal delta; the ebb tidal delta has a present volume of over 35,700,000 cubic meters. The only beach not severely eroding lies immediately south of the inlet where the ebb tidal delta affords protection from northeast storm wave approach. In this region the welding of swash bars to the beach supplies sediment to the longshore transport reversal.

A 10-percent (± 2 percent) reduction in the cross-sectional area of the inlet throat between the summer of 1974 and winter of 1975 was related to the increased frequency of high waves during the fall and winter months. By late spring 1975, the cross-sectional area had returned to within 3 percent (± 2 percent) of the area during the previous summer, indicating a seasonal response to the wave climate. Storms such as the severe northeaster of 10 and 11 February 1973, cause major infilling of the inlet throat which is then compensated for by tidal scouring as return to an equilibrium area takes place.

The flood tidal delta, which has been migrating steadily westward under the influence of wave action at high tide, includes a trailing ebb spit which divides the tidal flow between two main channels. This spit extends as far seaward as the inlet throat section but is eroding as the flood tidal delta moves westward. Differences in current velocity and salinity are found on either side of the ebb spit because the southern channel (Jones Creek) has a more direct connection with Winyah Bay, the only source of freshwater in the area.

Tidal current measurements, in conjunction with continuous recording of tidal elevations in the ocean, Jones Creek, and Town Creek, have been used to compute tidal prism volumes. The variation in volume between successive ebb and flood tidal prisms can be explained by the diurnal inequality, meteorological effects, and the presence of Winyah Bay brackish waters. Comparison of the tidal prism and the cross-sectional area of the inlet throat to geomorphological studies indicates that the inlet is presently in equilibrium.

Manning's n friction coefficient increased during the ebb phase of most tidal cycles, but tended to steadily decrease during flood phases, reflecting changes in channel shape and depth during the semidiurnal cycle. Calculation of Keulegan's (1967) repletion coefficient required consideration of Jones Creek and Town Creek channels separately due to different channel configurations and total lengths. The highest value of K = 3.72 was obtained for neap tidal flow through the Town Creek cross section. The lowest values, K = 1.45 and 1.83, were obtained for Jones Creek and Town Creek, respectively, when the North Inlet tidal prism was augmented by flow from Winyah Bay during mean tide and springtide.

The results show that variation in the computed Keulegan repletion coefficients is reasonably well explained by variation in the observed flow conditions, despite the assumptions made in Keulegan's analysis. This is an important result since many previous analyses have not dealt with the complexities of major and minor channels, marsh-filled lagoons, and tidal creek connection to another water body, as is found at North Inlet.

The results of this study have added new detail to process-response relationships in a complex coastal environment. The importance of seasonal variation in processes was emphasized by the significant differences in wave parameters, short-term morphologic response, and tidal parameters found during the quarterly studies. The applicability of certain theoretical relationships has been tested and data developed which will point to further research.

LITERATURE CITED

ABELE, R. W., Jr., "Analysis of Short-Term Variations in Beach Morphology (and Concurrent Dynamic Processes) for Summer and Winter Periods, 1971-72, Plum Island, Massachusetts," Final Report Contract DACW72-71-C-0023, U.S. Army, Corps of Engineers, Coastal Engineering Research Center, Fort Belvoir, Va., (in preparation, 1976).

ALAKA, M. A., "Climatology of Atlantic Tropical Storms and Hurricanes," Technical Report WB-6, Environmental Science Services Administration, Rockville, Md., May 1968.

ANAN, F. S., "Hydraulic Equivalent Sediment Analyzer (HESA)," Technical Report No. 3-CRC. Coastal Research Center, University of Massachusetts, Amherst, Mass., July 1972.

BEHRENS, E. W., WATSON, R. L., and MASON, C., "Hydraulics and Dynamics of New Corpus Christi Pass, Texas," Final Report, Contract DACW72-72-C-0027, U.S. Army, Corps of Engineers, Coastal Engineering Research Center, Fort Belvoir, Va., (in preparation, 1976).

BOOTHROYD, J. C., "Inner Channel-Margin Linear Bar, Stop Description," *Field Trip Guide: Inlet and Coastal Environments at North Inlet, South Carolina*, Coastal Research Division, Department of Geology, University of South Carolina, Columbia, S.C., Oct. 1973.

BOOTHROYD, J. C., and HUBBARD, D. K., "Bed Form Development and Distribution Pattern, Parker and Essex Estuaries, Massachusetts," MP 1-74, U.S. Army, Corps of Engineers, Coastal Engineering Research Center, Fort Belvoir, Va., Feb. 1974.

BROWN, E. I., "Inlets on Sandy Coasts," *Proceedings of American Society of Civil Engineers*, Vol. 54, 1928, pp. 505–553.

BUFFINGTON, R. M., and RANDALL, J. P., "Descriptive Report to Accompany Hydrographic Survey H-8838," Environment Science Services Administration, Rockville, Md., Apr. 1964.

CAMPBELL, R. C., *Statistics for Biologists*, Cambridge University Press, London, 1967.

CHOW, V. T., *Open-Channel Hydraulics*, McGraw-Hill, New York, 1959.

DAVIS, R. A., Jr., and FOX, W. T., "Beach and Nearshore Dynamics in Eastern Lake Michigan," Technical Report No. 4, ONR Contract 388-092, Office of Naval Research, Washington, D.C., 1971.

DEAN, R. G., and WALTON, T. L., "Sediment Transport Processes in the Vicinity of Inlets with Special Reference to Sand Trapping," Vol. II, *Estuarine Research*, Academic Press, New York, 1975, pp. 129–149.

DeWALL, A. E., PRITCHETT, P. C., and GALVIN, C. J., Jr., "Beach Changes Caused by a Northeaster Along the Atlantic Coast," *Abstracts from the Annual Meeting of the Geological Society of America*, Washington, D.C., Vol. 3, No. 7, Nov. 1971, pp. 542.

DIXON, W. J., and MASSEY, F. J., Jr., *Introduction to Statistical Analysis*, McGraw-Hill, New York, 1969.

DOLAN, R., FERM, J. C., and McARTHUR, D. S., "Measurements of Beach Process Variables, Outer Banks, North Carolina," Technical Report No. 64, ONR Contract 388-092, Office of Naval Research, Washington, D.C., Jan. 1969.

DRACUP, J. F., "National Geodetic Survey Data: Availability-Explanation-Application," National Oceanic and Atmospheric Administration, National Ocean Survey, Rockville, Md., 1973, 36 pp.

EMERY, K. O., "A Simple Method of Measuring Beach Profiles," *Limnology and Oceanography*, Vol. 6, No. 1, Jan. 1961, pp. 90–93.

FARRELL, S. C., "Growth Cycle of a Small Recurved Spit," *Coastal Environments, N. E. Massachusetts and New Hampshire*, Coastal Research Group, University of Massachusetts, Amherst, Mass., 1969, pp. 316–336.

FINLEY, R. J., "Tidal Inlet Morphology and Hydrodynamics of North Inlet, South Carolina," Final Report, Contract DACW72-72-0032, U.S. Army, Corps of Engineers, Coastal Engineering Research Center, Fort Belvoir, Va., 1973.

FINLEY, R. J., "Hydrodynamics and Tidal Deltas of North Inlet, South Carolina," Vol. II, *Estuarine Research*, Academic Press, New York, 1975, pp. 277–291.

FOLK, R. L., *Petrology of Sedimentary Rocks*, Hemphill's, Austin, Tex., 1968.

FOX, W. T., and DAVIS, R. A., Jr., "Computer Simulation Model of Coastal Processes in Eastern Lake Michigan," Technical Report No. 5, ONR Contract 388-092, Williams College, Williamstown, Mass., 1971.

FOX, W. T., and DAVIS, R. A., Jr., "Coastal Processes and Beach Dynamics at Sheboygan, Wisconsin, July 1972," Technical Report No. 10, Williams College, Williamstown, Mass., 1972.

GALVIN, C. J., Jr., "Longshore Current Velocity: A Review of Theory and Data," *Reviews of Geophysics*, Vol. 5, 1967, pp. 287–304 (also Reprint 2-68, U.S. Army, Corps of Engineers, Coastal Engineering Research Center, Washington, D.C., NTIS AD 672 614).

GALVIN, C. J., Jr., "Wave Breaking in Shallow Water," *Waves on Beaches and Resulting Sediment Transport*, Academic Press, New York, 1972, pp. 413–456 (also Reprint 4-73, U.S. Army, Corps of Engineers, Coastal Engineering Research Center, Fort Belvoir, Va., NTIS AD 766 106).

GALVIN, C. J., Jr., and NELSON, R. A., "Compilation of Longshore Current Data," MP 2-67, U.S. Army, Corps of Engineers, Coastal Engineering Research Center, Washington, D.C., Mar. 1967.

HARRISON, W., and KRUMBEIN, W. C., "Interactions of the Beach-Ocean-Atmosphere System at Virginia Beach, Virginia," TM-7, U.S. Army, Corps of Engineers, Coastal Engineering Research Center, Washington, D.C., Dec. 1964.

HAYES, M. O., "Forms of Sediment Accumulation in the Beach Zone," *Waves on Beaches and Resulting Sediment Transport*, Academic Press, New York, 1972, pp. 297–365.

HAYES, M. O., and BOOTHROYD, J. C., "Storms as Modifying Agents in the Coastal Zone," *Coastal Environments, N.E. Massachusetts and New Hampshire*, Coastal Research Group, University of Massachusetts, Amherst, Mass., 1969, pp. 245–265.

HAYES, M. O., GOLDSMITH, V., and HOBBS, C. H., III, "Offset Coastal Inlets," *Proceedings of the 12th Coastal Engineering Conference*, Washington, D.C., Vol. II, 1970, pp. 1187–1200.

HAYES, M. O., et al., "The Investigation of Form and Processes in the Coastal Zone," Coastal Geomorphology, *Proceedings of the Third Annual Geomorphology Symposium*, State University of New York at Binghamton, 1973, pp. 11–41.

HICKS, S. D., and CROSBY, J. E., "Trends and Variability of Yearly Mean Sea Level 1893-1972," Technical Memorandum No. 13, National Oceanic and Atmospheric Administration, Rockville, Md., Mar. 1974.

HUBBARD, D. K., "North Channel-Margin Linear Bar and Bedforms, Stop Description," *Field Trip Guide: Inlet and Coastal Environments at North Inlet, South Carolina*, Coastal Research Division, Department of Geology, University of South Carolina, Columbia, S.C., Oct. 1973.

INMAN, D. L., and QUINN, W. H., "Currents in the Surf Zone," *Proceedings of the Second Coastal Engineering Conference*, Council on Wave Research, University of California, Berkeley, Calif., 1951, pp. 24–36.

JARRETT, J. T., "Tidal Prism-Inlet Area Relationships," GITI Report 3, U.S. Army, Corps of Engineers, Vicksburg, Miss., Feb. 1976.

JOHNSON, J. W., "Characteristics and Behavior of Pacific Coast Tidal Inlets," *Journal of Waterways and Harbors Division,* Vol. 9, No. WW3, Aug. 1973, pp. 235–339.

KANA, T. W., "Beach Erosion During a Minimum Storm at Debidue Island, South Carolina," Coastal Research Division, Department of Geology, University of South Carolina, Columbia, S.C. (in preparation, 1976).

KEULEGAN, G. H., "Tidal Flow in Entrances: Water Level Fluctuations of Basins in Communication with Seas," Technical Bulletin No. 14, Committee on Tidal Hydraulics, U.S. Army, Corps of Engineers, Vicksburg, Miss., July 1967.

KING, D. B., "The Dynamics of Inlets and Bays," Technical Report 22, Coastal Oceanographic Engineering Laboratory, University of Florida, Gainesville, Fla., Mar. 1974.

LANDERS, H., "Climate of South Carolina," *Climatography of the United States,* No. 60-38, Environmental Science Services Administration, Rockville, Md., June 1970.

MEHTA, A. H., and HOU, H. S., "Hydraulic Constants of Tidal Entrances II: Stability of Long Island Inlets," Technical Report 23, Coastal Oceanographic Engineering Laboratory, University of Florida, Gainesville, Fla., Nov. 1974.

MUNK, W. H., "The Solitary Wave Theory and Its Application to Surf Problems," *Annals of the New York Academy of Sciences,* Vol. 51, 1949, pp. 376–462.

NATIONAL OCEANIC AND ATMOSPHERIC ADMINISTRATION, "Tidal Tables, 1975," National Ocean Survey, Rockville, Md., 1974.

NEIHEISEL, J., "Source and Distribution of Sediments at Brunswick Harbor and Vicinity, Georgia," TM-12, U.S. Army, Corps of Engineers, Coastal Engineering Research Center, Washington, D.C., Mar. 1965.

O'BRIEN, M. P., "Estuary Tidal Prisms Related to Entrance Areas," *Civil Engineering,* Vol. 1, No. 8, May 1931, pp. 738–739.

O'BRIEN, M. P., "Equilibrium Flow Areas of Inlets on Sandy Coasts," *Journal of Waterways and Harbors Division,* Vol. 95, No. WW1, Feb. 1969, pp. 43–52.

O'BRIEN, M. P., "Notes on Tidal Inlets on Sandy Shores," GITI Report 5, U.S. Army, Corps of Engineers, Vicksburg, Miss., Feb. 1976.

O'BRIEN, M. P., and CLARK, R. R., "Hydraulic Constants of Tidal Entrances I," Technical Report 21, Coastal Oceanographic Engineering Laboratory, University of Florida, Gainesville, Fla., Nov. 1973.

O'BRIEN, M. P., and DEAN, R. G., "Hydraulics and Sedimentary Stability of Coastal Inlets," *Proceedings of the 13th Coastal Engineering Conference*, Vancouver, B.C., Canada, 1972, pp. 761–780.

OWENS, E. H., "The Geodynamics of Two Beach Units in the Magdalen Islands, Quebec, Within the Framework of Coastal Environments of the Southern Gulf of St. Lawrence," unpublished Ph.D. Dissertation, Department of Geology, University of South Carolina, Columbia, S.C., 1975.

PRITCHARD, D. W., "What is an Estuary: Physical Viewpoint," *Estuaries, American Association for the Advancement of Science*, No. 83, Washington, D.C., 1967, pp. 3–5.

STEPHENS, D. G., et al., "Environmental Analysis of the Santee River Estuaries: Thirty Years After Diversion," *Southeastern Geology*, Vol. 16, No. 3, Feb. 1975, pp. 131–144.

THOM, B. G., "Coastal and Fluvial Landforms: Horry and Marion Counties, South Carolina," No. 19, Coastal Studies Series, Louisiana State University Press, Baton Rouge, La., 1967.

THOM, B. G., et al., "Aspects of the Texture and Mineralogy of Surficial Sediments, Horry and Marion Counties, South Carolina," Technical Report 117, Coastal Studies Institute, Louisiana State University, Baton Rouge, La., 1972.

U.S. ARMY ENGINEER DISTRICT, CHARLESTON, "Murrells Inlet, Survey Report on Navigation," Charleston, S.C., 1970.

U.S. ARMY, CORPS OF ENGINEERS, COASTAL ENGINEERING RESEARCH CENTER, *Shore Protection Manual*, 2d ed., Vols. I, II, and III, U.S. Government Printing Office, Stock No. 008-022-00077, Washington, D.C., 1975, 1,160 pp.

U.S. NAVAL WEATHER SERVICE COMMAND, "Summary of Synoptic Meteorological Observations, Atlantic and Gulf Coasts," Vol. 3, Area 10, Charleston, S.C., May 1970.

U.S. NAVAL WEATHER SERVICE COMMAND, "Summary of Synoptic Meteorological Observations, Atlantic and Gulf Coasts," Vol. 3, Area 19, Charleston, S.C., 1975, pp. 317–395.

WIEGEL, R. L., *Oceanographical Engineering*, Prentice-Hall, Englewood Cliffs, N.J., 1964.

BIBLIOGRAPHY

BASCOM, W. N., *Waves and Beaches*, Doubleday, New York, 1964.

DUANE, D. B., et al., "Linear Shoals on the Atlantic Inner Continental Shelf, Florida to Long Island," *Shelf Sediment Transport*, Dowden, Hutchinson and Ross, Inc., Stroudsburg, Pa., 1972, pp. 411–427 (also Reprint 22-73, U.S. Army, Corps of Engineers, Coastal Engineering Research Center, Fort Belvoir, Va., NTIS AD 770 172).

FAIRCHILD, J. C., "Correlation of Littoral Transport with Wave Energy Along Shores of New York and New Jersey," TM-18, U.S. Army, Corps of Engineers, Coastal Engineering Research Center, Washington, D.C., Nov. 1966.

FAIRCHILD, J. C., "Longshore Transport of Suspended Sediment," *Proceedings of the 13th Coastal Engineering Conference*, Vancouver, B.C., Canada, Vol. II, 1972, pp. 1069–1087.

GALVIN, C. J., Jr., "A Gross Longshore Transport Rate Formula," *Proceedings of the 13th Coastal Engineering Conference*, Vancouver, B.C., Canada, Vol. II, 1972, pp. 953–970.

GALVIN, C. J., Jr., and EAGLESON, P. S., "Experimental Study of Longshore Currents on a Plane Beach," TM-10, U.S. Army, Corps of Engineers, Coastal Engineering Research Center, Washington, D.C., Jan. 1965.

JOHNSON, D. W., *Shore Processes and Shoreline Development*, Columbia University Press, New York, 1919.

KING, C. A. M., *Beaches and Coasts*, Butler and Tanner, Ltd., France and London, 1972.

KOMAR, P. D., "The Mechanics of Sand Transport on Beaches," *Journal of Geophysical Research*, Vol. 76, No. 3, Jan. 1971, pp. 713–721.

KOMAR, P. D., and INMAN, D. L., "Longshore Sand Transport on Beaches," *Journal of Geophysical Research*, Vol. 75, No. 30, Oct. 1970, pp. 5914–5927.

LONGUET-HIGGINS, M. S., "Recent Progress in the Study of Longshore Currents," *Waves on Beaches and Resulting Sediment Transport*, Academic Press, New York, 1972, pp. 203–248.

OERTEL, G. F., "Sediment Transport of Estuary Entrance Shoals and the Formation of Swash Platforms," *Journal of Sedimentary Petrology*, Vol. 42, No. 4, Dec. 1972, pp. 858–863.

OERTEL, G. F., and HOWARD, J. D., "Water Circulation and Sedimentation at Estuary Entrances on the Georgia Coast," *Shelf Sediment Transport*, Dowden, Hutchinson and Ross, Stroudsburg, Pa., 1972, pp. 144–427.

PRITCHARD, D. W., and CARTER, H. H., "Estuarine Circulation Patterns," *The Estuarine Environment*, American Geologic Institute, Washington, D.C., 1971.

SHEPARD, F. P., and WANLESS, H. R., *Our Changing Shorelines*, McGraw-Hill, New York, 1971.

THORNTON, E. B., "Variation of Longshore Current Across the Surf Zone," *Proceedings of the 12th Coastal Engineering Conference*, Washington, D.C., Vol. I, 1970, pp. 291–308.

ZENKOVITCH, V. P., *Processes of Coastal Development*, Oliver and Boyd, London, 1967.

APPENDIX A

DEBIDUE ISLAND (DBI) AND NORTH ISLAND (NI)

1972-73 BEACH PROFILES

(Station locations in Fig. 10)

Vertical Exaggeration = 5X

MLW   25 June 1972

MLW   5 July

MLW   8 July

16 July

22 July

MLW   5 Aug.

13 Aug.

22 Aug. 1972

Meters
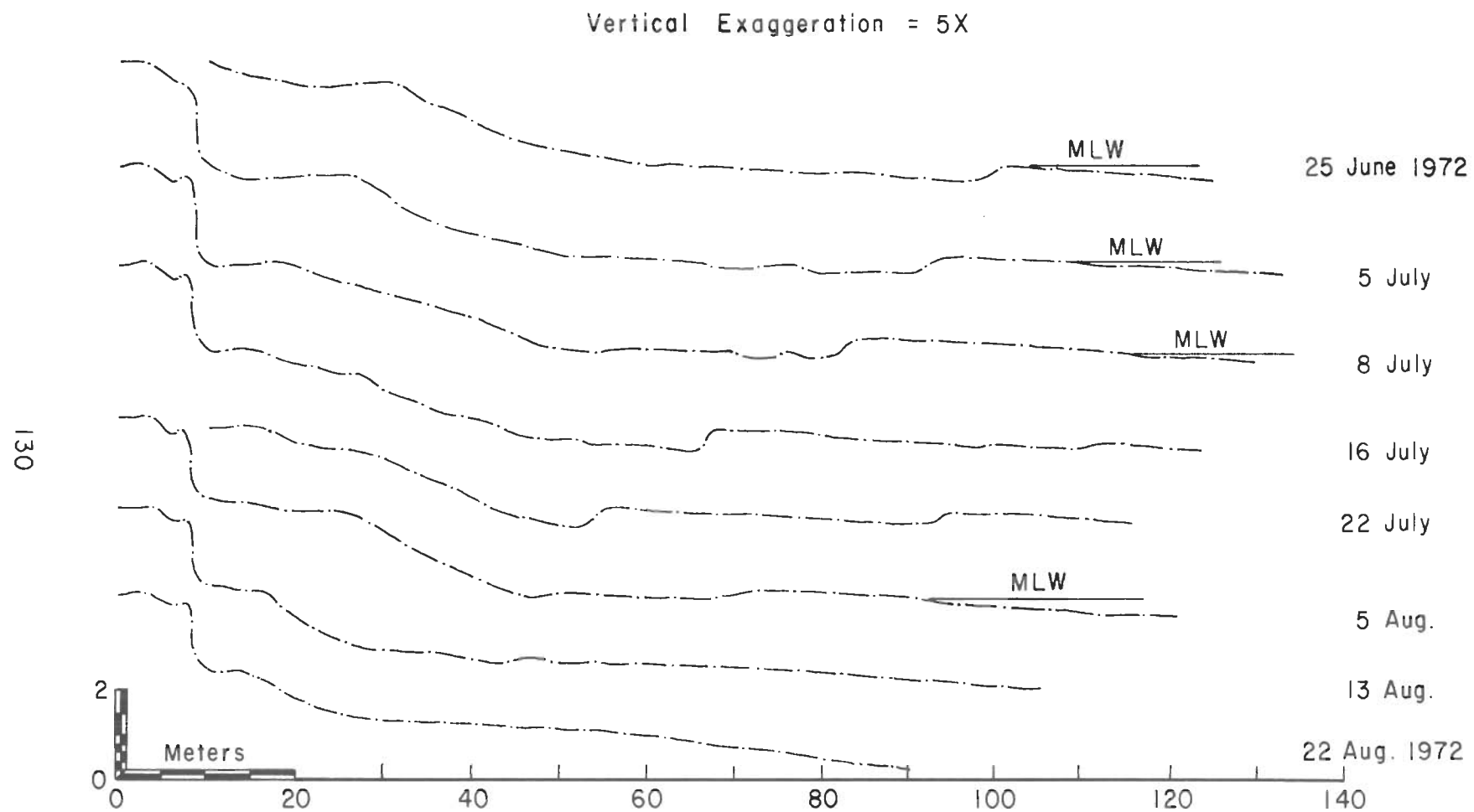
Figure A-1. Station DBI-10, 25 June to 22 August 1972.

Vertical Exaggeration = 5X

7 Oct. 1972

MLW

MLW

4 Nov.

MLW 2 Dec. 1972

MLW

15 Feb. 1973

16 Mar.

MLW

14 Apr. 1973

2

Meters

0

0   20   40   60   80   100   120   140
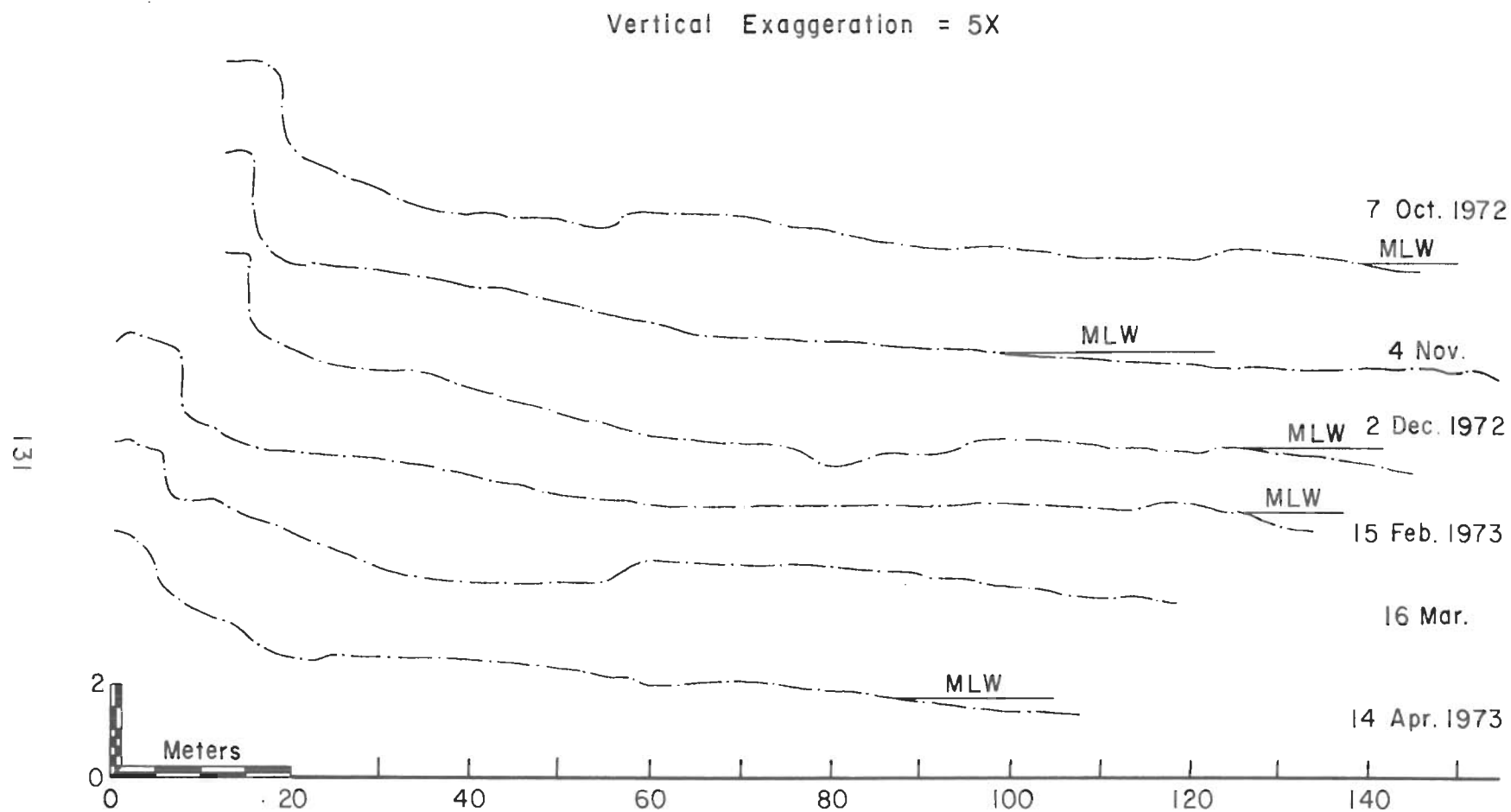
Figure A-2. Station DBI-10, 7 October 1972 to 14 April 1973.

Vertical Exaggeration = 5X

25 June 1972

MLW   5 July

MLW   8 July

16 July

22 July

MLW   31 July

MLW   5 Aug.

13 Aug.

22 Aug. 1972

Meters

0   20   40   60   80   100   120
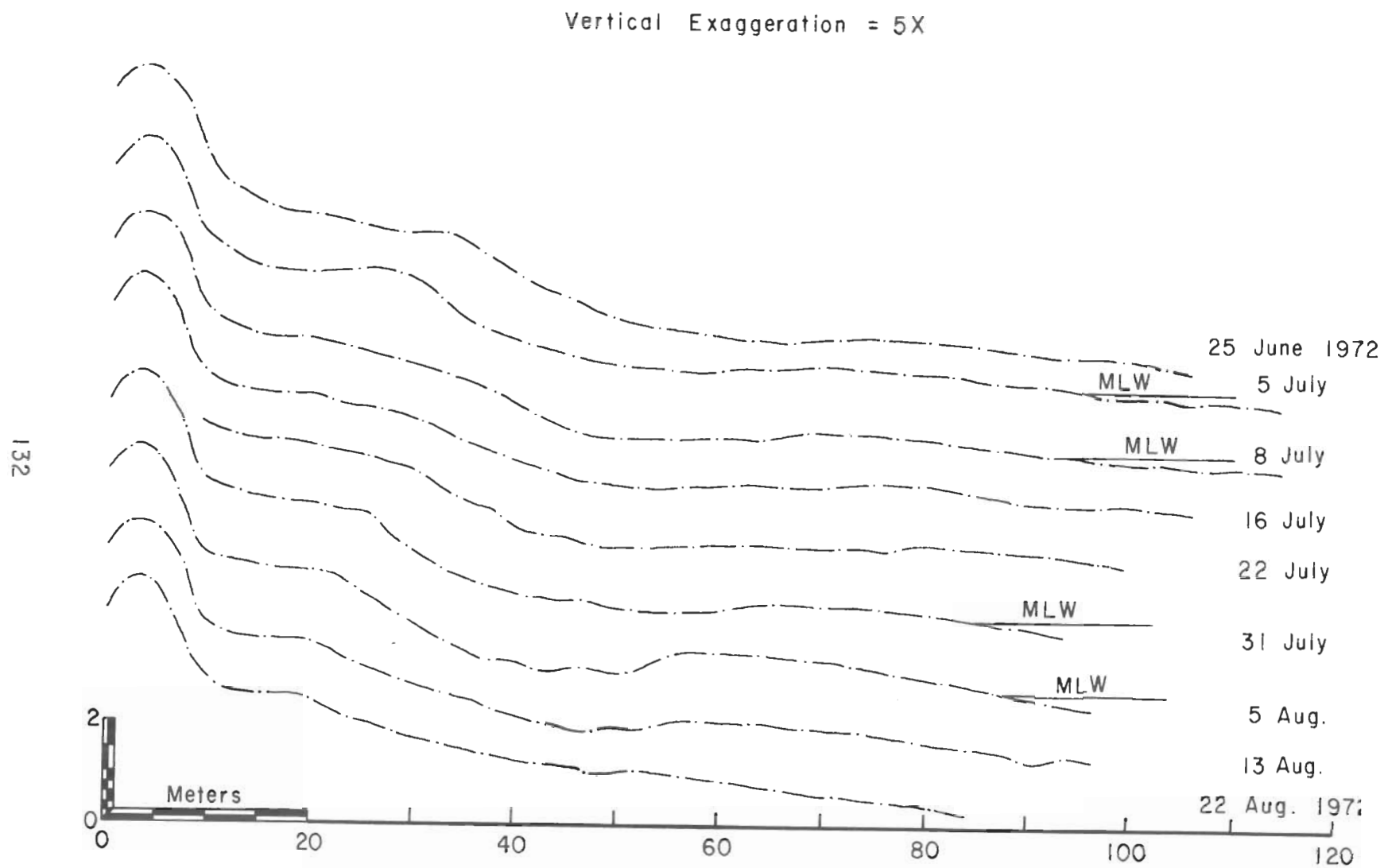
Figure A-3. Station DBI-20, 25 June to 22 August 1972.

Vertical Exaggeration = 5X

7 Oct. 1972

4 Nov.
MLW

2 Dec. 1972
MLW

MLW

15 Feb. 1973

MLW

16 Mar.

MLW
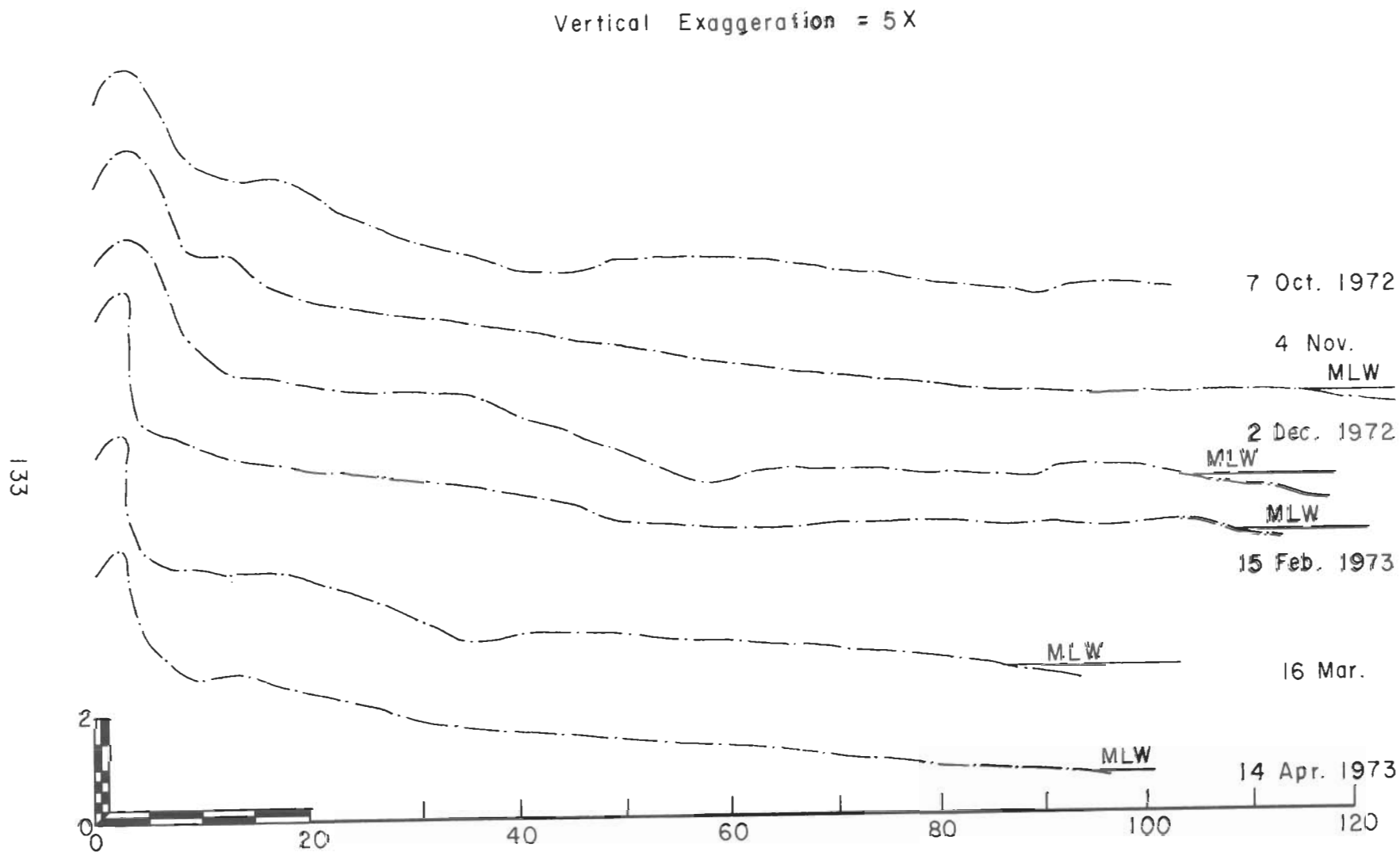
14 Apr. 1973

Figure A-4. Station DBI-20, 7 October 1972 to 14 April 1973.

133

Vertical Exaggeration = 5X

MLW

MLW

MLW

31 July 1972

5 Aug.

13 Aug.

22 Aug.

MLW

7 Oct.

MLW

2 Dec. 1972

MLW

15 Feb. 1973

MLW

16 Mar.

2

Meters

MLW

14 Apr. 1973

0

0   20   40   60   80   100

134
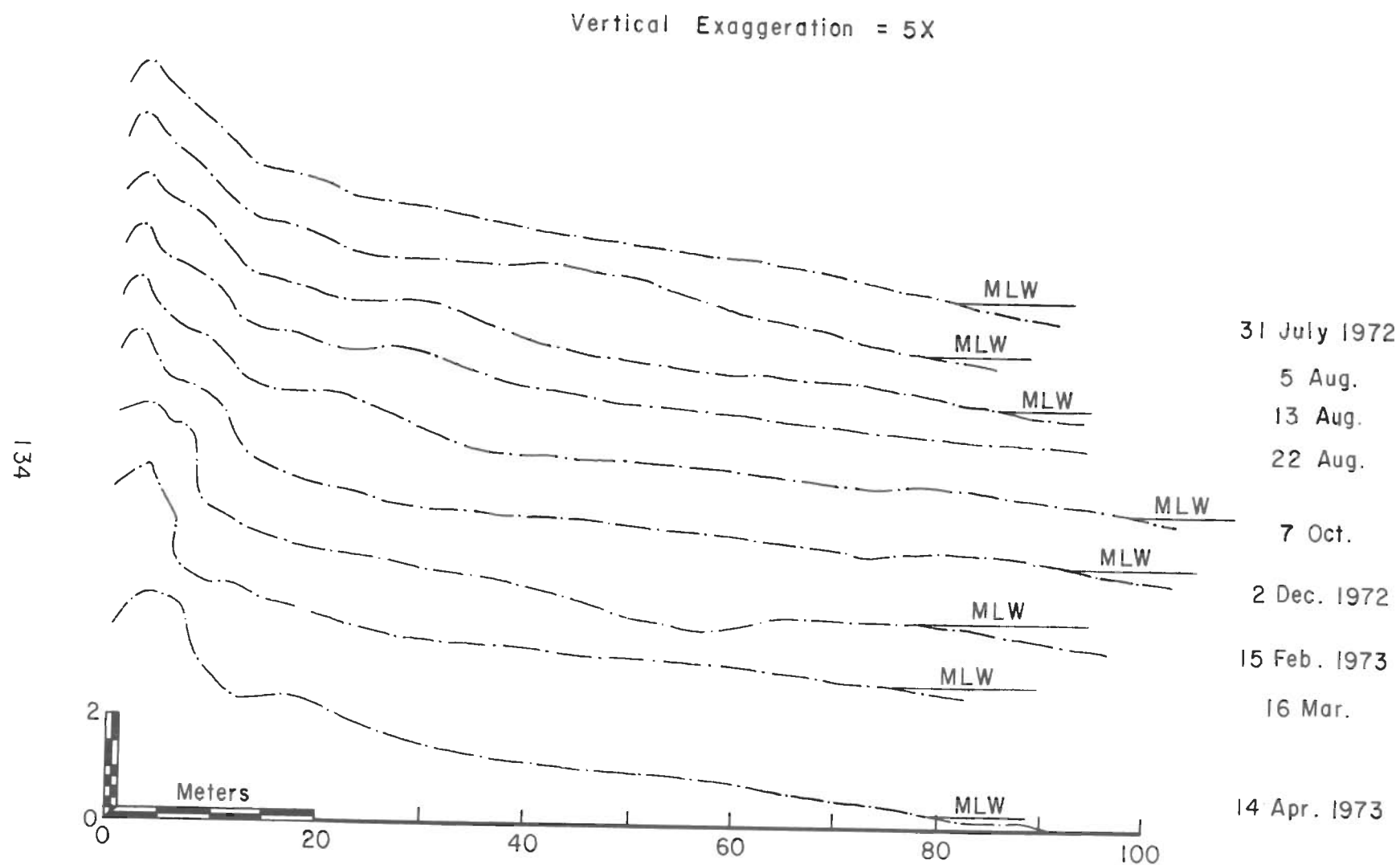
Figure A-5. Station DBI-25, 31 July 1972 to 14 April 1973.

Vertical Exaggeration = 5X

5 July 1972

MLW

8 July

16 July

MLW

22 July

MLW

31 July

MLW

5 Aug.

MLW

13 Aug.

MLW

22 Aug. 1972

135

2

Meters

0

0   20   40   60   80   100   120
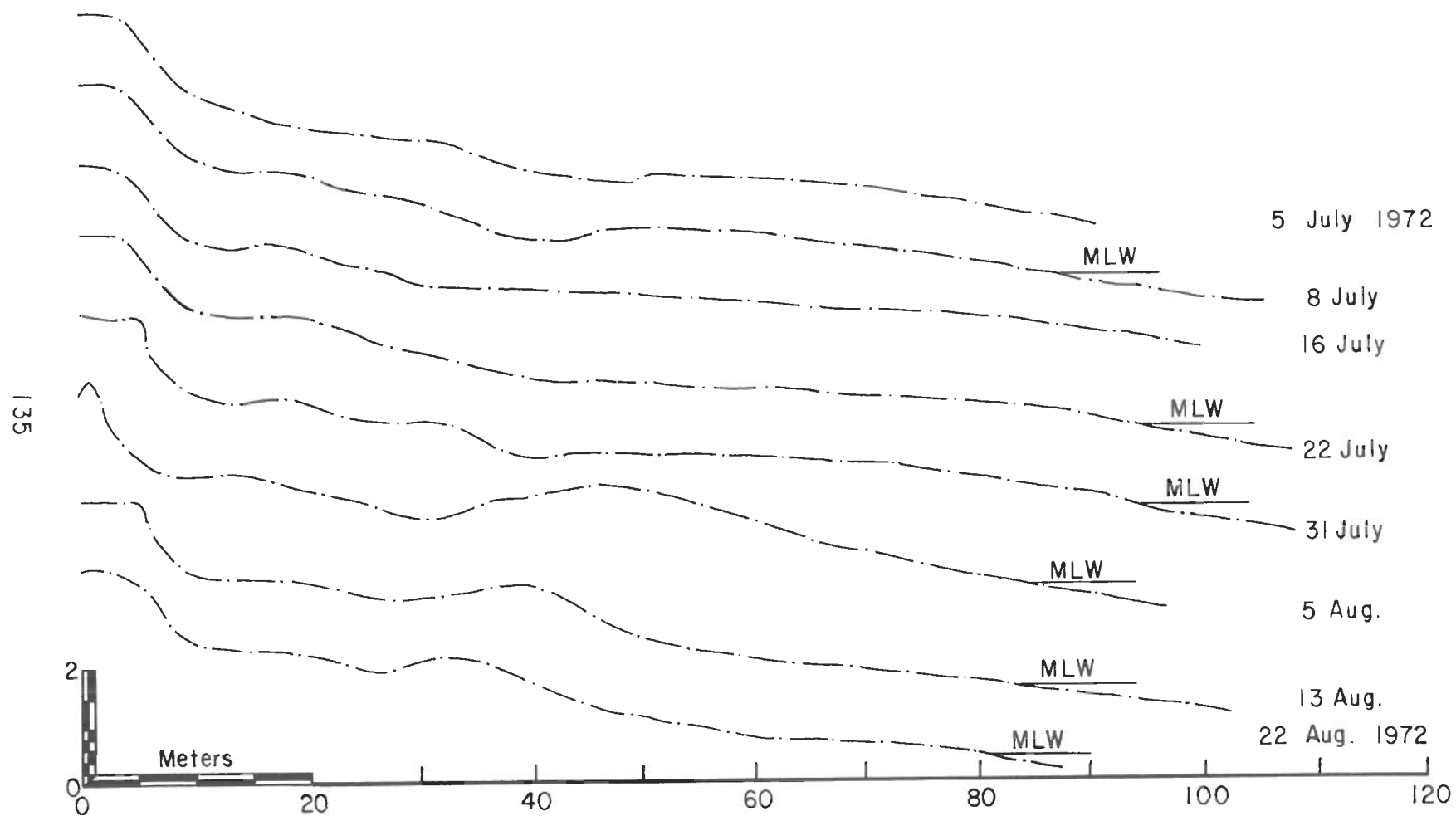
Figure A-6. Station DBI-30, 5 July to 22 August 1972.

Vertical Exaggeration = 5X

MLW

7 Oct. 1972

MLW

4 Nov.

MLW

2 Dec. 1972

MLW

15 Feb. 1973

MLW

16 Mar.

MLW

14 Apr. 1973

2

Meters

0

0   20   40   60   80   100
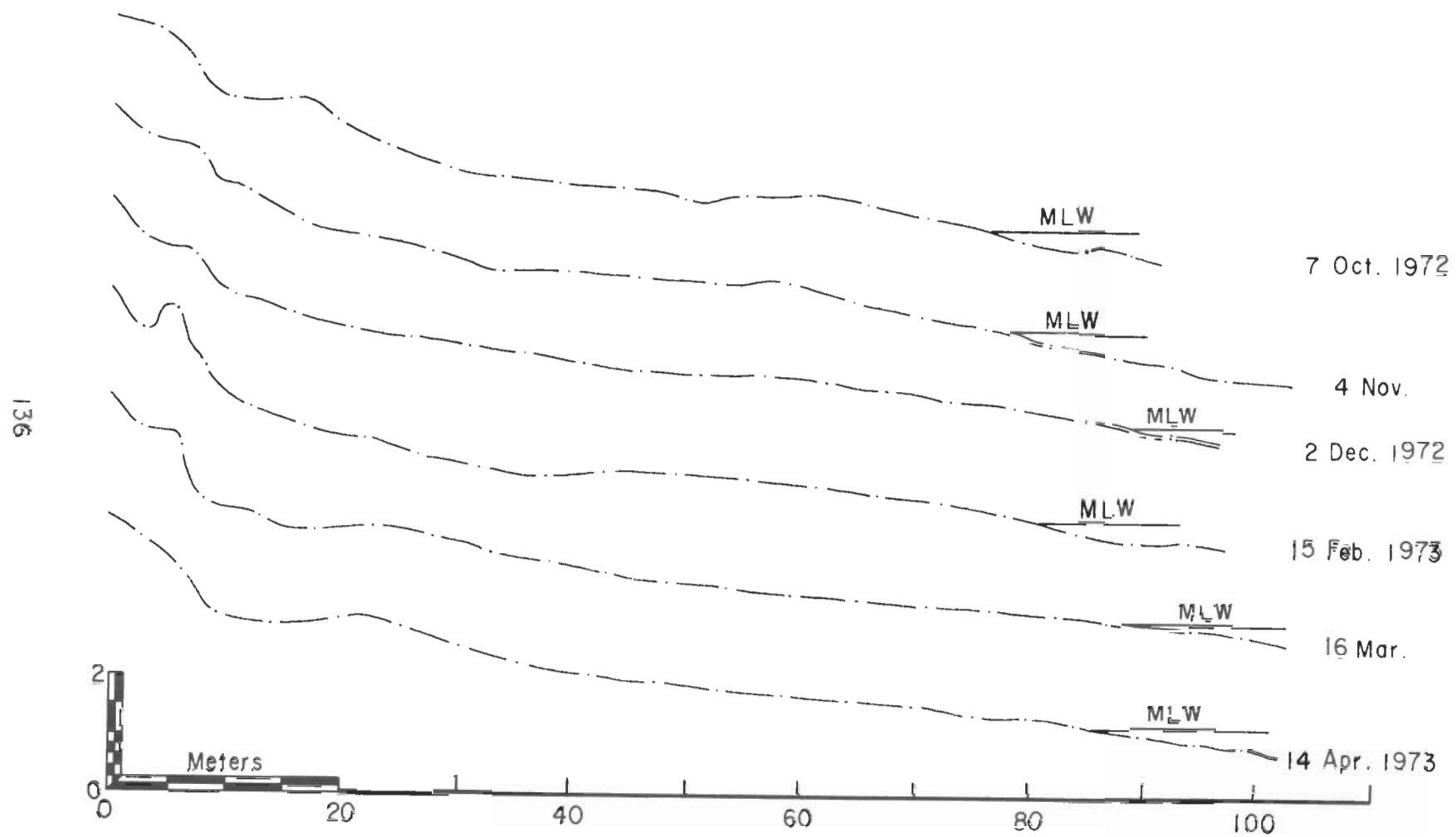
Figure A-7. Station DBI-30, 7 October 1972 to 14 April 1973.

Vertical Exaggeration = 5X

14 July 1972

MLW

21 July

137

MLW

4 Aug.

MLW

2

Meters

0

0   20   40   60   80   100

21 Aug. 1972
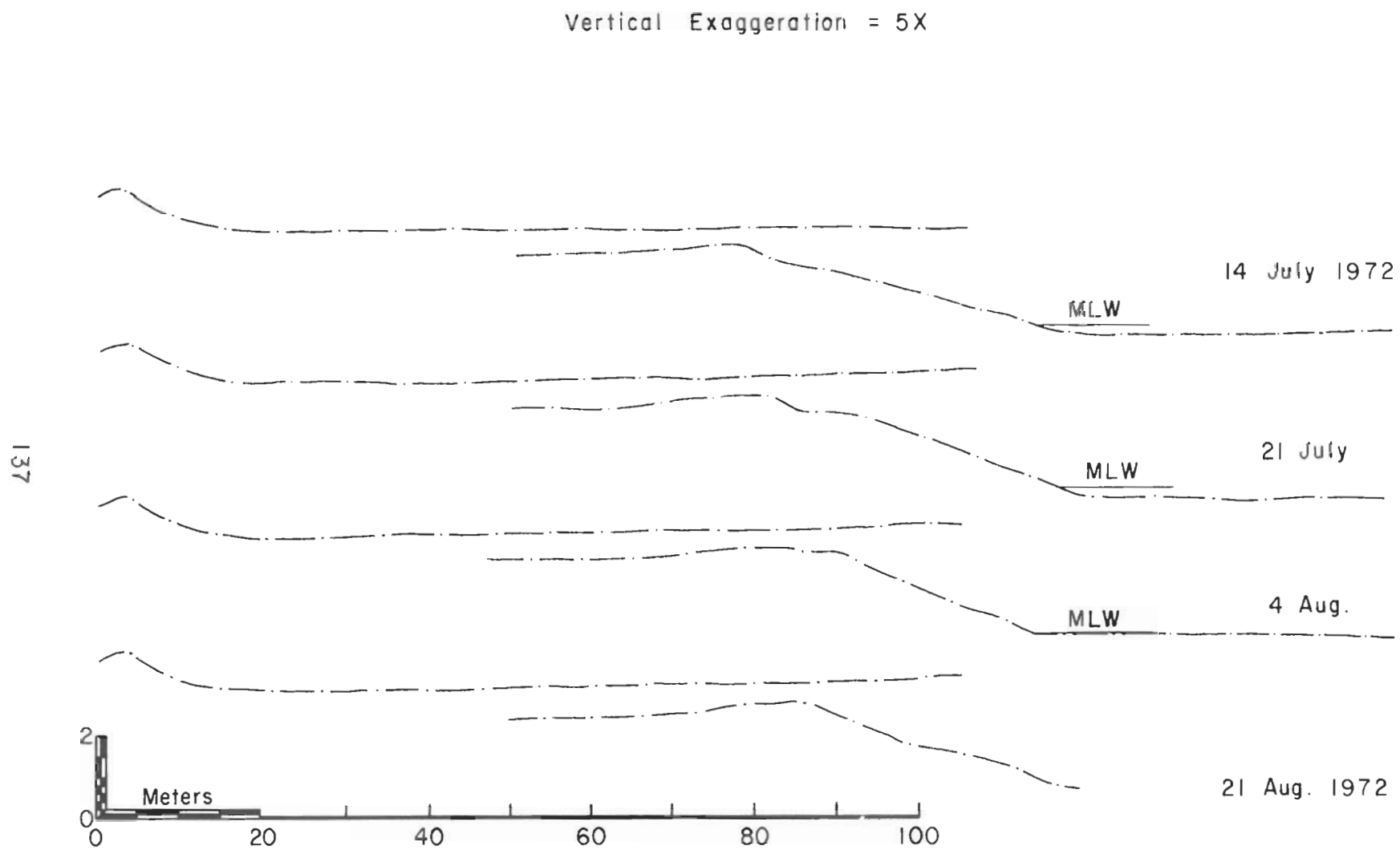
Figure A-8. Station NI-10, 14 July to 21 August 1972.

Vertical Exaggeration = 5X

6 Jan. 1973

MLW

12 Feb.

MLW

30 June 1973

MLW

2

Meters

0

0   20   40   60   80   100
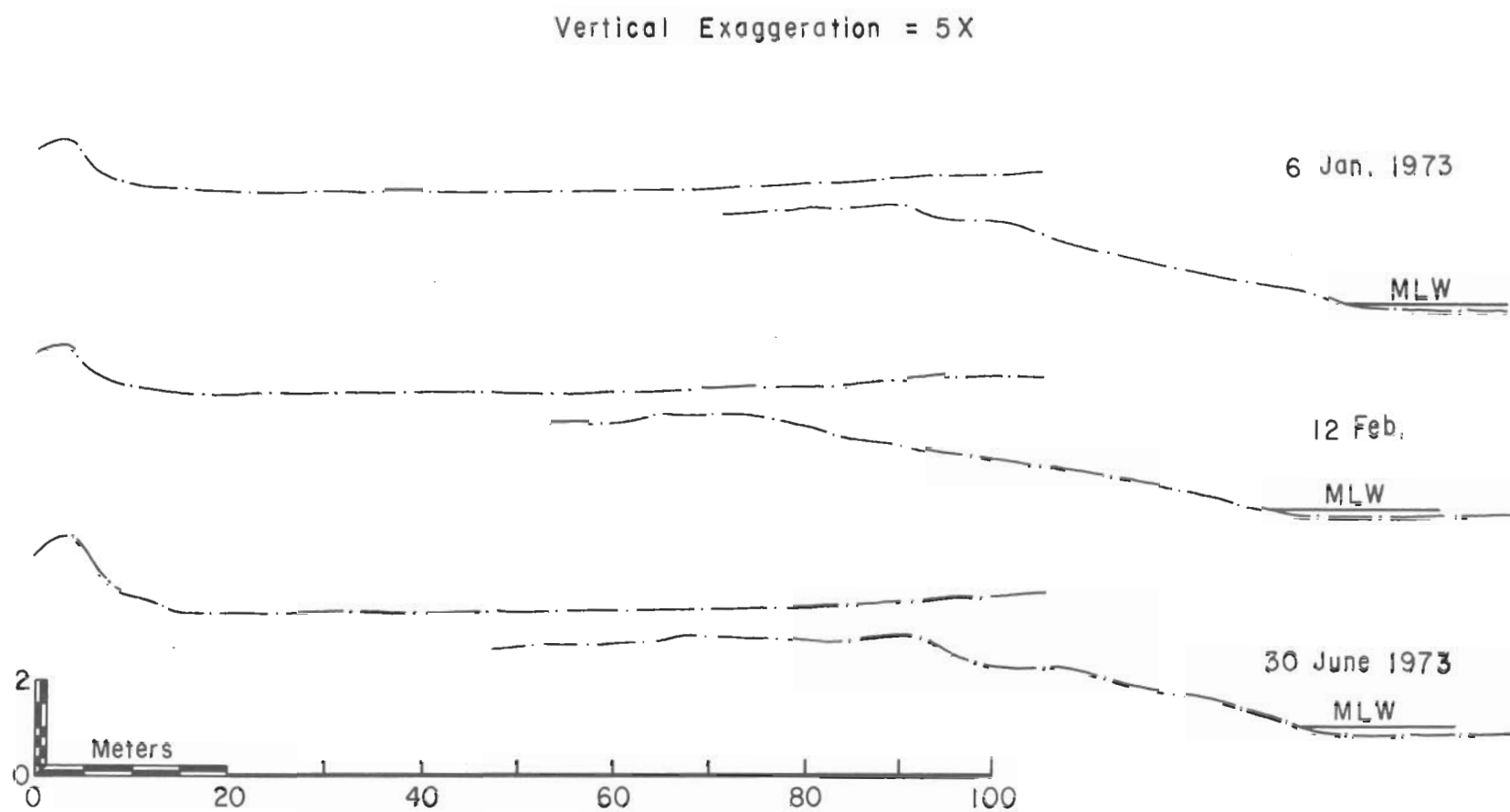
Figure A-9. Station NI-10, 6 January to 30 June 1973.

Vertical Exaggeration = 5X

MLW   21 July 1972

MLW   4 Aug.

MLW   12 Aug.

MLW   21 Aug. 1972

MLW   6 Jan. 1973

MLW   17 Feb.

MLW   30 June 1973

2

Meters

0

0   20   40   60   80   100   120   140   160

139
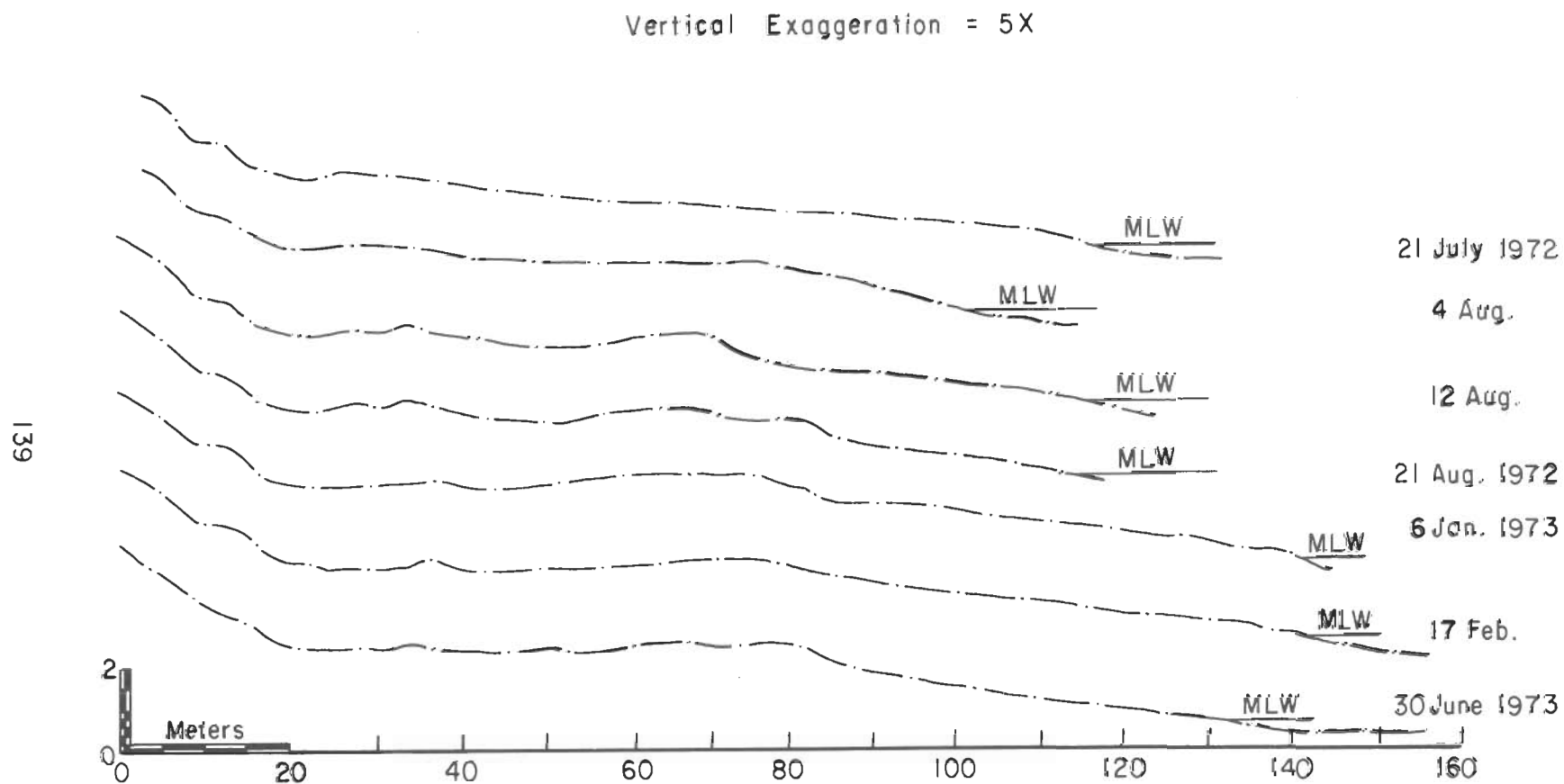
Figure A-10. Station NI-14, 21 July 1972 to 30 June 1973.

Vertical Exaggeration = 5 X

MLW

14 July 1972

MLW

21 July

MLW

4 Aug.

MLW

12 Aug.

MLW

21 Aug. 1972

MLW

6 Jan. 1973

MLW

17 Feb.

MLW

30 June 1973

2

Meters

0

0   20   40   60   80   100

140
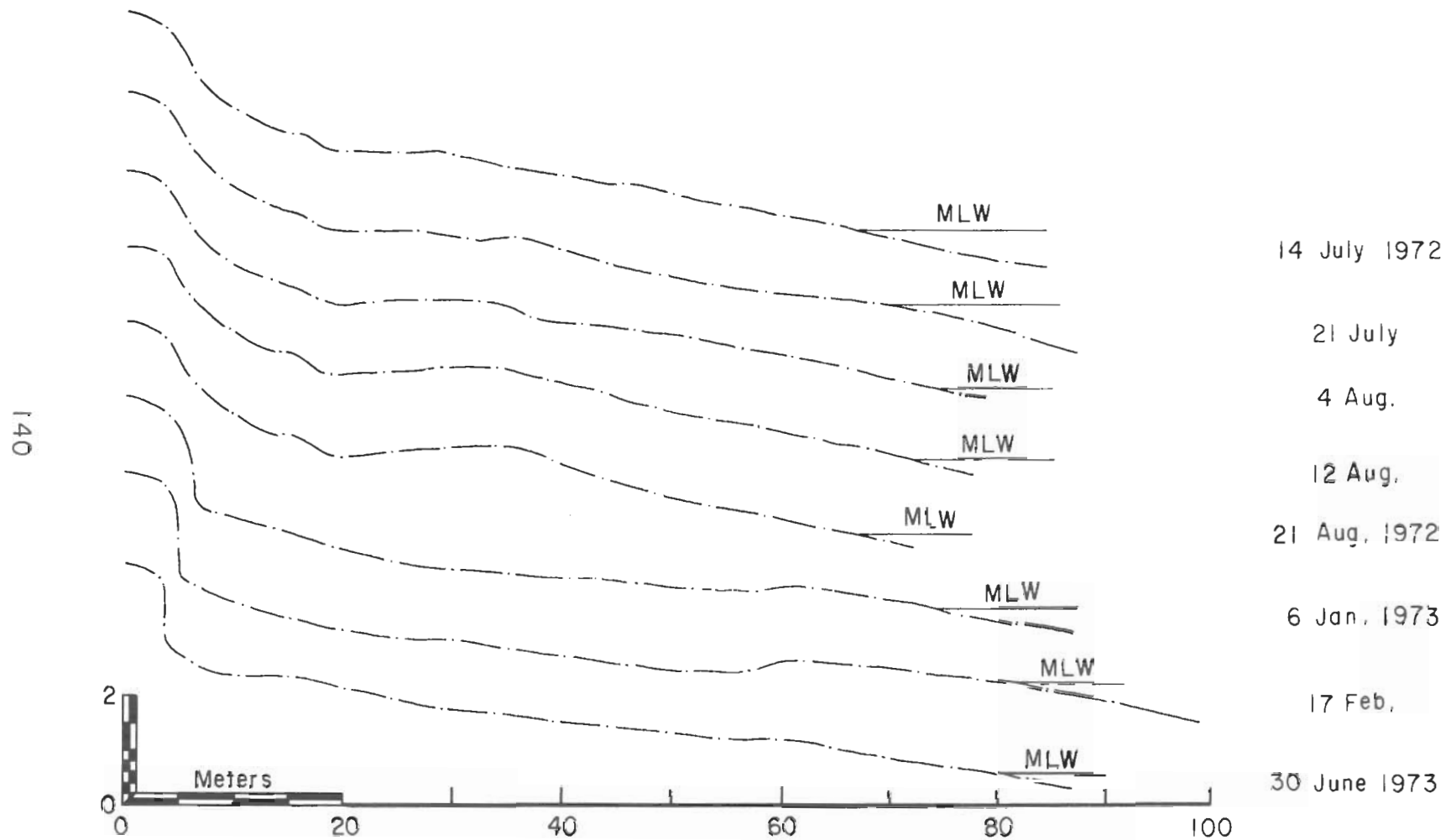
Figure A-11. Station NI-20, 14 July 1972 to 30 June 1973.

APPENDIX B

DEBIDUE ISLAND (DBI) AND NORTH ISLAND (NI)

1973-75 BEACH PROFILES

MLW   **23 Oct. 74**

MLW   **14 Dec. 74**

MLW   8 Jan. 75

23 Feb. 75

MLW   23 Mar. 75

2
1
m
0   20   40
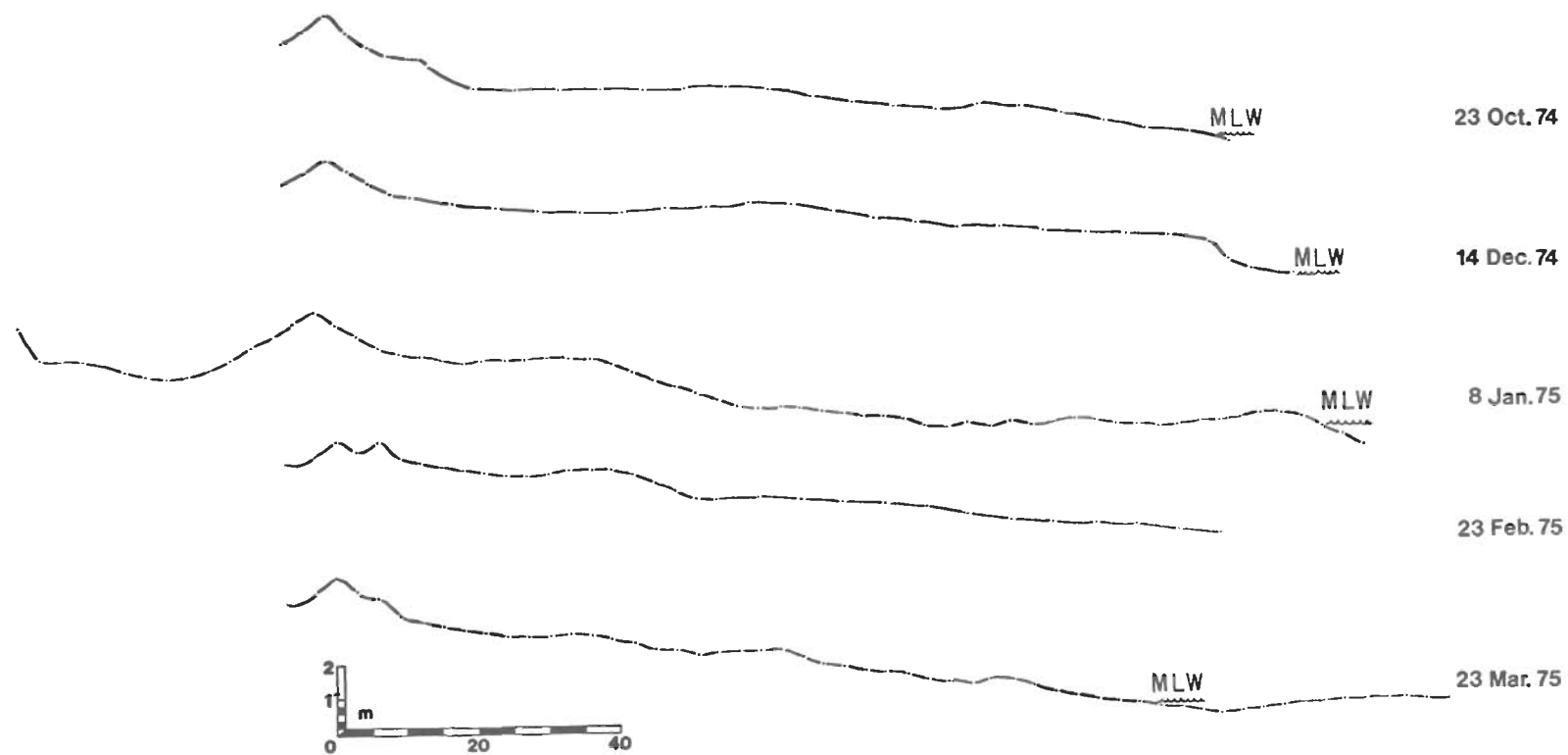
Figure B-1. Station DBI-TS, 23 October 1974 to 23 March 1975.

143

30 June 74

22 July 74

MLW

MLW

25 Aug. 74

MLW

18 Sept. 74

MLW

29 Oct. 74

MLW

14 Dec. 74

MLW

8 Jan. 75

23 Feb. 75

MLW

23 Mar. 75

2
1
m
0   20   40
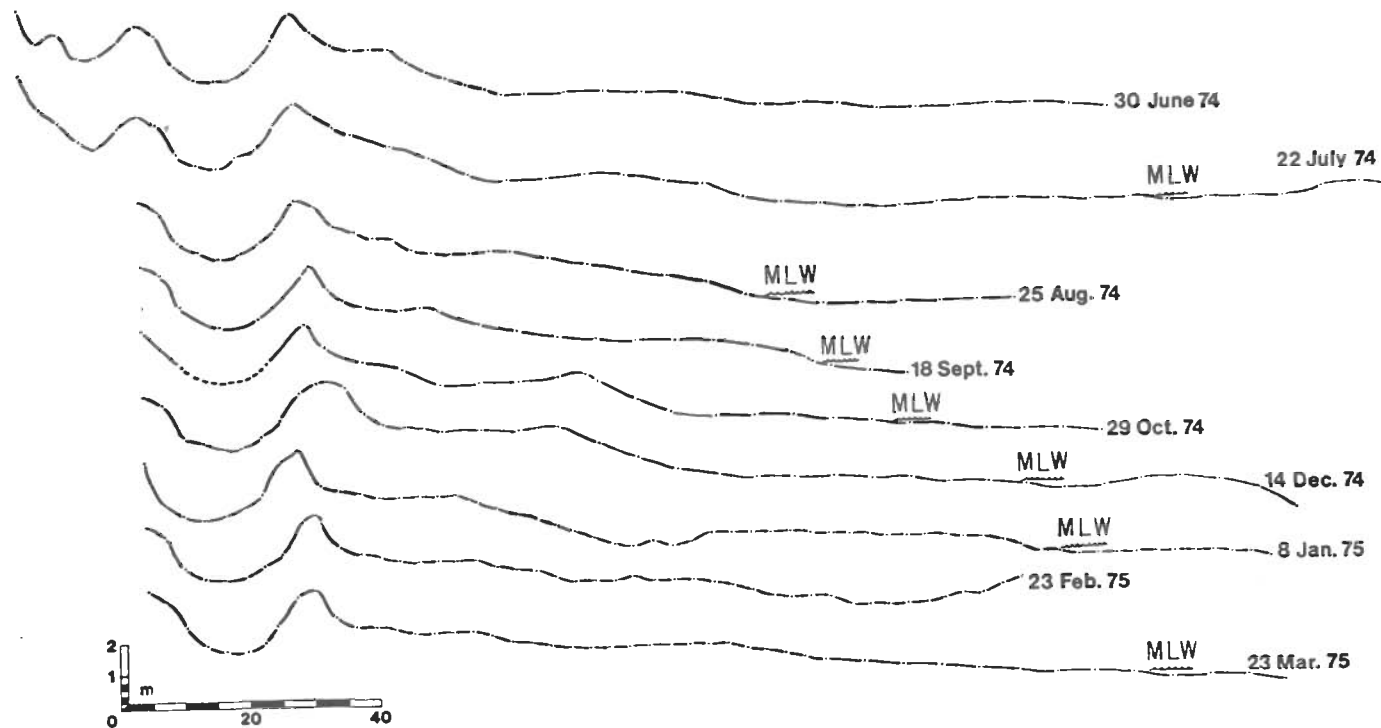
Figure B-2. Station DBI-6, 30 June 1974 to 23 March 1975.
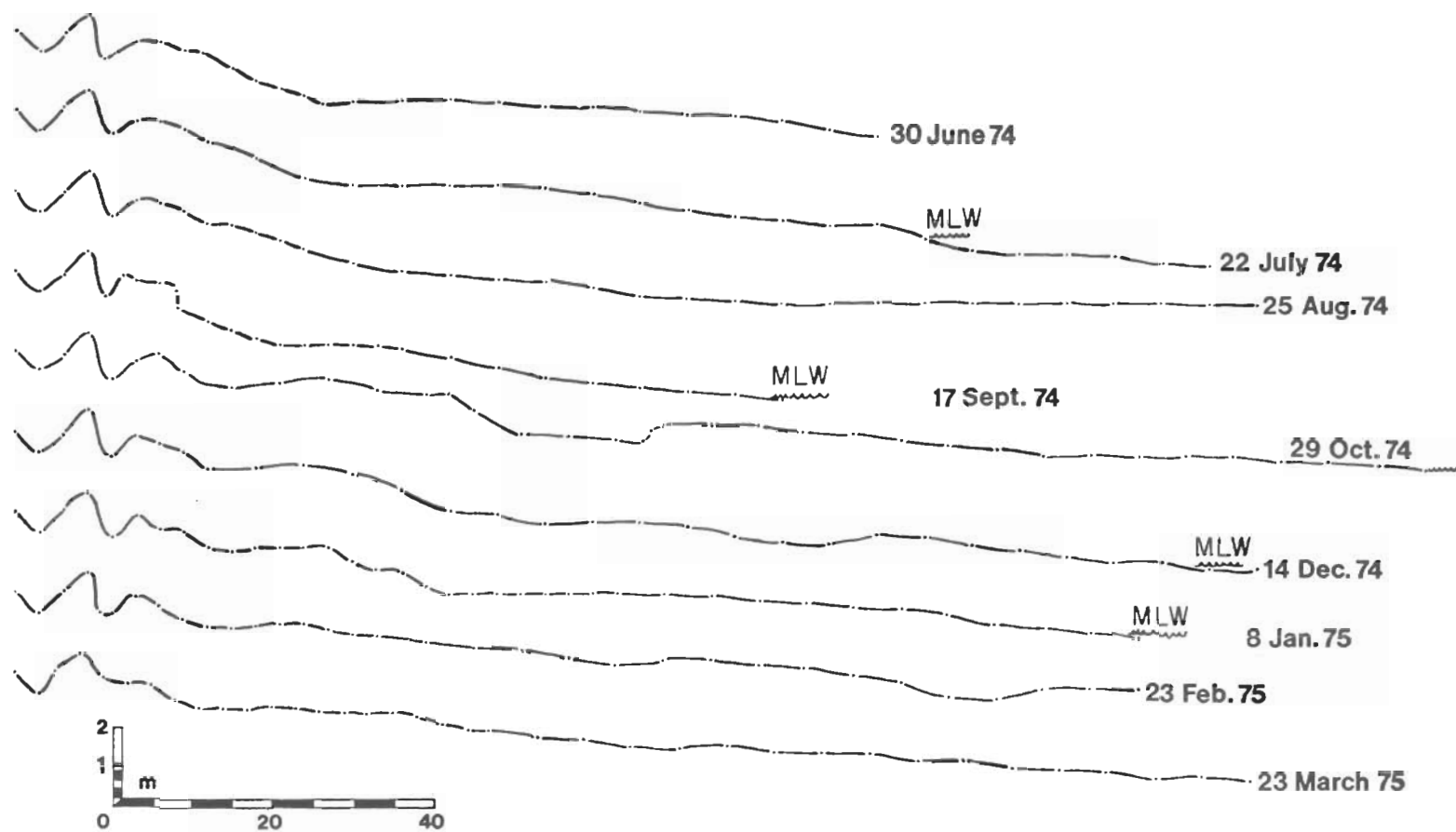
Figure B-3. Station DBI-8, 30 June 1974 to 23 March 1975.

MLW

MLW

MLW

MLW

MLW

MLW

MLW

MLW

28 July 73

26 Sept. 73

7 Oct. 73

24 Nov. 73

10 Dec. 73

19 Jan. 74

21 Mar. 74

2
1
m
0
20
40
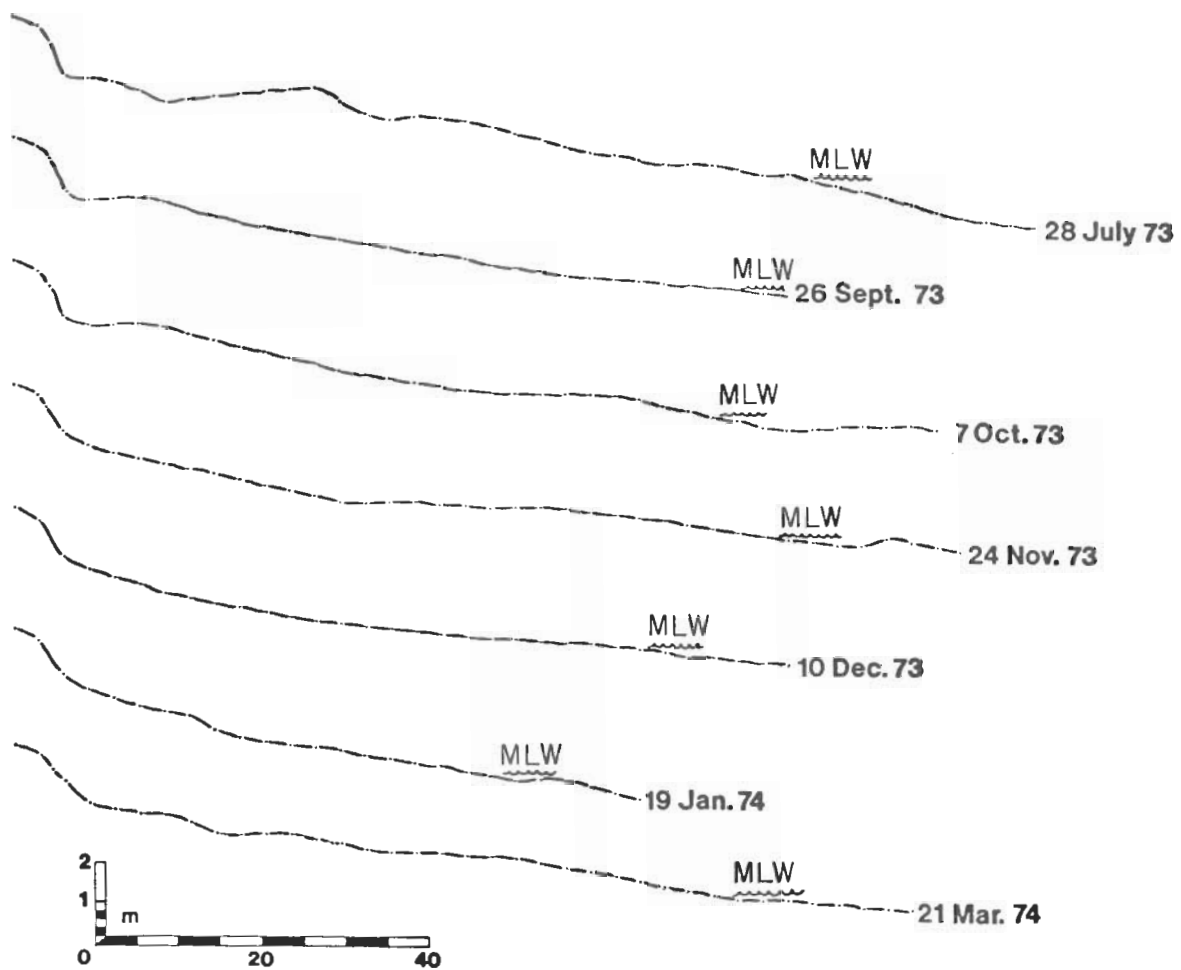
Figure B-4. Station DBI-10, 28 July 1973 to 21 March 1974.

MLW
30 June 74

MLW
22 July 74

MLW
25 Aug. 74

MLW
18 Sept. 74

MLW
29 Oct. 74

MLW
14 Dec. 74

MLW
8 Jan. 75

MLW
23 Feb. 75

MLW
20 Mar. 75

2
1
m
0   20   40
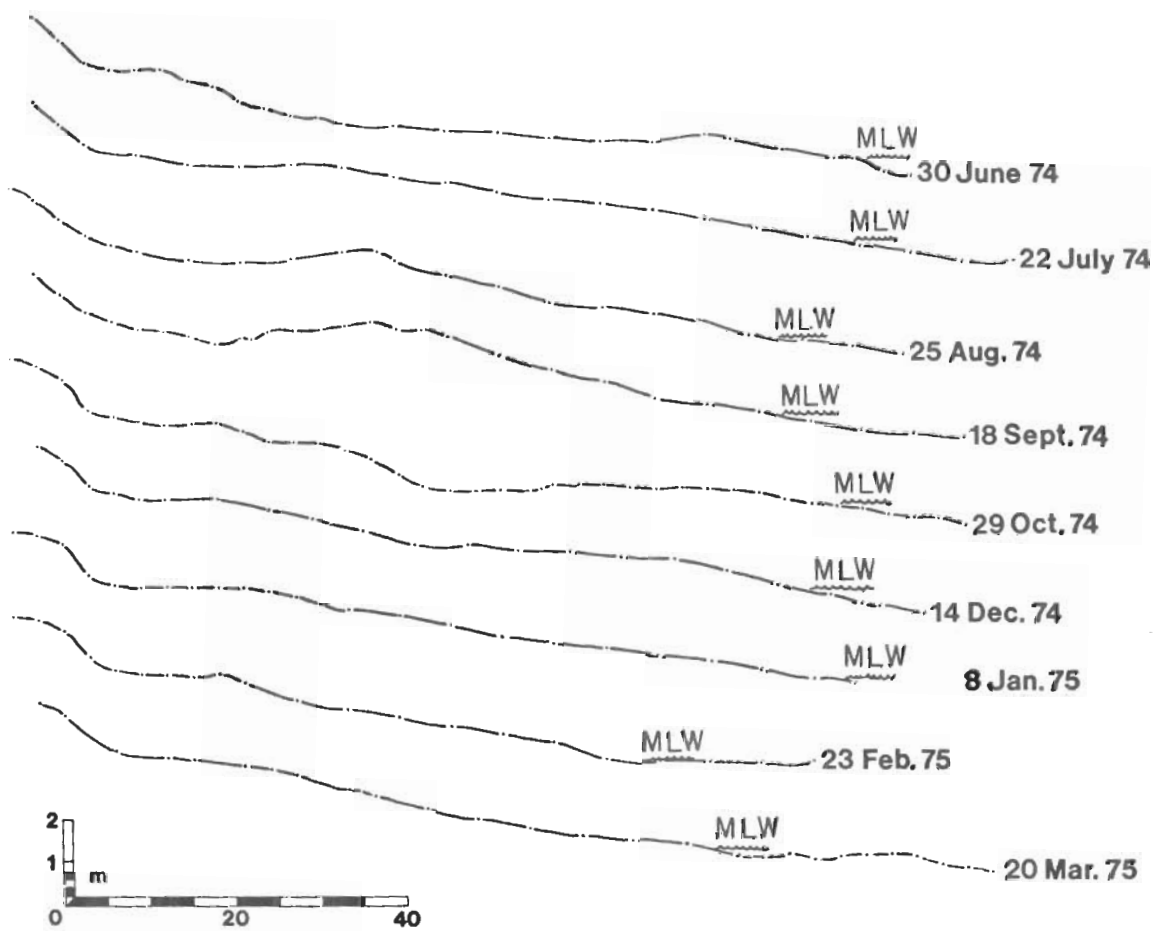
Figure B-5. Station DBI-10, 30 June 1974 to 20 March 1975.
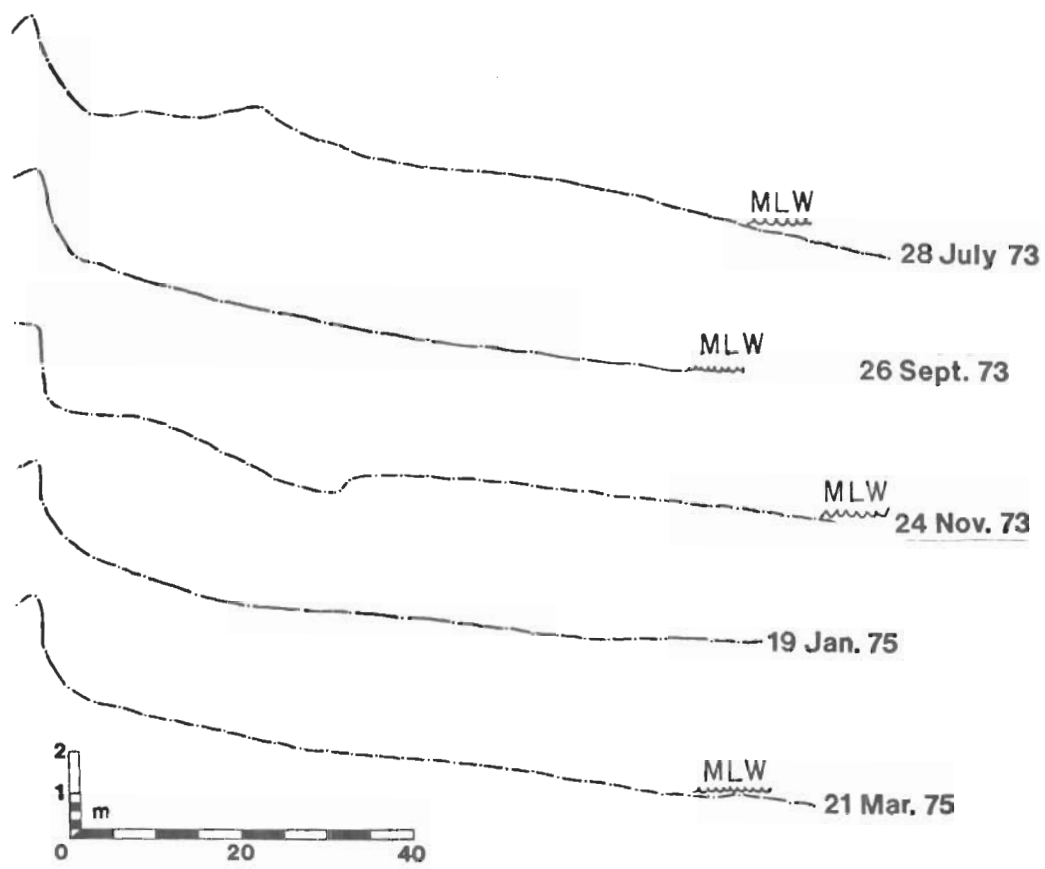
Figure B-6. Station DBI-20, 28 July 1973 to 21 March 1974.

MLW

28 July 73

MLW

26 Sept. 73

MLW 24 Nov. 73

19 Jan. 75

MLW

21 Mar. 75

2
1
m
0   20   40

a. **NI-10**

12 Aug. 73
MLW

10 Dec 73
MLW

b. **NI-14**

12 Aug. 73

MLW 10 Dec. 73

c. **NI-20**

MLW 12 Aug. 73

MLW 10 Dec. 73

2
1
m
0   20   40
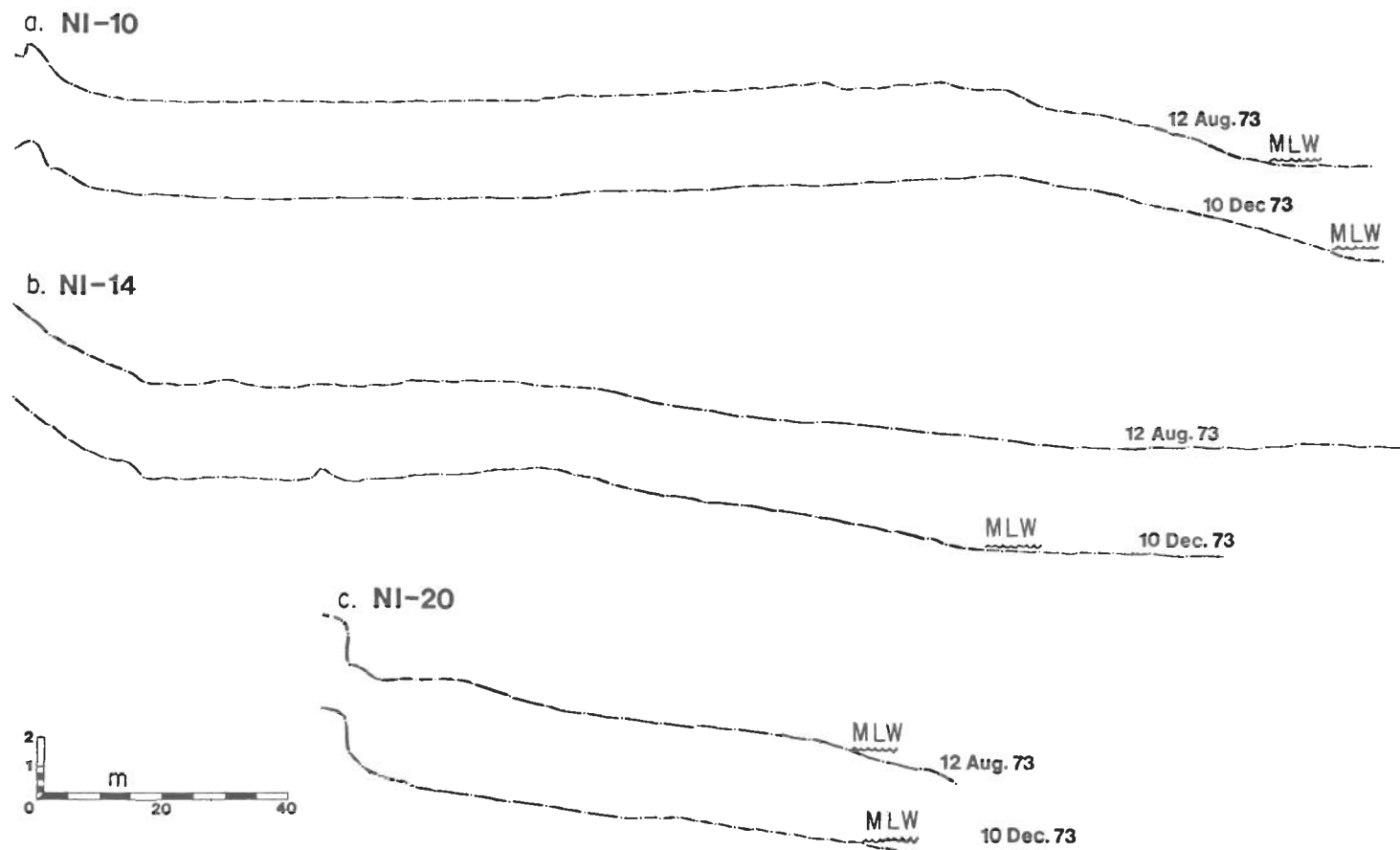
Figure B-7. Stations NI-10, NI-14, and NI-20, 12 August to 10 December 1973.

MLW 30 June 74

MLW 22 July 74

MLW 24 Aug. 74

MLW 18 Sept. 74

MLW 29 Oct. 74

MLW 14 Dec. 74

8 Jan. 74

23 Feb. 74

23 Mar. 74
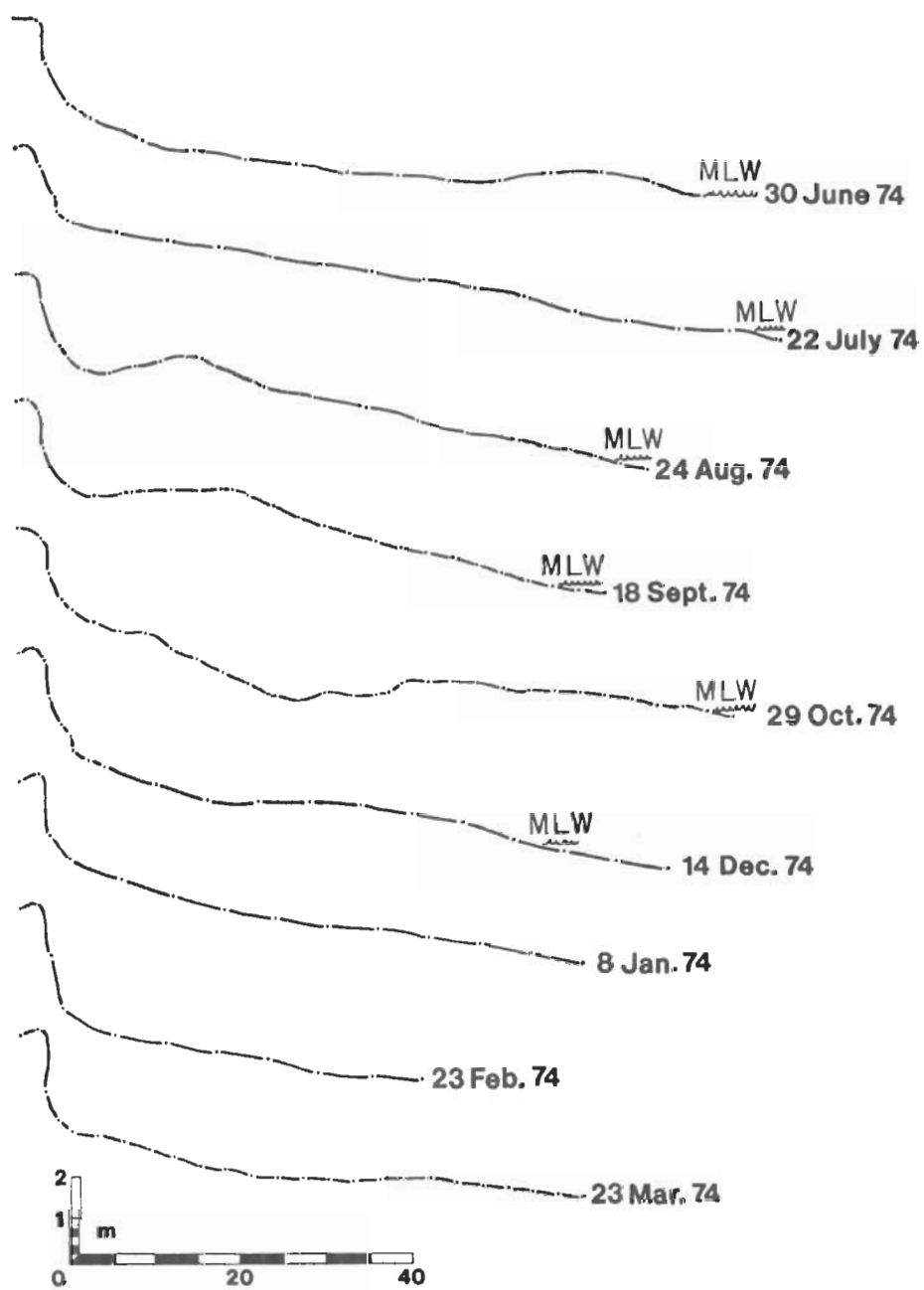
Figure B-8. Station DBI-20, 30 June 1974 to 23 March 1975.

MLW

28 July 73

26 Sept. 73

MLW

24 Nov. 73

MLW
19 Jan. 74

MLW
21 Mar. 74

2
1
m
0   20   40
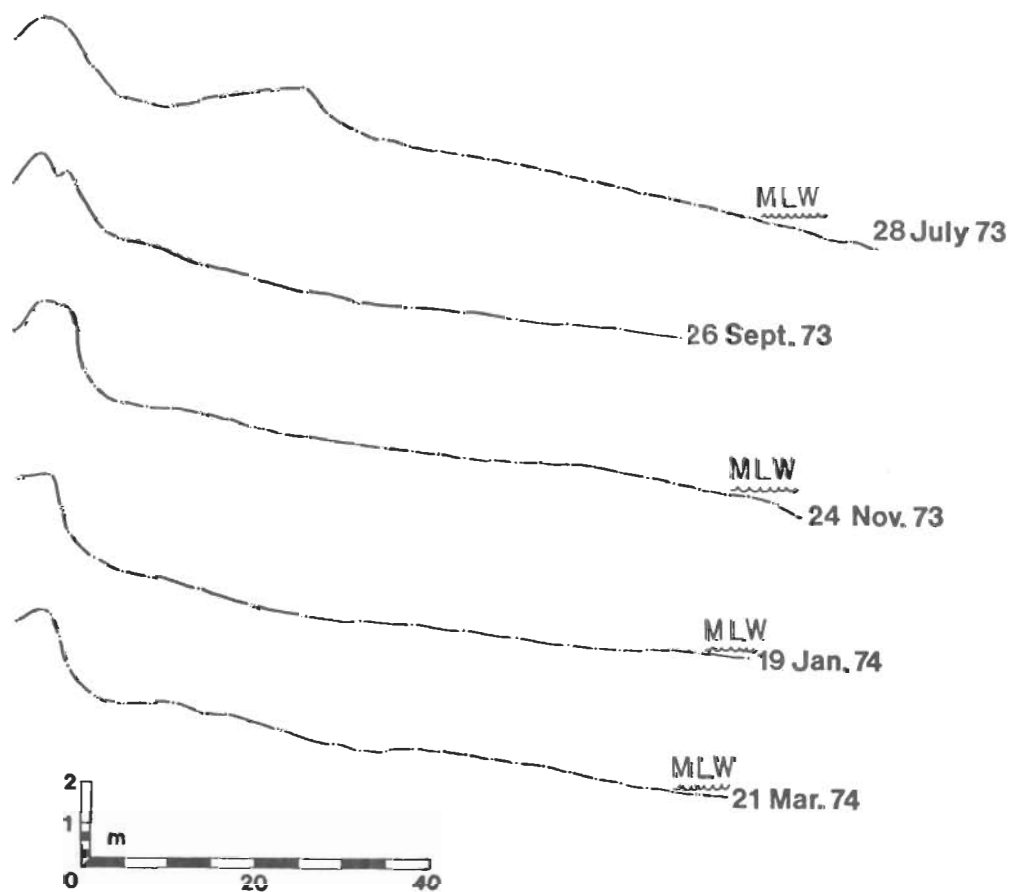
Figure B-9. Station DBI-25, 28 July 1974 to 21 March 1974.
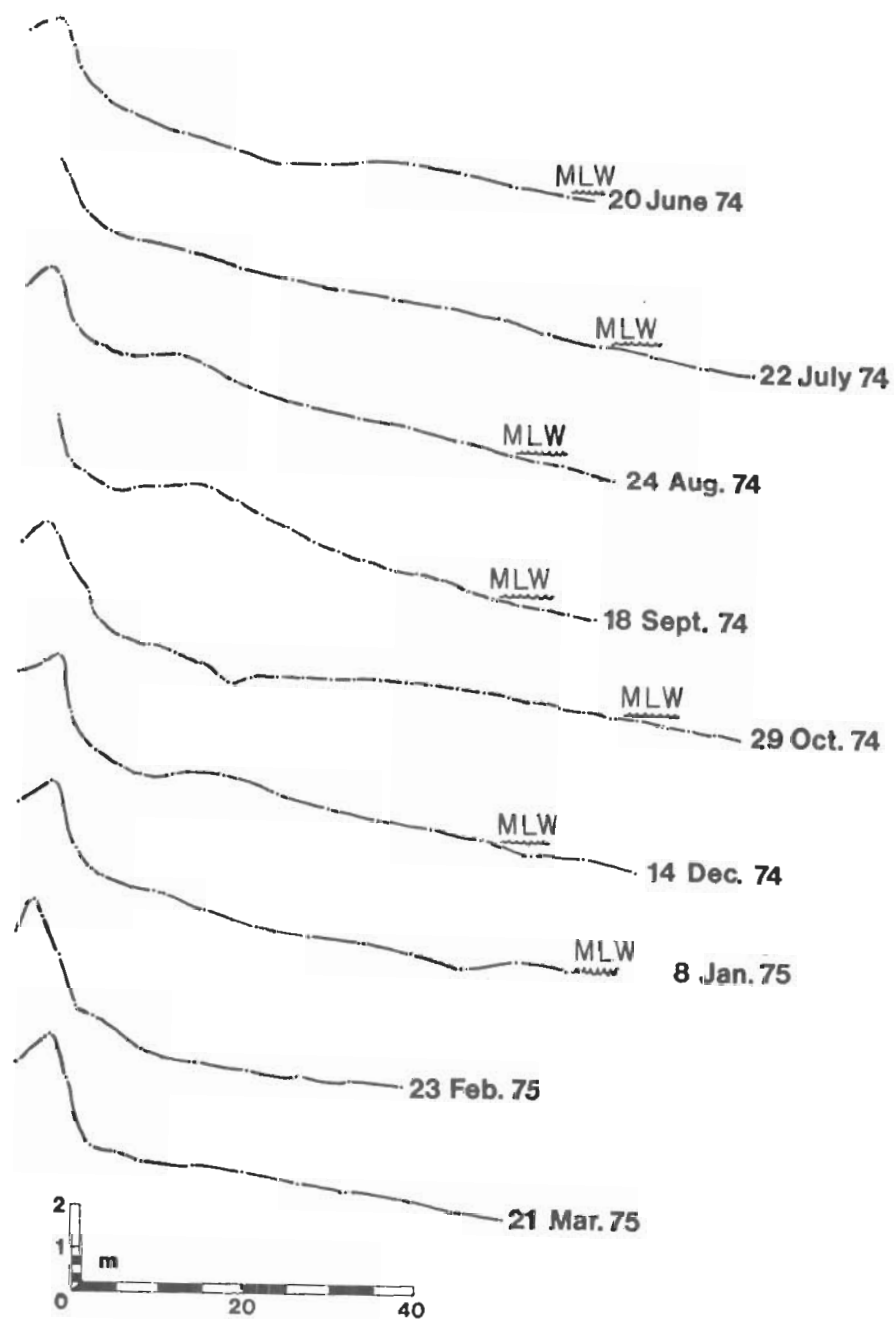
Figure B-10. Station DBI-25, 30 June 1974 to 21 March 1975.

MLW

27 July 73

26 Sept. 73

MLW
24 Nov. 73

MLW
19 Jan. 74

MLW
21 Mar. 74

2
1
m
0   20   40
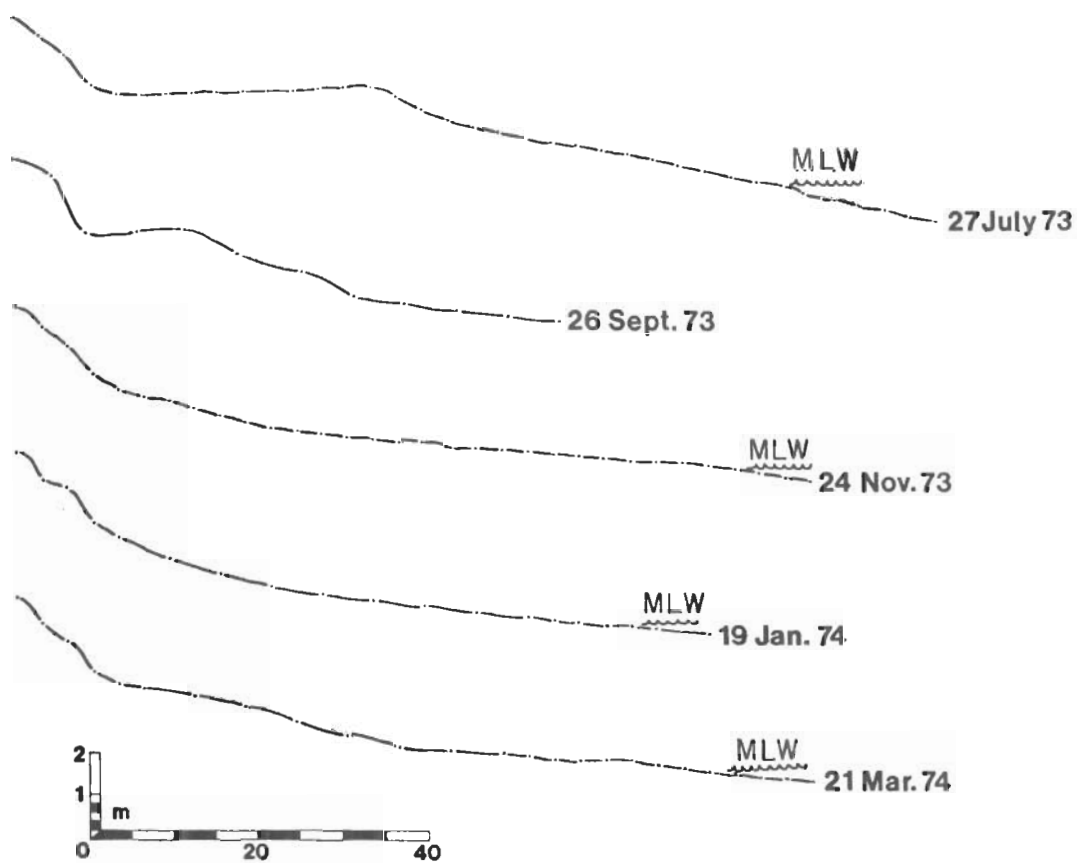
Figure B-11. Station DBI-30, 27 July 1973 to 21 March 1974.

30 June 74

22 July 74

24 Aug. 74

14 Sept. 74

29 Oct. 74

8 Jan. 75

23 Feb. 75

26 Mar. 75

2
1
m
0   20   40
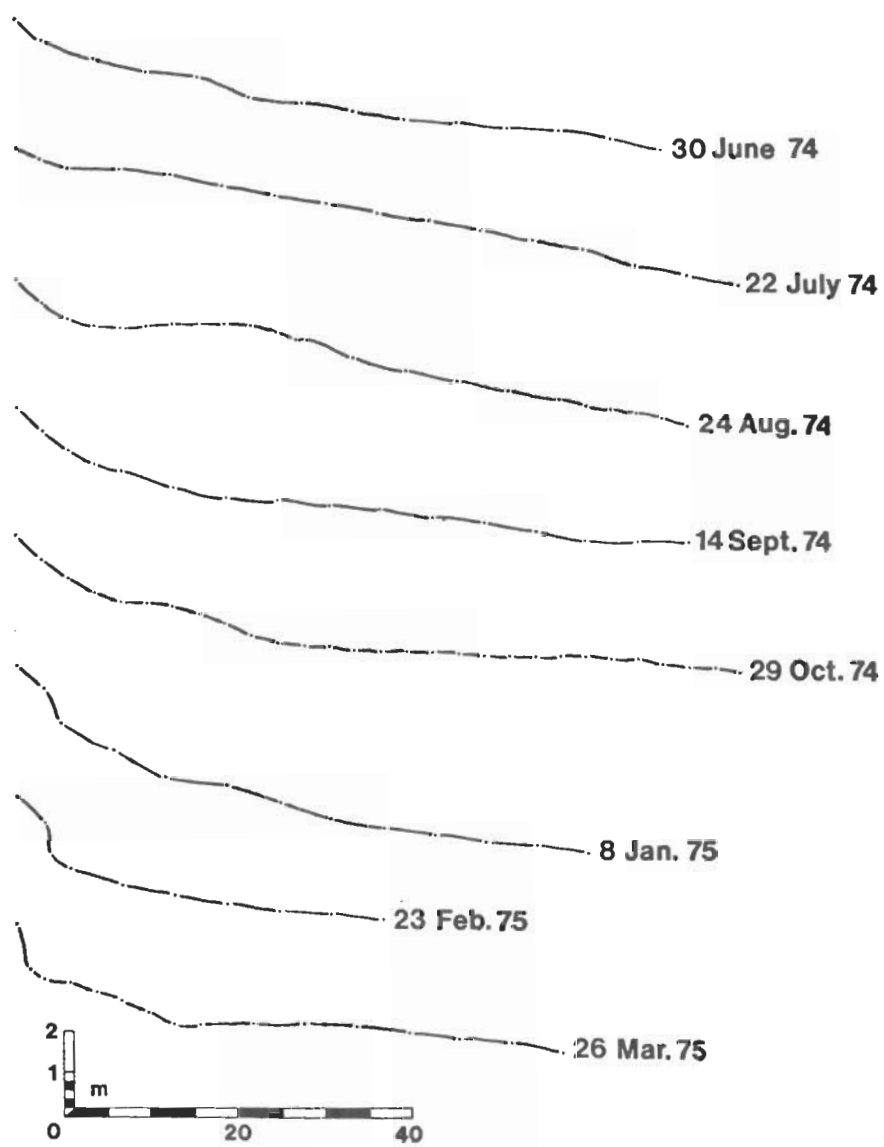
Figure B-12. Station DBI-30, 30 June 1974 to 26 March 1975.

MLW

24 Aug. 74

MLW

17 Sept. 74

MLW

27 Oct. 74

MLW

29 Nov. 74

MLW

10 Jan. 75

MLW

23 Feb. 75

MLW

25 Mar. 75

2
1
m
0   20   40
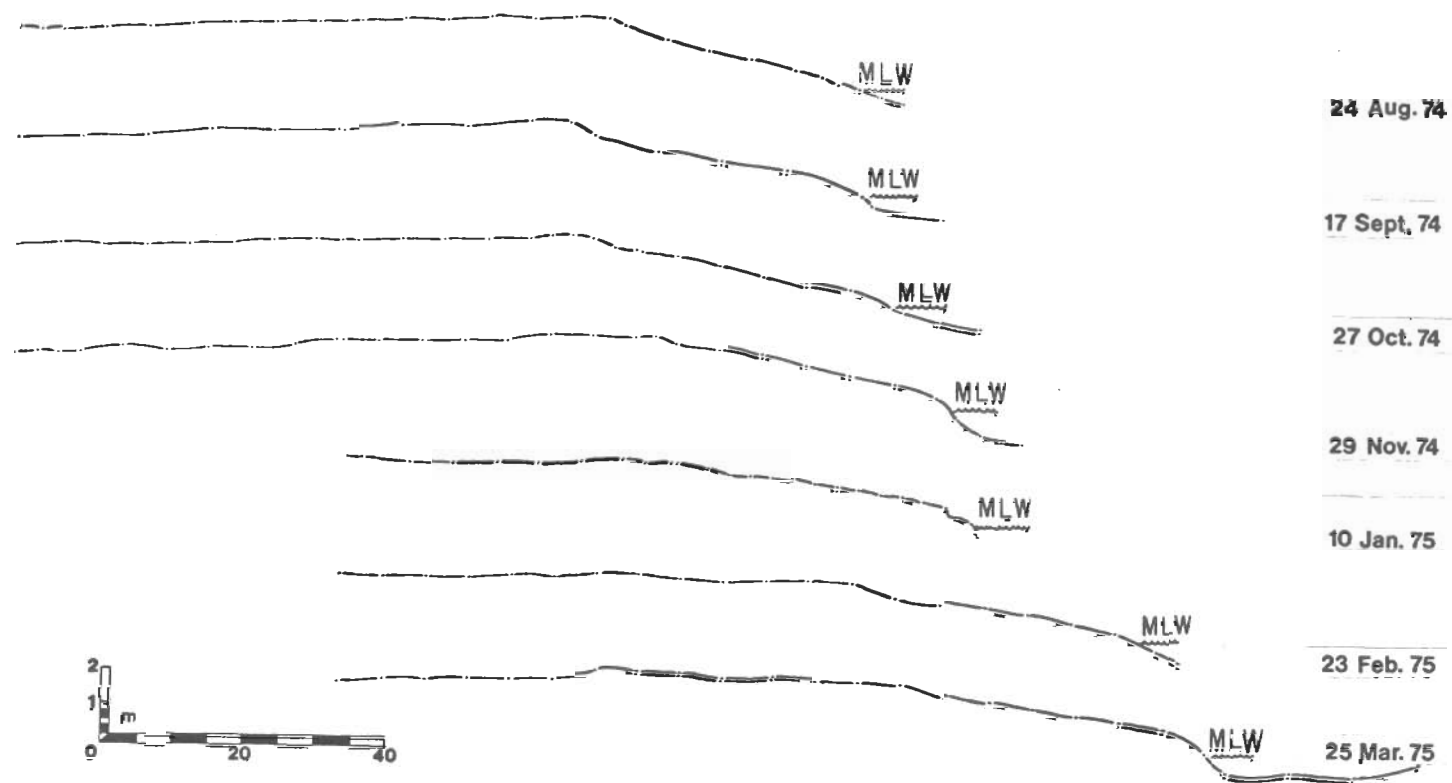
Figure B-13. Station NI-6, 24 August 1974 to 25 March 1975.

155
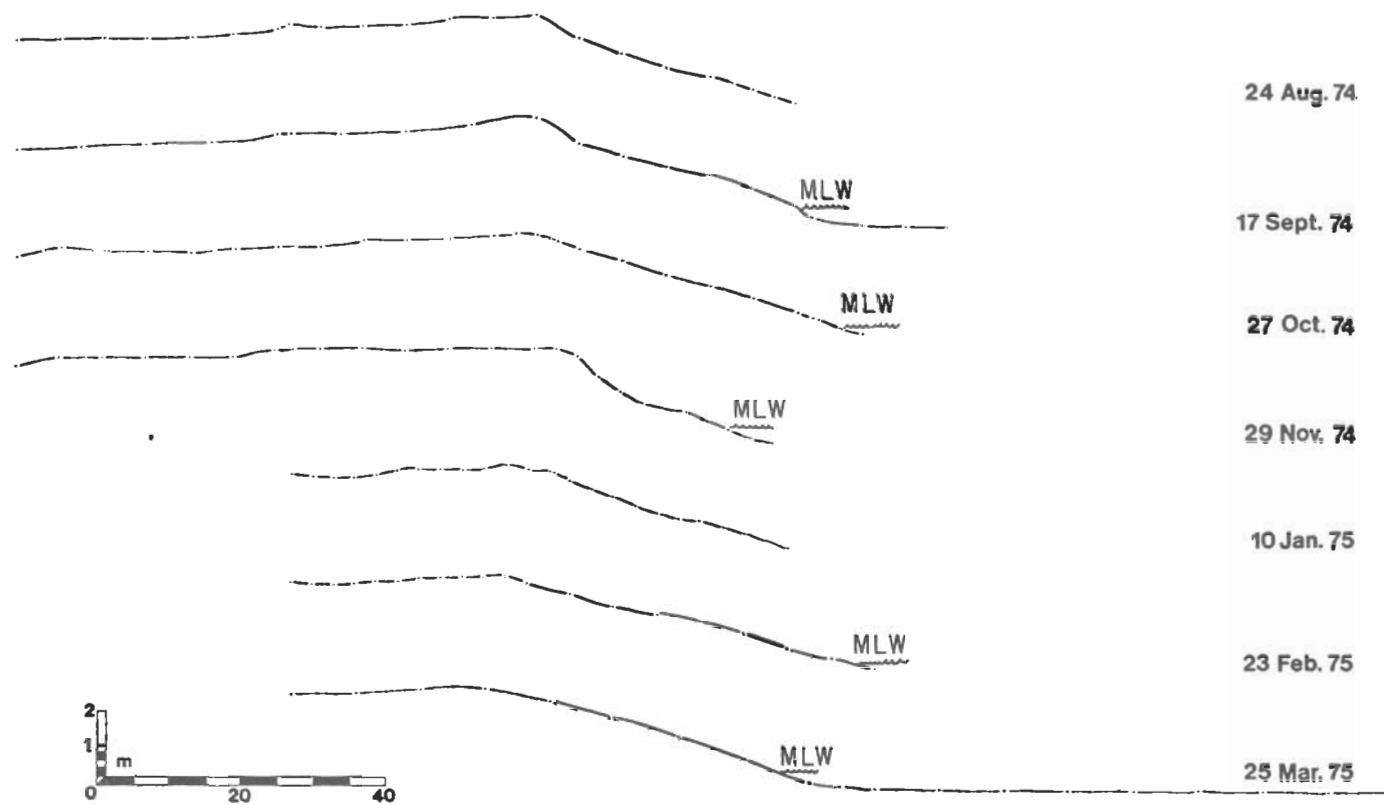
Figure B-14. Station NI-8, 24 August 1974 to 25 March 1975.

27 Aug. 74

17 Sept. 74

MLW

27 Oct. 74

MLW

29 Nov. 74

MLW

156
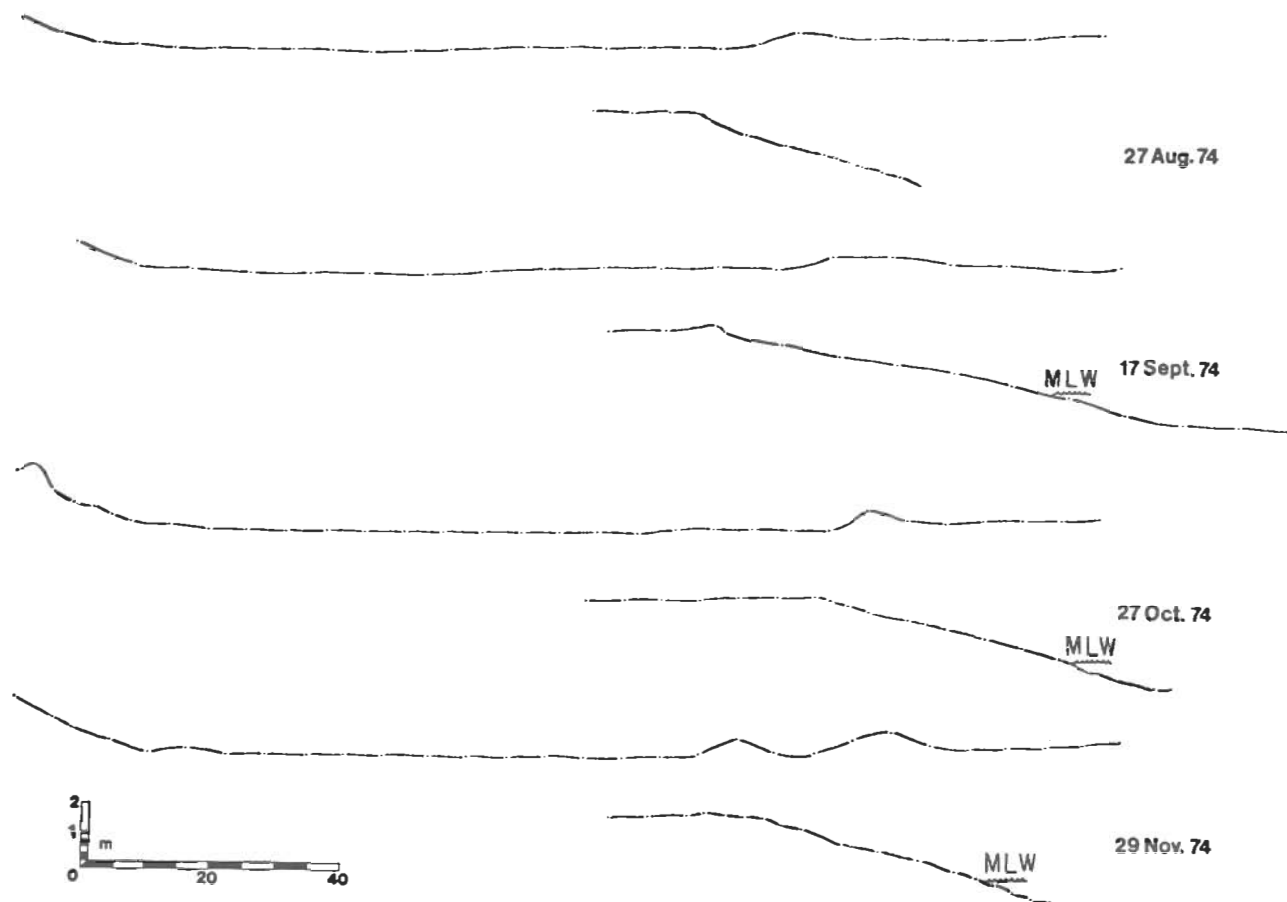
Figure B-15. Station NI-10, 27 August to 29 November 1974.
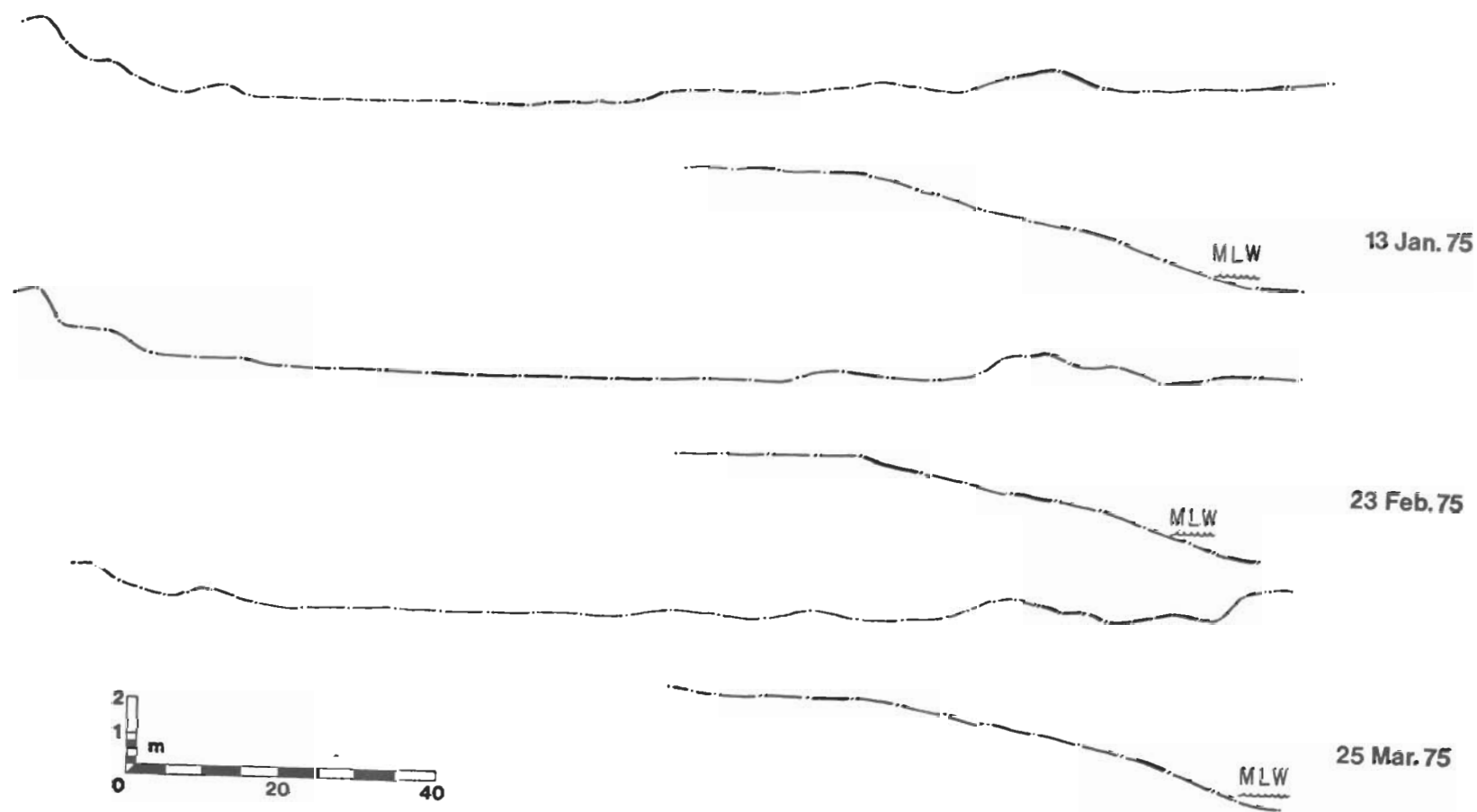
Figure B-16. Station NI-10, 13 January to 25 March 1975.

22 July 74

MLW   23 Aug. 74

19 Sept. 74

2
1
m
0   20   40

27 Oct. 74
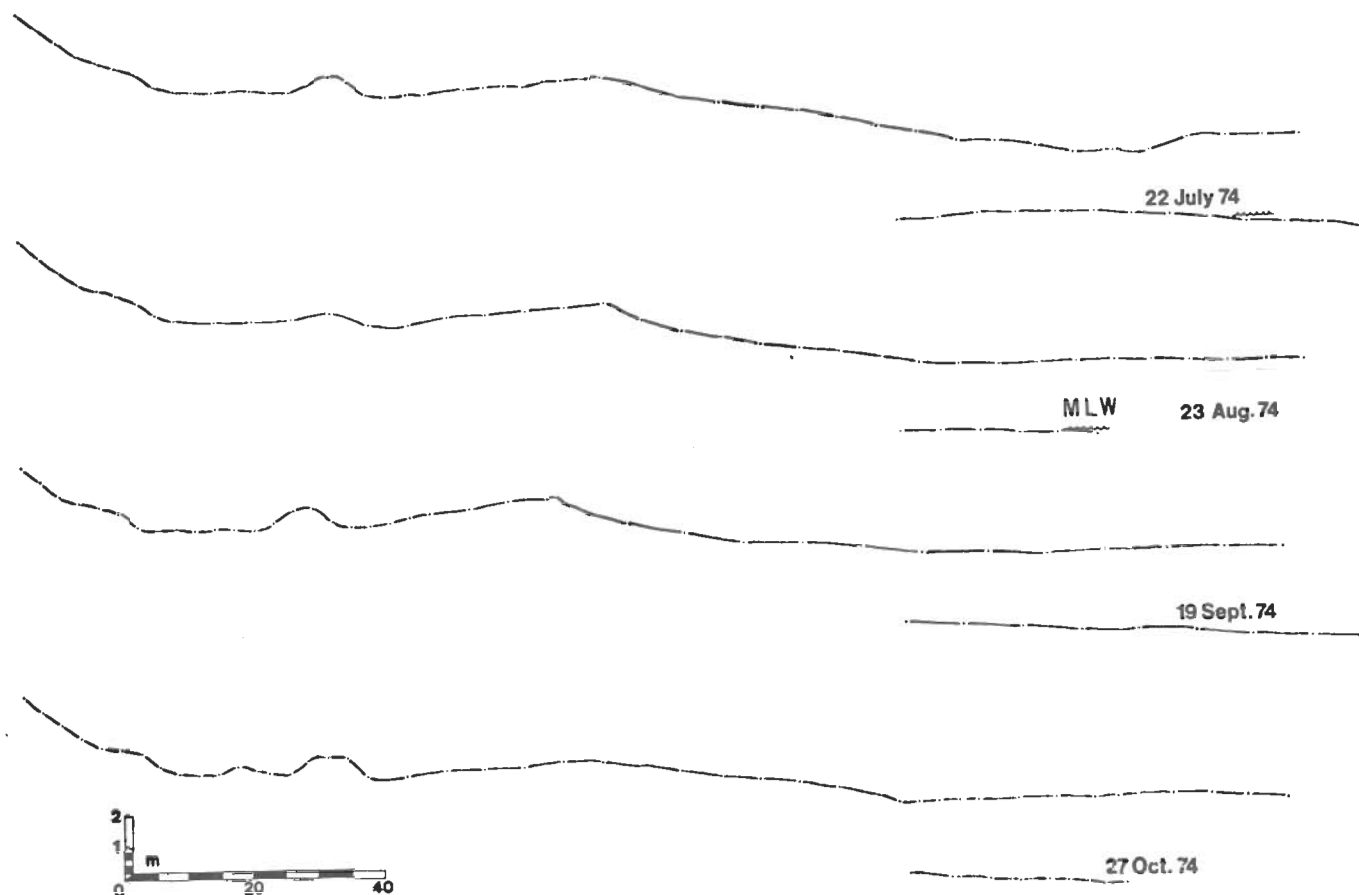
Figure B-17. Station NI-14, 22 July to 27 October 1974.

29 Nov. 74   MLW

9 Jan. 75   MLW

23 Feb. 75

25 Mar. 75
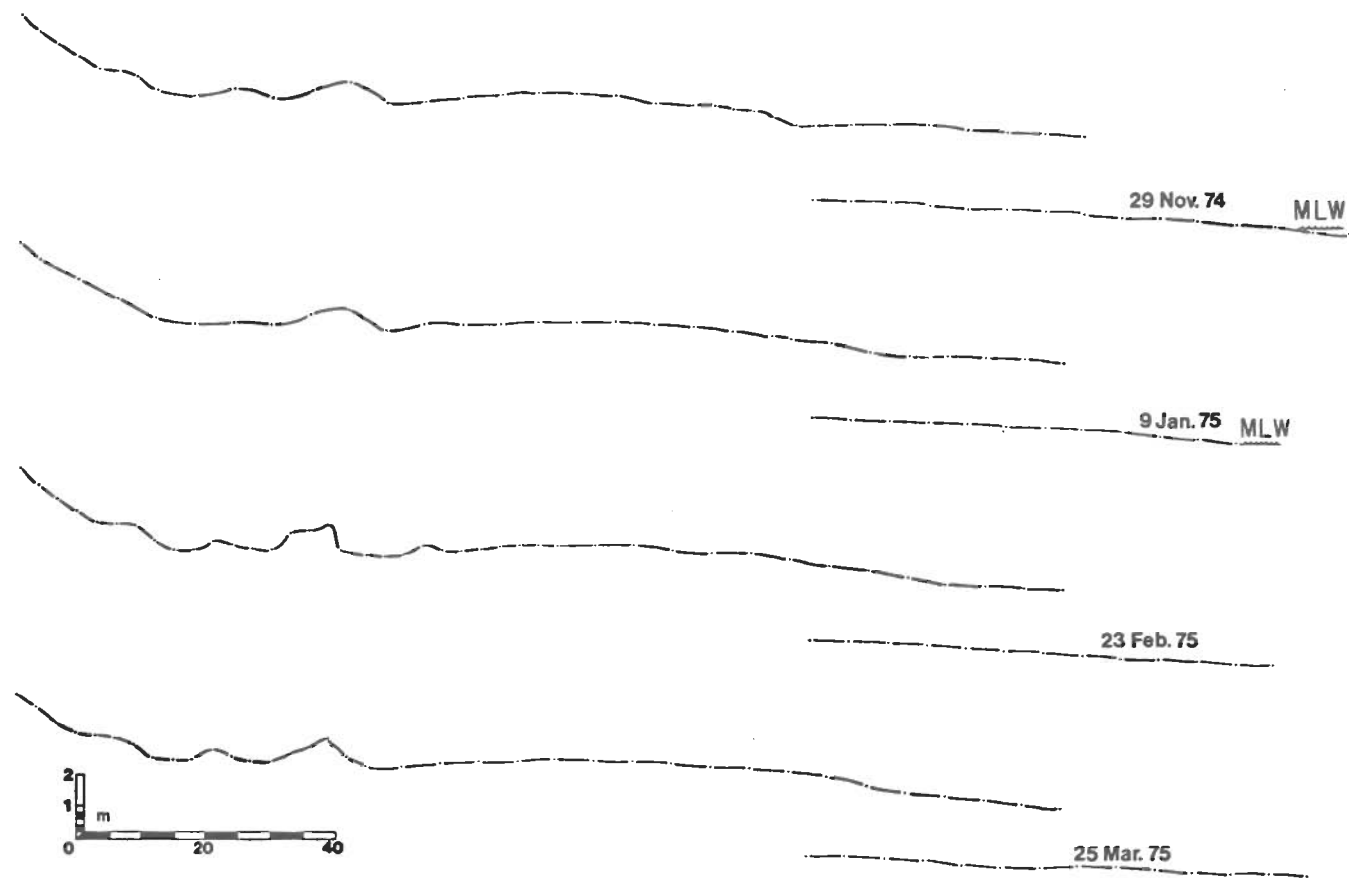
Figure B-18. Station NI-14, 29 November 1974 to 25 March 1975.

a. NI-FTD

10 Jan. 75

MLW
25 Mar. 75

b. NI-TS

27 Oct. 74

MLW
10 Jan. 75

23 Feb.75

MLW
25 Mar. 75

c. NI-20

MLW
22 July 74

17 Sept. 74

MLW
9 Jan. 75

25 Mar. 75

2
1
m
0   20   40
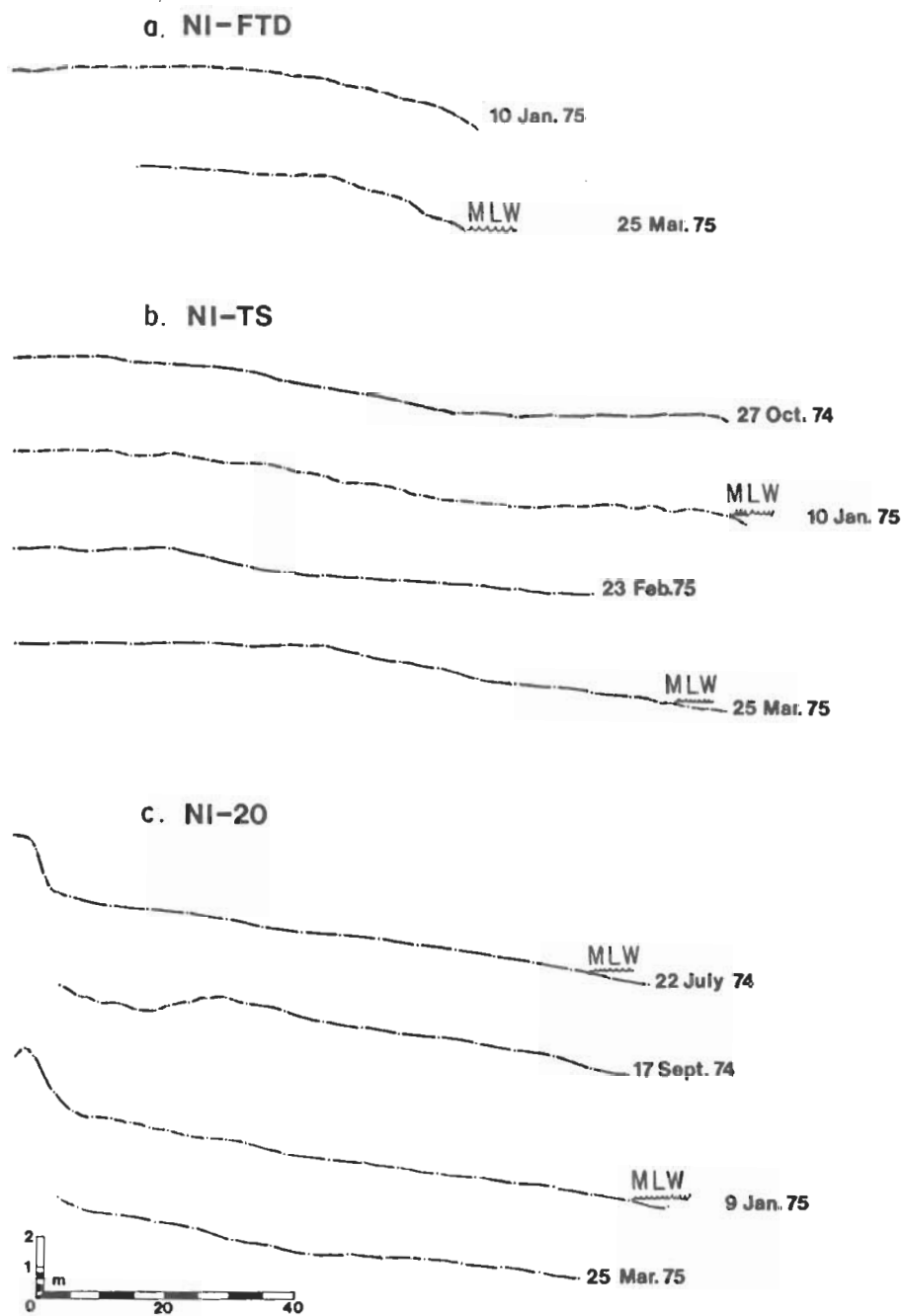
Figure B-19. Stations NI-FTD (10 January to 25 March 1975),
NI-TS (27 October 1975 to 25 March 1975), and NI-20
(22 July 1974 to 25 March 1975).

APPENDIX C

1972-73 TIDAL CURRENT TIME HISTORIES
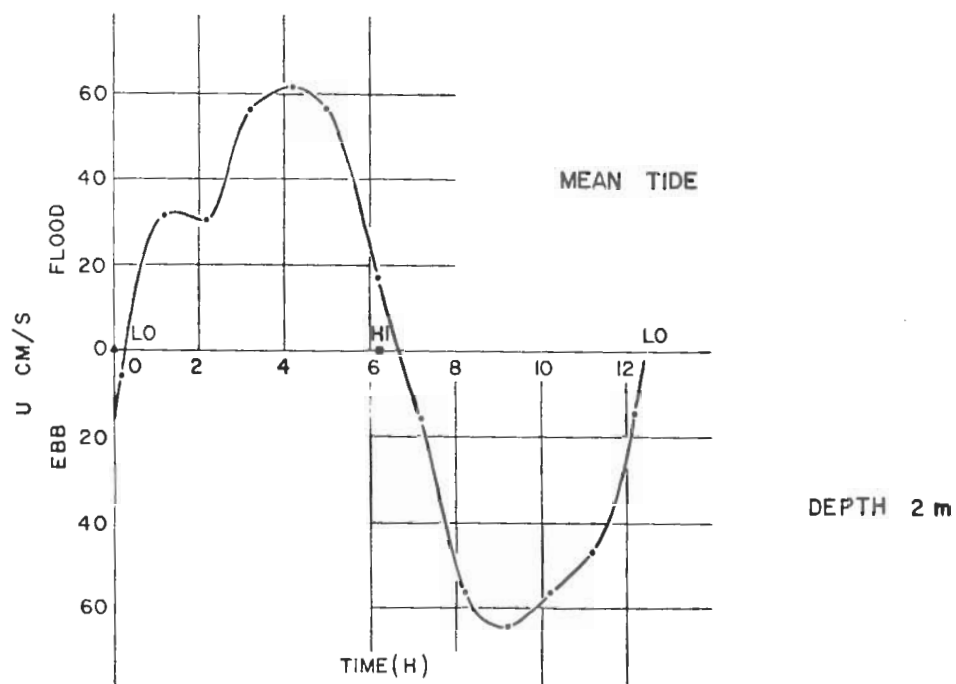
Figure C-1. Tidal current velocity, station IN-1, 25 July 1972.
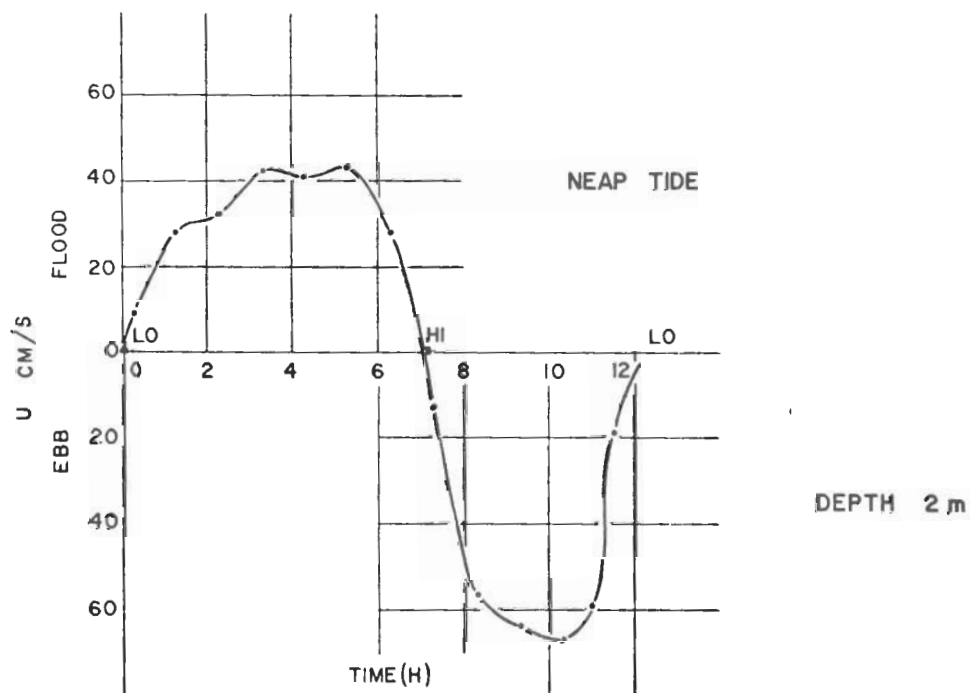
Figure C-2. Tidal current velocity, station IN-1, 18 July 1972.

162
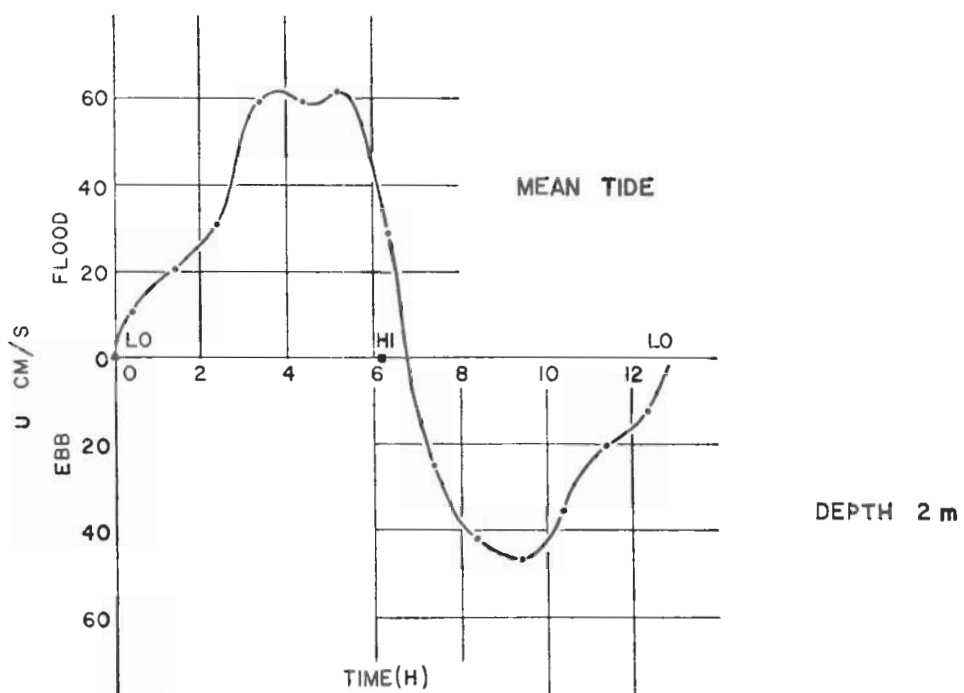
Figure C-3. Tidal current velocity, station IN-2, 25 July 1972.
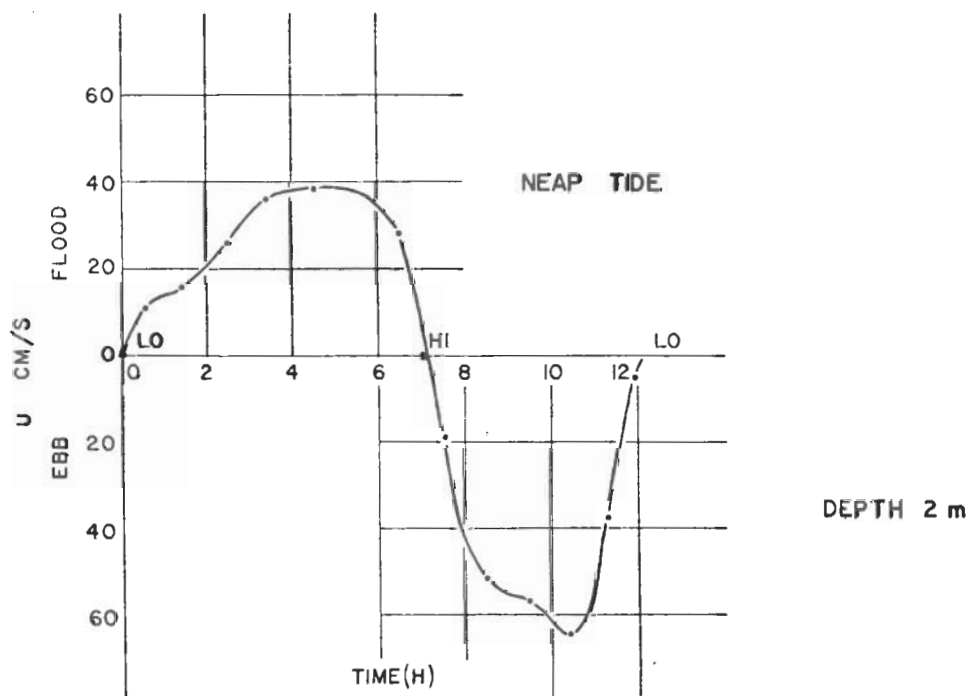
Figure C-4. Tidal current velocity, staion IN-2, 18 July 1972.

163
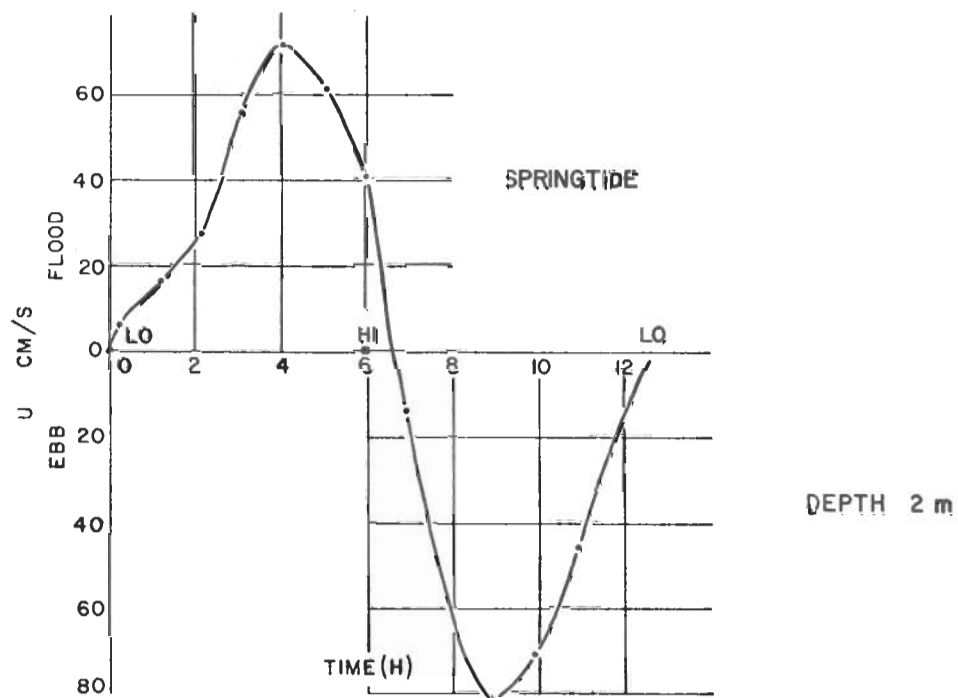
Figure C-5. Tidal current velocity, station IN-6, 14 April 1973.
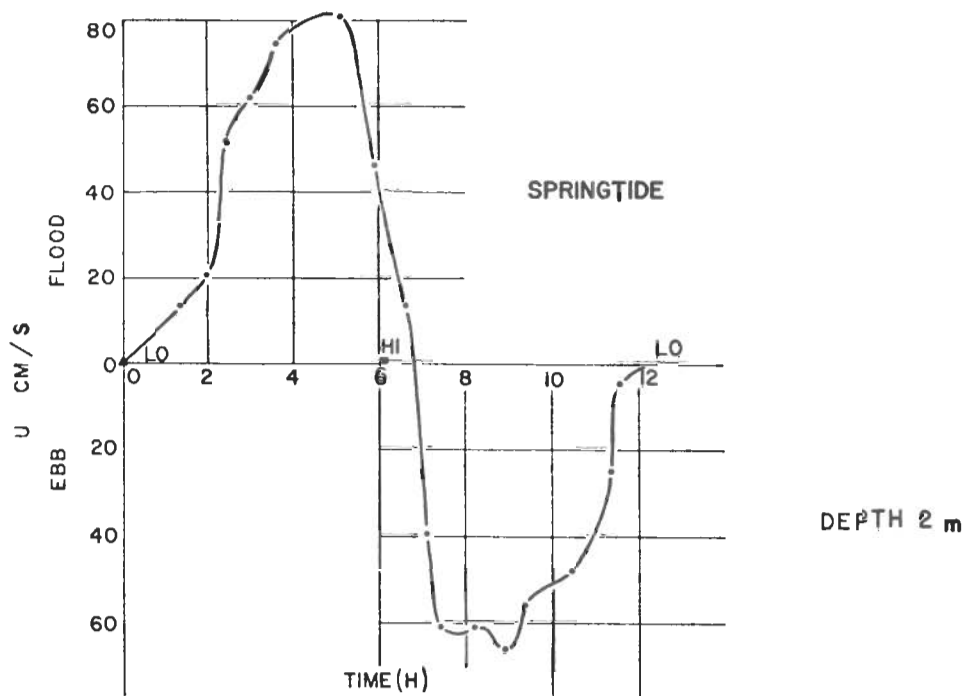
Figure C-6. Tidal current velocity, station IN-6, 5 May 1973.
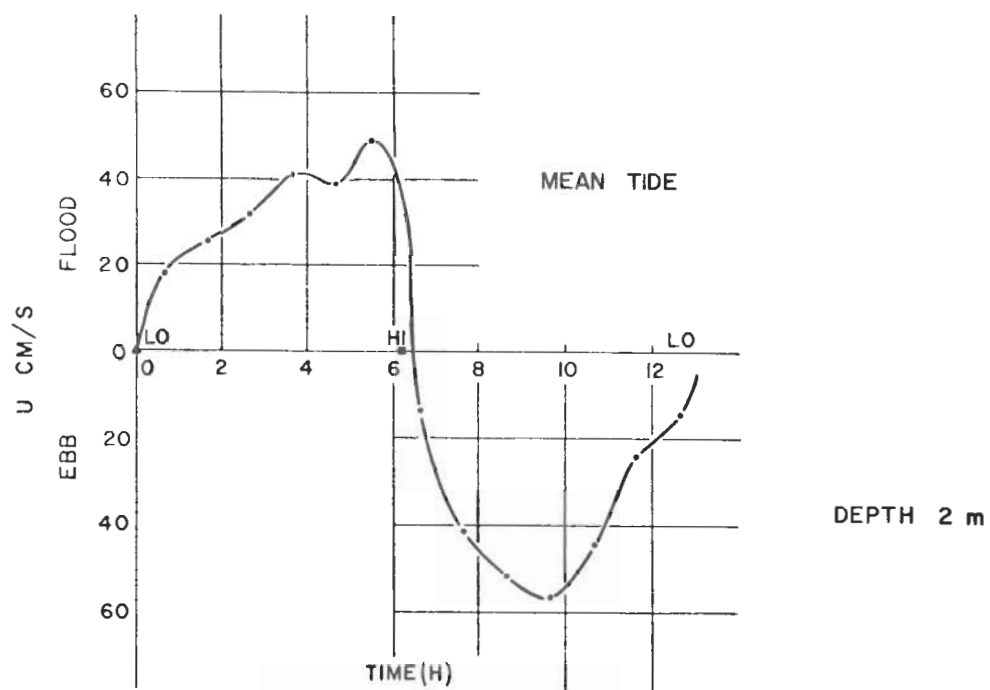
Figure C-7. Tidal current velocity, station TC-1, 25 July 1972.
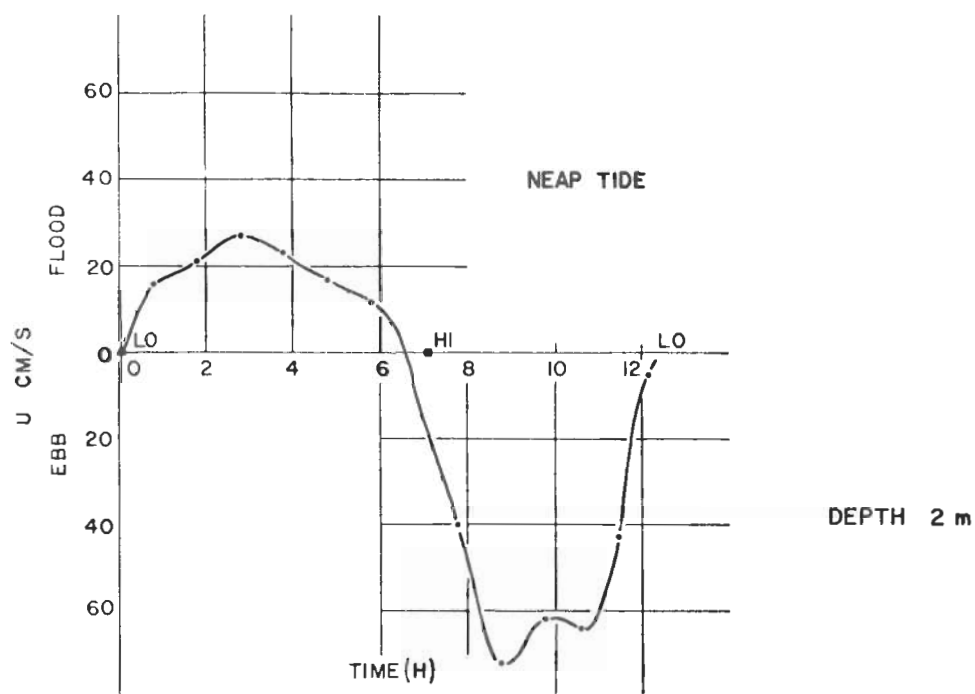
Figure C-8. Tidal current velocity, station TC-1, 18 July 1972.

165
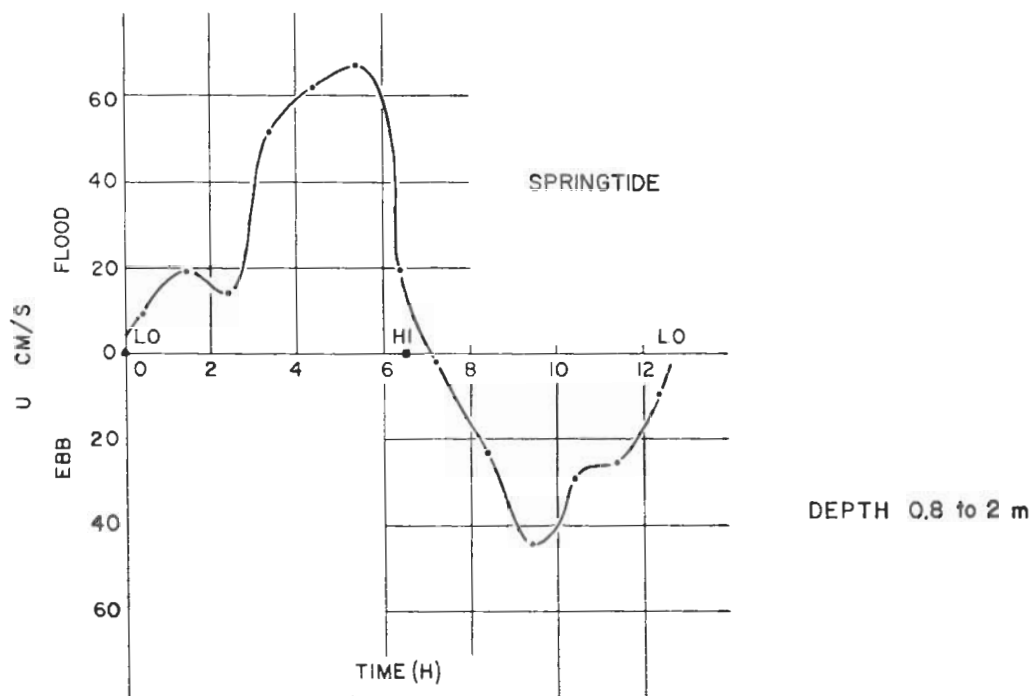
Figure C-9. Tidal current velocity, station TC-2, 6 August 1972.
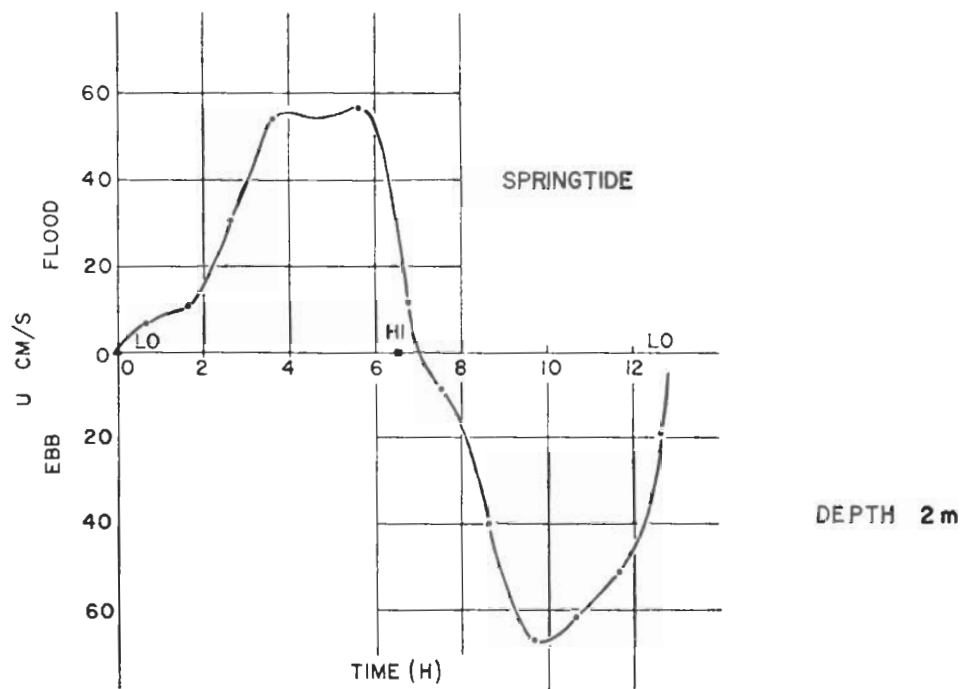
Figure C-10. Tidal current velocity, station TC-3, 6 August 1972.
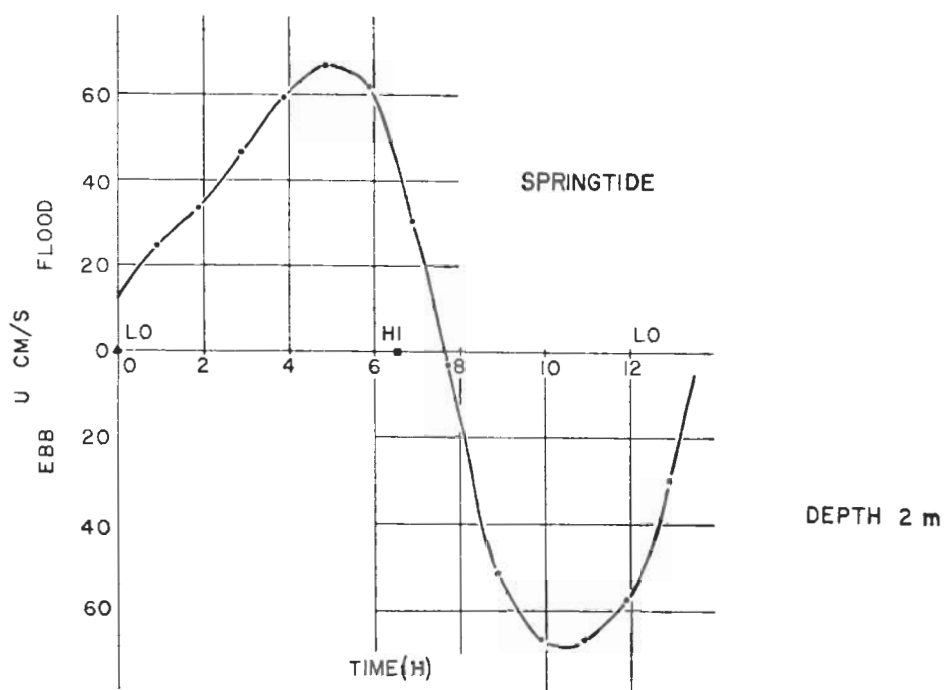
Figure C-11. Tidal current velocity, station TC-4, 6 August 1972.
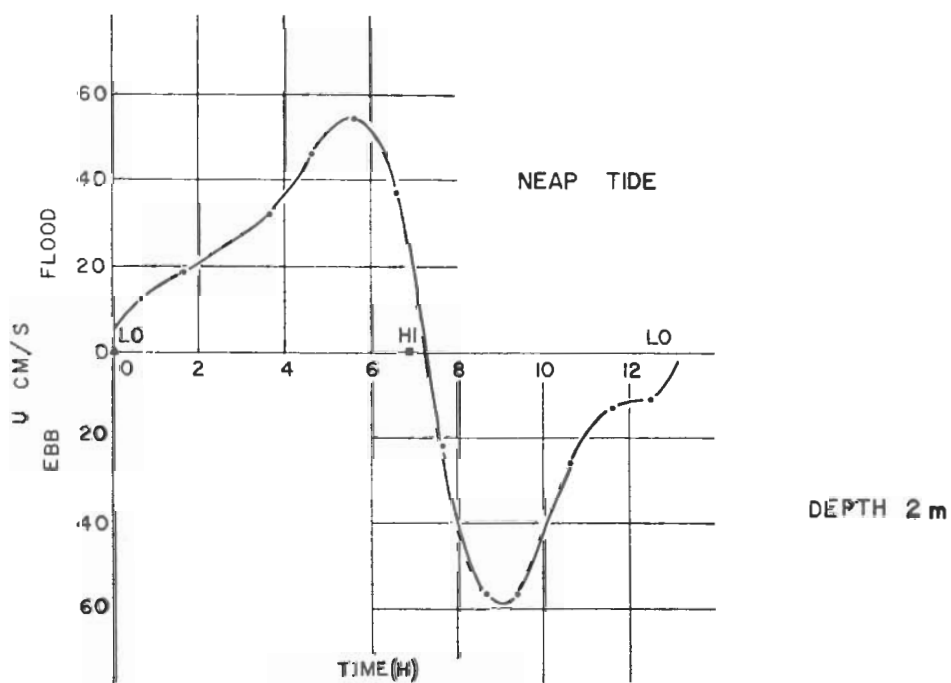
Figure C-12. Tidal current velocity, station JC-1, 20 July 1972.
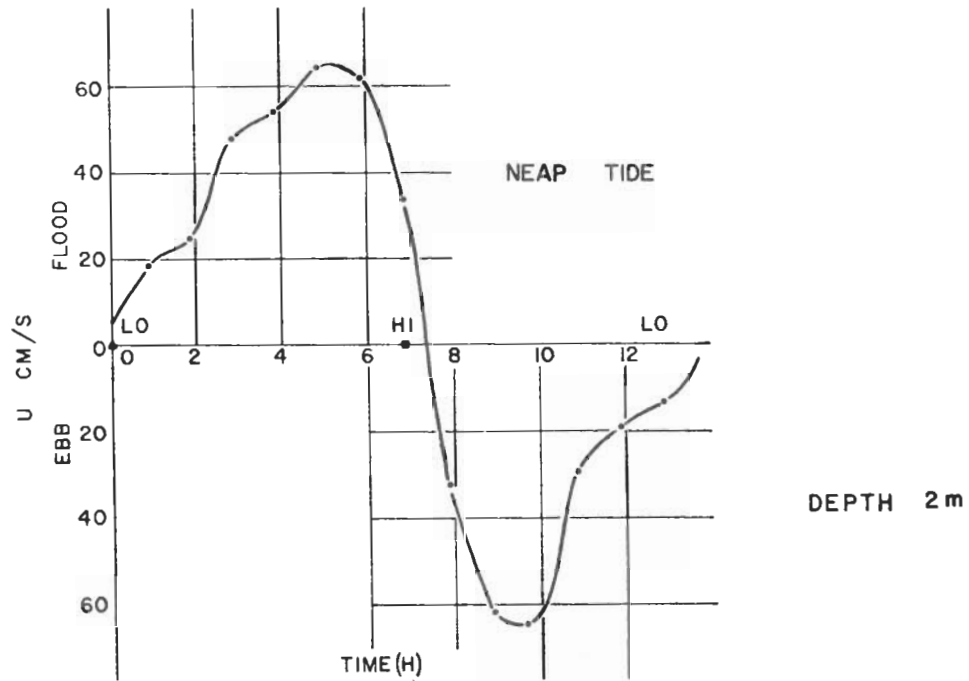
Figure C-13. Tidal current velocity, station JC-2, 20 July 1972.
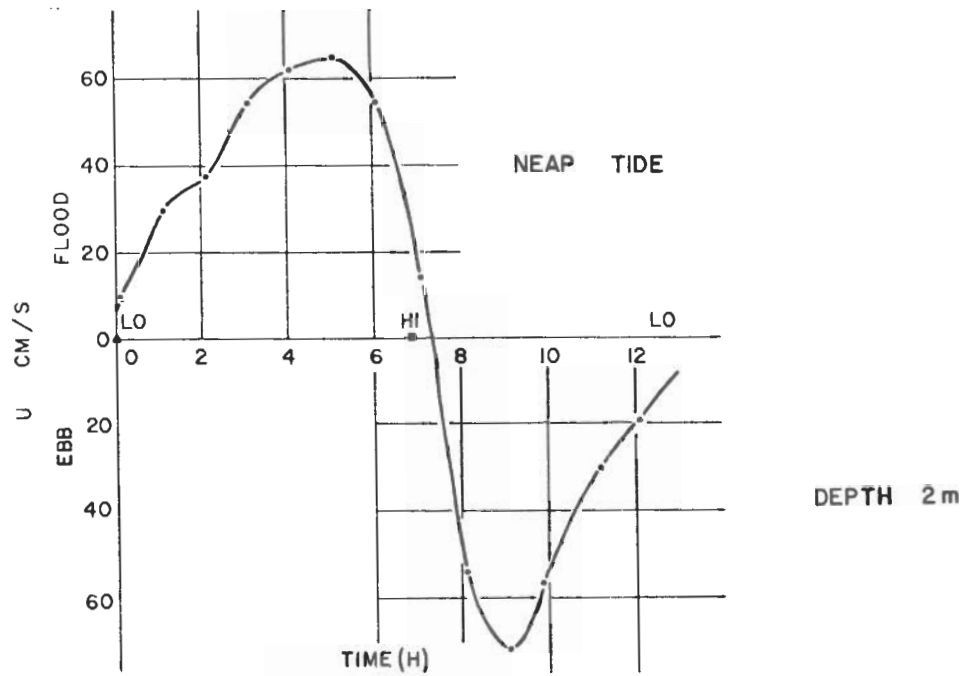
Figure C-14. Tidal current velocity, station JC-3, 20 July 1972.

APPENDIX D

TOTAL DISCHARGE TIME HISTORIES
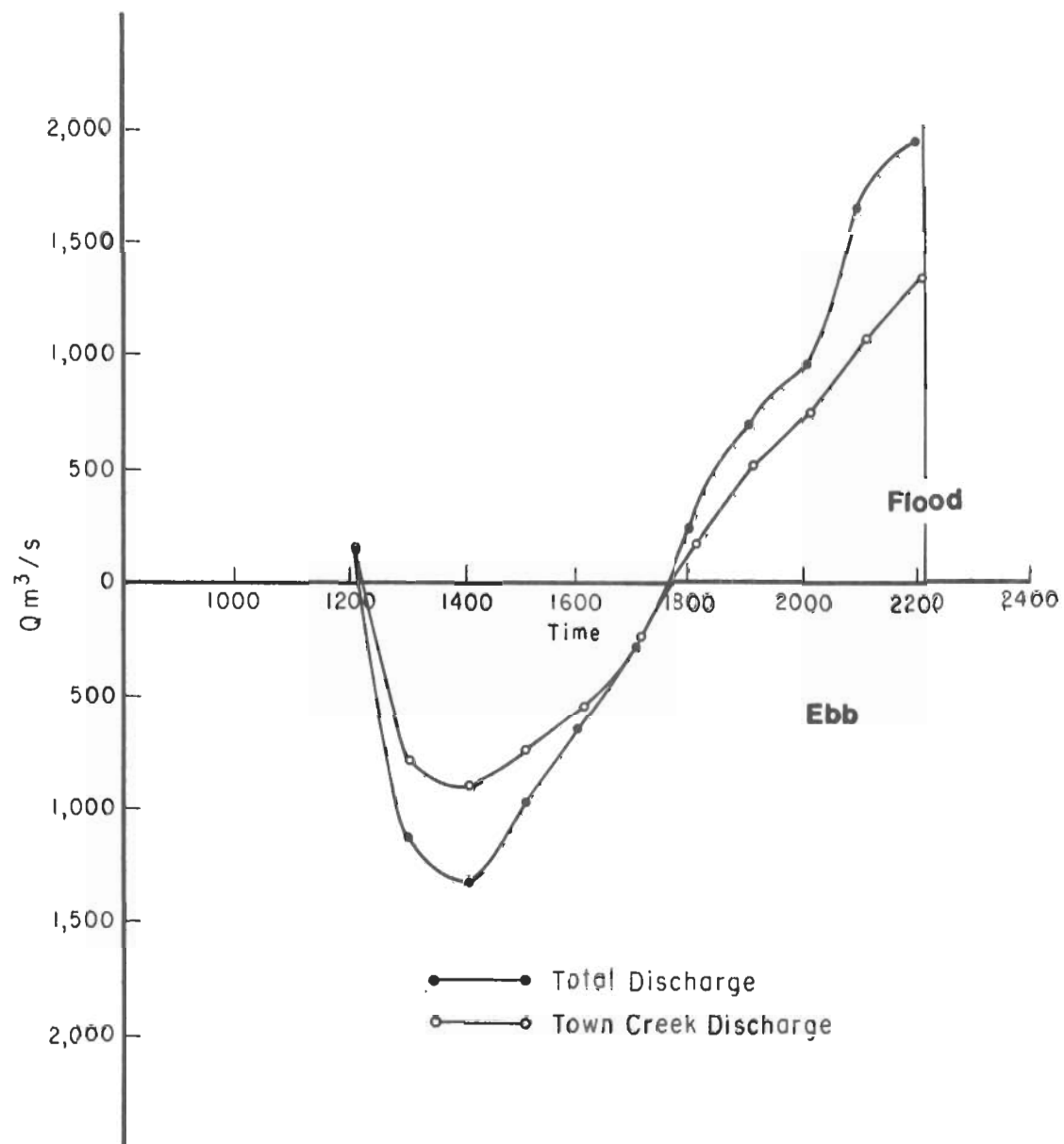
Figure D-1. North Inlet discharge, 20 July 1974.
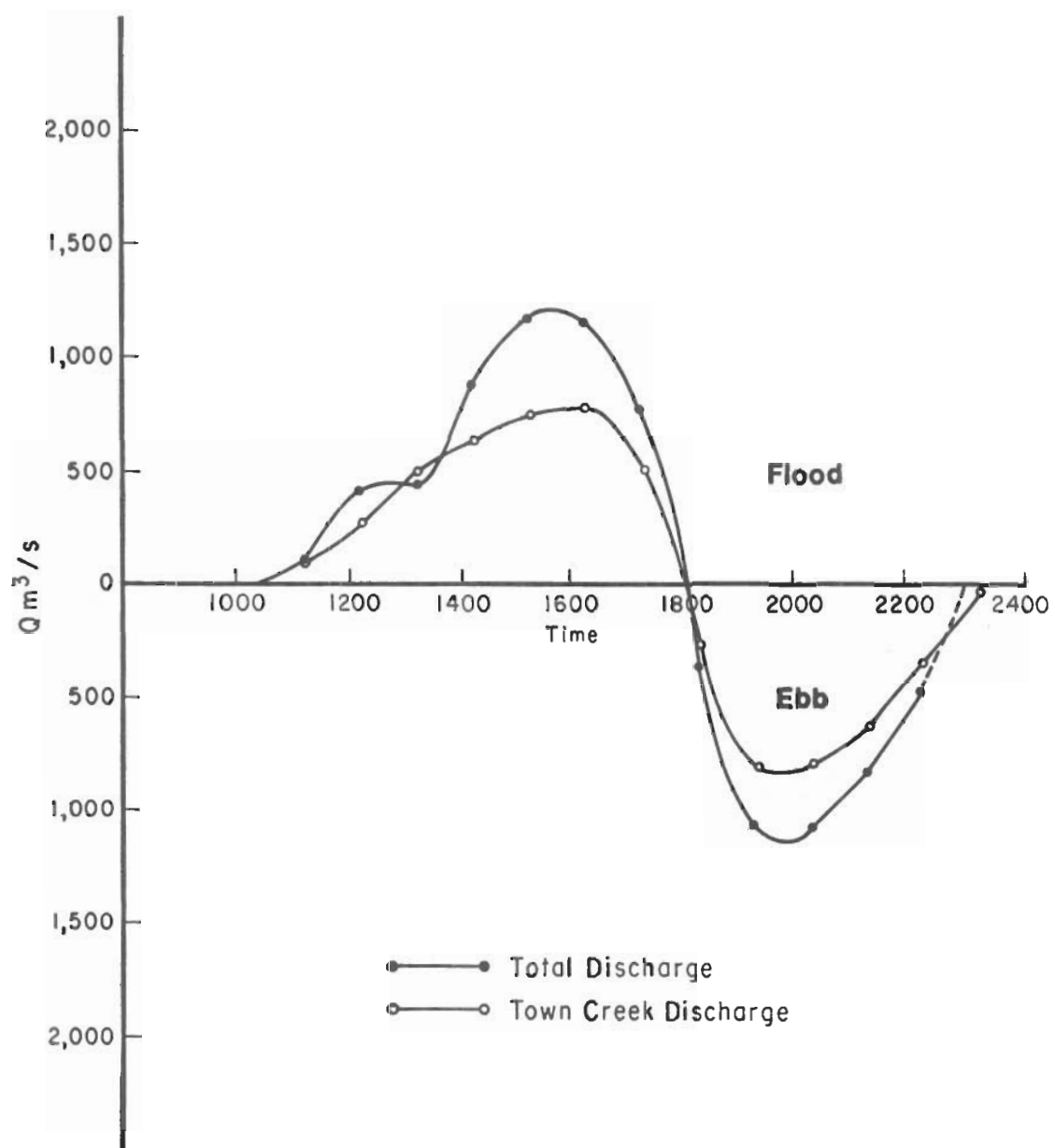
Figure D-2. North Inlet discharge, 26 July 1974.
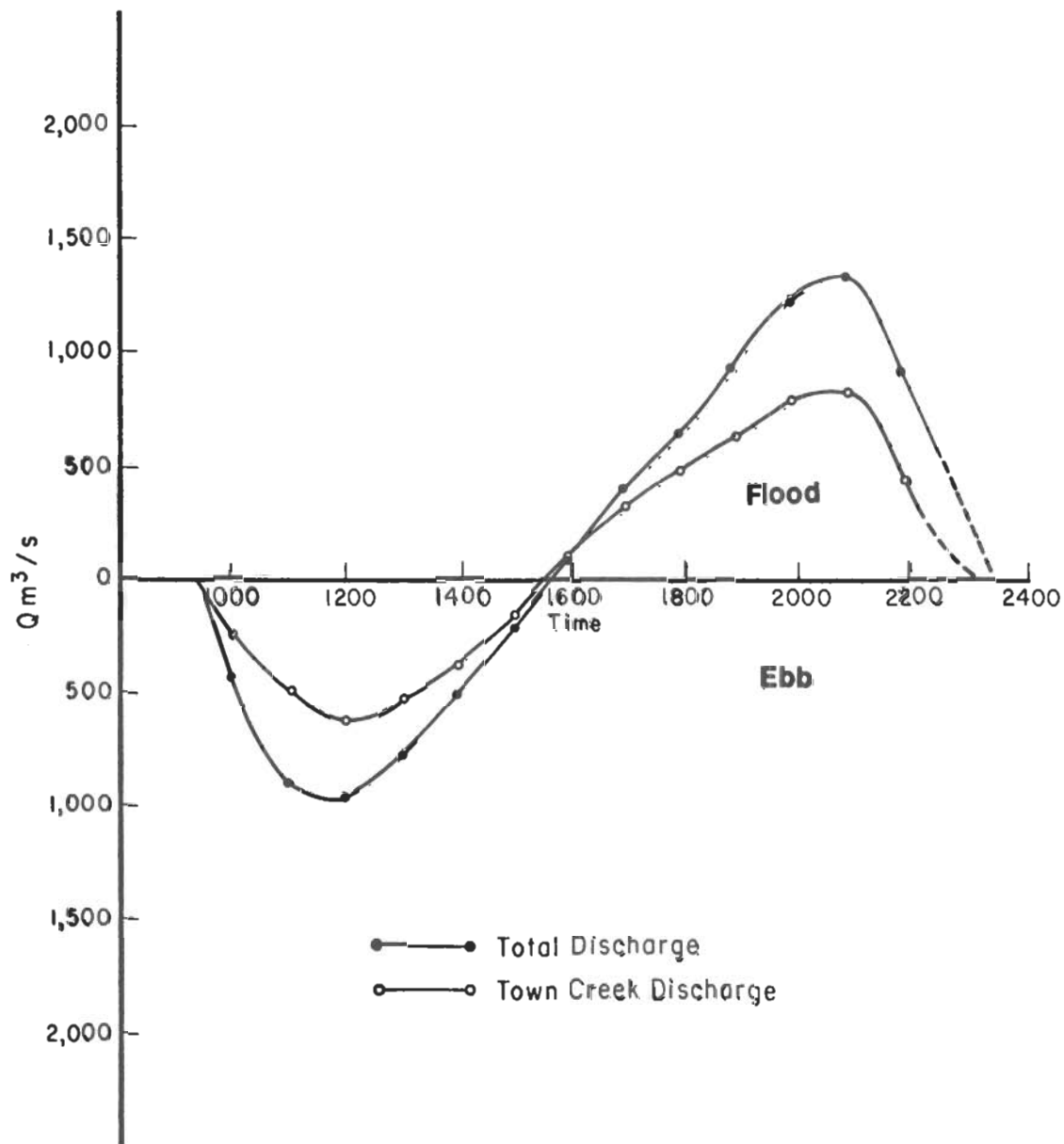
Figure D-3. North Inlet discharge, 1 August 1974.
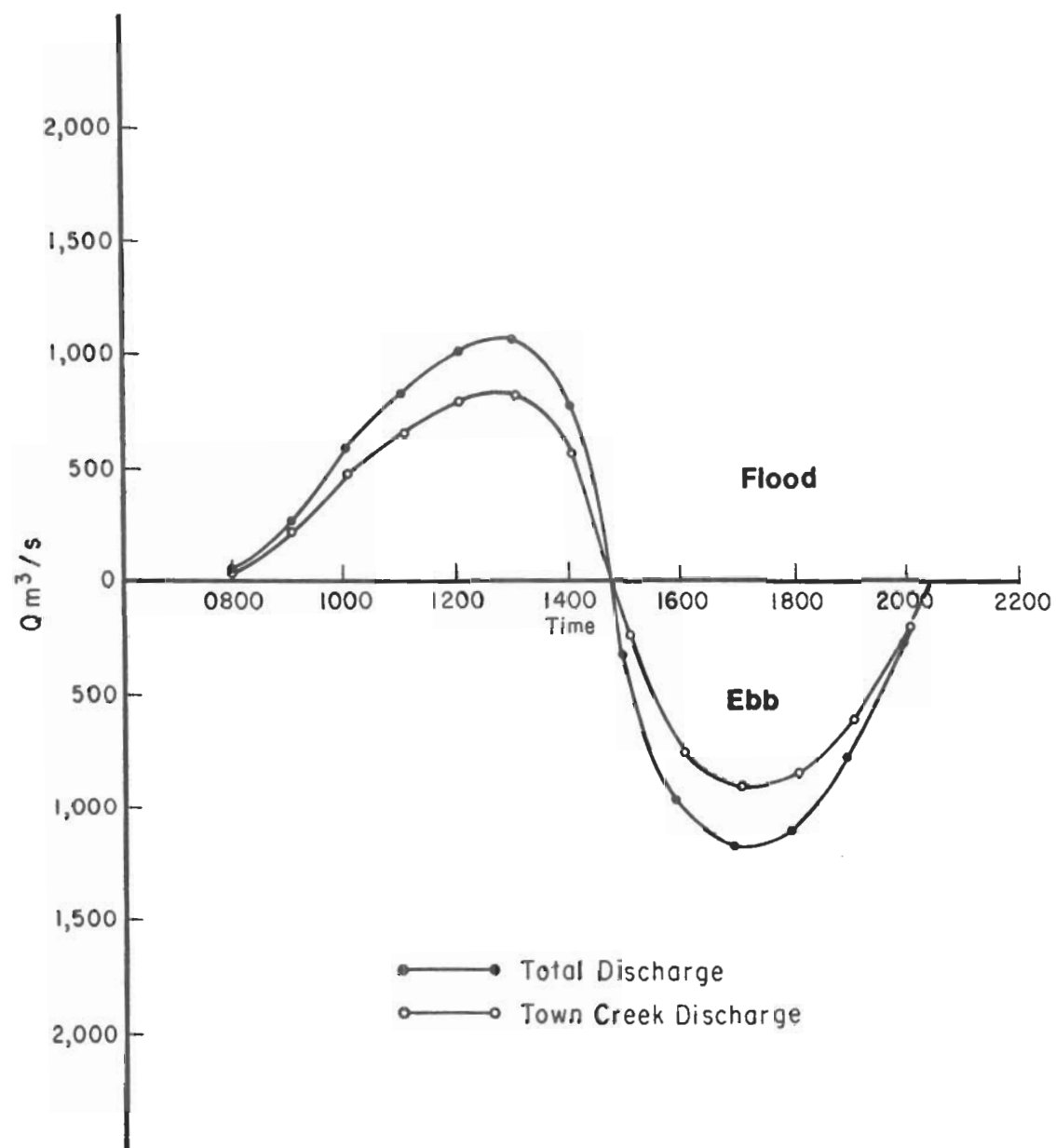
Figure D-4. North Inlet discharge, 24 August 1974.
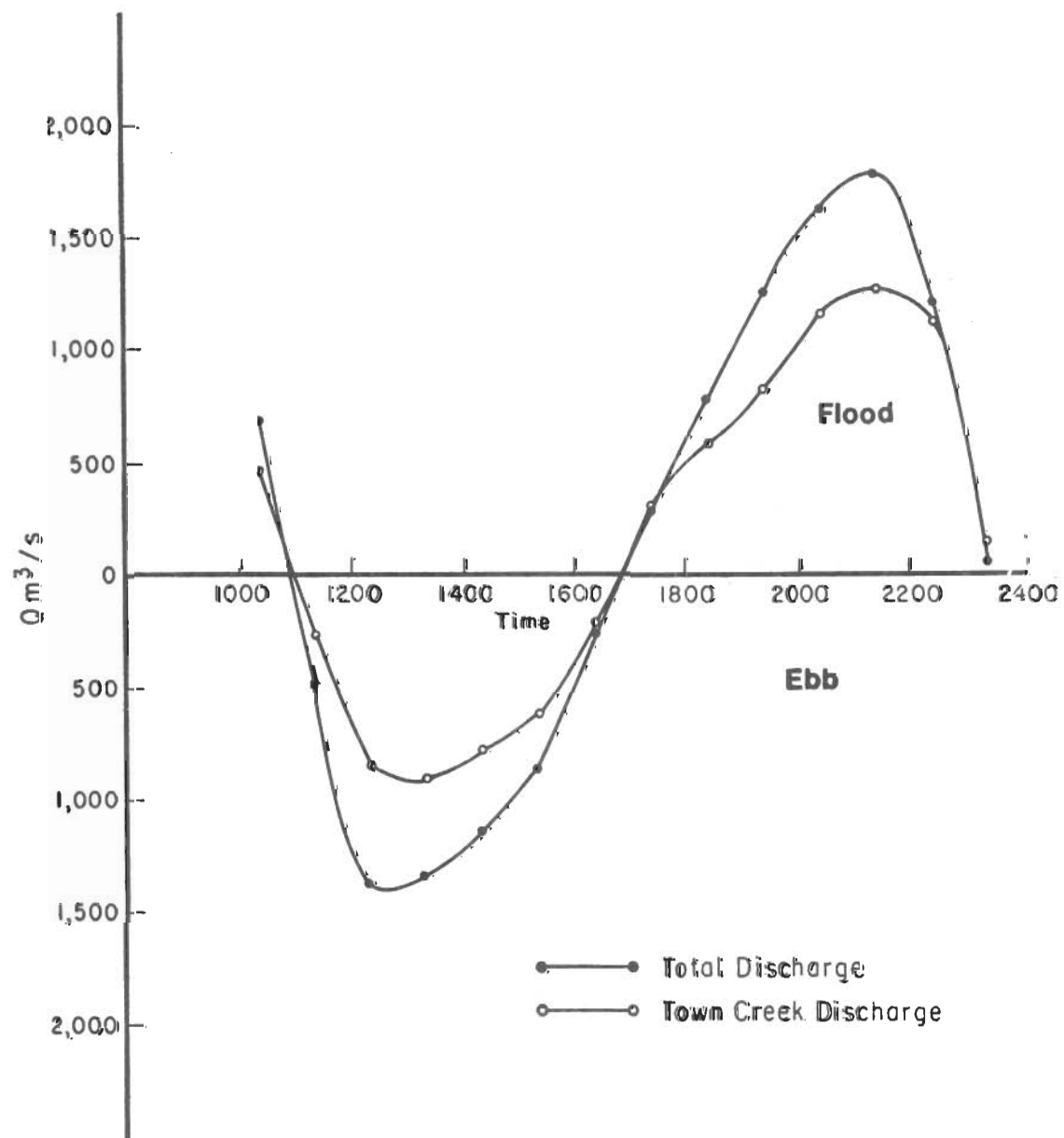
Figure D-5. North Inlet discharge, 15 September 1974.
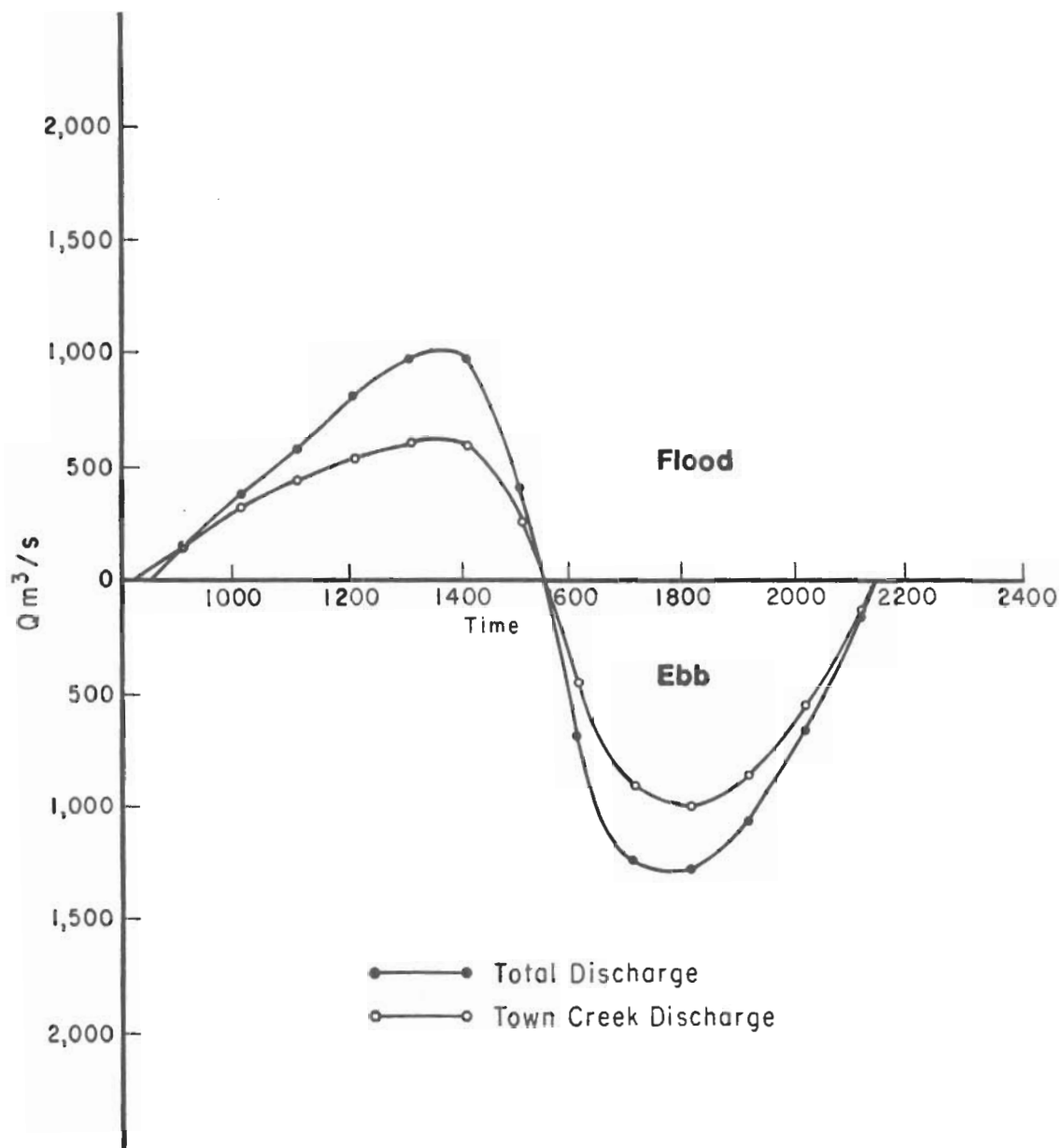
Figure **D-6.** North Inlet discharge, **21 September 1974.**
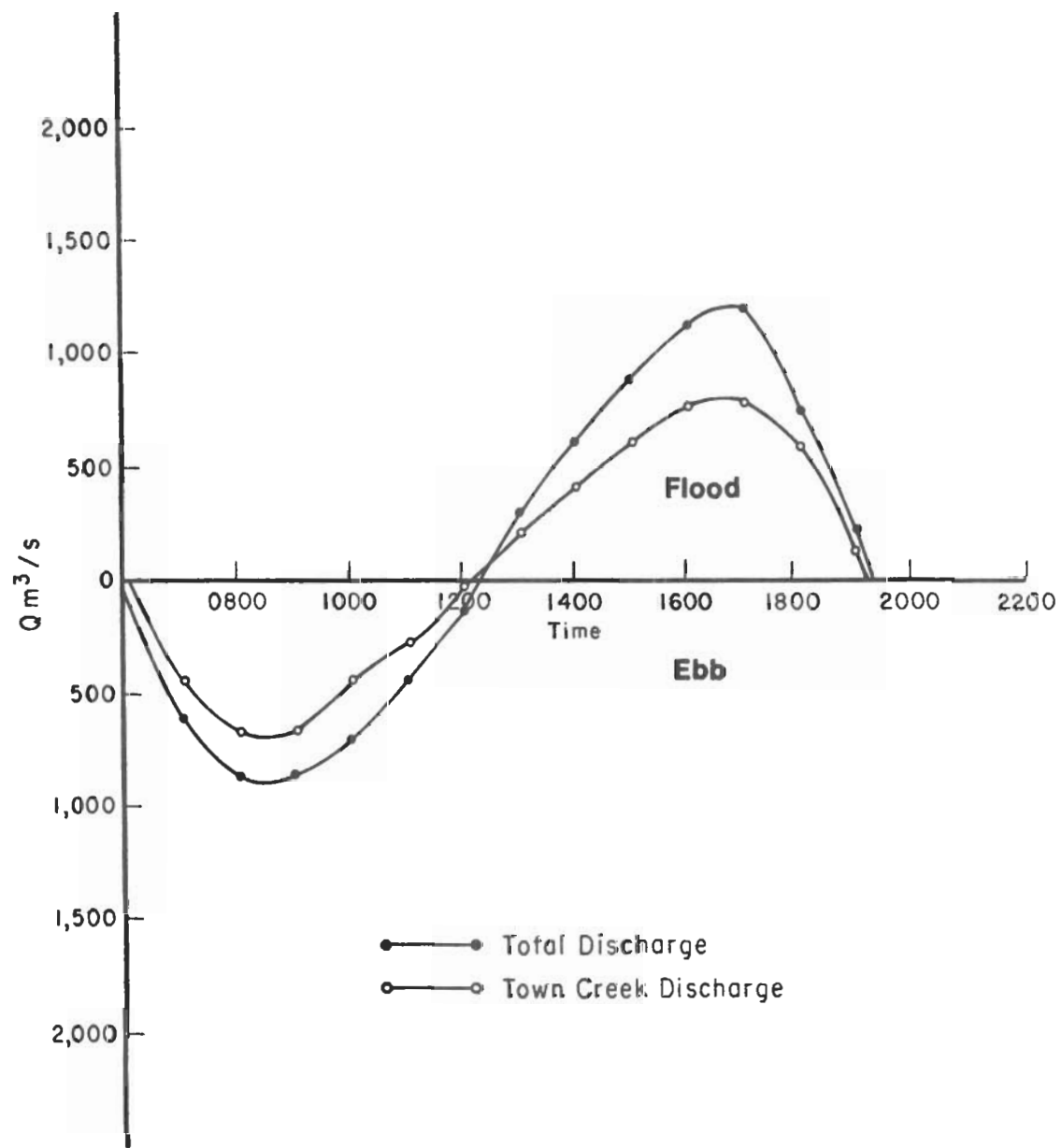
Figure D-7. North Inlet discharge, 27 September 1974.
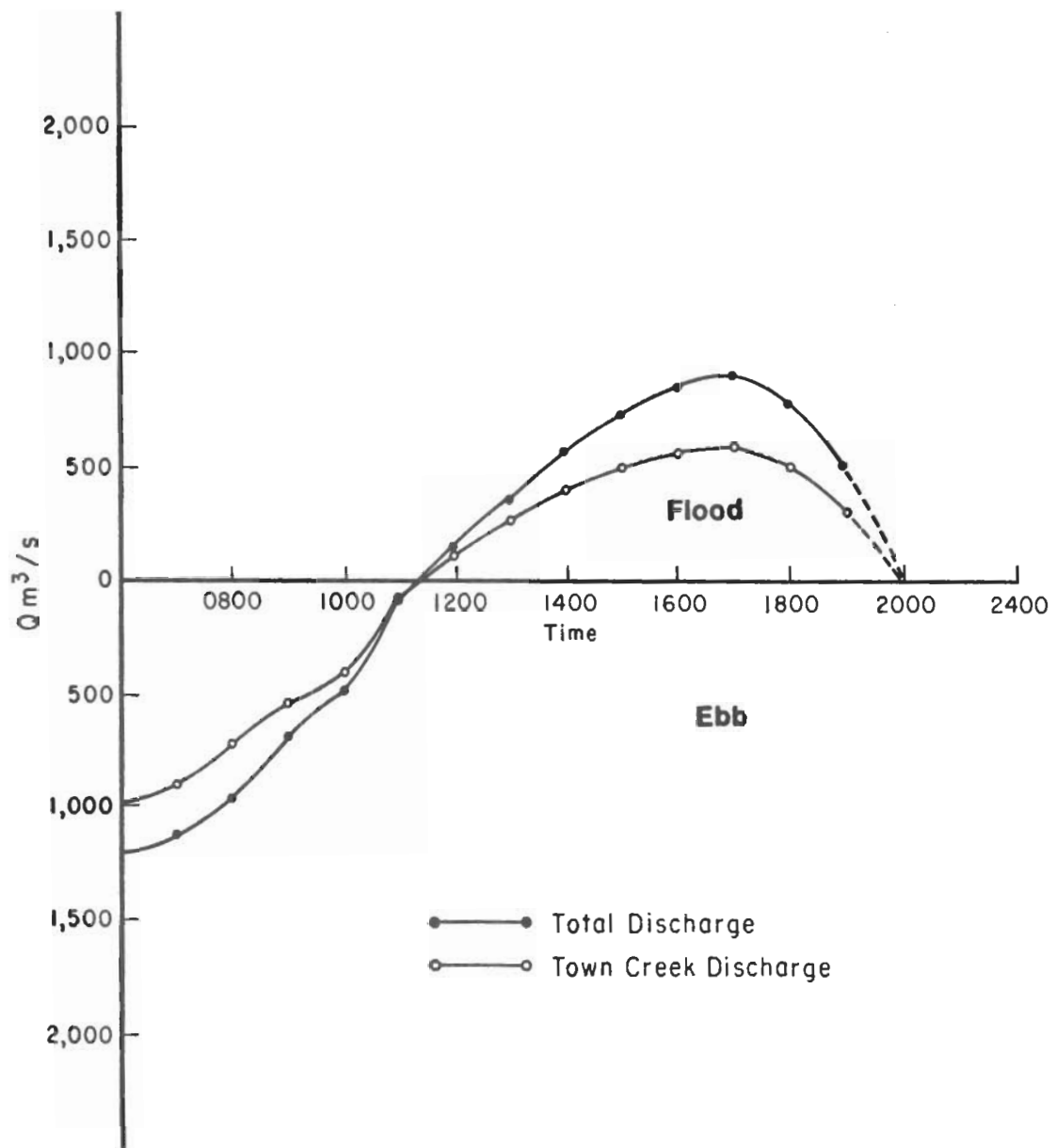
Figure D-8. North Inlet discharge, 27 October 1974.
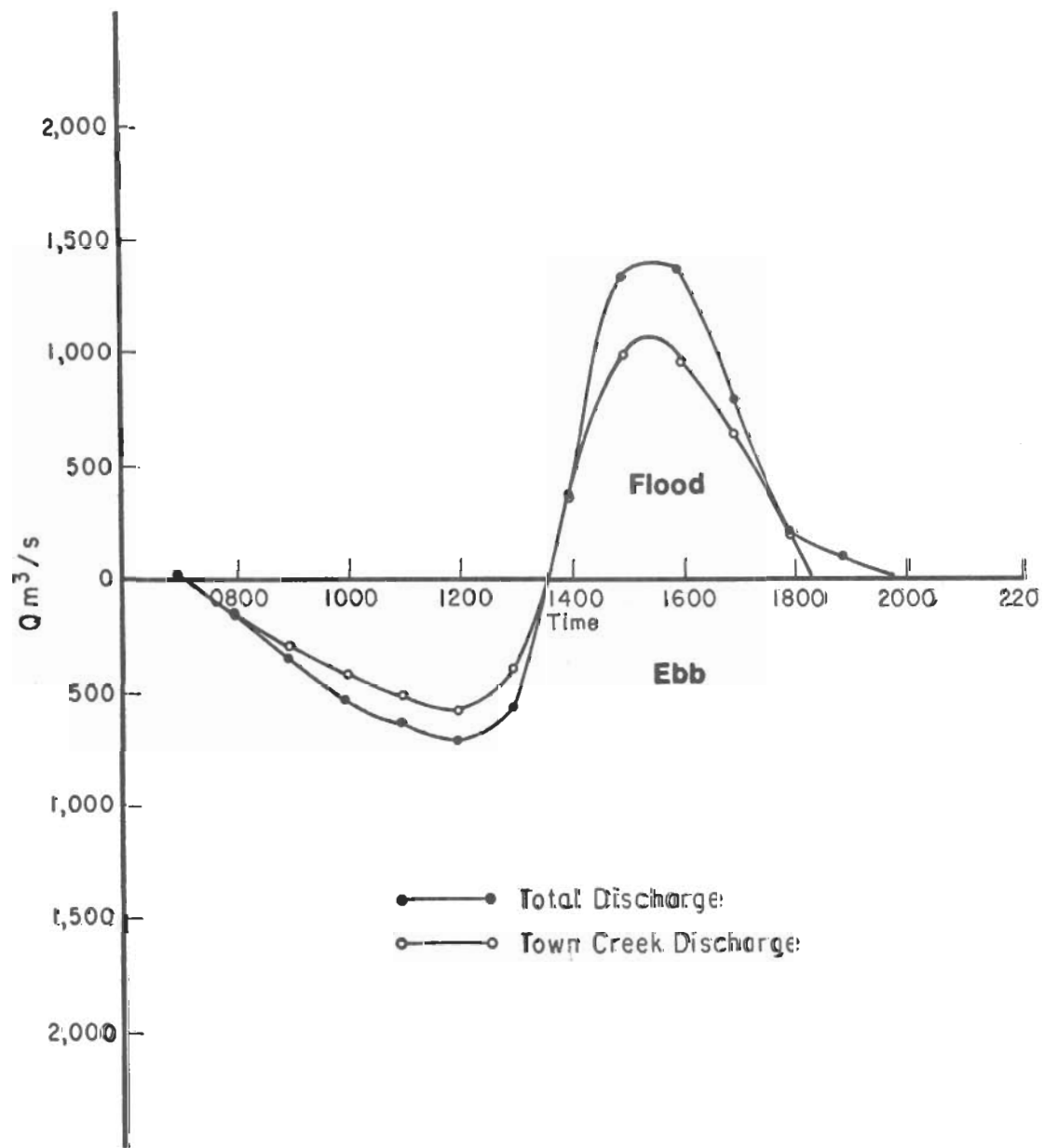
Figure D-9. North Inlet discharge, 4 January 1975.
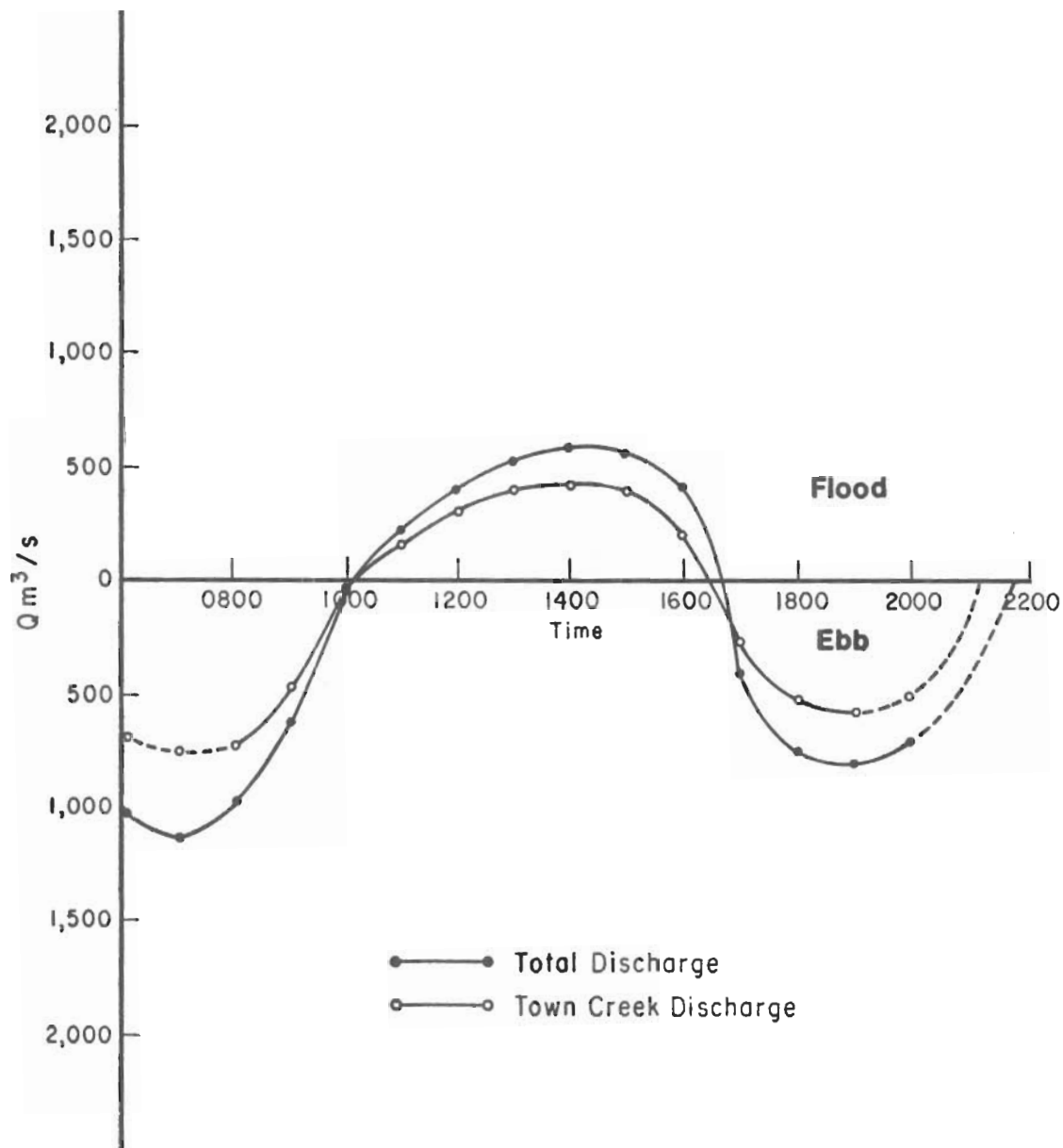
Figure D-10. North Inlet discharge, 7 January 1975.
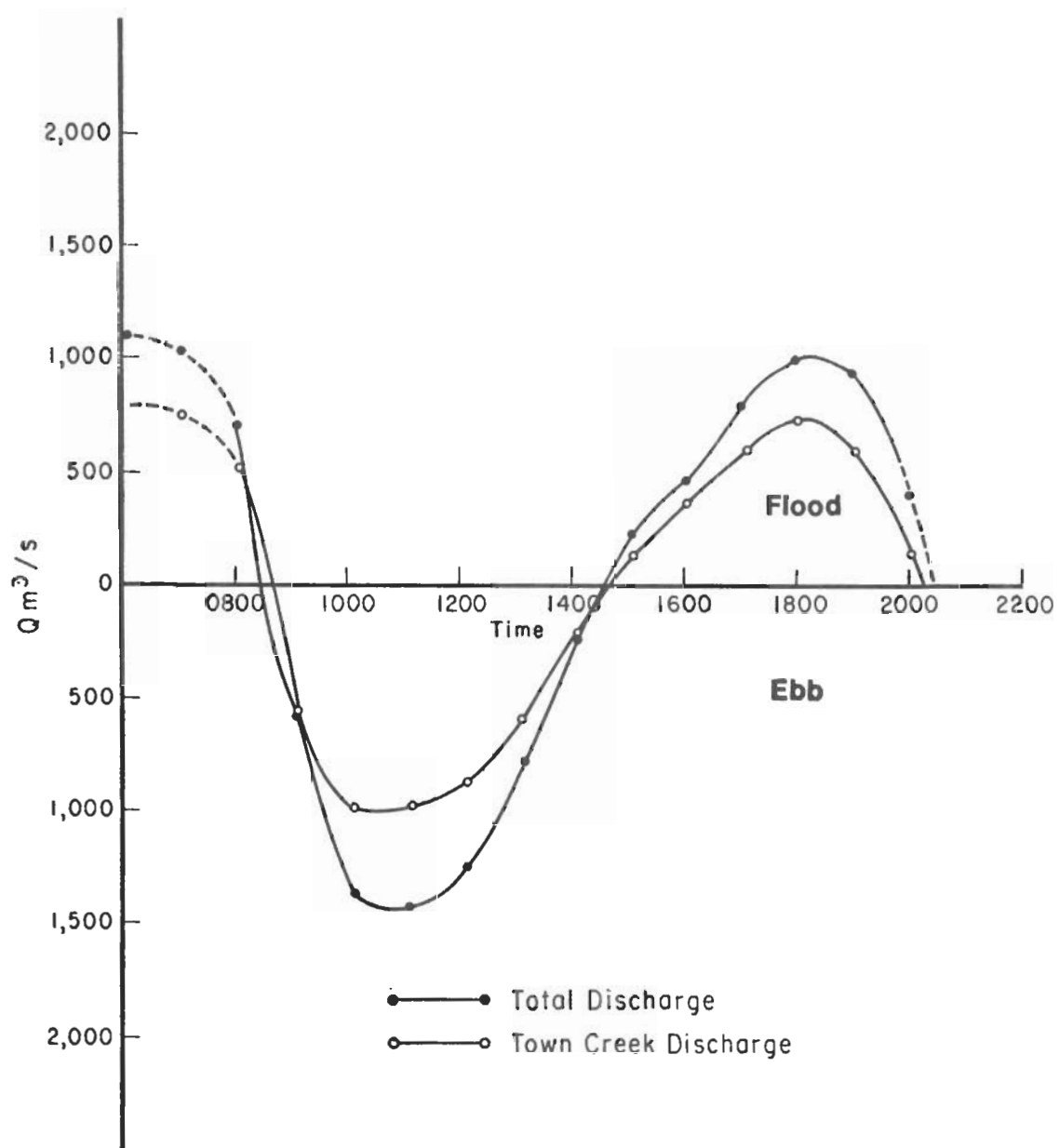
Figure D-11. North Inlet discharge, 12 January 1975.
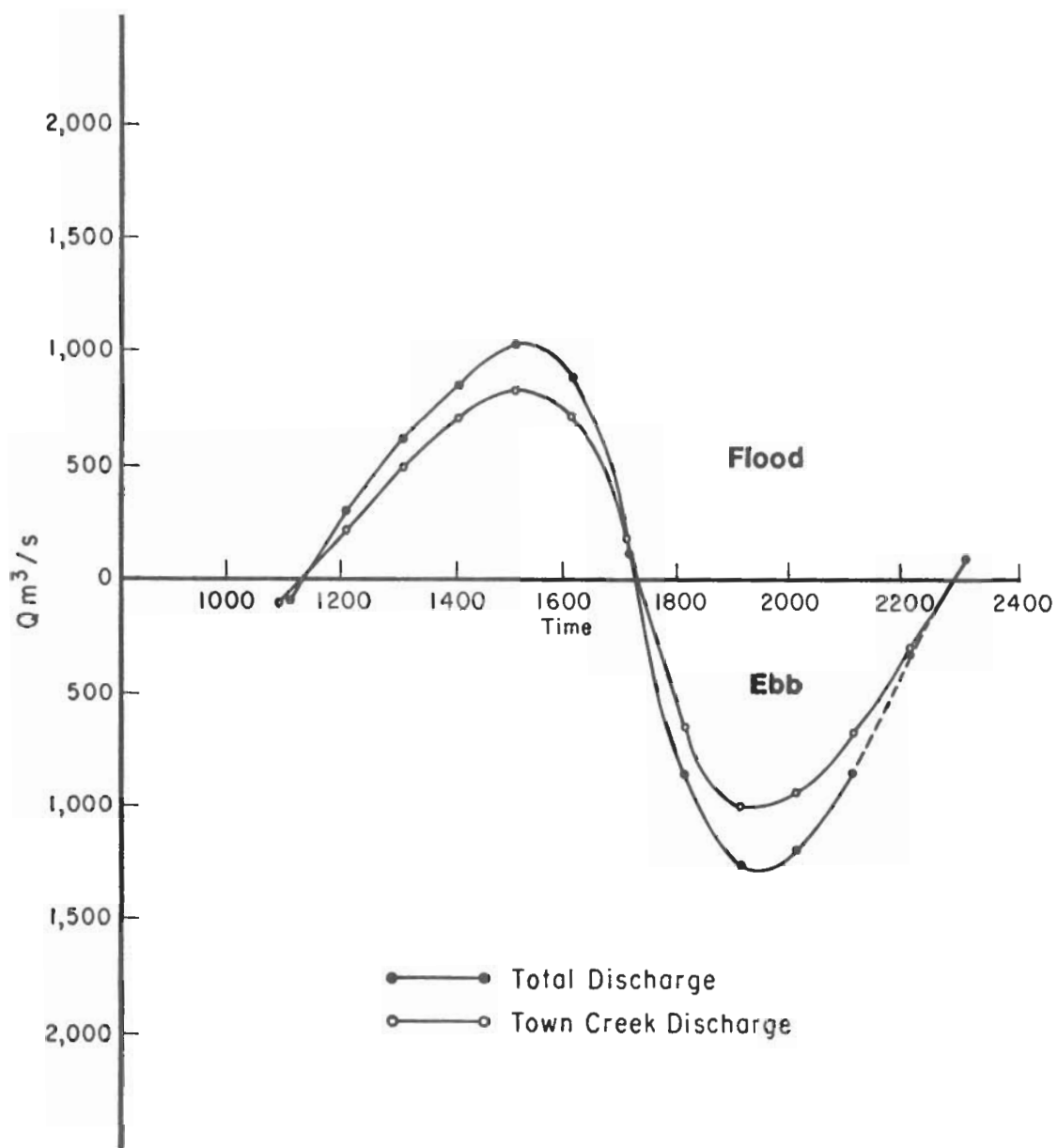
Figure D-12. North Inlet discharge, 22 February 1975.
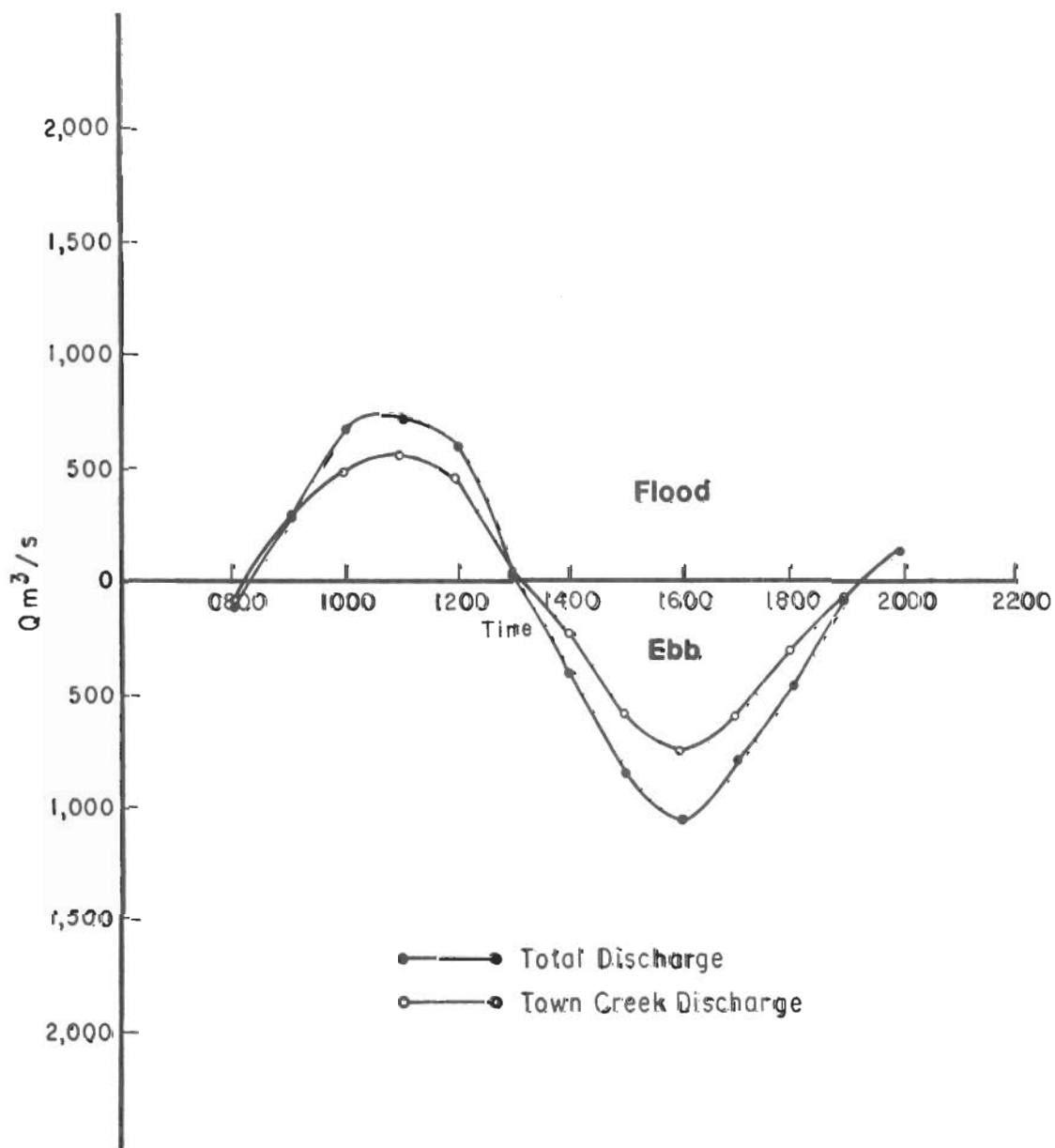
Figure D-13. North Inlet discharge, 19 March 1975.
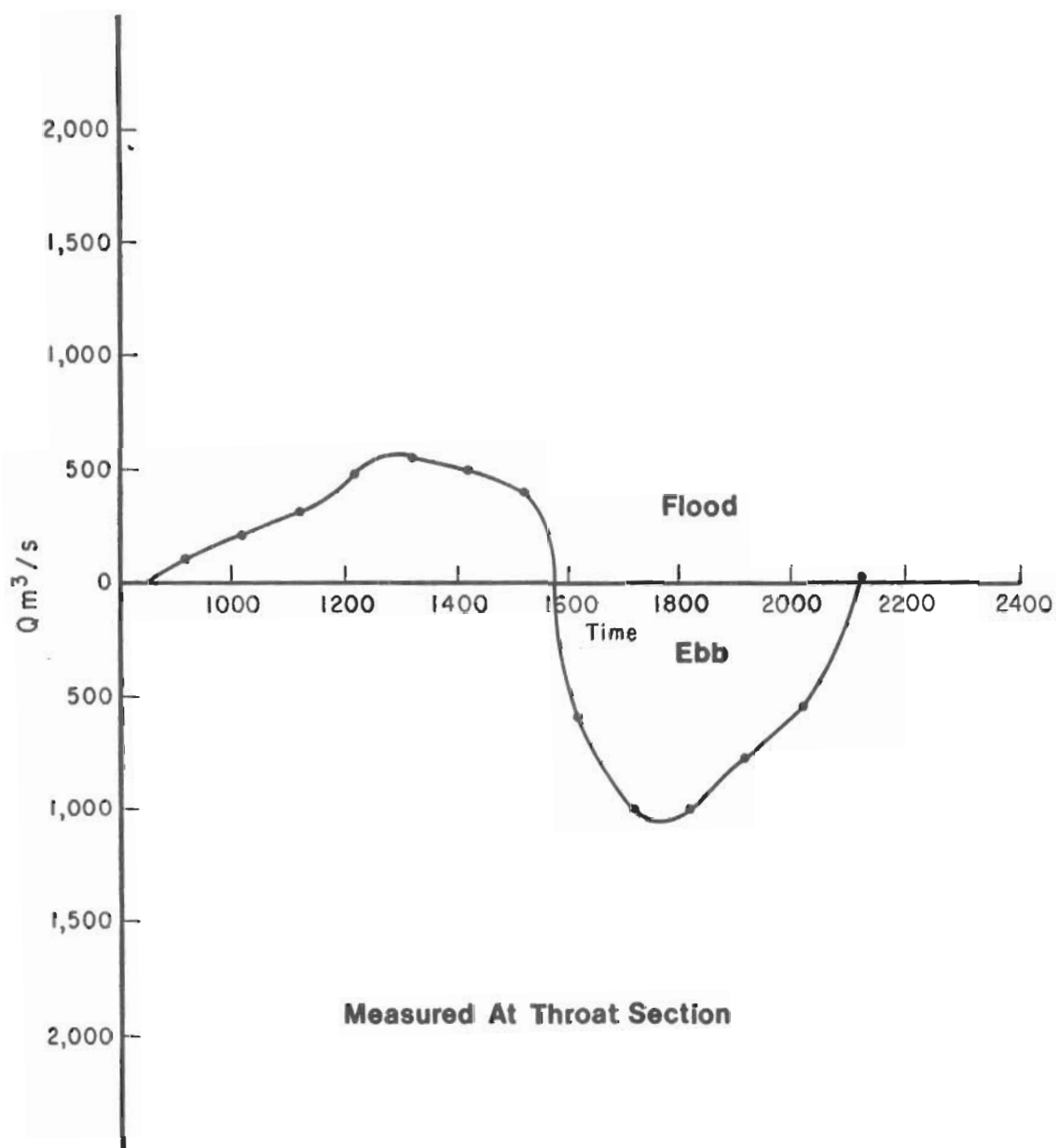
Figure D-14. North Inlet discharge, 21 March 1975.
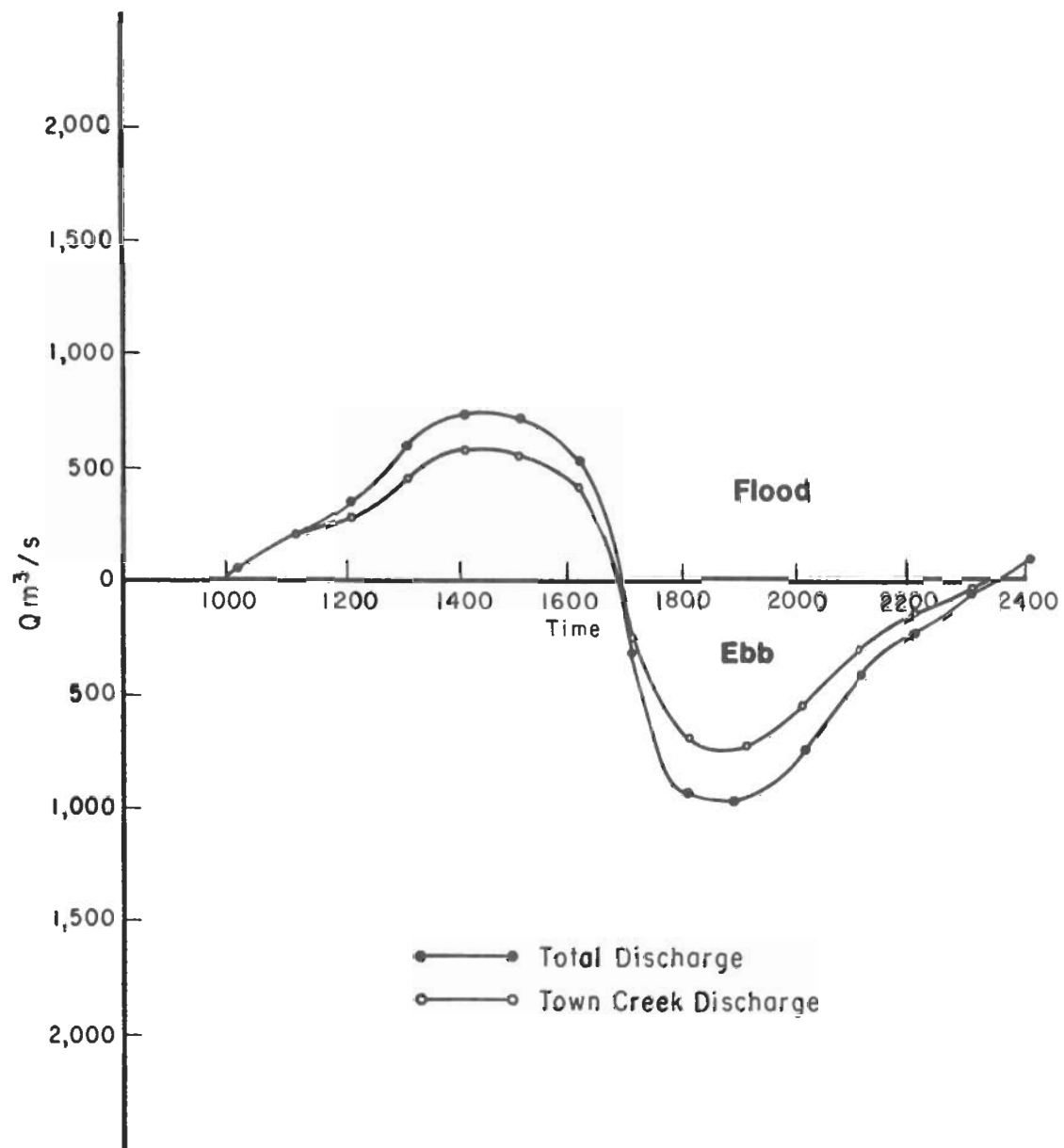
Figure D-15. North Inlet discharge, 22 March 1975.
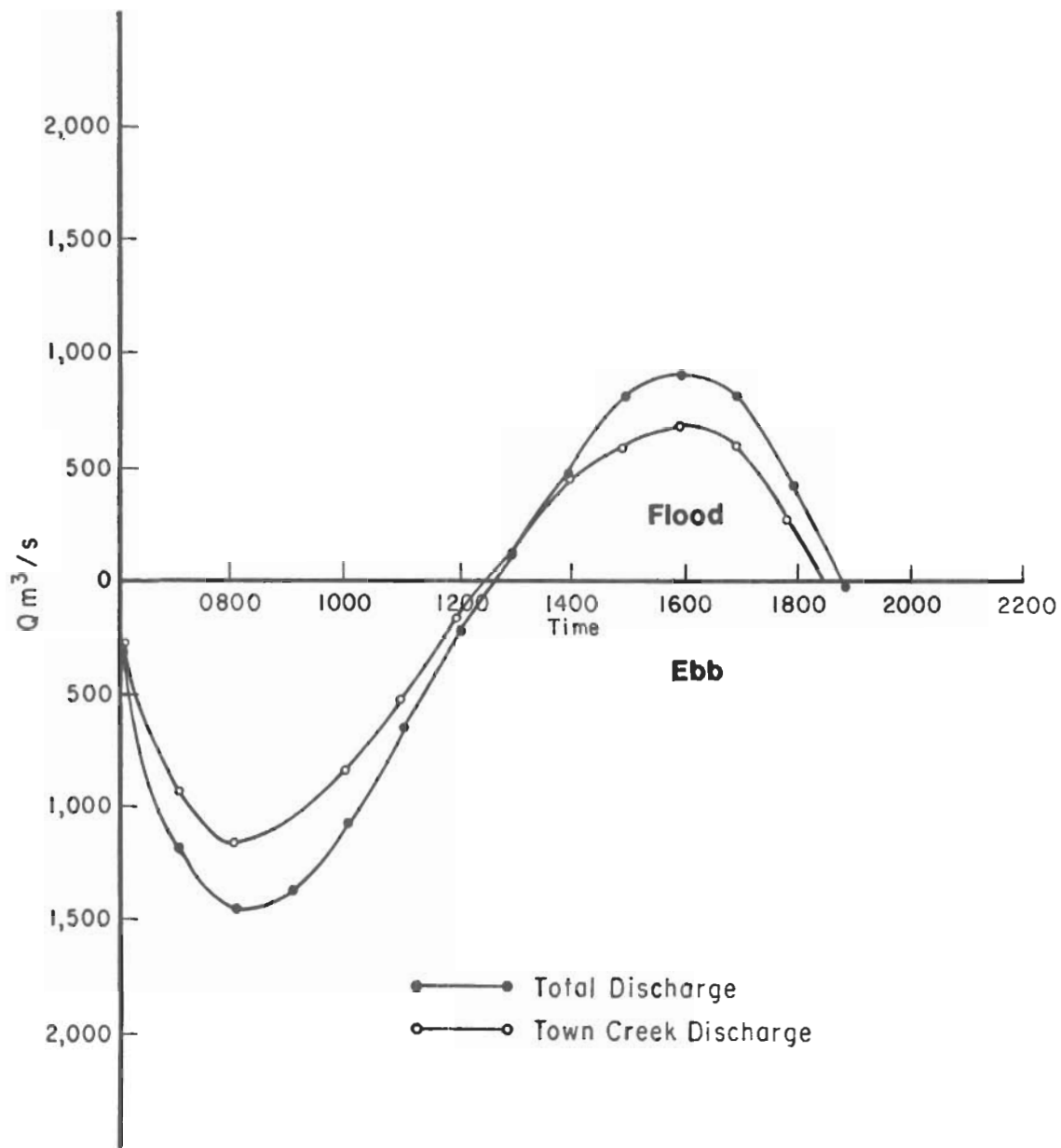
Figure D-16. North Inlet discharge, 24 March 1975.
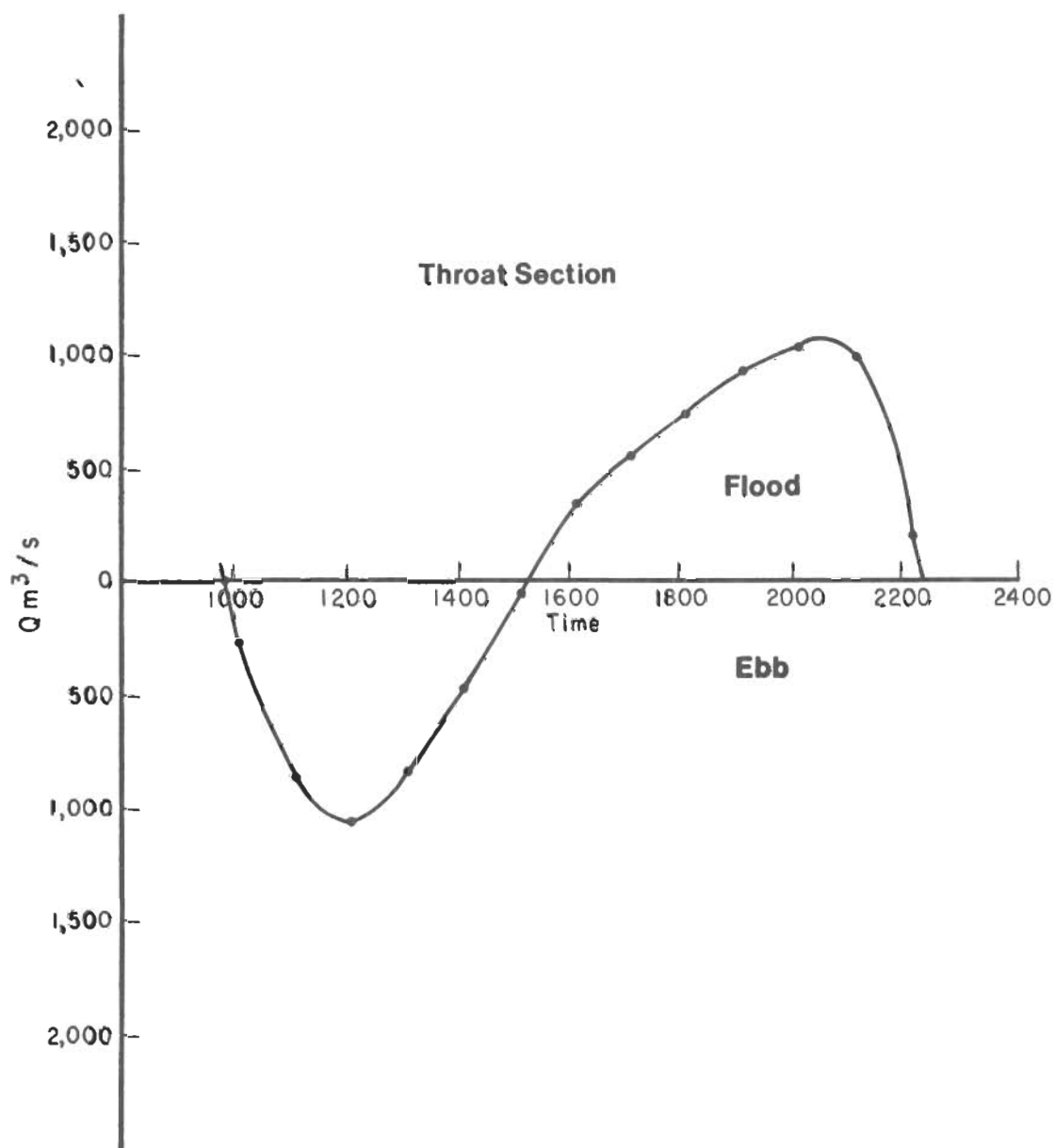
Figure D-17. North Inlet discharge, 26 April 1975.
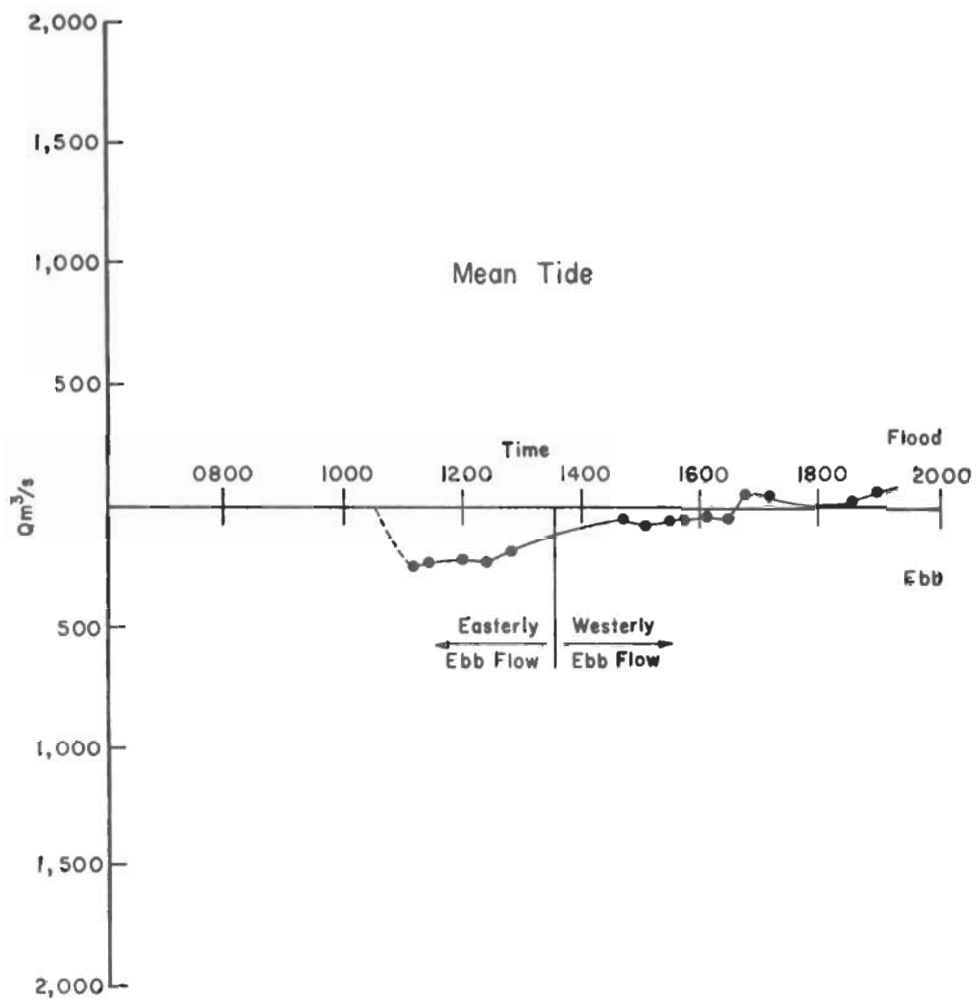
Figure D-18. Discharge of Sixty Bass Creek, 15 March 1975.
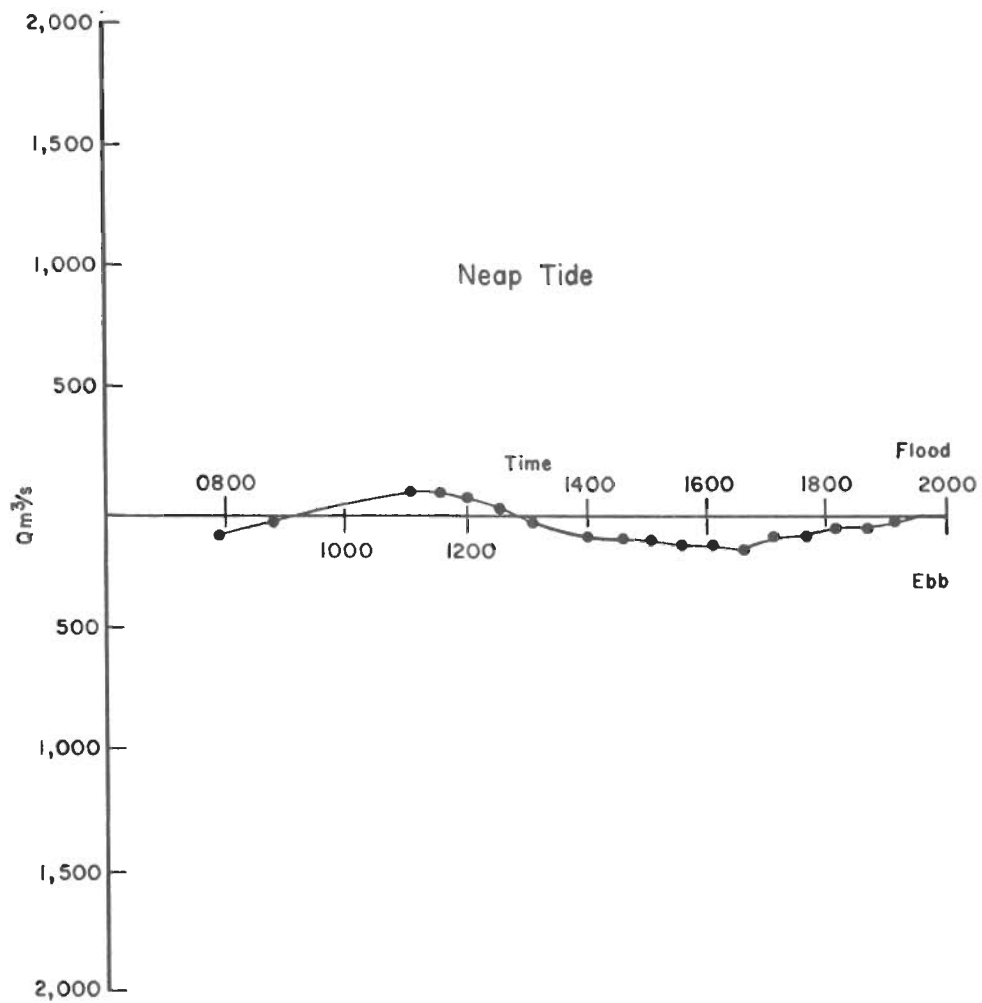
Figure D-19. Discharge of Jones Creek at Noble Slough, 19 March 1975.

Finley, Robert J.

  Hydraulics and dynamics of North Inlet, South Carolina, 1974-75 /
by Robert J. Finley. — Fort Belvoir, Va. : U.S. Coastal Engineering
Research Center, 1976.
  188 p. : ill. (GITI report 10) Also (Contracts - Coastal Engineer-
ing Research Center ; DACW72-72-C-0032 and DACW72-74-C-0018)
  Bibliography : p. 126.
  Variation in wave parameters, beach and inlet morphology, and tidal
hydraulics are discussed in relation to climatic patterns at North
Inlet, South Carolina.
  1. North Inlet, South Carolina. 2. Tidal hydraulics. 3. Tidal
inlets. 4. Coastal morphology. I. Title. II. South Carolina.
University. III. Series : U.S. Army Corps of Engineers. GITI report
10. IV. U.S. Coastal Engineering Research Center. Contract DACW72-
72-C-0032. V. U.S. Coastal Engineering Research Center. Contract
DACW72-74-C-0018.

GB454   .I5   U581r   no.10   551.4